Final Scientific/Technical Report

Complete Fiber/Copper Cable Solution for Long-Term Temperature and Pressure Measurement in Supercritical Reservoirs and EGS Wells.

Award Number: DE-EE0002786

Recipient: Prysmian Group (Draka Cableteq USA)
22 Joseph E. Warner Blvd.
North Dighton, MA 02764

Principal Investigators: Walter Constantine, walter.constantine@prysmiangroup.com
Kendall Waterman, kendall.waterman@prysmiangroup.com

Project Period: 1/29/2010 through 9/30/2014

Date of Report Submission: November 13, 2015

DOE Project Team: DOE Contracting Officer – Melissa Jacobi
DOE Project Officer – William Vandermeer
Project Monitor – Angel Nieto

Prysmian Group Team		
Draka Cableteq USA	North Dighton, MA, USA	Cable Development
Draka Telecomm	Claremont, NC, USA	Fiber Coating Development
Draka Telecomm	Deflzijl, NL	Cable Design & Manufacturing
Draka Telecomm	Eindhoven, NL	Fiber Development
Draka Telecomm	Marcousis, France	Fiber Development
Participants & Other Collaborating Organizations		
Tetramer Technologies	Pendleton, SC, USA	Subcontractor-fiber coatings
Sandia National Labs	Albuquerque, NM, USA	Fiber Testing
SensorTran (vendor)	Houston, TX, USA	DTS instrument vendor
Omnisens (vendor)	Morges, Switzerland	DTS instrument vendor
Chemours (vendor)	Wilmington, DE, USA	High Temp Material vendor
PermaWorks (vendor)	Albuquerque, NM, USA	High Temp P/T tool
AltaRock Energy	Seattle, WA, USA	Down-hole Trials
Lowell Innovation	Berkley, MA, USA	Consultant

Executive Summary

High Temperature insulated wire and optical fiber cable is a key enabling technology for the Geothermal Technologies Program (GTP). Without insulated electrical wires and optical fiber, downhole temperature and pressure sensors, flow meters and gauges cannot communicate with the surface. Unfortunately, there are currently no insulated electrical wire or fiber cable constructions capable of surviving for extended periods of deployment in a geothermal well (240-325°C) or supercritical (374°C) reservoir. This has severely hindered engineered reservoir creation, management and utilization, as hot zones and cool water intrusions cannot be understood over time. The lack of a insulated electrical wire and fiber cable solution is a fundamental limitation to the viability of this energy source.

The High Temperature Downhole Tools target specification is development of tools and sensors for logging and monitoring wellbore conditions at depths of up to 10,000 meters and temperatures up to 374^{o}C. It well recognized in the industry that no current electronic or fiber cable can be successfully deployed in a well and function successfully for more a few days at temperatures over 240^{o}C. The goal of this project was to raise this performance level significantly.

Prysmian Group's objective in this project was to develop a complete, multi-purpose cable solution for long-term deployment in geothermal wells/reservoirs that can be used with the widest variety of sensors. In particular, the overall project objective was to produce a manufacturable cable design that can perform without serious degradation:

- At temperatures up to 374°C;
- At pressures up to 220 bar;
- In a hydrogen-rich environment; and
- For the life of the well (> 5 years).

This cable incorporates:

- Specialty optical fibers, with specific glass chemistry and high temperature and pressure protective coatings for data communication and distributed temperature and pressure sensing, and
- High-temperature insulated wire conductors

Prysmian Group has developed a geothermal fiber optic cable (GFOC) solution which incorporates novel glass chemistry for optical fibers to operate at the required bandwidths in high temperature/high pressure hydrogen rich environments with fiber protection, high temperature insulated conductors and protective cladding for cable components. The cable solution has been tested in a geothermal installation for 10 months. The electrical insulation and optical fibers have been validated through laboratory testing to ensure successful operation for greater than 5 years at 300°C, with the possibility of higher temperatures depending on the particular well environment.

With the 300°C optical fiber and electrical insulation developments completed and validated in laboratory tests the greatest challenge to a complete 300°C cable solution was protecting the optical fibers in the cable. Optical fibers are typically incased in a protective tube where the tube

is filled with a gel. The gel serves as mechanical protection, prevent moisture ingress, and can include hydrogen scavenging materials. A suitable gel for use at 300°C could not be identified and an industrialized alternative was not fully attained.

Despite the problems encountered and the lower long-term operating temperature of the cable solution, the project showed success in developing a complete cable solution for a large portion of the geothermal wells in operation today. Further work to obtain the higher long-term temperature goal of the project can be achieved based on the knowledge gained in the current project.

This project is significant for many reasons including the new materials science, manufacturing technology, energy independence, and jobs created and will create.

Table of Contents

1.0 Project Introduction

All downhole sensors and tools require wire and fiber cable to operate. Therefore wire and cable are critical to the success of any Enhanced Geothermal System. Unfortunately, there are currently no wire or fiber cable constructions capable of surviving long-term deployment in a geothermal well (240-325°C) or supercritical (374°C) reservoir. This has severely hindered engineered reservoir creation, management and utilization, as hot zones and cool water intrusions cannot be understood over time. The lack of a wire and fiber cable solution is a fundamental limitation to the viability of this energy source.

Prysmian Group SA planned to develop a complete, multi-purpose cable solution for long-term deployment in geothermal wells/reservoirs that can be used with the widest variety of sensors.

This cable incorporates specialty optical fibers, with specific glass chemistry and high temperature and pressure protective coatings for data communication and distributed temperature and pressure sensing high-temperature insulated wire conductors.

The cable design originally proposed is depicted in Figure 1 below.

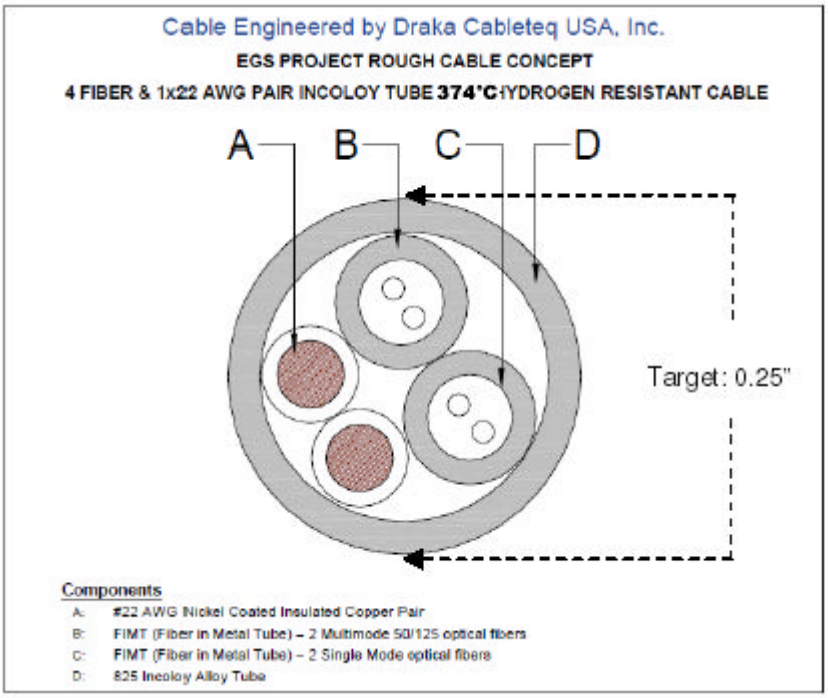

Figure 1: Proposed Design

Prysmian Group envisions this will become a standard platform for further geothermal sensor and tool development. The proposed cable will be able to provide continuous pressure and temperature sensing throughout the wellbore as well as offering multiple means of communicating between downhole tools and the surface.

The glass fiber portion of the cable will incorporate both step-index single-mode and graded-index multimode optical fibers made from a novel hydrogen-insensitive glass. These two fiber types will allow transmission of a wide variety of data and be used as sensors for temperature and pressure. The insulated electrical conductor portion of the cable will provide power and communications with downhole tools.

1.1 PROJECT OBJECTIVES

The overall project objective was to manufacture a cable that can perform without serious degradation with the follow criteria:

- At temperatures up to 374°C
- At pressures up to 220 bar
- In a hydrogen-rich environment
- For the life of the well (> 5 years)

The objectives achieved during this project are:

- Optical fiber coating chemistry for stability at high temperature (300°C or higher) and pressure (220 bar or higher);
- Glass chemistry for hydrogen-insensitive optical fiber;
- Electrical conductor insulation for both stability at high temperatures and manufacturability; and
- Cable packaging for mechanical and thermal protection of glass and electrical components during installation and deployment.

The work required for each of these advances was divided into discrete phases and tasks. It has been Prysmian's intent to bring each component of the cable (i.e. hydrogen-insensitive fiber, high temperature conductors, etc.) into commercial production at the conclusion of each phase – without waiting for project completion – so EGS developers can benefit from each new development as quickly as possible.

1.2 PROJECT ACCOMPLISHMENTS

Following is a short summary of the accomplishments for each phase of the project. A full summary of the project work is described in Part II of this report.

1.2.1 Phase 1 Optical Fiber Developments:

a. Selected optimal 300°C rated optical fiber coating.
b. Identified candidate MMF and SMF chemistries for optimized H2 tolerance.
c. Modeled H2 affects in SMF and MMF over a large range of temperatures.
d. Demonstrated that carbon coating not effective above 200°C.
e. Optimized macro and micro bending performance of both the MMF and SMF
f. Completed all originally planned H2 exposure testing at Sandia Labs.

1.2.2 Phase 2 Cable Developments:

a. Developed 300°C rated insulated conductor.
b. Developed base cable design for 300°C
c. Developed means of reinforcing cable needed for unsupported cables in wells depths greater than 8000 feet and temperatures up to 300°C.
d. Developed "non-conventional gel" -- novel means of supporting Fiber in Metal Tube (FIMT) at 300°C.
e. Manufactured all electric cable rated for 400°C.
f. Granted patent for "non-conventional gel"
g. Manufactured backup cable design to reduce risk of further downhole trial scheduling slips.

1.2.3 Phase 3: Cable Testing and Validation Accomplishments

a. Short-term test: Cable installed in the well to a depth of 6210 feet. Measurements were performed using DTS systems for multimode and singlemode fibers, as well as single point temperature/pressure measurements from the transducer and attenuation measurements with an Optical Time Domain Reflectometer (OTDR). All measurement systems performed as designed.
b. Medium-term test: Cable condition was evaluated and DTS measurements were performed after cable was installed in well for one month. All cable elements performed as designed.
c. Long-term test: Cable condition was evaluated and DTS measurements were performed after cable was installed in well for four months and again after 10 months. Cable was removed from well and condition was evaluated. All cable elements were operational.

2.0 PHASE I – Development of Hydrogen-Insensitive High-Temperature Fiber

2.1. INTRODUCTION

Optical glass fiber can be used for both data communication and distributed sensing in geothermal wells. Optical data transmission is ideal for communication with downhole sensors, tools and equipment, while fiber sensing allows real-time monitoring of the temperature and pressure along the entire length of the well. A temperature profile obtained during, or shortly after drilling provides important information on the well's potential use for power generation, while long-term monitoring of temperature and pressure is essential to maximize well production. Thus, the use of optical fiber is a key technology. However, there is currently no fiber that can survive the well environment long enough to be of practical use.

To understand Prysmian's proposed fiber solution, some background on distributed sensing is required: Distributed optical fiber sensing is a technique that allows spatially continuous measurement of temperature, pressure or both, along the length of an optical fiber. Distributed sensors take advantage of the fact that the scattering characteristics of light traveling down an optical fiber vary with the temperature and pressure along the length. In a distributed sensor,

both the input and backscattered light are guided along the sensing fiber so all measurement interpretation can be performed at a single location, typically above ground in an accessible location. Distributed fibers sensors can be graded index multimode fibers (GIMMF) or step index single mode fibers. Most distributed temperature sensor (DTS) systems measure Raman backscattered light. The intensity of Raman backscattered light is much lower than the initial laser pulse, so in order to get enough backscattered signal to make a temperature measurement it is important that the fiber core is as large as possible. Multimode fiber has a larger core size and therefore a larger backscatter signal than singlemode fiber. Therefore most distributed temperature sensors operate in the 900-1150nm wavelength window and use GIMMF. By comparison most distributed pressure sensors measure Brillouin backscatter signal along the fiber length. These systems operate in the 1550nm telecommunications wavelength window and are based on step-index singlemode fibers. Prysmian's solution will contain both GIMMF and singlemode fibers to optimize the cable's ability to sense both temperature and pressure.

To understand Prysmian's approach to the fiber core and cladding chemistry, some background on fiber failure is required: One major barrier preventing the widespread deployment of optical fiber in downhole environments is the rapid environmental degradation of the fiber. In environments such as a geothermal (or petrochemical) well, temperatures and pressures are significantly higher than found in traditional fiber applications such as telecommunications. The downhole environment also contains chemicals that react negatively with the glass in the fiber. Hydrogen, in particular, creates severe attenuation increase (signal loss) via a phenomenon called hydrogen darkening. To date, the practical use of fiber optics in downhole applications has been limited due to the fiber-darkening effects of hydrogen, with the fiber often failing within days or even hours after installation.

Fiber darkening often referred to as hydrogen induced loss (HIL) is known to result from one or both of the following mechanisms:

- Solubility of hydrogen within the silica network
- Reaction of hydrogen with the silica network resulting in the formation of OH groups (SiOH, SiOOH, GeOH, etc.)

In addition to hydrogen induced loss, geothermal (EGS) wells have additional unique environmental attributes. EGS wells have sharp, non-linear temperature gradients caused by "hot rocks" in geothermally active areas and cold water intrusions. This make distributed optical fiber sensing much more advantageous as single point sensors are likely to miss these critical transition areas. However, these sharp temperature gradients can cause glass fiber to weaken and shatter. Similarly, water under pressure in the well can easily penetrate most current fiber coating technologies, thereby destroying the glass. A unique and robust fiber and cable design is therefore critical to withstand these temperature transitions.

2.2 TASK 1: FIBER DEVELOPMENT

The technical challenge is to develop specialty optical fibers having specific hydrogen-insensitive glass chemistry and high temperature and pressure protective coating, both in step-index SMF and graded index MMF designs. In this view, Prysmian involved capabilities of Plasma Chemical Vapor Deposition (PCVD) technology to manufacture preforms and fibers

with tightly control of glass composition and the refractive index profile. These fibers must allow transmission of a wide variety of data in the wavelengths of interest without serious degradation at temperatures up to 374°C and pressures up to 220 bar for the life of the well (> 5 years).

2.2.1 Glass-chemistry/drawing conditions to enhance hydrogen resistance

The first task requires the development of hydrogen-insensitive SMF and MMF fibers with appropriate glass composition for core and cladding and draw conditions. For this, it has been taken into account the main processes by which hydrogen impacts fiber attenuation.

Hydrogen induced losses (HIL) in optical fibers can result from solubility of hydrogen within the silica network and/or reaction of hydrogen with the silica network.

The first mechanism is related to the ability of small hydrogen molecules existing in the external environment to diffuse through the fiber glass part.

In conventional fiber applications, external hydrogen concentration is very small and this impact is always neglected, however in geothermal (or petrochemical) well environments it is not the case and the reversible losses due to the presence of hydrogen molecules in glass have to be taken into account as they can represent the main cause of attenuation fluctuations in the telecom window.

As shown in the Figure 2, it is a reversible process which directly follows the diffusion laws. Diffusion of hydrogen in glass mainly depends on temperature, but defects concentration in glass cladding can also have an impact by slowing down hydrogen diffusion.

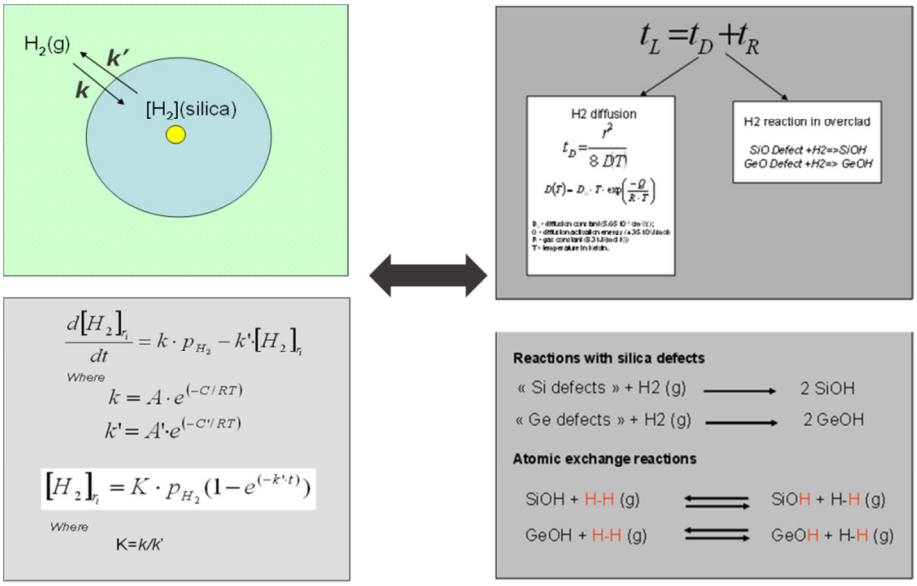

Figure 2: Schematic view of hydrogen diffusion process in optical fibers

Hydrogen molecules reaching the fiber core result in the apparition of totally reversible new absorption bands as represented in Figure 3 and Table 1 below. In the 700nm-1600nm window, the most intense bands are the 1240nm peak corresponding to the first overtone of fundamental

hydrogen vibration band and the tail of the fundamental vibration of hydrogen in silica above 1600nm.

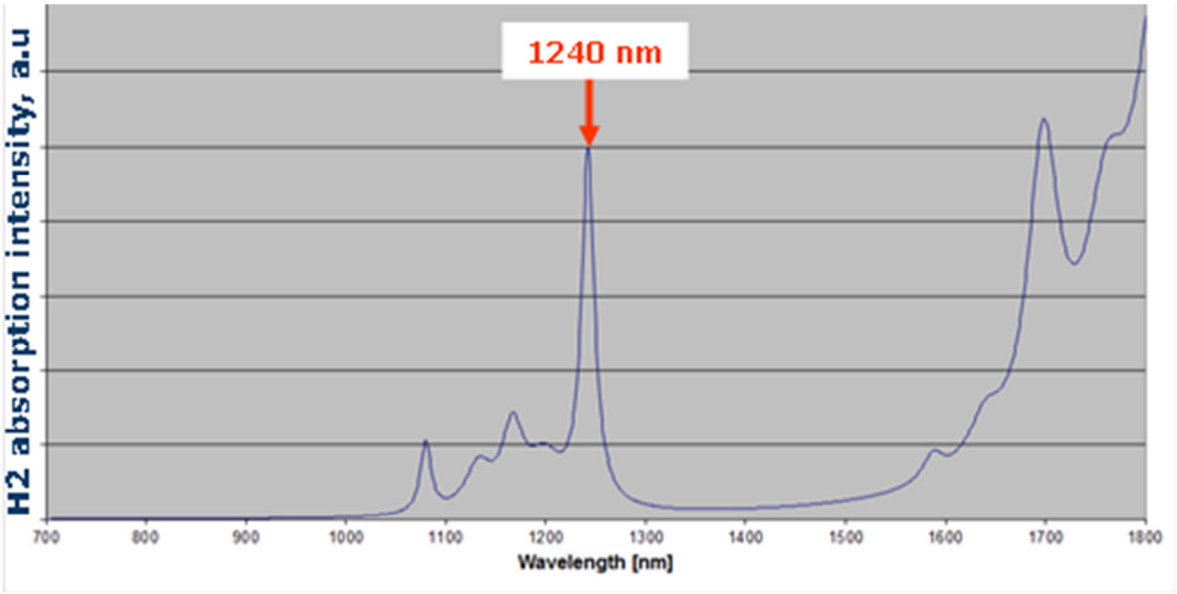

Figure 3: Main reversible molecular hydrogen bands in the telecom window

Wavelength (nm)	Normalized intensity relative to 1240 nm	Comments
2240	100	
2140	38	
2040	20	
1880	19	Fundamental H2 vibrations in silica
1700	1.4	
1630	0.5	
1590	0.3	
1240	**1**	Most intense first overtone of H2 vibrations in silica in the 1000-1700 nm window
1200	0.3	
1170	0.4	First overtone of H2 vibrations in silica
1130	0.2	
1080	0.3	

Table 1: Absorption peaks of hydrogen in silica fiber together with their relative intensity versus 1240nm band

The intensity of bands due to hydrogen molecules depends on its external concentration (partial hydrogen pressure) and temperature.

The general trend is that at a given temperature, the hydrogen band intensities increase with external hydrogen partial pressure, while at a given hydrogen partial pressure, band intensities decrease with increasing external temperature.

Figure 4 underlines, through evolution of the 1240nm band intensity over time, the reversible process of hydrogen diffusion towards fiber at a given external hydrogen partial pressure together with the impact of temperature on hydrogen concentration in fiber core. The other bands related to hydrogen follow the 1240nm band evolution according to the relative intensities mentioned in Table 1.

The problem here is to be able to anticipate and control the effect of hydrogen ingression in glass in the wavelengths of interest according to temperature and external hydrogen partial pressure over time.

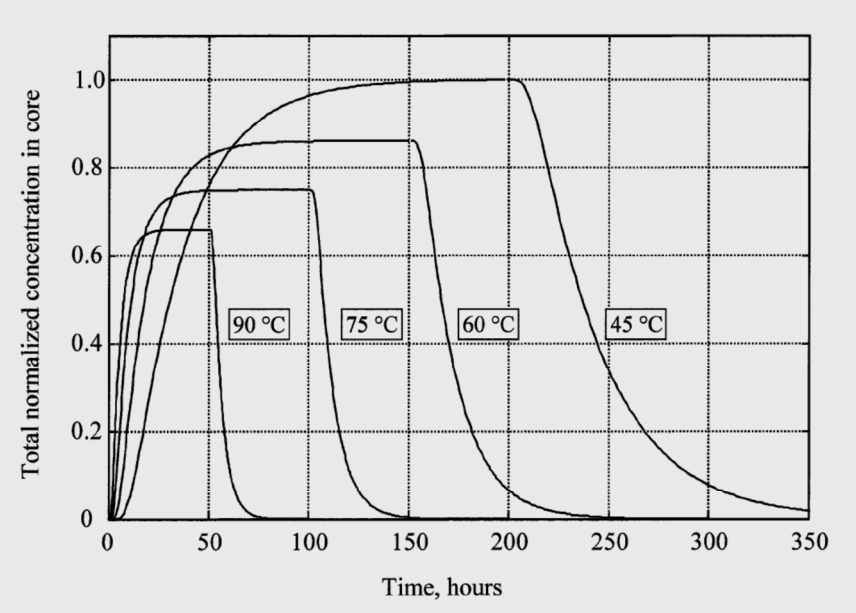

Figure 4: Reversible hydrogen diffusion process in fiber core through 1240nm band versus time at different temperatures for a given external partial pressure

Second mechanism is basically related to the reaction of hydrogen molecule with glass defects to form OH groups (SiOH, SiOOH, GeOH, etc.) and leading to irreversible HIL mostly in the 1350-1450nm area.

It has been well documented that the glass dopants have a strong influence on the reaction of hydrogen with glass defects and formation of OH species (Figure 5).

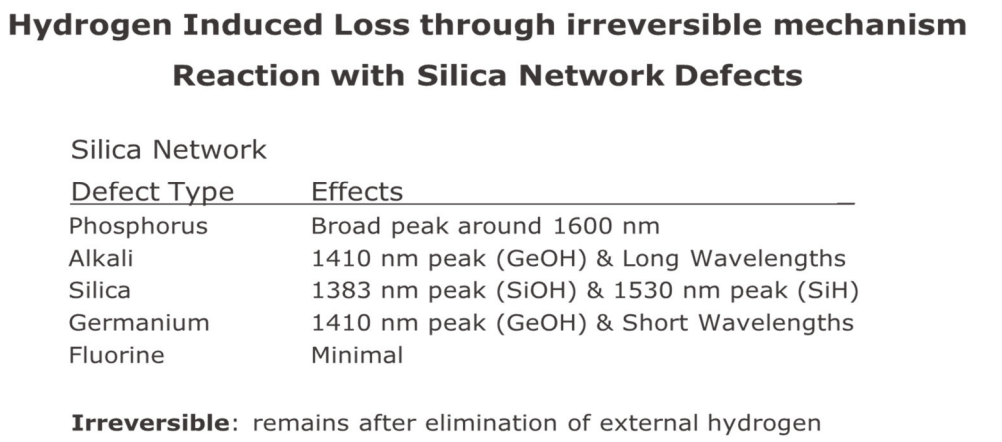

Figure 5: Effect of main core dopants on irreversible HIL

A common practice in the manufacture of optical fiber is to introduce germanium in the core to increase the refractive index. However, it has been found that glass doped mainly with germanium will lead to OH formation in hydrogen rich environments resulting in strong irreversible HIL. Other dopants such as phosphorus have also a negative influence on fiber hydrogen sensitivity.

Finally, manufacturing conditions also have a strong effect on the formation of OH species, especially the drawing conditions, which directly impact the number of silica point defects, and therefore the content of hydrogen-induced -OH groups.

In downhole environment, this mechanism is much more intense as the formation of -OH groups can result not only from the reactivity of hydrogen with point defects but also with weakened bonds of the SiO2-GeO2 glass. Notably at temperatures above 250°C, germanium-based glass network can give rise to new reactions with hydrogen creating severe attenuation increase and thus signal losses via a so-called “hydrogen darkening” effect. Figure 6 below shows the effect of hydrogen exposure at high temperature (300°C) on a standard germanium-doped singlemode fiber.

It strongly limits the practical use of fiber optics in harsh applications, with the fiber often failing within days or even hours after installation. Irreversible HIL is extremely dependent on the environmental conditions to which the fiber is exposed, in particular the temperature, hydrogen partial pressure and exposure time.

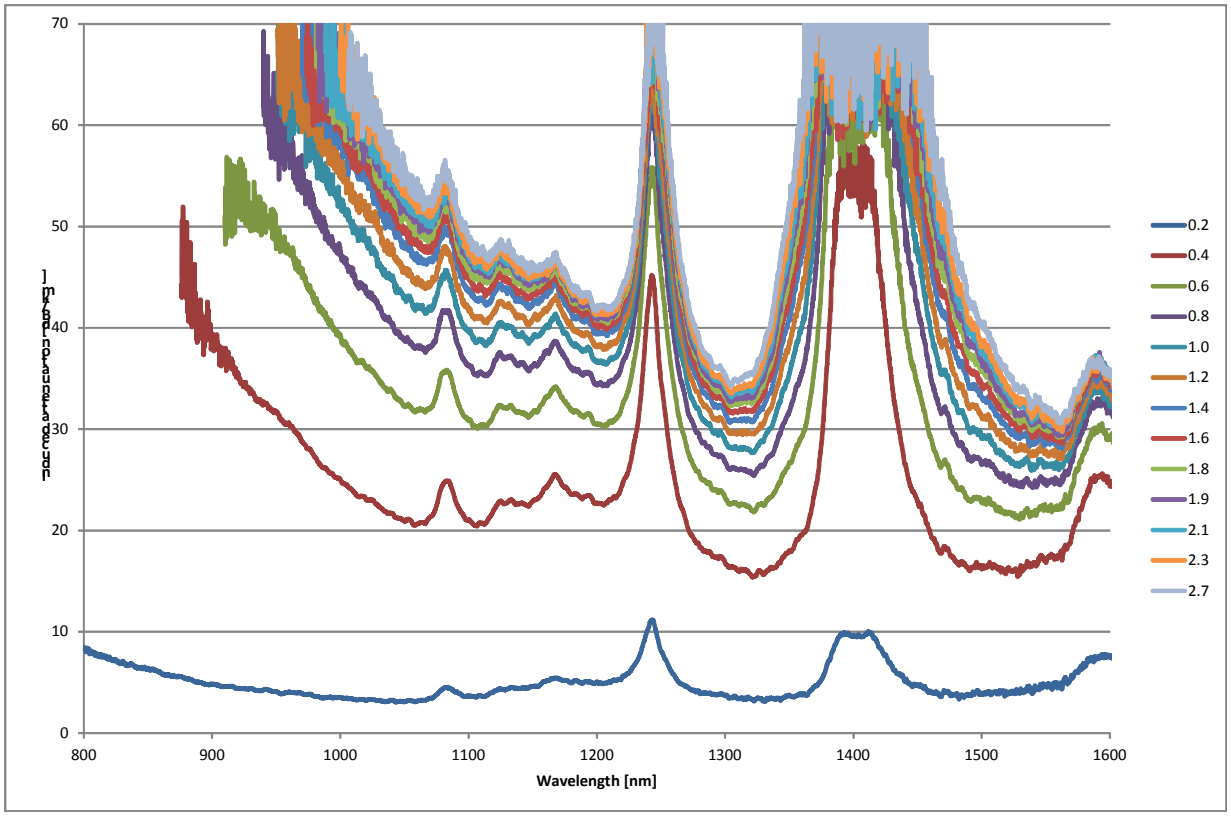

Figure 6: Irreversible HIL in GFOC conditions for a standard germanium doped single mode fiber according to time in hour (h) up to 2.7h

However, fluorine doping is known to actually help the hydrogen tolerance of glass and can be advantageously involved in the design of optical fibers in GFOC conditions.

In order to increase the hydrogen resistance of the fiber for GFOC application, the problem here is to limit or manage as much as possible the content of germanium in fiber core and take profit of capabilities of PCVD fiber manufacturing process in incorporating fluorine and finely control refractive index profiles.

2.2.2 Bandwidth and Optical Properties Optimization

An important parameter for the measurement resolution of a DTS system is the fiber bandwidth [MHz.km]. A relation of this parameter exists with length. To obtain enough measurement resolution in deep geothermal wells high bandwidth fibers are necessary. To fulfill these requirements a specification limit has been defined for this project for the fiber bandwidth, being at least 500 MHz.km in the 900 – 1100 nm range.

Step index multimode fibers have too low bandwidths (< 100 MHz.km). To fulfill above bandwidth specification graded index multimode profiles are necessary. The Prysmian Group has a lot of experience with producing high bandwidth multimode fibers with graded index profiles for DataCom applications (OM3, OM4 and OM4+).

Graded Index multimode core refractive index profiles are described with the parameter alpha (see Figure 7 and formula 7a & 7b). The bandwidth of a fiber relates with this alpha. A maximum bandwidth can be found at a certain alpha. Bandwidth is also dependent on the error with respect to the optimal alpha profile. Modeling shows an optimal alpha to obtain as high as possible bandwidths around 1.98. Error needs to be as small as possible to obtain as high as possible bandwidths.

Figure 7: Refractive index profiles with different alpha values.

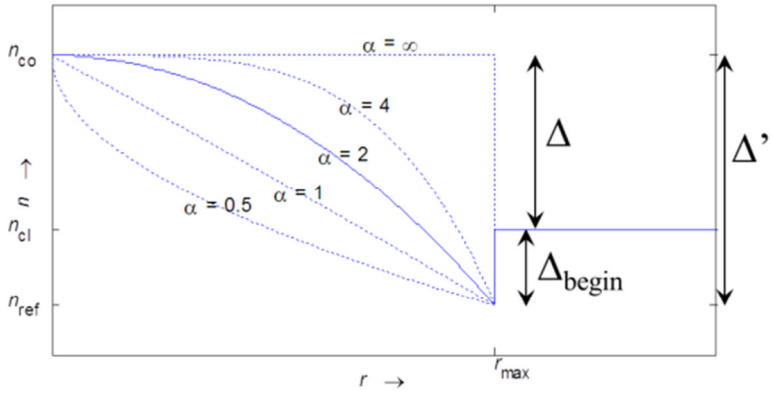

7a $$n_{\text{fit}}(r) = n_{\text{co}}\sqrt{1-2\Delta'\left(\frac{r}{r_{\max}}\right)^{\alpha}} \qquad \text{voor} \quad 0 \le r \le r_{\max}$$

7b $$\Delta' = \frac{n_{\text{co}}^2 - n_{\text{ref}}^2}{2n_{\text{co}}^2}$$

To obtain the correct alpha profile the refractive index profile is corrected with special refractive index correction programs. These programs have been developed for Germanium doped cores as used in DataCom applications. Building on the Prysmian Group's knowledge a refractive index correction program has been developed for Fluorine doped multimode fibers. Objective is to obtain bandwidths with Fluorine doped multimode fibers higher as 500 MHz.km over the 850 - 1300 nm range.

Results

The correction curve program has been changed to work with Fluorine doped profiles instead of Germanium doped profiles. To check this newly developed Correction Curve program for Fluorine doped Depressed Graded Index multimode fibers several core rods with different target alpha profiles have been produced. Refractive index profiles of these core rods have been measured along the length of the core rod. Alpha value and error value have been defined per position (see Figure 8).

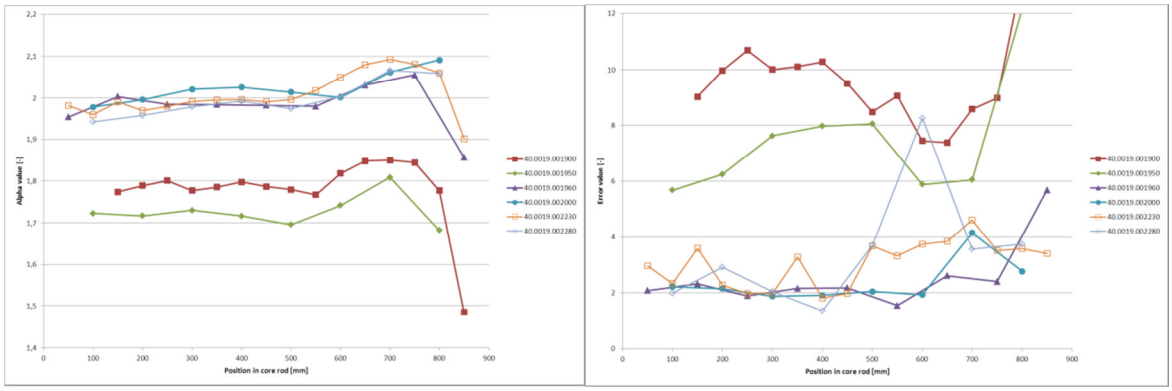

Figure 8: Alpha and error values along the length of several core rods.

The optimal part lies in the middle of the core rod. In this part a stable alpha region exists. Average alpha and error have been calculated for this region (see Table 2). Visible in below table is that the developed correction curve program was able to correct the profile step by step from a value of 1.79 with an high error to an optimal alpha of 1.98 with a small error in this alpha.

Core rod ID	Alpha	Error in alpha
40.0019.001900	1.788	9.87
40.0019.001950	1.715	7.47
40.0019.001960	1.984	2.07
40.0019.002000	2.014	1.99
40.0019.002230	1.989	2.42
40.0019.002280	1.976	2.50

Table 2: Average alpha and error

The core rods presented in Table 2 have been drawn with PolyImide (PI) coating. From every core rod a fiber from the middle part of the core rod has been measured on bandwidth at 850 and 1300 nm (see Table 3).

Fiber ID	Alpha	Error in alpha	Bandwidth at 850 nm [MHz.km]	Bandwidth at 1300 nm [MHz.km]
40.0019.001950.030	1.715	7.47	273	294
40.0019.001900.010	1.788	9.87	326	309
40.0019.001960.040	1.984	2.07	2786	2150
40.0019.002000.020	2.014	1.99	1369	1303
40.0019.002230.010	1.989	2.42	985	1011
40.0019.002280.100	1.976	2.50	1549	1277

Table 3: Bandwidth measurements at 850 and 1300 nm

Putting these values in a ‘butterfly’ diagram (bandwidth at 850 nm against bandwidth at 1300 nm, see Figure 9) shows interesting results. While bandwidths of Germanium doped fibers are very wavelength dependent, the bandwidths of Fluorine doped fibers seems to be wavelength independent.

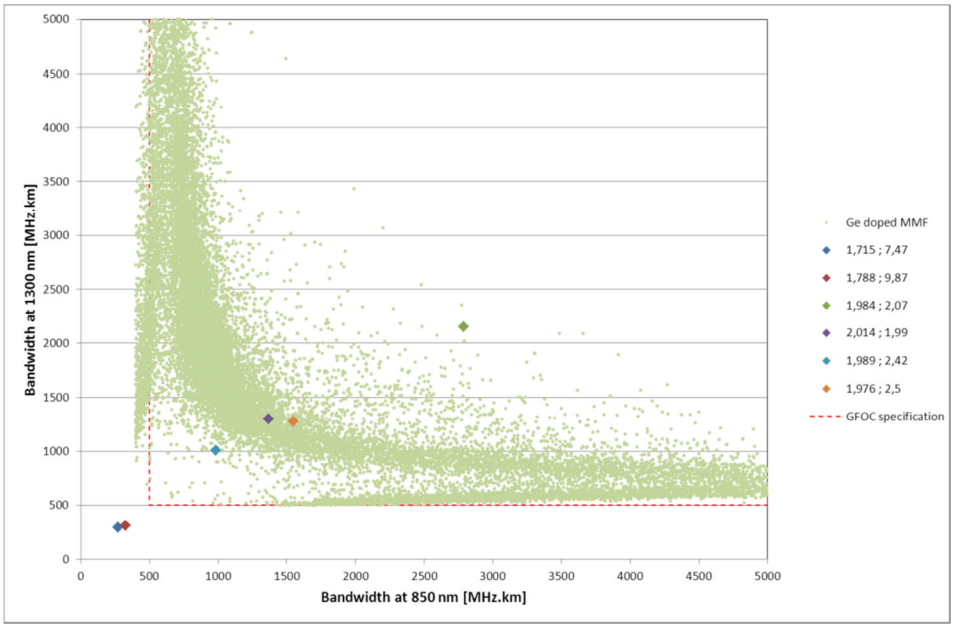

Figure 9: Bandwidth diagram for Fluorine doped depressed MMF's with different alpha's and error in alpha's.

Bandwidth Conclusions

With help of the newly developed correction curve program for Fluorine doped depressed multimode fibers, bandwidth can be optimized to values above 500 MHz.km in the 900 – 1100 nm range. Fluorine doped depressed multimode fiber bandwidths are wavelength independent when compared with Germanium doped 'Datacom' multimode fibers. Measuring bandwidth at 850 and 1300 nm (standard wavelengths for 'Datacom') is enough to check bandwidths in the 900 – 1100 nm range.

Bend loss optimization

Polyimide coated fibers are known for attenuation problems, especially in the cabling process. These problems are caused by the hardness and smaller diameter of the PolyImide coating, when compared with standard Acrylate coated fibers. Both are detrimental for micro bending induced attenuation, the main cause for the higher attenuation of PolyImide coated fibers.

Prysmian Group's experience with TeleCom fibers is that some changes in the glass refractive index profile, like a trench in the cladding, can be positive for micro and macro bending induced attenuation. Using such kind of glass refractive index profiles in combination with Polyimide coating can minimize attenuation increases in cabling process.

SMF Results

Experience with Telecom fibers is that adding a trench to single mode fibers improves both micro and macro bending results. With modeling proper profiles have been defined for depressed single mode fibers. For this a trade-off has to be made between the leakage losses of the fundamental mode (target leakage losses contribution below 0.005 dB/km at 1550nm) and the leakage losses of highest order modes (keep the cable cut-off wavelength as low as possible). Based on this trade-off 4 profiles have been defined (see Table 4 and Figure 10). Three of these

were based on an overcladding process, resulting in a larger preform diameter. The last one was a copy of the first profile, but based on bare core rod drawing process.

Profile ID	R1 [mm]	R2 [mm]	R3 [mm]	R4 [mm]	Δn_1 [10^{-3}]	Δn_2 [10^{-3}]	Δn_3 [10^{-3}]	Δn_4 [10^{-3}]	OC diam [mm]
PSCF_SMF_T1	0.97	2.33	3.66	10.0	-0.3	-5.6	-10.7	-5.7	30.5
PSCF_SMF_T2	1.43	3.01	5.58	10.0	-0.3	-5.3	-13.3	-5.3	39.5
PSCF_SMF_T3	1.25	3.13	5.18	10.0	-0.3	-6.1	-14.3	-6.1	39.3
PSCF_SMF_T1b	0.80	1.91	3.00	8.2	-0.3	-5.6	-10.7	-5.7	25.0

Table 4: Proposed depressed SMF profiles with trench from modeling (on preform)

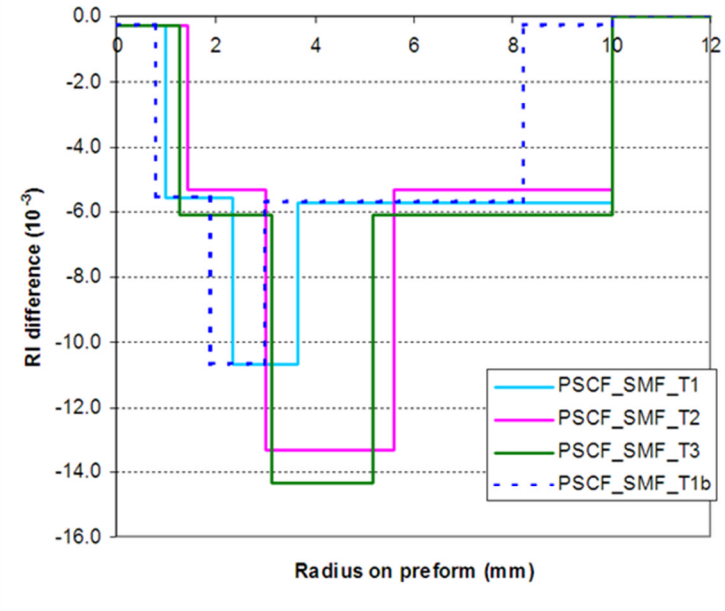

Figure 10: Proposed depressed SMF profiles with trench from modeling (on preform)

Because bare core rod drawing is the chosen process for PolyImide coating drawing it has been decided to start with profile PSCF_SMF_T1b. Several core rods have been produced with this profile and drawn with High Temperature Acrylate coating and PolyImide coating. Fiber results were far from the desired G.652 specifications. Based on these fiber results a new profile PSCF_SMF_T4 has been proposed (see Table 5). Fibers produced with this profile were inside G.652 specification.

Profile ID (on core rod)	R1 [mm]	R2 [mm]	R3 [mm]	R4 [mm]	Δn_1 [10^{-3}]	Δn_2 [10^{-3}]	Δn_3 [10^{-3}]	Δn_4 [10^{-3}]	OC diam [mm]
PSCF_SMF_T4	0.852	2.188	3.108	10.0	-0.30	-5.57	-10.80	-5.57	25.9

Profile ID (on fiber)	R1 [µm]	R2 [µm]	R3 [µm]	R4 [µm]	Δn_1 [10^{-3}]	Δn_2 [10^{-3}]	Δn_3 [10^{-3}]	Δn_4 [10^{-3}]	diam [µm]
PSCF_SMF_T4	4.11	10.56	15.00	48.26	0.00	-5.27	-10.50	-5.27	125

Table 5: Proposed depressed SMF profiles with trench from modeling (on core rod & fiber)

Fibers produced with profile PSCF_SMF_T4 have been used for comparison with depressed single mode without trench. The chosen fibers for micro and macro bending comparison are presented in Table 6. For this comparison the use of High Temperature Acrylate coating has been to make the measurements in both tests easier. Fibers are chosen to have comparable MAC values (MAC value is the ratio of Mode Field Diameter (MFD)to cutoff wavelength of a fiber at 1310 nm) and coating diameters. These parameters are known to influence micro and macro bending results. Because no comparable MAC values could be found in the available fibers, 2 trench assisted fibers have been selected, with MAC values surrounding the MAC value of the selected non trench assisted fiber. Due to measurement issues an extra fibers has been added for the micro bending measurement.

Fiber ID	MFD @ 1550 nm [µm]	Cut-off [nm]	MAC	Prim. diam. [µm]	Sec. diam. [µm]	Type
10.0019.023270.020	10.25	1316	7.79	190	243	Trench
10.0019.021680.030	9.89	1355	7.30	193	245	Trench
10.0019.019230.030	9.39	1249	7.52	188	244	No trench
10.0019.011490.020	10.07	1269	7.94	185	234	No trench

Table 6: Fiber parameters chosen fibers for micro and macro bending comparison

Micro bending

Mechanical stress might cause local discontinuities into a fiber. This is called micro bending and will cause additional attenuation.

In IEC TR 62221 four methods to determine micro bending are described. In the Prysmian Group the Fixed Diameter Drum method is used. Prysmian Group's experience is that this method is the most reliable method for measuring micro bending.

In this method 400 m of fiber is winded on a Ø=500 mm drum with sandpaper (grade 40 µm). Winding force is 3.5 N. Attenuation is measured with and without bending with a PK2500. The difference between both measurements is the micro bending induced attenuation. In Figure 11 the results for the 3 measured fibers are presented.

The better micro bending results of both fibers with a trench are clearly visible. At 1550 nm micro bending resistivity is a factor 5 better for the trench assisted fibers.

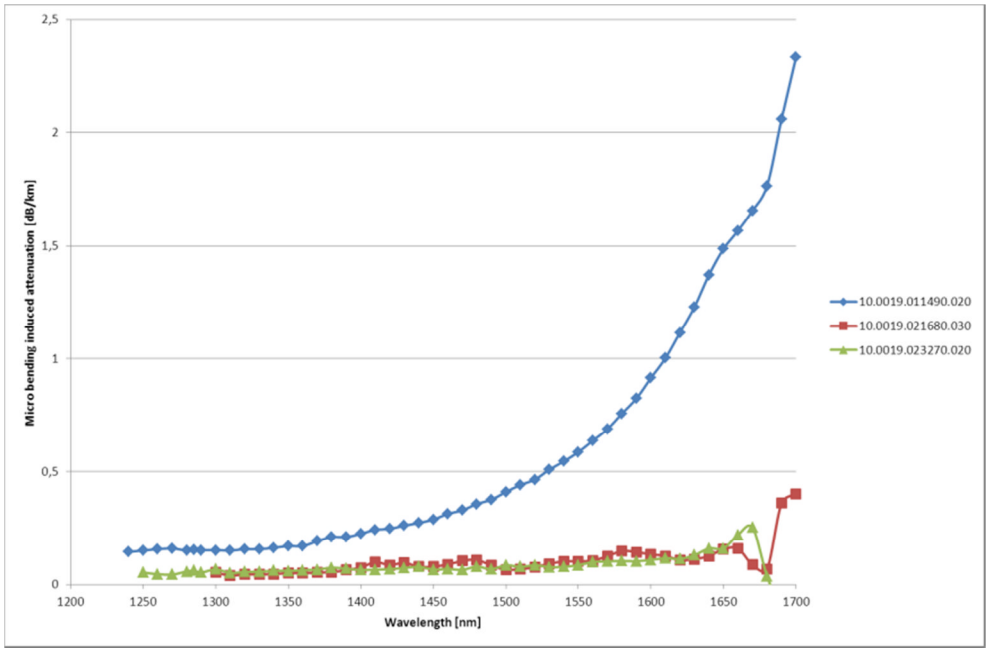

Figure 11: Micro bending results of trench and non-trench assisted depressed SMF's

Macro bending

Prysmian Group uses for macro bending measurements the own developed ball bearing test. This test has been developed for G.657 fibers (bend insensitive fibers), and uses smaller bend radii (necessary for G.657) as in standard IEC 60793-1-47 described.

With this method a fiber of a certain length will be placed between 2 rows of ball bearings, both rows will be pushed together, to obtain a certain amount of 180° bends. Attenuation will be measured with and without introduced macro bending for several ball bearing radii (6, 7.5, 9, 11, 15 and 20 mm). In this way the bending induced attenuation is determined.

In Figure 12 the macro bending results of the 3 selected fibers are presented.

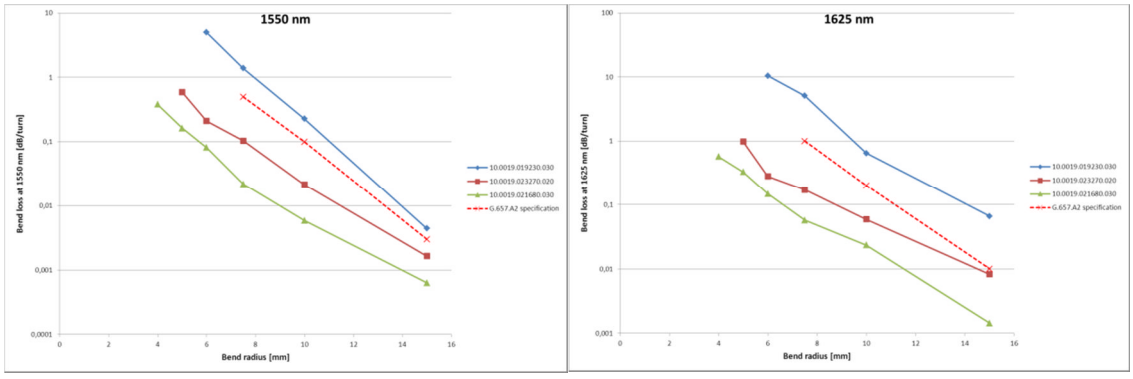

Figure 12: Macro bending induced attenuation at 1550 and 1625 nm for trench and non trench assisted depressed single mode fibers with High Temperature Acrylate coating

The better macro bending results of both fibers with a trench are clearly visible. Both trench assisted fibers fulfill the G.657.A2 specification for bend loss. The fiber without trench is outside this specification.

MMF results

Like with the depressed single mode profile a trench has been added to the depressed multimode profile. Modeling group has proposed 2 profiles (see Table 7 and Figure 13).

Profile ID	a [µm]	R1 [µm]	R2 [µm]	R3 [µm]	W1 [µm]	W2 [µm]	Δn_1 [10^{-3}]	$\Delta n_{cladding}$ [10^{-3}]	Δn_{trench} [10^{-3}]
DGIMMF_T401	25.0	26.5	31.5	45	1.5	5.0	-0.6	-16.4	-20.4
DGIMMF_T402	24.5	26.0	31.0	45	1.5	5.0	-0.6	-15.9	-19.9

Table 7: Depressed GIMM profiles with trench

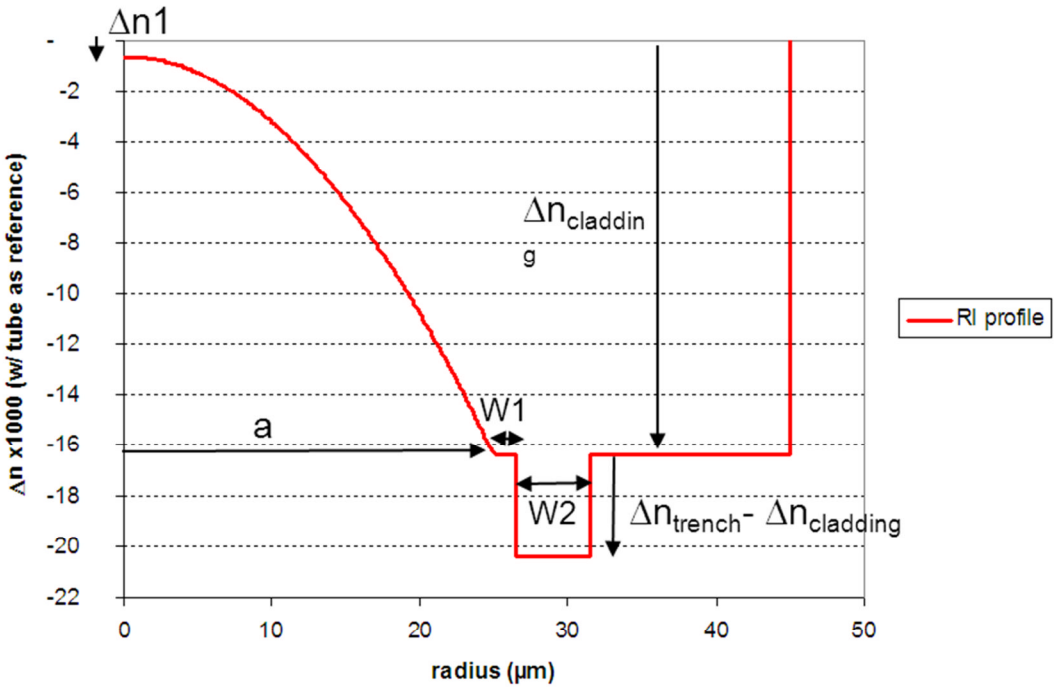

Figure 13: Example depressed GIMM profile with trench (DGIMMF_T401)

Several core rods have been produced with both profiles. DGIMMF_T401 profile gave the best fiber characteristics (core diameter, bandwidth etc.), so has been used for the bend loss comparison with the non-trench assisted depressed multimode fibers. For these tests two as much as possible comparable fibers have been selected (similar NA and coating characteristics, see Table 8).

Fiber ID	Profile	NA	Core diam. [µm]	Clad. diam. [µm]	Coat. diam. [µm]
40.0019.002840.020	No trench	0.214	50.7	125.3	240.5
40.0019.002850.020	With trench	0.214	49.1	125.0	244.5

Table 8: Fiber parameters chosen fibers for micro and macro bending comparison

A big difference exists between bending measurements of single and multimode fibers. Because of the multimode character of multimode fibers the launch conditions used in the tests are very important for the test results. These launch conditions have been standardized.

In the bending tests a launch fiber is used, with nominal core size and NA. With a mandrel the launch conditions are tuned until they fulfill the specifications set with-in the IEC specifications (Encircled Flux masks used date from 26-12-2008, see Figure 14).

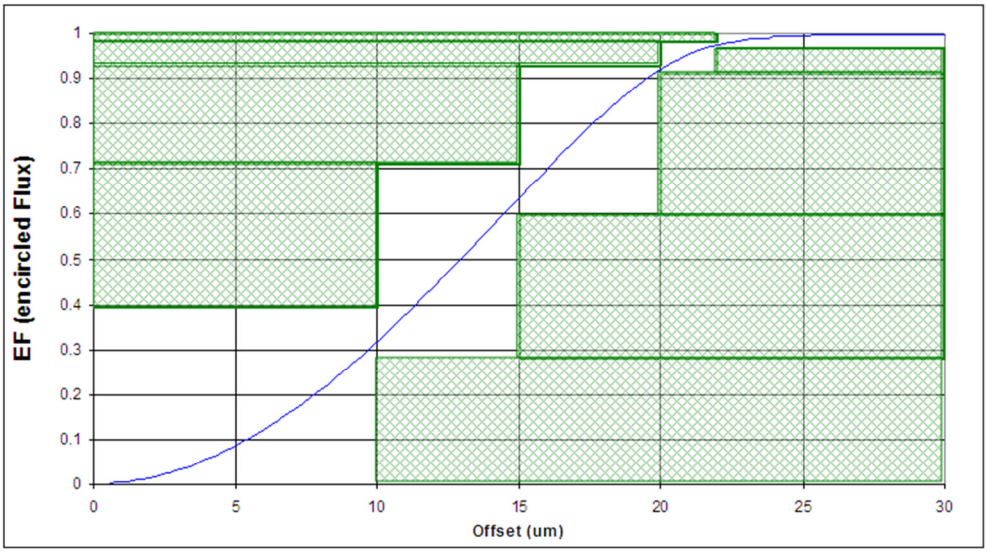

Figure 14: Encircled Flux curve

Above a typical Encircled Flux curve is plotted, the green areas are the Encircled Flux mask. A tested fiber should not have an Encircled Flux which is within the green area. These launch conditions are checked with a launch analyzer at 850 nm (MPX-1 from Arden Photonics) before the bending measurement.

When the correct mandrel setting to obtain the correct launch conditions is determined, the launch fiber is spliced to the fiber under test. Hereafter the bend-loss measurement for multimode fibers is started.

Micro bending

Mechanical stress might cause local discontinuities into a fiber. This is called micro bending and will cause additional attenuation. In multimode fibers micro bending also influences the mode coupling negative.

The test method used is similar to the one for single mode, except the above described launch conditions. Results are presented in Figure 15.

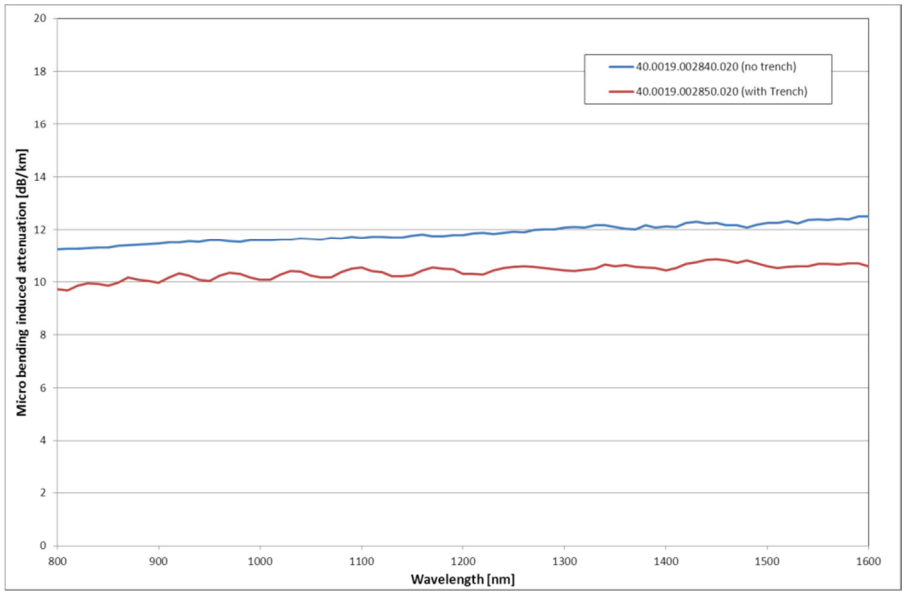

Figure 15: Micro bending results trench and non-trench assisted depressed multimode fibers

As can be observed in Figure 15 a slight improvement in micro bending sensitivity is possible with trench-assisted depressed multimode fibers. The improvement however is not that big when compared with single mode fibers.

Macro bending

For multimode basically the same measurement technique is used as for single mode. Differences are the controlled launching "Encircled flux“ and the number of turns.

Macro bending on multimode fibers is measured with 2 turns on a 5 mm, 7.5 mm, 10 mm and a 15 mm radius spool (IEC/PAS 62614 Ed 1.0). Only 2 full turns (or in case of the ball bearing test 4 half turns) are used, because most of the bend loss in multimode fiber takes place in these first 2 bends. In this respect macro bending is different in multimode as in single mode fibers. In single mode fibers the bend loss is proportional with the amount of turns. This is not the case for multimode fibers.

Macro bending results of the selected fibers are presented in Figure 16.

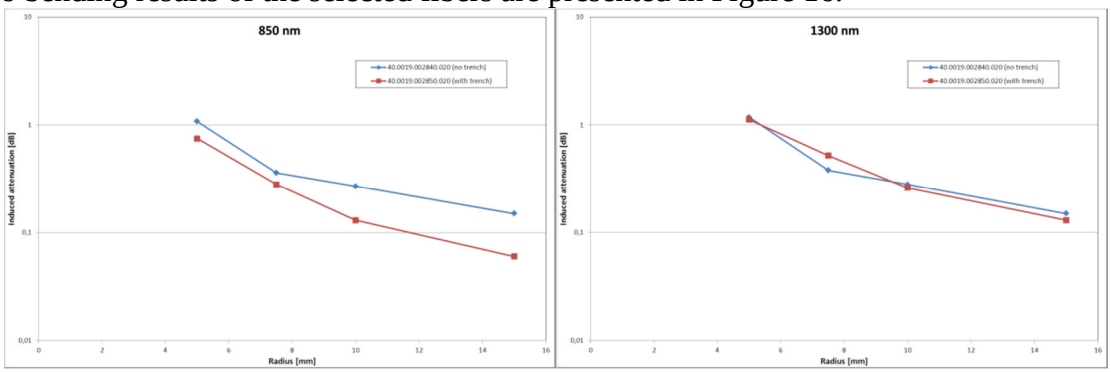

Figure 16: Macro bending (4 half bends) results depressed GIMM fibers with and without trench at 850 and 1300 nm (PK2500, ball bearing test).

At 850 nm a slight improvement in macro bending sensitivity is visible for the trench assisted multimode fiber. At 1300 nm no difference is visible.

Results

Results presented in this investigation clearly show the positive effect of a trench on the micro and macro bending for single mode fibers. No clear or a slight improvement is visible for multimode fibers.

2.2.3 Drawing with High Temperature Coating

Using the information found on optical fiber preform design in the previous sections, Prysmian drew fibers with high temperature coatings to establish a reference point in the development of new fiber coatings reported starting with Section 2.3. This investigation was included and is reported on in Section 2.3

2.2.4 Conclusions

To increase the hydrogen resistance of the fiber for GFOC application, the content of germanium in the fiber core must be limited or managed as much as possible. The capabilities of the PCVD fiber manufacturing process will facilitate the incorporation of Fluorine and help finely control refractive index profiles.

Bandwidth for the GFOC fiber can be optimized to values above 500 MHz.km in the 900 – 1100 nm range with the help of the newly developed correction curve program for Fluorine doped depressed multimode fibers. Fluorine doped depressed multimode fiber bandwidths are wavelength independent when compared with Germanium doped ‘Datacom’ multimode fibers. Measuring bandwidth at 850 and 1300 nm (standard wavelengths for ‘Datacom’) is enough to check bandwidths in the 900 – 1100 nm range.

Finally, it is clear from the experiments that there is a positive effect of a trench on the micro and macro bending for single mode fibers. No clear or a slight improvement is visible for multimode fibers.

With this information, a novel class of fibers that includes unique hydrogen-insensitive glass chemistry and a defined refractive index profile for proper bandwidth has been developed for the GFOC application.

2.3 TASK 2: HIGH TEMPERATURE POLYMERS FOR OPTICAL FIBER COATINGS

Optical fiber has a very high tensile strength when it is drawn from the preform boule. However, it is extremely susceptible to surface damage from dirt, glass shards, or other bits with a hardness at or above that of pure silica. Also, environmental moisture immediately begins to degrade the strength of the silica fiber by attacking the silicon-oxygen bonds, converting them to -Si-OH. When silica is under strain, moisture catalyzes rapid flaw growth through this mechanism.

This sensitivity to the environment was recognized straight from the initial experiments with optical fiber. Thus from the beginning some form of coating was applied to the glass when the fiber was drawn. The first coatings literally were sprayed-on varnishes applied by hand from the can during draw. In a short time, coatings were being formulated to give some protection against lateral stress while at the same time offering some toughness against abrasion. Some of these early coatings were compounded from oil-extended thermoplastics (hot melts) and some from acrylated oligomers and monomers that in a mix could be cured with actinic irradiation. Over the first few years of commercialization of optical fiber, the radiation-curable approach won out.

Today's optical fiber coatings typically comprise a soft primary coating on the glass and a harder and tougher secondary coating on top of the primary to give the fiber handle-ability and resistance to abrasion. These modern coatings are ideal for most applications in long-lines deployment, metropolitan installations and for fiber to the curb or to the business. However, some special applications require an optical fiber toughened against high temperature, and these standard UV-curable coatings cannot be exposed more than a few days to temperatures higher than about 100°C.

UV-curable coatings are available that can withstand months-to-years at temperatures as high as 150°C and even up to 170°C for several weeks. Thermally-cured silicones may be used for exposures up to 260°C (but silicones bring handling problems and are not widely accepted). For geothermal energy well conditions, a coating system is needed that can withstand temperatures as high as 374°C in a normal air atmosphere. Nothing is known for this application short of metal coatings, which are extremely expensive, reduce the glass tensile strength, and are difficult to work with on fiber in splicing and terminating. Phase I/Task 2 targets a new material that will most closely meet the requirements for GFOC designs.

Deliverable

The deliverable is a new high temperature polymeric material that is practical for applying and curing during the fiber optic draw process and that can enable the optical fiber to function properly (as designed) in temperatures up to 374°C for as long as possible, up to 5 years being desired.

Candidate Materials

It was not a goal of this project to invent a new polymeric material for high temperature applications. High temperature thermoplastics and thermosets are plentiful, and new materials are regularly introduced that are stable at very high temperatures. Poly(ether-ether ketones) and polyphenylene sulfides are examples of classes of engineering thermoplastics that withstand temperatures approaching the range of interest.

Many high temperature polymeric materials are not suitable for optical fiber coatings unless complicated and expensive fiber draw and material application equipment designs are developed, witness the above engineering thermoplastics. Since the goal of the Geothermal Optical Fiber Cable project is a viable commercial product, this approach was not considered. Coating application at optical fiber draw speeds limits the range of material candidates to those that can be applied as liquids having a viscosity in the range of perhaps 1000 centipoise to 25,000 centipoise.

The parameters set for investigating materials for high temperature coatings eliminate all known 100 percent solids materials, UV-curable and thermally-curable. Materials soluble in a reasonably safe solvent provide the preferred path to a new high temperature coating.

Tetramer Technologies LLC

Tetramer Technologies was formed in 2001 as a faculty-driven start-up company commercializing high value research activities pursued at Clemson University. The company currently employs 20 people- 10 PhD, 6 Masters, and 4 BS level in an incubator facility located in Pendleton, SC 29670. Their business model is to focus on developing specialty polymeric or oligomeric materials with high value molecular architecture in close research and development relationships with downstream customers.

Tetramer has developed three major technology platforms:

- Perfluorocyclobutyl (PFCB) and polyimide polymer materials for integrated optics, fuel cell membranes, gas separation membranes, high temperature optical fiber coatings, nanocrystal encapsulation and fluoropolymer adhesion promoters.
- Biorenewable materials such as proprietary lactide and unsaturated vegetable oils into industrial products.
- Piezopolymers involving proprietary polyvinylidene fluoride and other poleable polymer nanocomposites.

Tetramer Technologies was chosen as a partner for the development of a new high temperature fiber coating because of their experience with the PFCB and polyimide chemistries. The company has considerable expertise in building molecular structures for specific properties, and they formed the core of the material research group investigating new materials for optical fiber coatings under Prysmian Group leadership.

2.3.1 Synthesis of New High Temperature Materials

Existing coating materials for fiber optic applications above 200°C and up to 300°C are limited to polyimides. These are typically applied as solutions of polyamic acid in dimethyl sulfoxide or in n-methyl pyrrolidinone. After application to fiber, the solvent is driven off and the polyamic acid exposed to temperatures up to 500°C for a few seconds, converting the amic acid to imide and expelling H_2O as the byproduct. At the start of the project, available polyimide coatings were limited to a few days at 300°C before thermal degradation resulted in excessive attenuation in the transmission properties. Another disadvantage of existing polyimide coatings is that the polymer is insoluble as applied to optical fiber and must be stripped from the glass fiber by boiling, concentrated sulfuric acid or by a flame. This disadvantage is not a stopper, but it would be useful to have a high temperature coating that is removable by solvents or mechanical means.

PFCB

Tetramer Technologies has commercialized the PFCB for its unique properties as a membrane filter and as an optical conductor. Examples of structures utilizing PFCB are shown in Figure 17.

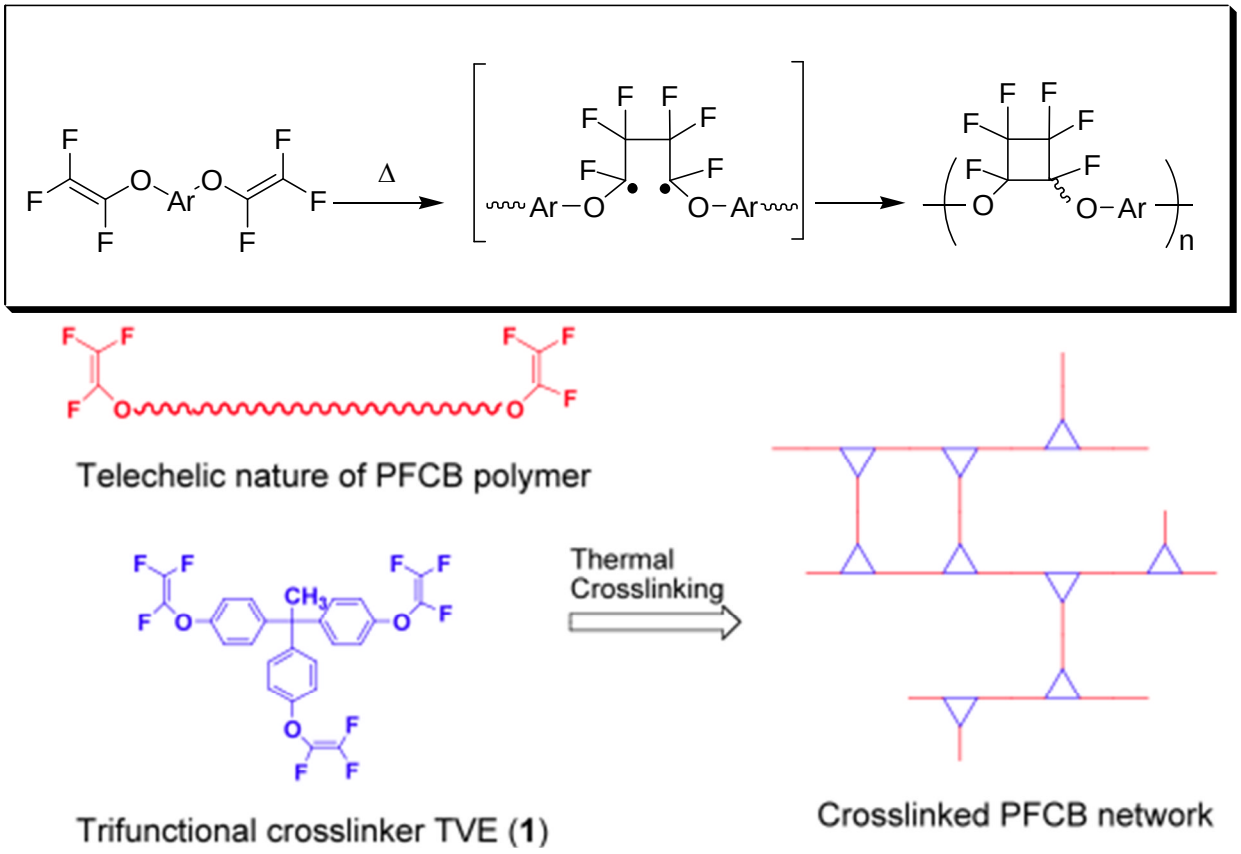

Figure 17: An example of a poly(fluorocyclobutane) structure is at top. Below is an example of how the PFCB polymer can be thermally crosslinked if desired for a greater resistance to high temperature.

PFCB polymer is soluble in polar solvents such as cyclopentanone. This is a relatively low-boiling point and effective solvent, so solutions of 25 percent solids by weight can be applied and the solvent driven off at practical fiber draw speeds. Even if crosslinked on the fiber, the PFCB can be swelled and removed by strong polar solvents such as cyclopentanone, cyclohexanone, or even acetone.

Soluble Polyimides

Tetramer worked with polyimides, already converted from the polyamic acid before application to fiber, functionalized to make the polyimide soluble in polar solvents. Several examples tested are shown in Figure 18. These materials can be put into solution at up to 15 weight percent solids, applied to optical fiber, and the solvent driven off to leave a polyimide coating that can be

removed from the fiber again using polar solvents. The drawback is that the soluble functionality could reduce the thermal stability of the coatings.

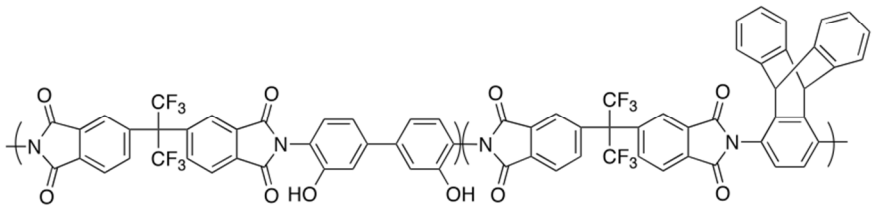

THT1000 copolyimide

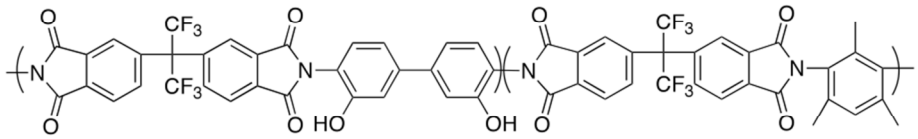

THT2000 copolyimide

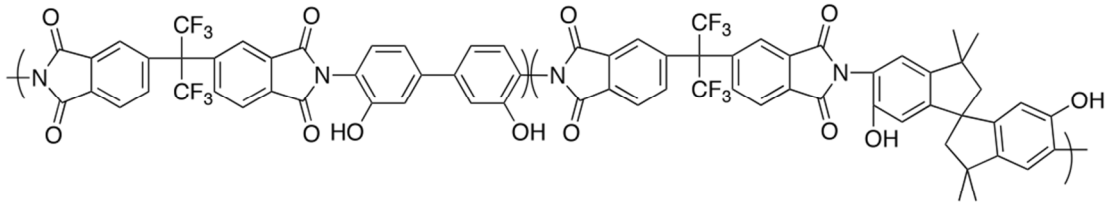

THT3000 copolyimide

Figure 18: Examples of soluble PIe structures examined as fiber coatings.

Strippable Poly(benzodioxanes)

This class of material is known to have excellent thermal stability at high temperatures and can also be applied from solution with no further reaction on the fiber. Thus they would be easily strippable with strong polar solvents. An example of a poly(benzodioxane) is shown in Figure 19.

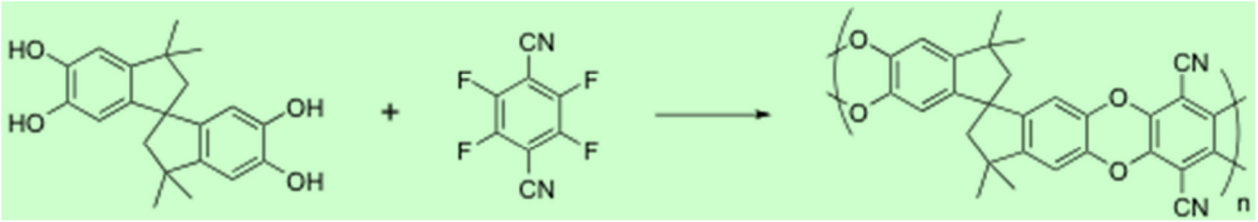

Figure 19: Example of a strippable (polar solvent) poly(benzodioxane) THT 6000A.

Strippable Poly(phenylenes)

Poly(phenylenes) comprise another class of molecular structures known to have a high thermal stability. The THT11 series of candidate materials from Tetramer are in this class of material. They are soluble and undergo no thermal reaction after application to fiber, so they would also be strippable by the appropriate solvent. Figure 20 shows the basic structures of the THT11 poly(phenylene) and a fluorinated version THT11F, illustrating the basic Diels-Alder reaction to obtain the molecule from available precursors.

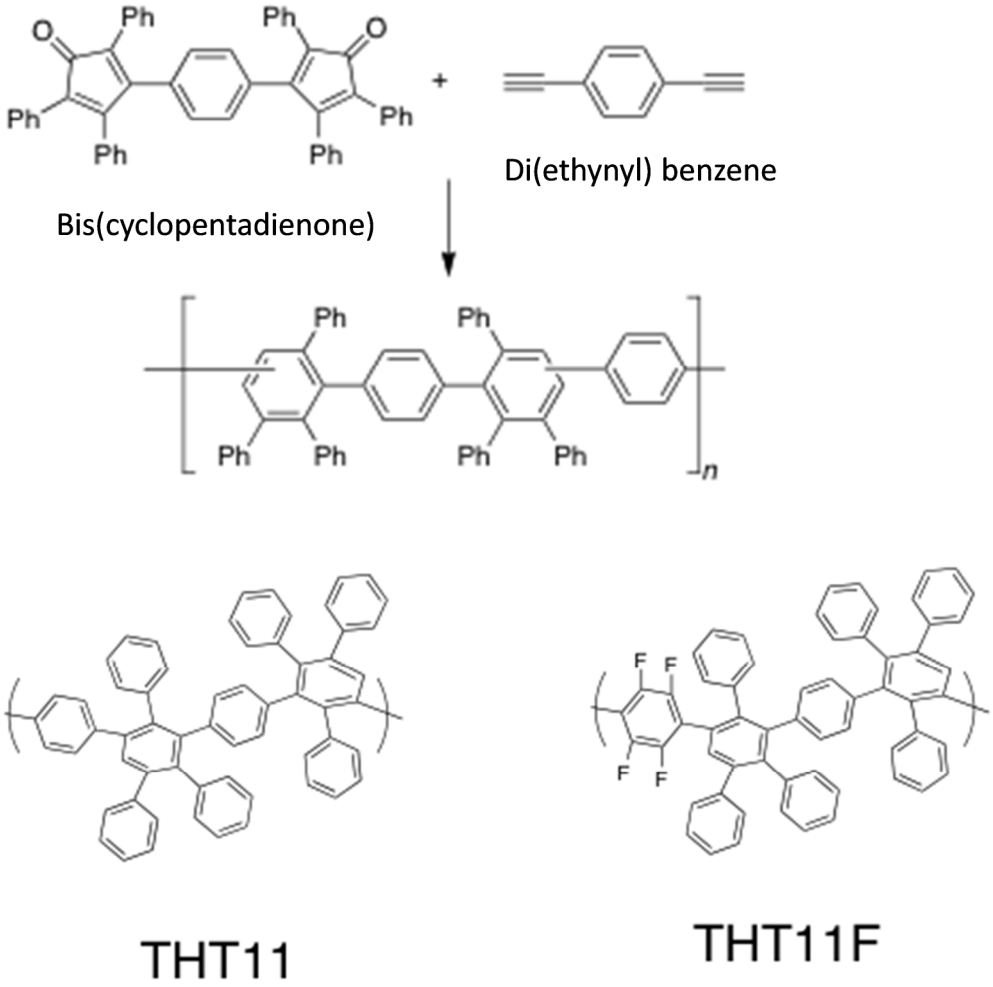

Figure 20: Obtaining the poly(phenylene) from precursor molecules, and the two types of poly(phenylene) examined in the project.

Insoluble Polyimides

If soluble materials prove to have less than the desired thermal stability as a fiber coating, Tetramer would investigate new polyamic acid precursors that would be converted to polyimide on fiber following solution application. These would be based on new building blocks for polyamic acids designed for improved thermal stability.

Currently there are several companies commercializing polyimides suitable for optical fiber applications. The basic building blocks are known, although the suppliers do not offer their formulation details. Some of these molecular chemistries are shown in Figure 21. Tetramer will investigate some new molecular approaches shown in Figure 22, molecules they believe may be superior to those on the market today.

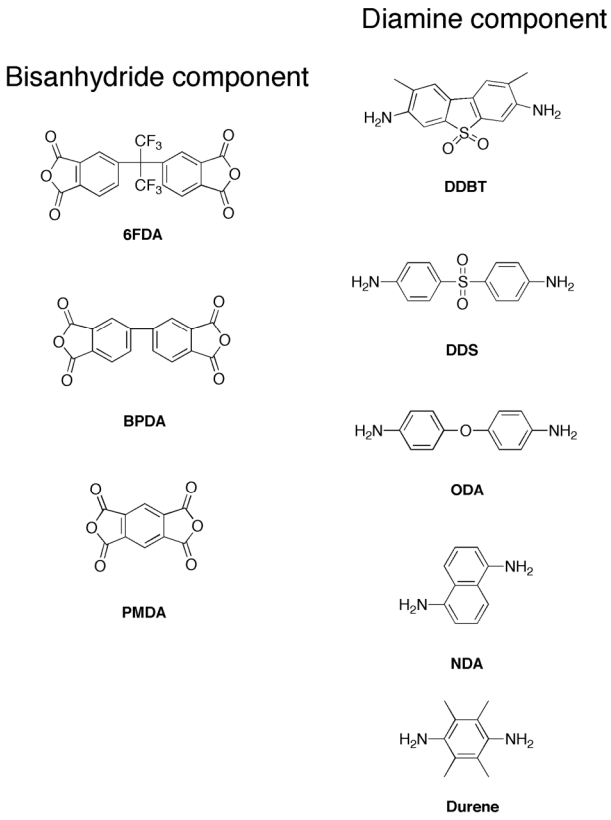

Figure 21: Components used in commercially available polyamic acid precursors to PI coatings for optical fiber.

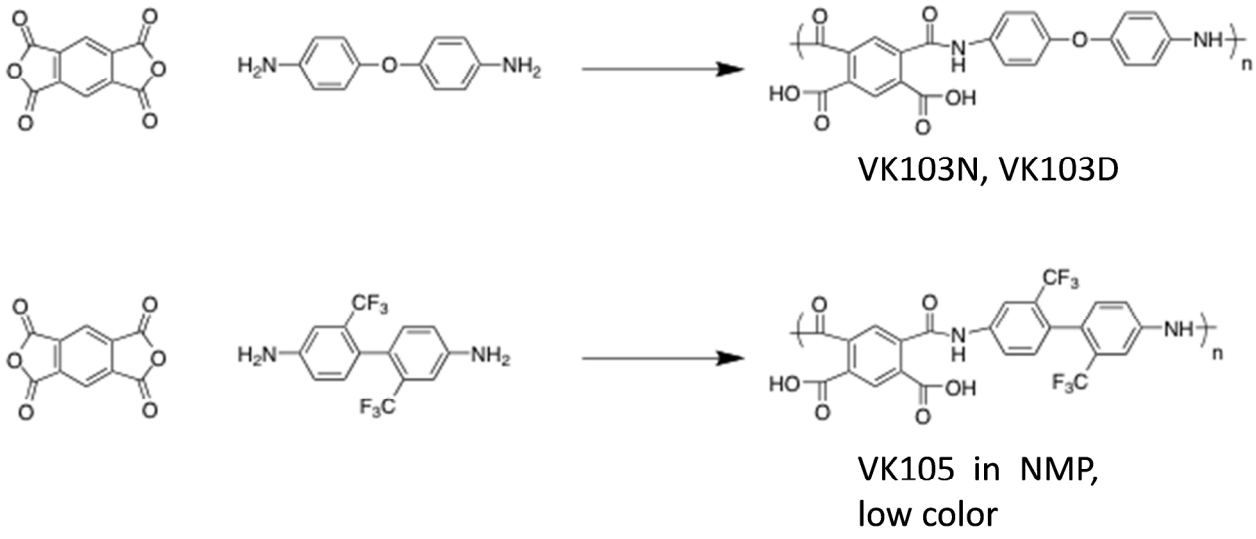

Figure 22: "Standard" PI precursor, above, and new fluorinated precursor designed for optical fiber.

Poly(benzoxazole)

There is potential for polyimides carrying hydroxyl groups to rearrange at high temperature (typically greater than 350°C, or above the glass transition temperature of the polyimide precursor) to form a class of compounds called benzoxazoles. Benzoxazoles are known to have very good stability at high temperatures. An example of a poly(benzoxazole) to be studied is shown in Figure 23, illustrating the condensation thermal rearrangement reaction.

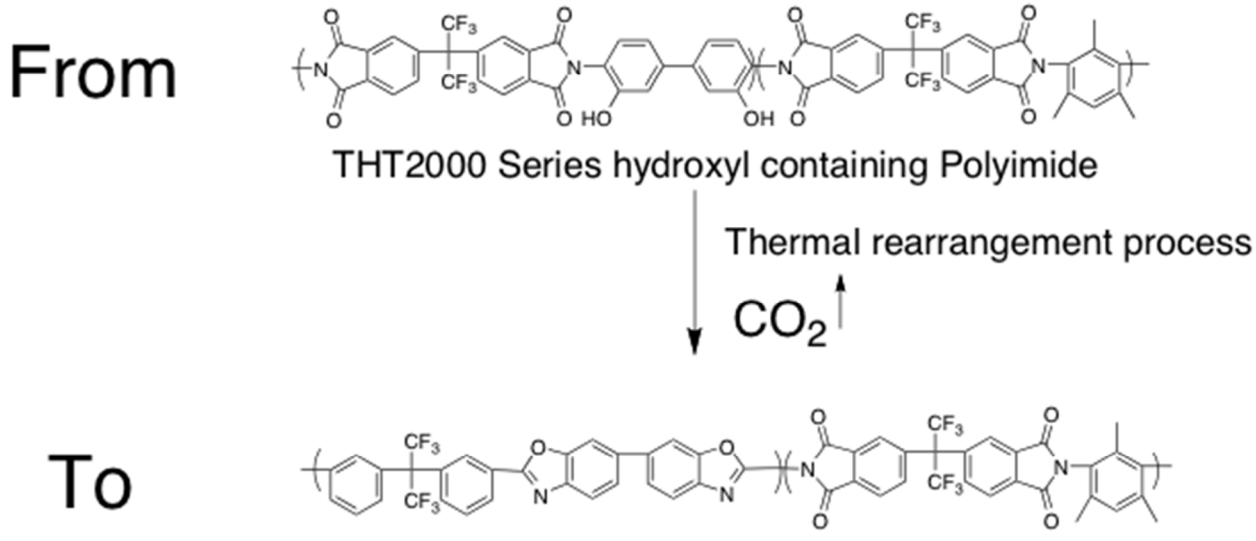

Figure 23: Thermal rearrangement of a hydroxyl-containing PI molecular segment to form a benzoxazole, based on the THT2000 series of high temperature compounds from Tetramer.

2.3.2 Preliminary Screening of New Materials

Methodology: TGA Method I

An accelerated thermal aging technique was needed in order to evaluate the various coating candidate materials. This would involve aging films of the candidates at several high temperatures and monitor some metric related to thermal degradation over time, determining a rate of degradation at each temperature, and finally constructing some type of Arrhenius plot for the rate of degradation versus temperature. This would provide the basis for extrapolation to the long times expected at in-use temperatures in the range of 300°C to 400°C.

Manually handling films of candidate materials, weighing them periodically or measuring mechanical properties, lacks precision and introduces opportunity for uncertainty in the actual aging times at temperature, for contamination of samples, or for mistakes in measuring properties. Therefore it was decided to use a dynamic thermogravimetric approach and use weight loss as the metric for degradation. The candidate materials are neat, not mixtures of raw materials (as are standard acrylate coatings), and so thermal degradation is depolymerization that should be accompanied by some kind of regular weight loss that can be measured with precision via the TGA balance.

Over the course of the project, two techniques were applied using dynamic TGA. The first technique is based on the dynamic TGA protocol described by Stolov, Simoff and Li[1]. In it, thermogravimetric measurements of weight loss versus temperature were made on each of the materials in dried film form. A TA TGA Q500 instrument was used for all experiments. Temperature ramp runs were completed at several rates of temperature increase, e.g., 2°C/min., 5°C/min., 7°C/min. An example of the TGA data is shown in Figure 24. The figure shows an overlay of candidate THT2000A soluble polyimide, where the dashed line shows weight versus temperature for a specimen without any pretreatment, and the solid line shows the weight loss versus temperature for the material that has first been taken to 350°C under nitrogen and held for 30 minutes before running at 2°C/minute from room temperature to 800°C. The heating and holding at 350°C first drives off any residual solvent remaining in the film and converts the polyimide to the poly(benzoxazole). The weight change due to the molecular rearrangement is observed in the non-pretreated specimen occurring between 350°C and 400°C. The weight loss due to residual DMSO solvent is observed in the non-pretreated specimen at around 200°C.

[1] A. Stolov, D. Simoff, J. Li, "*Thermal Stability of Specialty Optical Fibers*", Journal of Lightwave Technology, vol. 26, (2008).

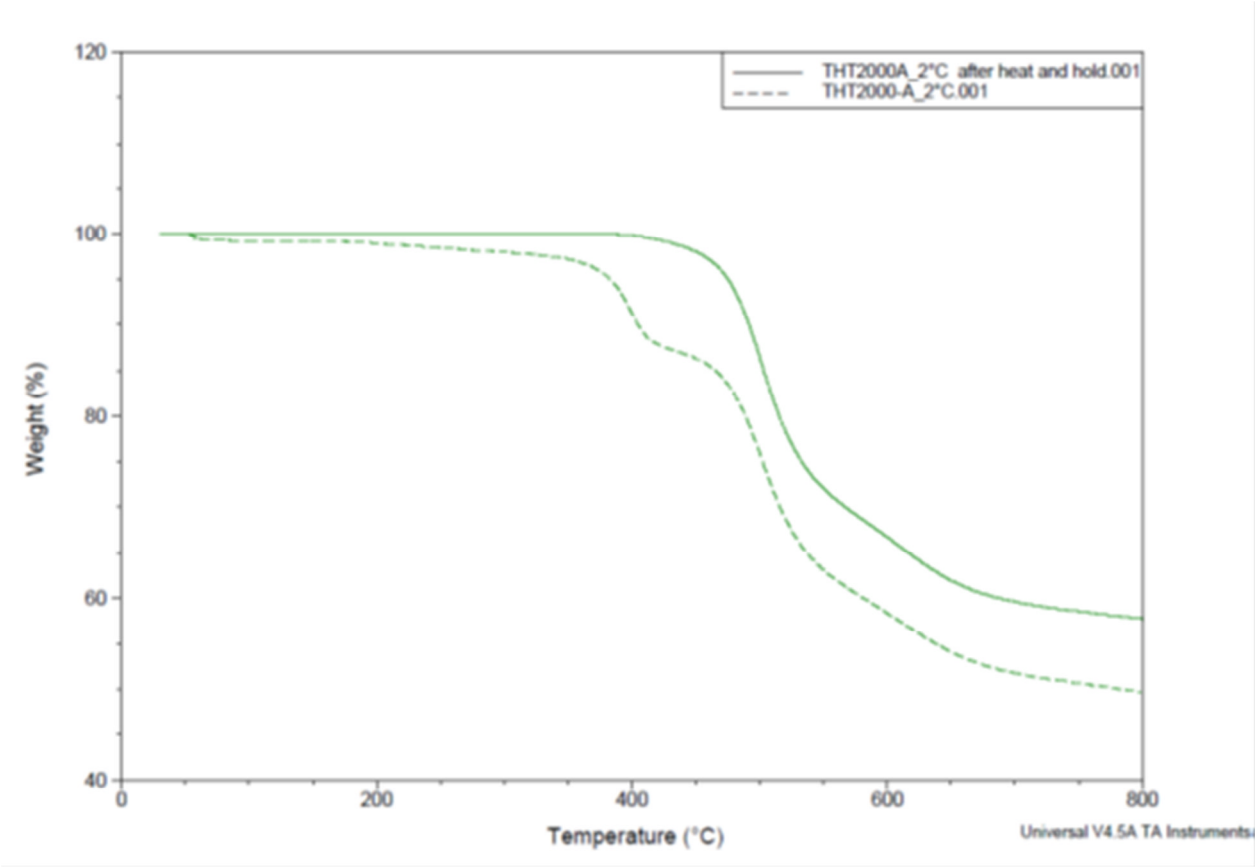

Figure 24: Example of a TGA run, here THT2000A soluble PI with and without heating to 350°C for 30 minutes prior to running from 25°C to 800°C under a nitrogen atmosphere.

For each TGA run of each coating material, the temperature T_{xi} corresponding to a weight loss of x_i% was determined for several values of x_i%, typically 1%, 2%, 3%, 5%, 7%, and 10% weight loss. The average temperature in going from a weight loss x_i % to a weight loss x_k % is $(T_{xk}-T_{xi})/2$ and the equivalent time τ at this average temperature T_{av} is $(T_{xk}-T_{xi})/\beta$, where β is the temperature ramp rate. This gives an equivalent steady state weight loss (x_k-x_i) for an equivalent time τ at a steady temperature T_{av}, and it does so without the inevitable early weight loss that would be experienced if an attempt were made to go directly to that steady state temperature and hold for a period. It is also a much faster method of getting the weight loss over time τ (that is, the rate of weight loss) at temperature T_{av} for a number of possible average temperatures. Then the log(time to failure) can be plotted versus $1/T_{av}$,K to obtain the activation energy via the Arrhenius relation

$$dt/dT=Aexp((-E)/RT) \ ,$$

and the slope of the relation used to project time to failure at temperatures in the range of interest. Figure 25 shows the Arrhenius plot for the example of THT2000A (converted to the benzoxazole) from TGA runs at 2°C/min, 5°C/min, 7°C/min and 10°C/min.

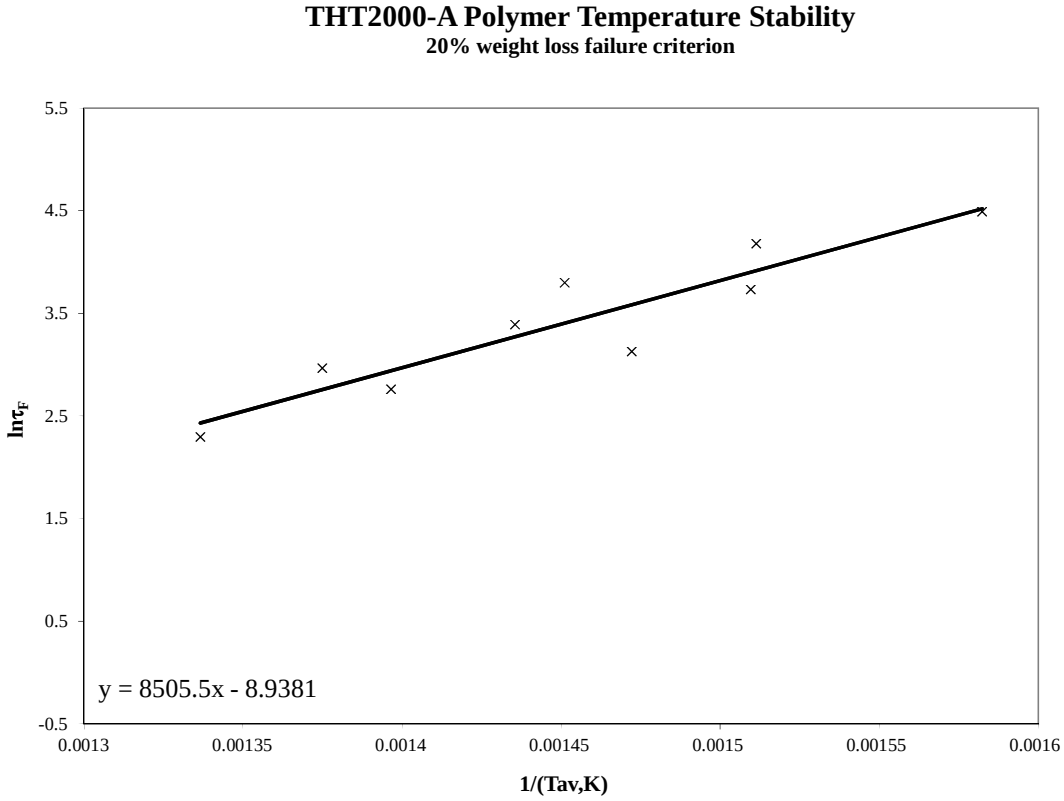

Figure 25: Arrhenius plot for time to failure versus temperature, example for THT2000A soluble PI pretreated to convert to the poly(benzoxazole) form.

Methodology: TGA Method II

Midway through the project, a modified version[2] of the dynamic TGA was developed (details in Section 4.3.1). By this procedure, samples of candidate material or of coated fiber are loaded into a platinum crucible to a sample weight of 6 to 8 milligrams, or between 25 and 30 milligrams of fiber (enough fiber to provide 6 to 8 milligrams coating). Less material had been found to give proportionately more scatter in the weight loss versus temperature measurements.

The goal is to estimate the kinetics of the overall degradation process, so it is important to eliminate extraneous factors from the data. These factors can include residual solvent, even nanogram levels, and incomplete imidization of the coating on the glass. The first step in a measurement was to take the loaded crucible to 300°C under dry nitrogen and hold for 15 minutes to drive off any last solvent and to complete any conversion to imide. Since imidization is a condensation reaction it involves weight loss that is not associated with degradation.

Next, the samples were cooled and then taken through a temperature ramp under dry air at 2°C per minute to 800°C. This end-temperature fully pyrolized all the organic material and left bare

[2] B. Overton, F. Gooijer, G. Krabshuis, "*An Optical fiber with Advanced Polyimide Coating*", Proceedings of the 61st International Wire and Cable Symposium, 2012.

silica in the case of coated fiber specimens. The weight of the silica was subtracted from the weight of the fiber sample after the 300°C pretreatment.

A dynamic TGA run per the method II described above is shown in Figure 26 for a non-soluble polyimide coating cured or converted from the polyamic acid form on fiber.

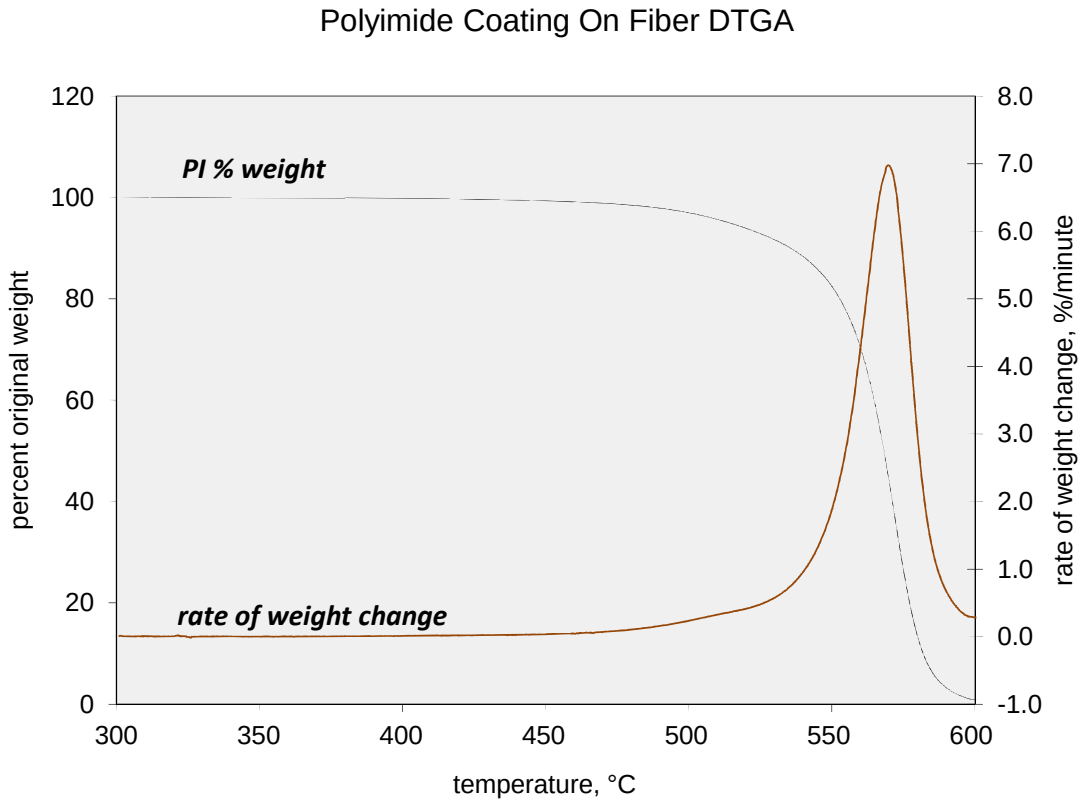

Figure 26: Example of a dynamic TGA run of a PI coating candidate cured on fiber. The weight of the glass is subtracted from the total weight of the sample after the 300°C pretreatment in order to obtain the original coating material weight.

In Figure 26, the running rate of weight change is shown. This is where this method differs from the Method I. The instantaneous rate of change of weight W at temperature T is a function of T, or dW/dt(T). It is approximated in Figure 26 by the running average of the change in weight over small intervals of temperature.

Applying the Arrhenius relation:

$$dW/dt=Aexp((-E)/RT)$$

the plot may be generated for *ln(dW/dt)* versus *1/(T,K)*, as shown in Figure 27. Then with the activation energy known the lifetime at temperatures of interest can be projected.

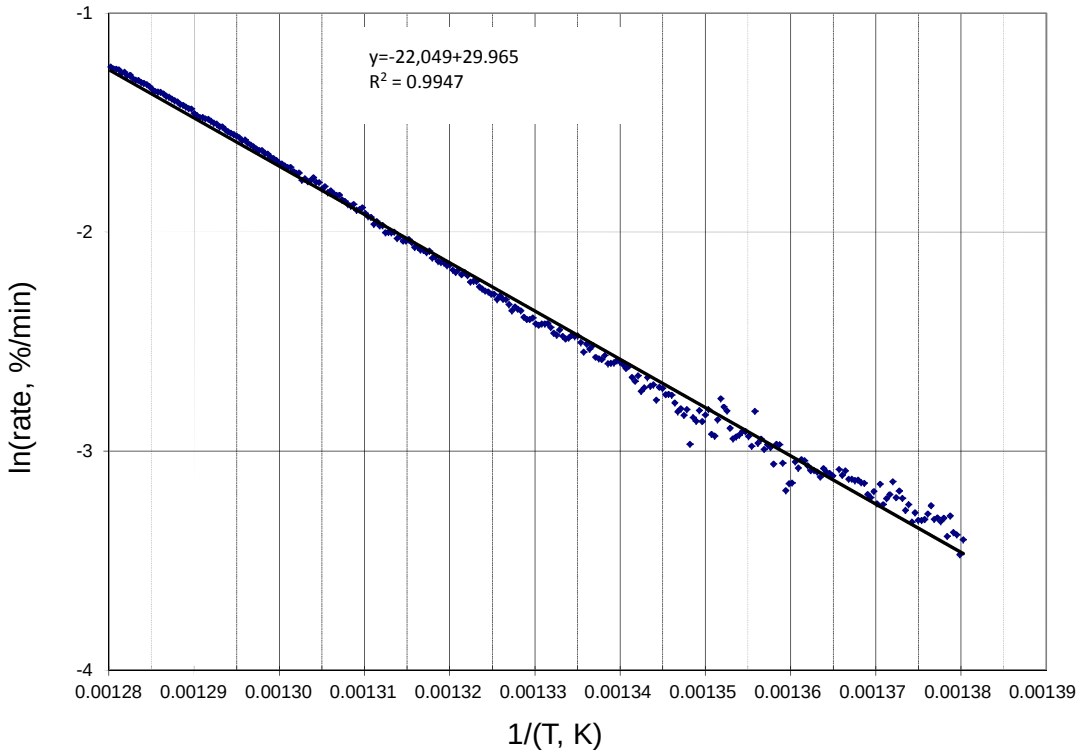

Figure 27: Arrhenius plot of rate of weight loss versus temperature for the example PI candidate.

Fiber Drawing: Viscosity Considerations

Any coating material or solution of coating material for optical fiber must be applied as a liquid. It is important to be able to utilize existing coating applicators to avoid excessive cost in design and fabrication of special applicators for different coating systems. A coating prepolymer or coating solution is delivered from a reservoir to the coater under pressure, and then applied as a very thin layer to the bare glass fiber as the glass passes through from the draw furnace down to the take-up spool.

The fiber draw process speed has a minimum limit due to the feedback controls controlling the fiber diameter. Below this minimum the controls cannot maintain the fiber diameter within specification requirements. Thus, all in all, the practical range of coating viscosity for existing coating applicators and process speeds is about 1000 cPs minimum to about 10,000 cPs maximum. This range limitation was found to be a difficulty for some of the most promising candidate materials, as will be discussed.

Fiber Drawing: Filtration

The high temperature coating is a thin layer of about 15 microns on the silica glass. It is the only protection the fiber has for this type of design, and it must be free of hard particles greater than 1

or 2 microns in diameter. So filtration is absolutely necessary. Here the viscosity is again important, because it is extremely difficult to force a high viscosity liquid through a filtration device rated at 1 micron absolute in a realistic timeframe and without rupturing the filter through high pressure.

Before moving to fiber draw trials, all the candidates that made it to this point had to be demonstrated as filterable to 1 micron particle size maximum. Silver-metal membrane filters were used to remove contamination.

Fiber Drawing: Delivery On Tower

All candidate solutions drawn had been filtered into pristinely clean glass containers. These containers were not opened until it was time to draw fiber. Then, with lid removed, they were always placed directly into a reservoir with a cleaned dip tube inserted into the bottom of the container. The entire delivery line system was always new for each material, and the coaters had been scrupulously cleaned and rinsed with pure electronic grade propanol. The coating material is always forced through the system by pressurized nitrogen. Nitrogen is essential to use for all polyimides, though normally air is used for UV-curable acrylate coatings.

Characterization of Performance on Fiber

The key metric for the candidate coating on fiber was the dynamic TGA Method II test protocol. As a 15 micron thick film on the silica, the performance could be different than when cut from a much thicker film made in the laboratory. All TGA runs at this stage were done under a clean air atmosphere, since air is the medium in which the fiber will be deployed.

Some tests were also run in an intensely accelerated environment to judge the fiber strength in the presence of steam. These tests were run at Southwest Research Institute in San Antonio, Texas, where a facility for high pressure, high temperature, and moisture in the atmosphere is maintained. Polyimide coatings on fiber were compared with fiber having both a hermetic carbon coating and polyimide coatings to see if there is an additional benefit to be realized from the hermetic coating.

Results and Discussion: Laboratory Screening

PFCB

In the early stages of the project, thermogravimetric tests were run under a dry nitrogen atmosphere to observe thermal decomposition without the influence of oxidation. This was in consideration of the fiber being deployed inside sealed steel tubes and with considerable additional barrier surrounding the tubes as part of the cable design. (Later in the project, the decision was made to change to an air atmosphere in the TGA experiments because it will be impossible to guarantee an inert atmosphere in the cable.)

The first films of fully-soluble PFCB (non-crosslinked) were cast from a solution of 40,000 average molecular weight polymer in cyclohexanone. Specimens of 5 to 10 milligrams were prepared for the TGA. It was determined to run everything under dry nitrogen at this time. The specimens in the tarred platinum crucible were taken first to 200°C for 10 minutes to ensure no

remaining solvent, then returned to room temperature for starting the temperature ramps. The temperature was then increased at one of several ramp rates to 600°C.

As described in TGA Method I, the temperature at which a specimen exhibited a given weight loss was recorded, using weight loss points of

- 1%
- 2%
- 5%
- 7%
- 10%
- 15%

The temperatures at these weight loss points were a function of ramp rate as well. Ramp rates β, °C/minute, were

- 1
- 2
- 5
- 10
- 15
- 20

The time period τ_{xy} at a given ramp rate to go from one weight loss point *x* to another *y* was determined as $(T_y - T_x)/\beta$. The average temperature T_{av} between these two weight loss points was also calculated, simply $(T_x + T_y)/2$. Then the rate of weight loss at *Tav* is $(y\%-x\%)/\tau_{xy}$. Table 10 gives detailed data for this non-crosslinked PFCB.

	Temperature, °C, at indicated weight loss										
β °C/min	1%	2%	5%	7%	10%	15%		τ_{xy} (2% to 7%)	T_{av}	rate, %/min	$1/(T_{av},K)$	ln rate
1	391.3	404	417.1	421.8	426.9	433.2		17.80	412.9	0.28	0.001458	-1.26976
2	399.5	413.4	427.8	432.6	437.9	444.3		9.60	423	0.52	0.001436	-0.65233
5	414.1	429.3	444.6	449.8	455	462.3		4.10	439.55	1.22	0.001403	0.198451
10	427.2	442.7	458.1	463.3	469	476.2		2.06	453	2.43	0.001377	0.886732
15	428.2	451.9	469.1	475	481.3	488.9		1.54	463.45	3.25	0.001358	1.177655
20	441.3	461.4	478.3	484.1	490.4	498.1		1.14	472.75	4.41	0.001341	1.482805
	Temperature, °C, at indicated weight loss										
β °C/min	1%	2%	5%	7%	10%	15%		τ_{xy} (5% to 15%)	T_{av}	rate, %/min	$1/(T_{av},K)$	ln rate
1	391.3	404	417.1	421.8	426.9	433.2		16.10	425.15	0.62	0.001432	-0.47623
2	399.5	413.4	427.8	432.6	437.9	444.3		8.25	436.05	1.21	0.00141	0.192372
5	414.1	429.3	444.6	449.8	455	462.3		3.54	453.45	2.82	0.001376	1.038458
10	427.2	442.7	458.1	463.3	469	476.2		1.81	467.15	5.52	0.001351	1.709258
15	428.2	451.9	469.1	475	481.3	488.9		1.32	479	7.58	0.00133	2.024953
20	441.3	461.4	478.3	484.1	490.4	498.1		0.99	488.2	10.10	0.001313	2.312635
	Temperature, °C, at indicated weight loss										
β °C/min	1%	2%	5%	7%	10%	15%		τ_{xy} (7% to 10%)	T_{av}	rate, %/min	$1/(T_{av},K)$	ln rate
1	391.3	404	417.1	421.8	426.9	433.2		5.10	424.35	0.59	0.001434	-0.53063
2	399.5	413.4	427.8	432.6	437.9	444.3		2.65	435.25	1.13	0.001412	0.124053
5	414.1	429.3	444.6	449.8	455	462.3		1.04	452.4	2.88	0.001378	1.059392
10	427.2	442.7	458.1	463.3	469	476.2		0.57	466.15	5.26	0.001353	1.660731
15	428.2	451.9	469.1	475	481.3	488.9		0.42	478.15	7.14	0.001331	1.966113
20	441.3	461.4	478.3	484.1	490.4	498.1		0.31	487.25	9.52	0.001315	2.253795

Table 10. TGA weight loss data for the non-crosslinked PFCB

Table 10 shows the temperature at given weight loss points and as a function of the ramp rate for the 6 different ramp rates used for the PFCB sample. It also shows how the calculations of rate of weight loss under the conditions are made. Finally the key data are obtained to get ln(rate) versus temperature. For TGA Method I this protocol is always used, but the detailed data need not be shown for every material.

The data in Table 10 allow the Arrhenius plot of rate of weight loss to be obtained for the PFCB. In this case it is ln(rate, %/min) and not ln(time to failure, τ_f) that is used. The same Arrhenius parameters are obtained either way, except the signs are reversed for A and E_a/R. Figure 28 shows the plot of the date in Table 10. The linear regression obtains

- $E_a/R = -24{,}081$
- $A = 34.033$

so projections of rate of weight loss can be made for lower temperatures where the rate of weight loss is far slower. Figure 29 gives the results for the non-crosslinked PFCB in the temperature range of 200°C to 350°C.

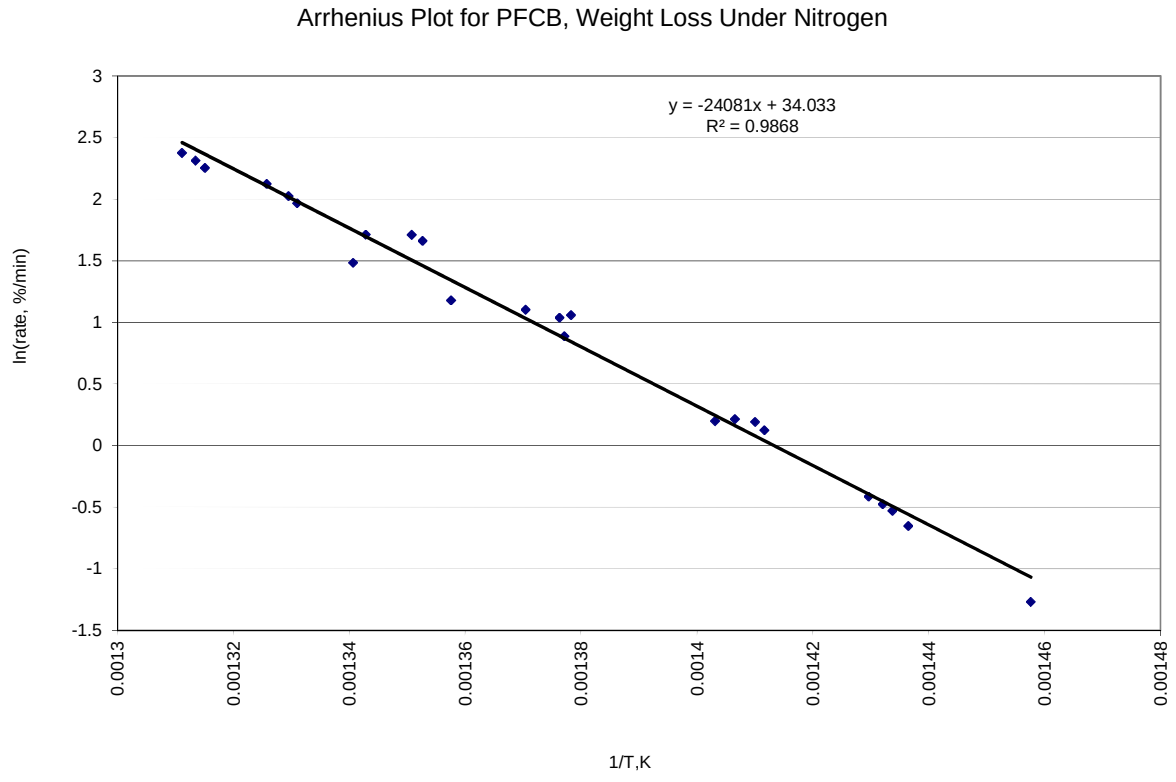

Figure 28: Arrhenius plot of rate of weight loss versus temperature for non-crosslinked PFCB under dry nitrogen.

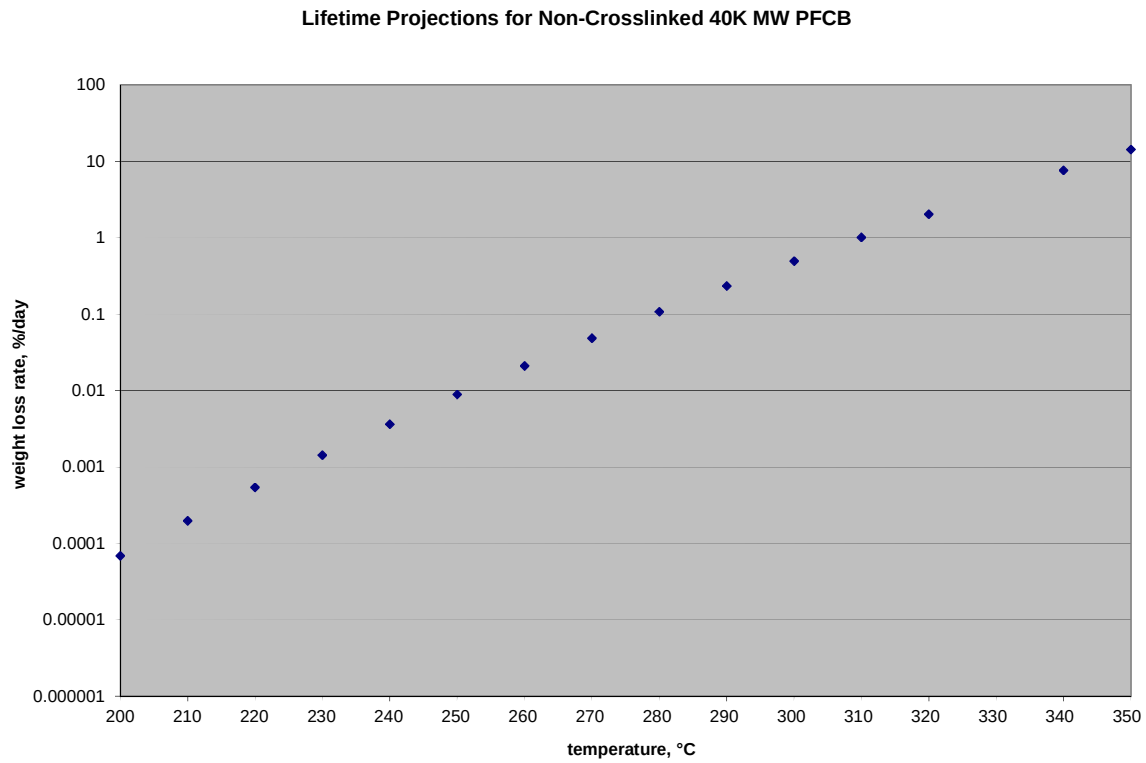

Figure 29: Projections of rate of weight loss for the non-crosslinked PFCB in a nitrogen atmosphere.

There are several ways to look at the lifetime projects, rate of weight loss versus temperature, time to X% weight loss (for example, 20 percent weight loss is often taken as a failure criterion for high temperature fiber coatings), etc. From the data in Figure 29, at 300°C under nitrogen the rate of weight loss is 0.5% per day, so clearly the desired goal of years at temperatures above 300°C are not realized by this non-crosslinked soluble polymer. Instead, the soluble PFCB can be considered an upper mid-temperature range fiber coating. It could perhaps be useful under certain conditions at temperatures as high as 250°C, but not for the geothermal fiber optic cable.

Tetramer Technologies prepared a series of cross-linkable PFCB polymers incorporating TVE as a crosslinking agent.

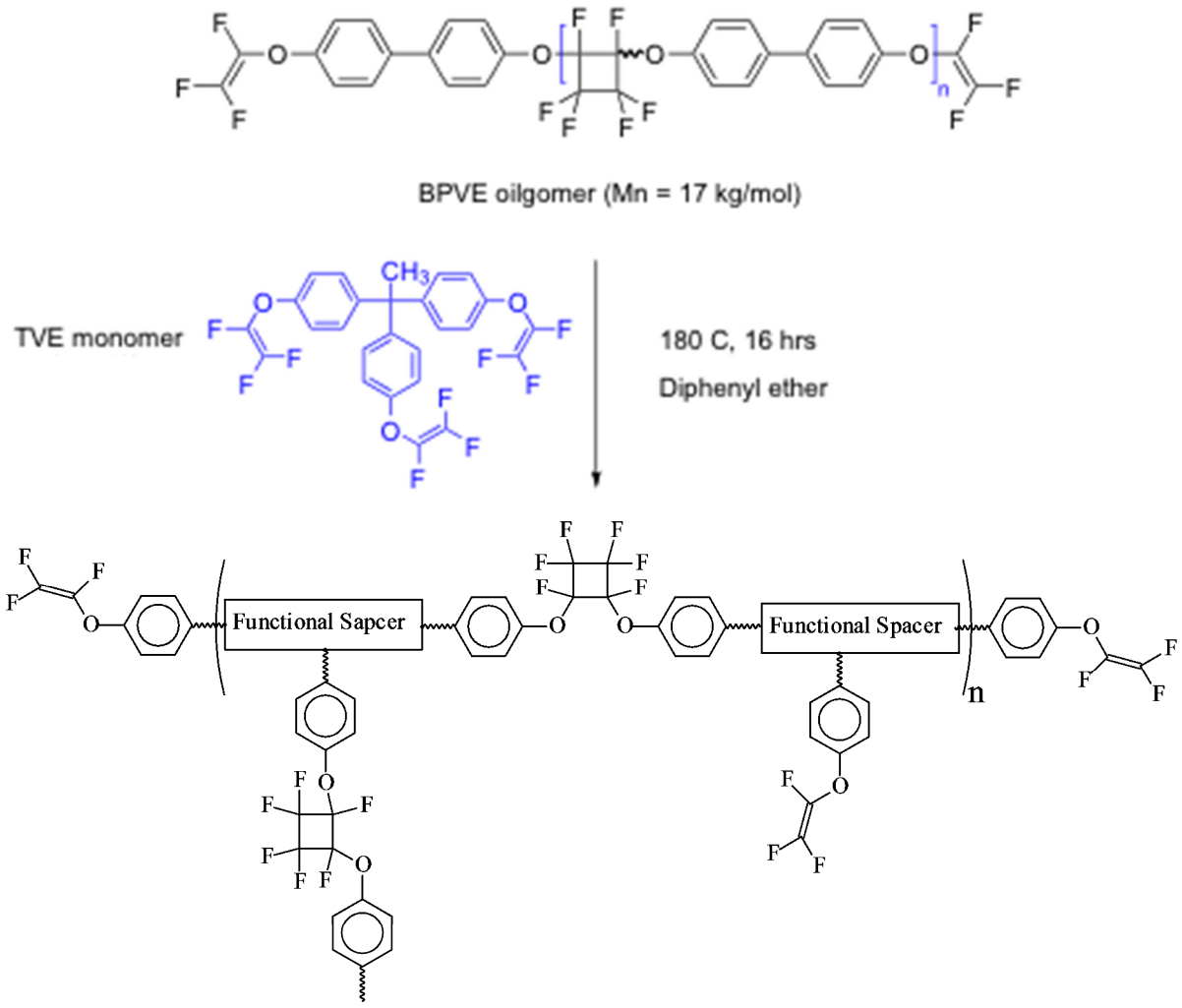

Figure 30: General route of preparation of crosslinked PFCB, Pendant reactive groups remain for further crosslinking in post-processing or in-situ as deployed in high temperature environments.

Table 11 shows the materials that were prepared.

Sample	Starting Materials	%TVE
TRJ 4043-6	BPVE Mn ~17,000 + TVE	0
TRJ 4043-5	BPVE Mn ~17,000 + TVE	1
TRJ 4043-1	BPVE Mn ~17,000 + TVE	5
TRJ 4043-2	BPVE Mn ~17,000 + TVE	10
TRJ 4043-3	BPVE Mn ~17,000 + TVE	15
TRJ 4043-4	BPVE Mn ~17,000 + TVE	20
TRJ 4043-3-2	BPVE Mn ~17,000 + TVE	15
TRJ 4043-4-2	BPVE Mn ~17,000 + TVE	20
TRJ 4043-7	BPVE Mn ~17,000 + TVE	25

Table 11: PFCB crosslinked with TVE for evaluation by TGA Method I.

The thermal stability of these materials was evaluated according to TGA Method I, closely following the same procedures as used for the non-crosslinked PFCB above. The projections of weight loss over time at temperature are shown in Figure 31.

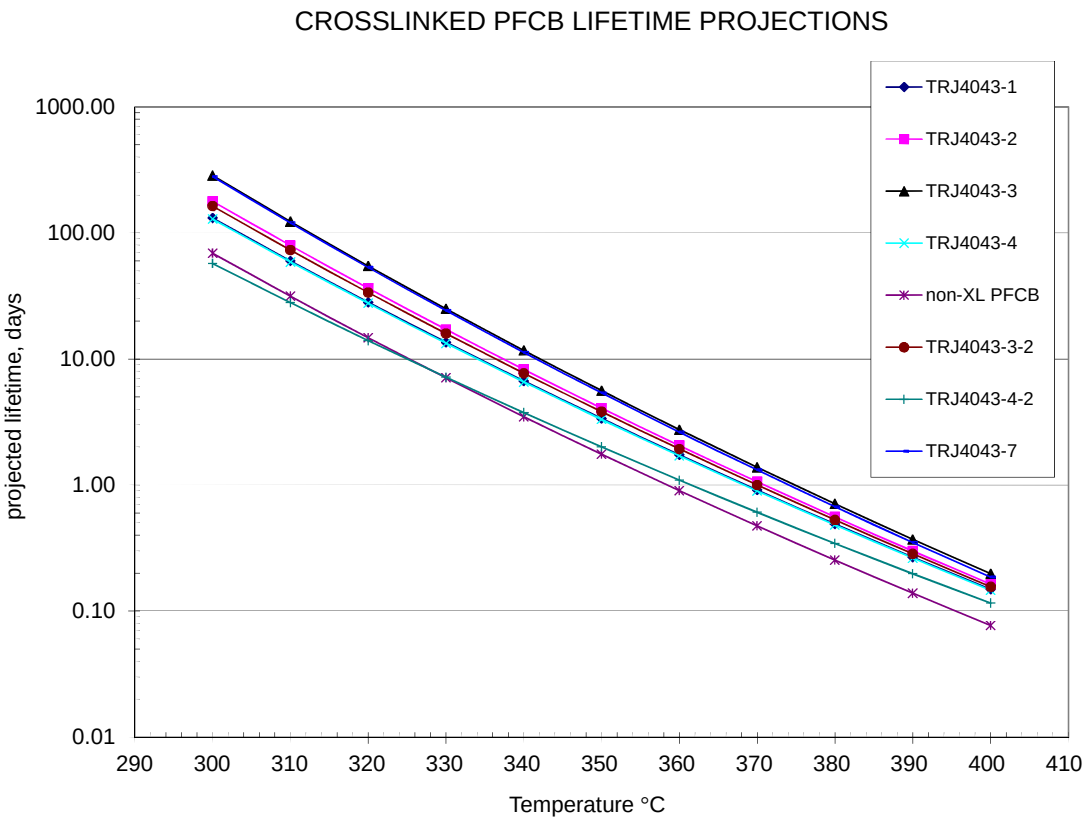

Figure 31: Projected lifetime (time to 20% weight loss) in Nitrogen for the crosslinked PFCB formulations.

Unexpectedly, it was found that a limit in thermal stability is obtained at a 15 percent TVE level, with higher concentrations of the agent moving the results back to lower projected lifetime at temperature. At best, the 15 percent TVE gives about a 4-fold increase in lifetime at high temperature, 70 days at 300°C for non-crosslinked polymer to 300 days for the crosslinked. Nevertheless, the target performance is not approached, even when the inert nitrogen atmosphere is the environment.

Soluble Polyimides and Poly(benzodioxane)

Tetramer next turned to preparation of soluble polyimides, polyimides to be applied in solution instead of reacted on the fiber surface. In theory, these materials would have greater thermal stability than the PFCB family but still be strippable by solvent means on fiber. Three classes of candidate materials were prepared in the following series, Figure 32. Table 12 below also shows as an example how the copolymer ratio was varied for the THT2000 series.

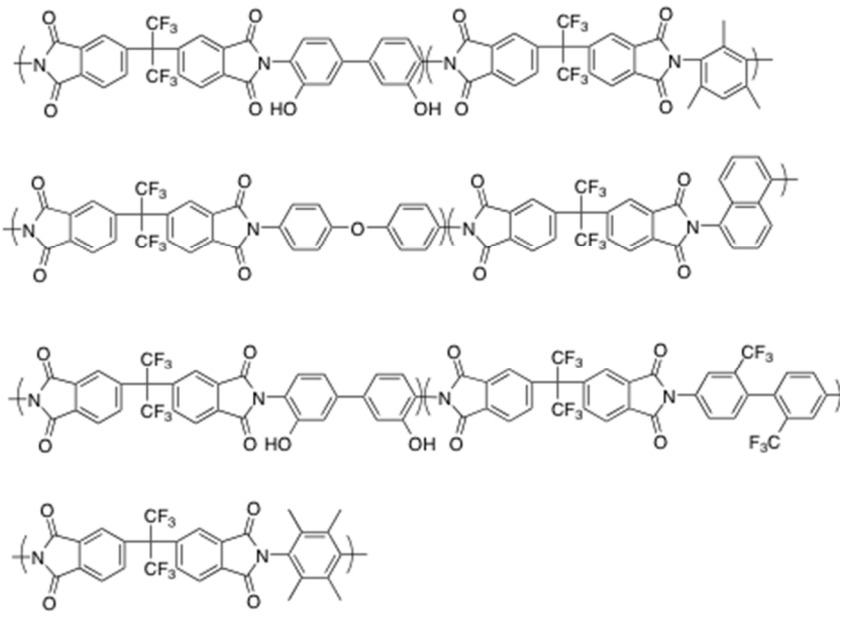

THT2000 series, copolymer ratio varied from 0 to 80%

THT4000 series, copolymer ratio varied from 0 to 100%

THT5000 series, copolymer ratio 50/50 only

Figure 32: Soluble PI candidate series, structures and range of copolymer ratios studied.

THT2000	**X weight %**	**Y weight %**
A	80	20
B	60	40
C	40	60
D	100	0

Table 12: Copolymer ratios for the THT2000 series of soluble PIs.

The THT2000 series, THT4000 series and THT5000 series materials were evaluated using the TGA Method I in inert nitrogen atmosphere. The homopolymer was not studied as it is a building block of the three series and not a candidate in itself.

THT2000A was evaluated as a straight polyimide and also after it was converted in the TGA to the poly(benzoxazole) form (THT2000A PBO). THT6000 poly(benzodioxane) was also provided for this part of the study because it is also a soluble material.

All materials behaved well in the TGA scans, so that data the reduction procedure gave linear regressions for the Arrhenius parameters with high R^2 values in all cases. With the activation energies and pre-exponential factors, the lifetime projections were obtained, Figure 33.

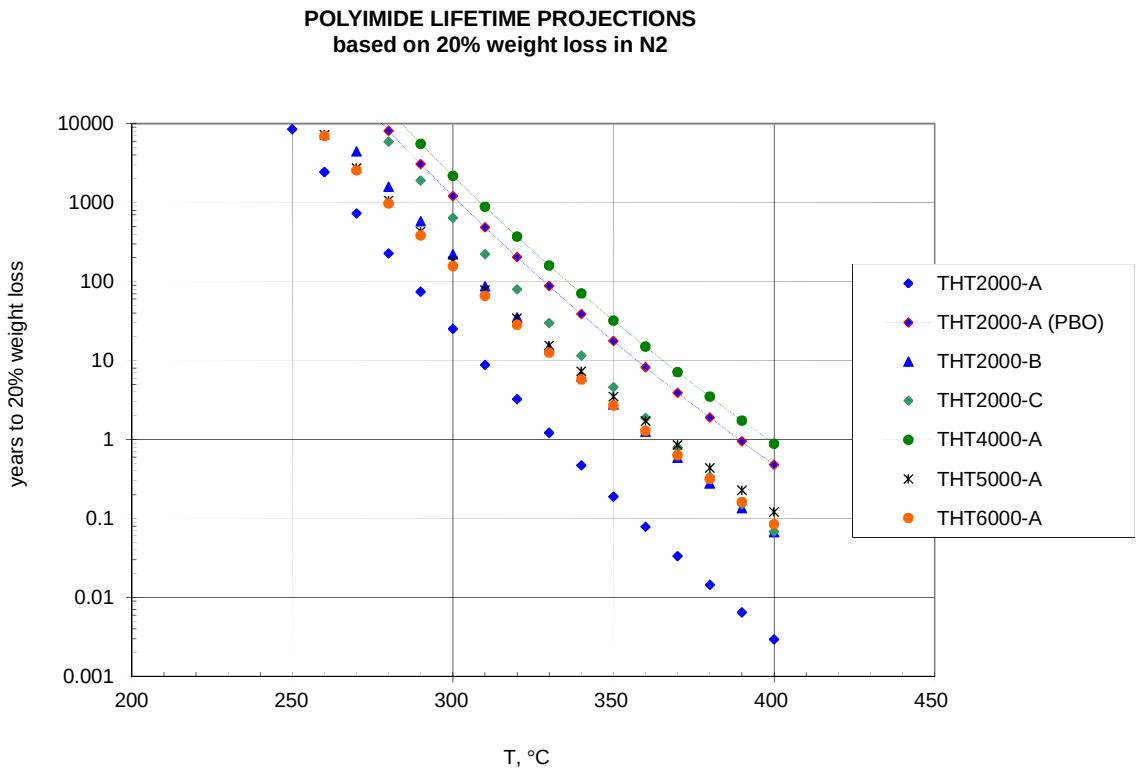

Figure 33: Lifetime projections in inert nitrogen for soluble PIs THT2000 series THT4000A, THT5000A, for the PBO form of THT2000A, and for THT6000A poly(benzodioxane).

The THT2000A, having the greatest hydroxyl content of the series and thus the highest potential for conversion to the PBO form, illustrates the benefit of rearrangement to PBO. The increase in thermal stability is roughly two orders of magnitude. However, the rearrangement was found to result in ~10 percent weight loss (see Figure 24). This is a considerable loss of mass. Since the conversion to PBO will have to take place in-situ on the glass, it is certain that the 15 micron thick coating will realize cracks, exposing the glass underneath.

Another blow to the PBO approach is that THT4000A performed better in the TGA test, projecting to endure twice as long at a given high temperature. Suprisingly, THT6000A did not do very well. The poly(benzodioxane) was expected to provide a very thermally stable coating.

THT4000A proved very interesting and was given additional studies. Ultimately it was chosen as a candidate with which to draw fiber for on-fiber testing. At this point in the project two changes in the test protocol came about. The potential for the cable to be in a high temperature air environment was being discussed and the decision was made to examine candidate materials by TGA but in a pure air atmosphere. Also, TGA Method II had been developed, providing a more direct and precise means of obtaining the instantaneous rate of weight loss versus temperature for the materials. In effect, this modification of the method takes the rate of weight change from being an average rate at an average temperature to being in the limit, almost $^{\partial w}/_{\partial t}$(T).

The TGA modification is shown in the scan below in Figure 34. This is a TGA scan in an air atmosphere at 2°C/minute for the THT4000A. The weight is shown over the temperature ramp, and also the running rate of weight loss is shown.

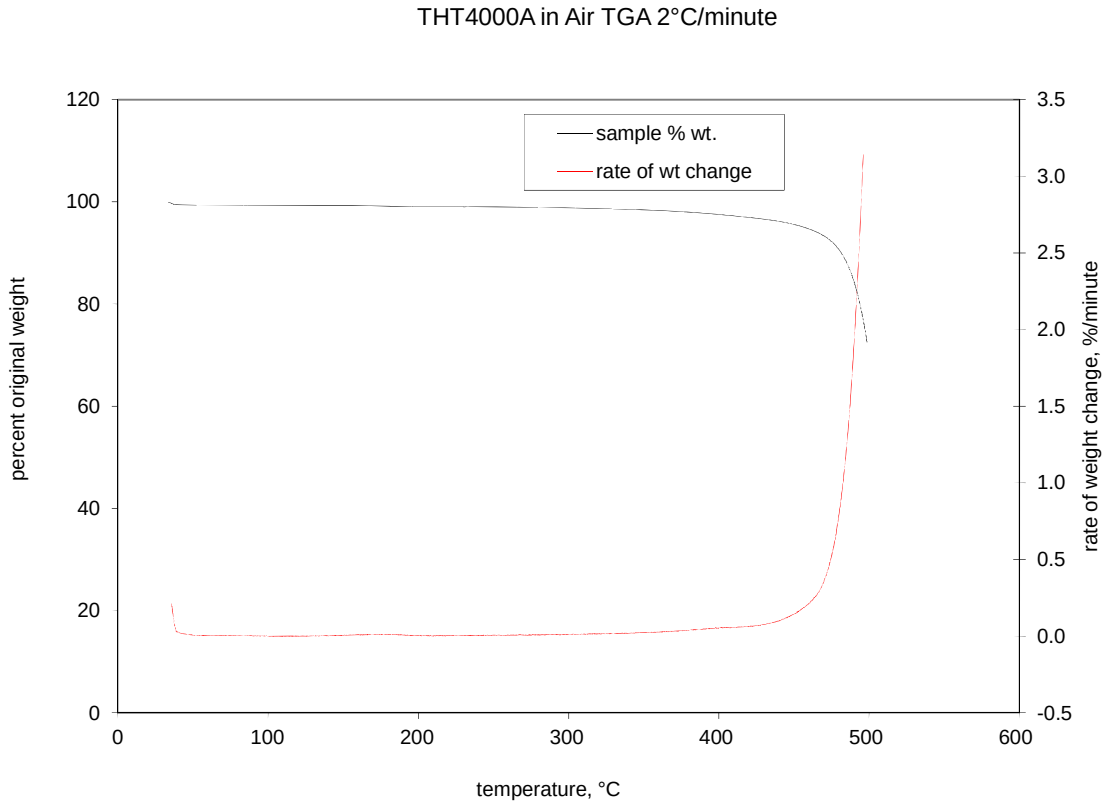

Figure 34: TGA in air, weight versus temperature in a 2°C/minute ramp experiment. The rate of weight change is also shown.

It is necessary to take the data from a region in the TGA scan where the rate of weight loss has become great enough that scatter in the data is under control while getting as close to the temperatures of interest as practical. Otherwise the linear estimate of an Arrhenius plot to obtain the activation energy and pre-exponential factor is meaningless. For these materials this region is generally between 400°C and 500°C, and for the THT4000A in particular the best range is 430°C to 460°C. Figure 35 gives the Arrhenius plot from the above data.

Figure 36 compares the lifetime projections for THT4000A in air versus in an inert nitrogen atmosphere. It was immediately clear that if there is a probability of an oxygen containing atmosphere available to the fiber then the impact on lifetime projections is profound, 1.5 to 2 orders of magnitude reduction in projected lifetime. Nevertheless, it was determined to go ahead with on-fiber experiments using THT4000A as a benchmark against which to measure further improvements.

From this point on, TGA Method II is the screening test protocol. All TGA was run in an air atmosphere as well, but first samples were taken to 300°C under nitrogen for 15 minutes to ensure the absence of solvent and the full cure of any material.

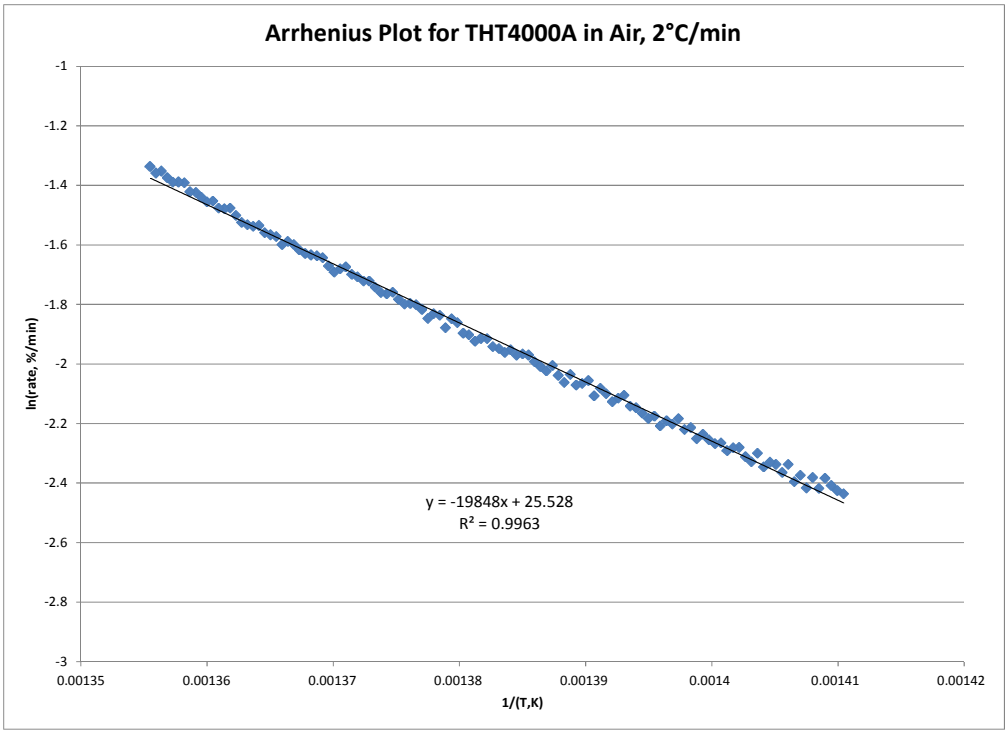

Figure 35: Arrhenius plot, rate of weight loss as a function of temperature for THT4000A, air atmosphere, 2°C/minute temperature ramp rate.

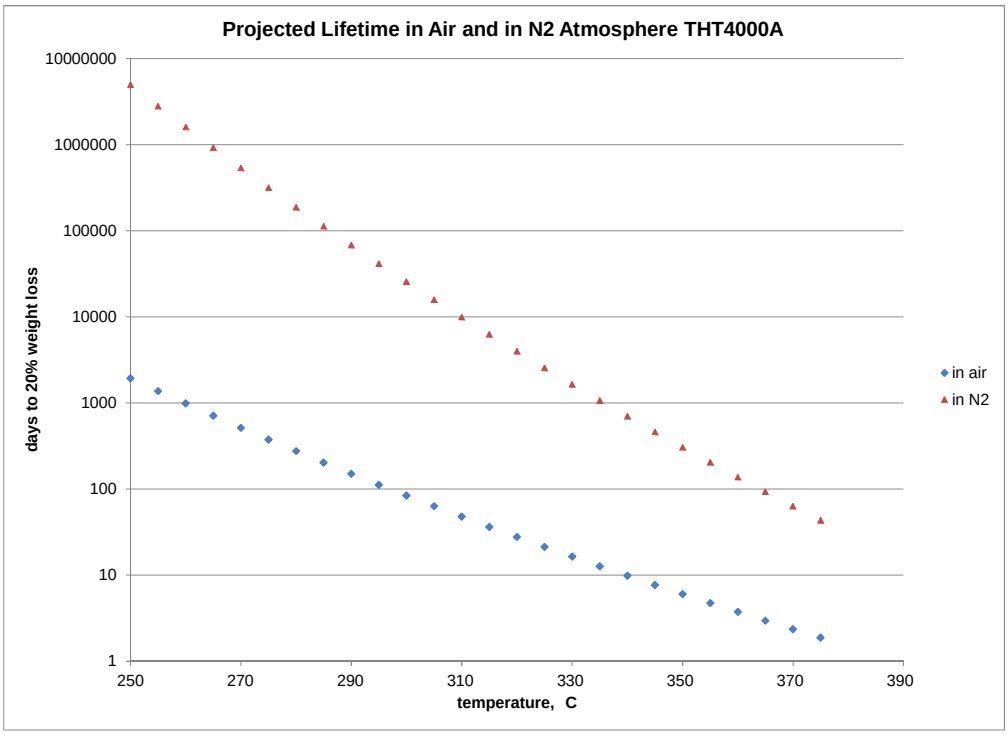

Figure 36: Lifetime projections for THT4000A in air versus in a nitrogen atmosphere.

Soluble Poly(phenylene)

Films of THT11 soluble poly(phenylene) were cast for TGA evaluation. Following Method II, the specimens were always taken to 300°C under nitrogen for 15 minutes to drive off all solvent, then given a temperature ramp at 2°C/minute under air. THT11 was also evaluated under nitrogen, this time to see if a similarly extensive impact is found in the presence of oxygen. Figure 37 shows the results as lifetime projections (rate of weight loss) versus temperature when the material is in air versus in nitrogen.

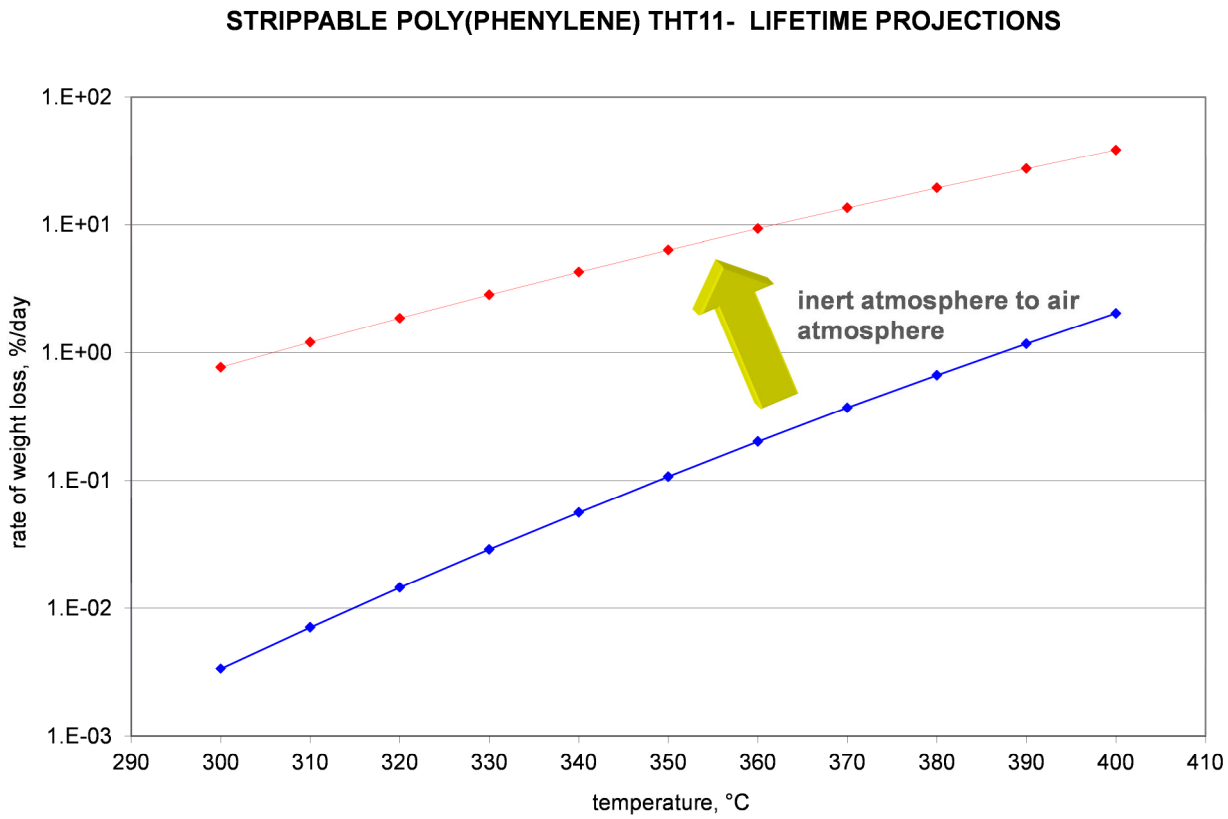

Figure 37: Projected rate of weight loss versus temperature for THT11 poly(phenylene) in an inert nitrogen atmosphere and in an air atmosphere.

Again, and not surprisingly, it is found that the air atmosphere accelerates the degradation by a factor of 100 at 300°C and of 60 at 350°C. The extensive aromatic nature of the poly(phenylene) was hoped to provide a greater thermal stability than soluble polyimides. Comparing the lifetime projected for THT11 and THT4000A in Figure 38, this is not found to be the case. The rate of weight loss in deployment temperatures will be several times higher for THT11 than for THT4000A.

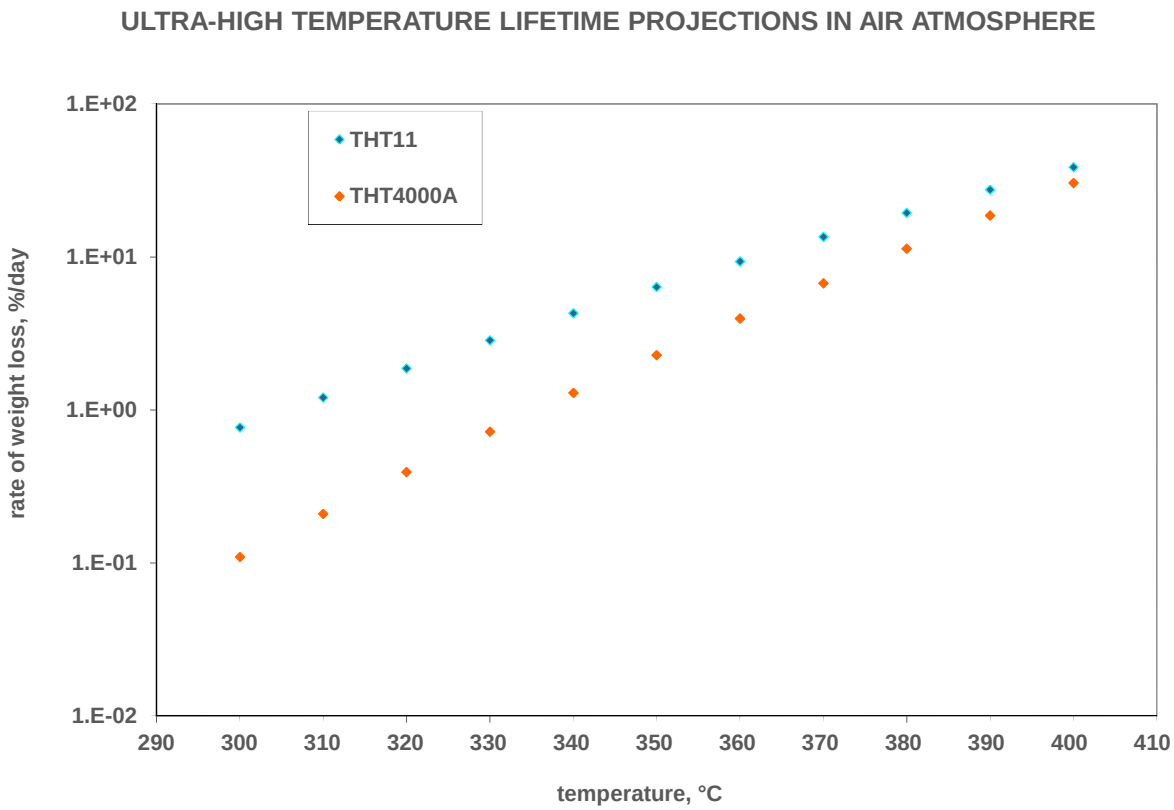

Figure 38: Projected rate of weight loss versus temperature for THT11 and THT4000A in air atmosphere.

Insoluble Polyimides

Insoluble polyimides are coatings applied to optical fiber as the polyamic acid precursor in solution in Dimethyl Sulfoxide (DMSO) or N-Methyl-2-pyrrolidone (NMP). After coating the fiber, the solvent is driven off and the amic acid converted to imide form through a condensation reaction at high temperature on the tower. Tetramer Technologies built several polyamic acid molecules for this study in an attempt to achieve a higher thermal stability than can be obtained from commercially available polyimides coatings.

Commercially available polyamic acid solutions suitable for coating on optical fiber and converting to polyimide during draw include:

- HD Microsystems
  - PI2574 inner layer
  - PI5878G outer layer
  - PI2525 outer layer
- R. Blaine Industries
  - VTEC1388 single layer
- Microquartz
  - Inner layer
  - Outer layer

Evaluation of cured polyimide films of VTEC1388 demonstrated very poor thermal stability, even though this material is in use on commercially available optical fiber, so it was eliminated from consideration immediately. The Microquartz polyimide system has never been used as a coating for optical fiber, but was developed primarily to coat silica capillaries for high temperature analytical instrumentation. It is believed that the HD Microsystems polyimides may be used on commercially available optical fiber, so these materials are of interest as well.

Where an inner layer is used, this layer includes a component to promote adhesion to the silica glass. Most polyimides do not have a very high natural adhesion to polar substrates, sometimes no adhesion at all. Tetramer would have to design a polyimide with this feature in mind.

Tetramer provided a polyamic acid solution in DMSO, VK115D, for evaluation after extensive internal investigations of the estimated thermal stabilities of various molecular building blocks and bonds. This material was considered to have suitable adhesion to glass already due to the nature of the moieties comprising the backbone.

The VK115D was cast in film, converted to polyimide by 30 minutes at 350°C under dry nitrogen, and tested by TGA Method II. Several runs were made, as illustrated in Figure 39.

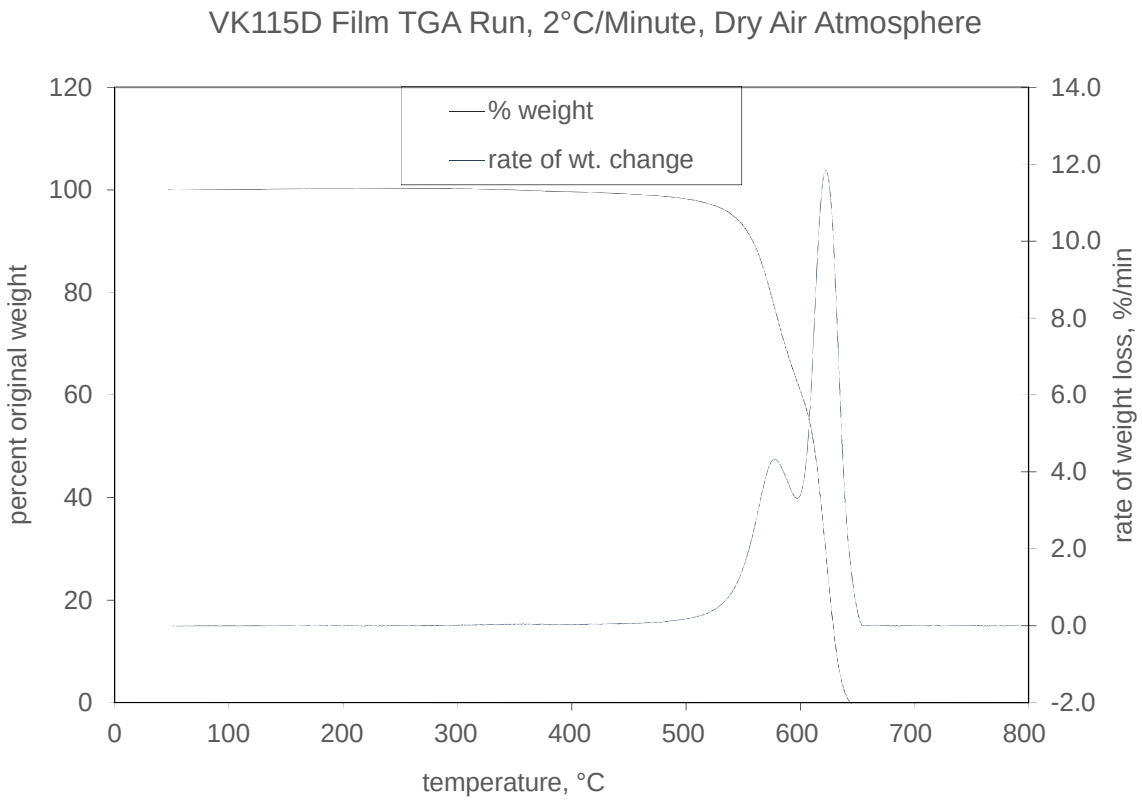

Figure 39: TGA run in air atmosphere for VK115D cast film converted to PI.

The Arrhenius plot for rate of weight loss was determined by the same method as above, Figure 40. Figure 41 compares the lifetime projection as days to 20% weight loss for VK115D with THT4000A soluble polyimide. Clearly the fully-cured and fully-bonded polyimide has significantly better thermal stability than the best of the soluble polyimides studied, by an order of magnitude.

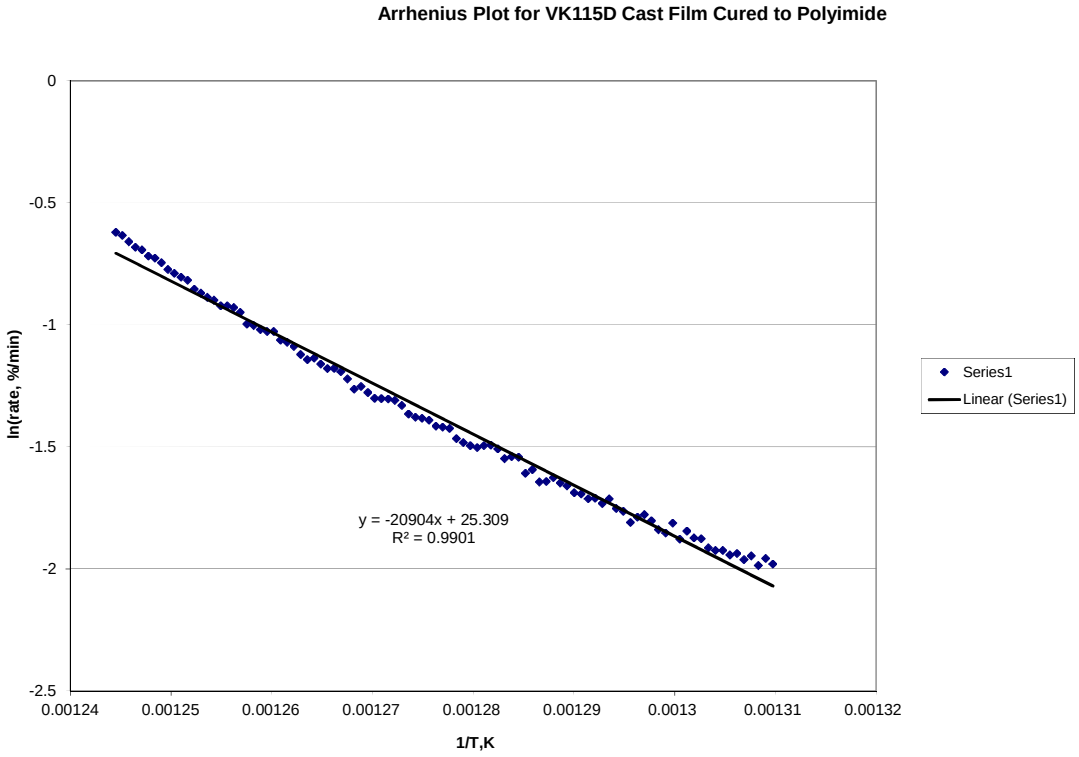

Figure 40: Arrhenius plot for VK115D cured film.

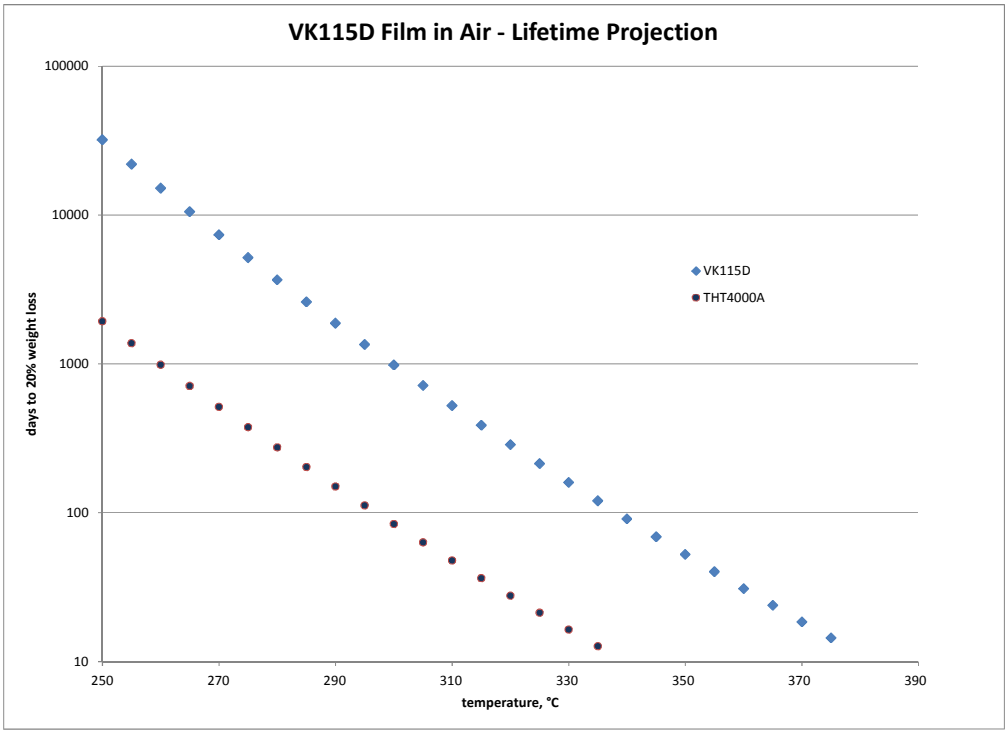

Figure 41: Lifetime projection for VK115D compared to THT4000A, in air.

2.3.3 Scale Up/Down Selected Polymer(s)

Draw Process Experience

Finally, Tetramer Technologies provided three materials for draw, based on the best performing of the soluble and insoluble candidates in terms of thermal stability. THT4000A was the soluble candidate, and VK105N and VK115D were the polyamic acid solution candidates. VK115D was proven in the screening to be at the optimum of thermal stability of all materials studied. VK105N was not optimized for adhesion to glass, and the purpose of including it was to determine the severity of the problem if the adhesion was not good enough, through comparison of handling and aging of fiber with VK105N compared with VK115D.

The first draw with VK105N proved disastrous. The fiber could not be kept from breaking during the draw process. Inspection of the dried amic acid from the solution, under a microscope, showed the presence of metallic-appearing particles. These would make it impossible to keep the glass from breaking at fiber draw.

Tetramer determined the particles were from a metal mixing device used to make the solution up. The filtration equipment had evidently failed, ruptured or opened up during use. The solution was filtered again, as well as the solutions of VK115D and of THT4000A, then returned to the draw facility in Eindhoven, Netherlands.

This time there was no problem with fiber breaking. Filtration had proven successful.

The VK105N, VK115D, and a test run with the Microquartz system were accomplished in Eindhoven. The draw process parameters are shown on the next page. There were two coating stages on the draw tower, each with two furnaces below them. The furnaces have 0.5 meter long hot zones with the fiber shielded by a quartz tube as it passes through each furnace. The tubes are completely inerted with a flow of dry nitrogen, required for the conversion of polyamic acid to polyimide. The temperature of the first furnace was set at 380°C, to drive off all the solvent. Then the second furnace, immediately after, was set to 600°C to effect the conversion to polyimide in a short time. The draw tower was run at a steady-state 30 meters/minute, so the dwell time in each furnace was one second.

For the VK115D, the viscosity of the solution was about 15,000 cPs, but on driving off the solvent the deposited layer of polyimide at each station was only about 1.5 microns. It was necessary to draw the fiber, coating it with two layers, and then pass the fiber down the tower at least twice or three times more again for more coating layers in order to build the necessary coating thickness.

The VK105N showed similar results as the VK115D, requiring three to 6 passes down the tower to obtain the desired coating thickness. The THT4000A proved to be so thin that no more than 8 microns could be put on in total. This is insufficient protection, and a problem of the low solids content possible to get into a solution that could be filtered and applied at draw.

With the Microquartz coating, two passes down the tower obtained the precise thickness desired on the fiber, 15 microns.

At different times, draws were accomplished in Eindhoven with other combinations of commercially available polyimides suitable for optical fiber coating (in addition to the Microquartz system run at the same time as the Tetramer candidates). These were:

- HD Microsystems PI2574 primary/PI5878G secondary
- HD Microsystems PI2574 primary/PI2525 secondary

The top one above was also used by a partner, and they provided a sample of their fiber for inclusion in our on-fiber evaluations.

Table 13: Draw Process Parameters

	trek 2		trek 3		trek 4		trek 5	
furnace temp °C	1735		1735		1735		1735	
lenght (m)			1000		1000		1000	
feedrate (mm/min)			0.7		0.7		0.7	
speed (m/min)			30		30		30	
position core rod		VK115D coating	25	VK115D coating	25	micro quartz coating	32	VK115D coating
furnace 1 (°C)	380		380		380		380	
furnace 2 (°C)	600		600		600		600	
furnace 3	380		380		380		380	
furnace 4	600		600		600		600	
coating wet measured with handheld beta(µm)								
BetaØ coating second layer (µm)	125	die 190 µm	125	die 190 µm	128	die 190 µm	122.2	die 150 µm
beta glass (µm)			125	nat coating	125		125	nat coating
pressure upper body				159µm				138µm
pressure lower body								
pressure secondary lower body			0.345		0.331		0.37	
temp upper body	room		room		room		room	
temp lower body	room		room		room		room	
bruto draw lenght (m)	375		3750		900		6500	

Because of the problems at draw with high viscosity, relatively low solids solutions of VK105N and VK115D, Tetramer investigated if VK115D could be altered to allow for higher solids content. (There was no need to do this for VK105N, as it was only interesting as a comparison for adhesion to glass and not a serious candidate for this application.) It was desired to increase the solids content from 15% to at least 25% by weight.

Tetramer found that by heating the polyamic acid precursor at relatively low temperatures, ~100°C, at a certain point in preparation, they could effectively cut the molecular weight in half while hopefully maintaining the full capability for conversion to polyimide during draw. They provided this VK115D Modification 1 for a second draw in Eindhoven. This time they were able to get the solids content to 25% by weight. This material ran well, and two passes down the draw tower for four layers gave no problems.

Fibers with every combination of candidate material were delivered to the laboratory for evaluation of the thermal stability of the coating as processed on fiber.

2.3.4 Optimize Process and Performance Properties of Polymer/Additive Formulation

Thermogravimetric Analysis

TGA Method II was adapted to measurements of high temperature coating weight loss on fiber in the following way:

1. Fiber is cleaned with 2-proponol to remove all dirt and oil
2. Further handling is with powder-free latex gloves
3. 155 micron diameter coated fiber is cut into 5mm lengths
4. The platinum crucible of the TGA is cleaned, flamed, and tared in the instrument
5. Enough 5mm lengths are placed into the crucible to total about 35 milligrams, giving 6 to 7 milligrams of coating resin
6. The TGA furnace is closed and programmed to 300°C at 20°C/min, holding at 300°C for 15 minutes, all under dry nitrogen
7. The furnace is cooled to 25 °C, then the atmosphere changed to clean, dry air
8. The instrument is programmed to go from 25°C to 550°C at 2°C/minute
9. At 550°C the ramp rate is changed to 20°C/minute until 800°C is reached (completely consuming all the resin), then returned to room temperature
10. The TGA data file now has the original weight of the coated specimen and the final weight of the silica only
11. The weight of the silica is subtracted from the total weight of the coated specimen at every datapoint in the file, effectively taring out the silica weight from the sample weight
12. At this point the reduction of the data goes as TGA Method II for films of resins already discussed

The datafiles resulting from each run were huge, more than 16,000 points. After removing the weight of the inert silica from the total fiber sample weight, the datafile was reduced to 10% the original size by removing 9 of every 10 points. The running weight loss rate versus temperature

was calculated, effectively (as mentioned) $\partial w/\partial t$(T). Then the data were plotted as shown in the Figure 42 example for the VK115D on fiber.

In Figure 42, it can be seen that even at the slow rate and in the air atmosphere accurately measureable weight loss begins well above 400°C. Staying as near as possible to the temperature range of interest, 300°C to 375°, but high enough to limit the scatter in the rate of weight change, the Arrhenius plot as in Figure 43 was generated for each coating-fiber sample. (Note that for the PFCB example analyzed by TGA Method I, Table 10, significant weight loss begins as the temperature approaches 400°C. This temperature range for these more thermally stable materials on fiber is usually about 450°C to 500°C.)

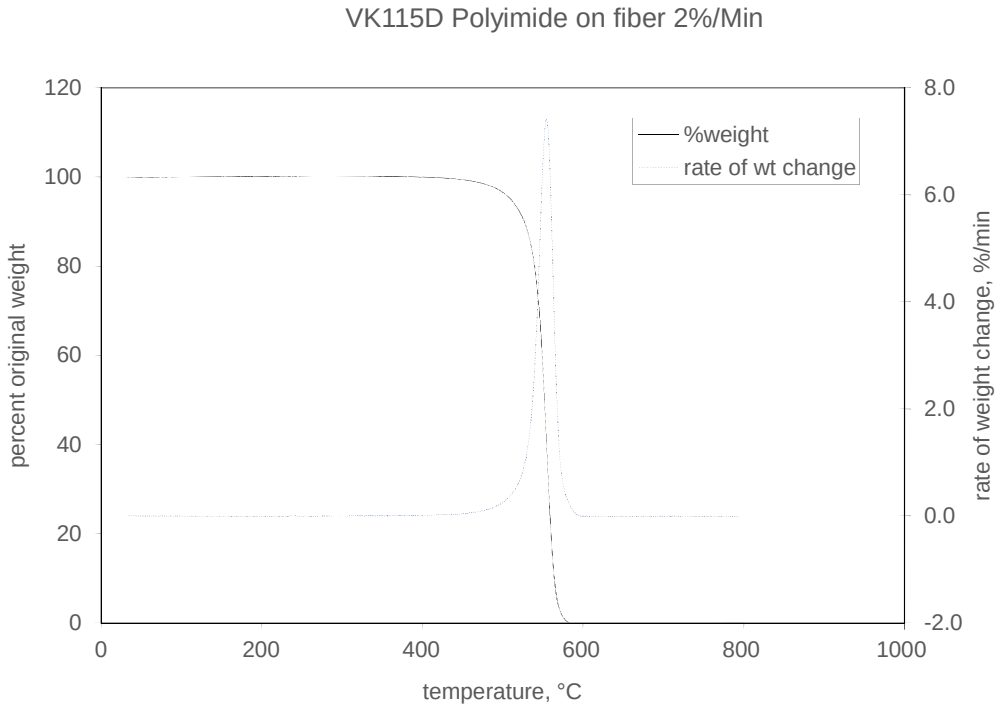

Figure 42: Coating resin weight vs temperature and rate of weight change vs temperature for VK115D on fiber.

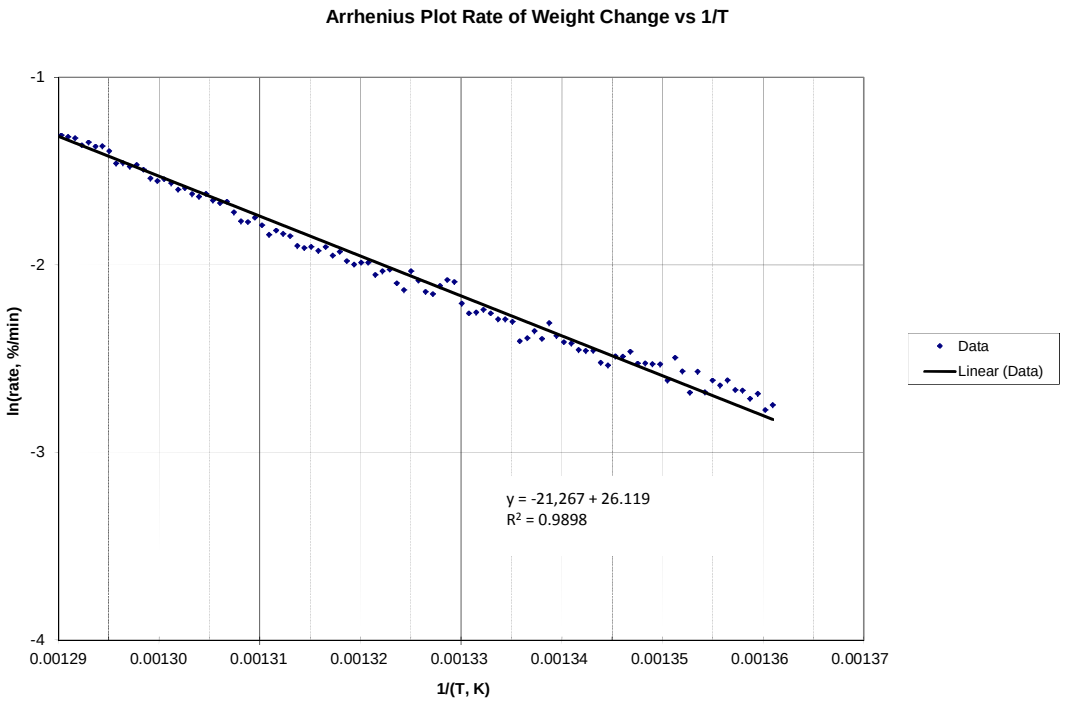

Figure 43. Arrhenius plot of rate of weight change vs temperature for the VK115D on fiber.

Weight loss data for the fibers drawn in Eindhoven were obtained by the modified TGA Method II described at the beginning of this section. In addition, a commercially available polyimide coated fiber was tested, as well as one of the HD Microsystems polyimide systems applied to fiber by an industry partner. For reference, here is the list of materials tested.

- MicroQuartz primary and secondary polyimide coatings drawn in Eindhoven
- HD Microsystems PI2574/PI5878G drawn by a partner
- HD Microsystems PI2574/PI5878G drawn in Eindhoven
- HD Microsystems PI2574/PI2525 drawn in Eindhoven
- Tetramer VK115D drawn in Eindhoven
- Tertramer VK115D Modification I drawn in Eindhoven
- Polyimide system on a commercially available fiber

The activation energy and pre-exponential factor for thermo-oxidative degradation was obtained for each material on fiber, and the lifetime projections were calculated based on these parameters. The lifetime projections given as days to 20% weight loss in an air atmosphere versus temperature are illustrated in Figure 44. The figure is reproduced on a full page to facilitate inspection.

We see from the analyses that the Tetramer VK115D and the Microquartz polyimides are the best of the group up to about 350°C. At that temperature the HD Microsystems PI2574/PI5878G drawn in Eindhoven is equal. For reasons not well-understood the PI2574/PI5878G drawn by the partner is far lower in thermo-oxidative stability than the same coatings applied in Eindhoven. This could be due to processing conditions, where higher temperatures could have

been used in converting the polyimide by the partner. Exact conditions are not known. In Eindhoven, the cure conditions are kept conservative in order to avoid excess degradation by processing, knowing that complete cure will be effected by the deployment temperatures in the field at any rate.

The commercially available polyimide on fiber is by far the worst, so significant progress has been made in terms of identifying advances for the coating on the GFOC fibers.

Fiber samples long enough for attenuation measurements were tested at 350°C to failure, following attenuation with time. The high temperature was chosen for the acceleration factor it gives versus the more normal use temperature of 300°C, where polyimide fibers are expected to last years.

The samples available were:

- VK115D polyimide coated 50 micron MMF
- MicroQuartz polyimide coated 50 micron MMF
- Partner HD Microsystems polyimide coated SMF
- Commercial polyimide coated SMF
- Commercial polyimide/carbon coated SMF

One km of each sample was spooled off and removed from a collapsible spool. For all samples, the coils were placed loosely into an aluminum pan 30cm by 50cm in dimension. The coils were heavily dusted with fine talcum powder, which was then worked into the coils until the whole lengths were coated. The fiber turns would slide easily, virtually friction-free, over each other. More talcum was placed on top, and the ends were left out of the pans.

The pans were placed carefully into 350°C ovens, in air with no humidity control, and the fiber ends were placed through the portals and labeled on the outside of the ovens. Initial measurements were made on the loose coils, and the temperature in both ovens was taken to 350°C. Measurements were made on the fiber samples regularly until the OTDR's could not launch through the fibers. Figures 46-49 show attenuation versus time in aging as well as the weight loss projected by the TGA Method II analyses over the same time period for the several fiber specimens. Thermo-oxidative weight loss is assumed to be linear from the beginning of the exposure in this first-order approximation.

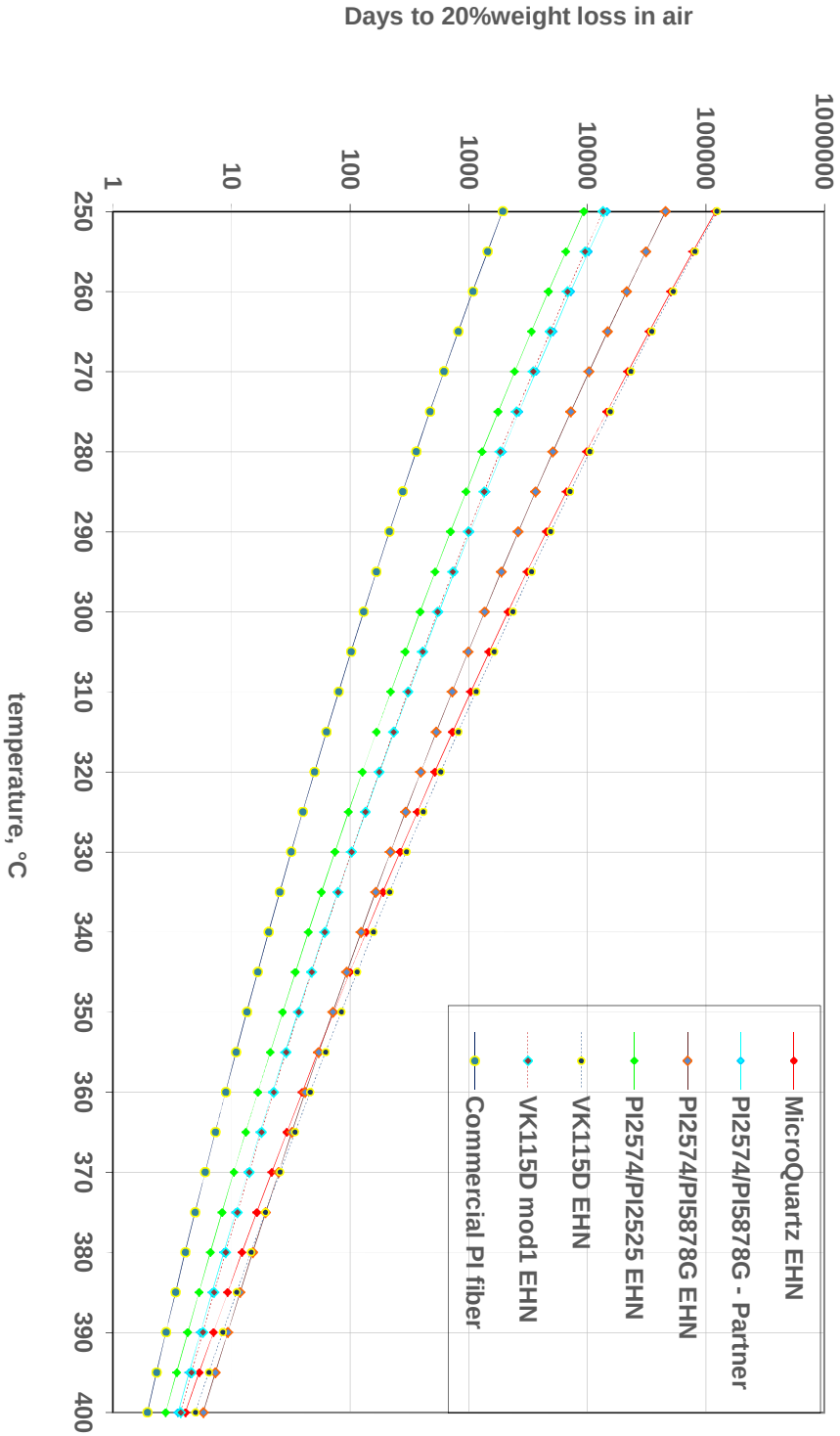

Figure 44: Lifetime projections for the high temperature coatings as applied on optical fiber.

nitrogen atmosphere. This represents the extreme expectation of best protection by the sealed steel tube and high temperature filling compound. Figure 45 shows the projected lifetime as time to 20 percent weight loss versus temperature under these conditions.

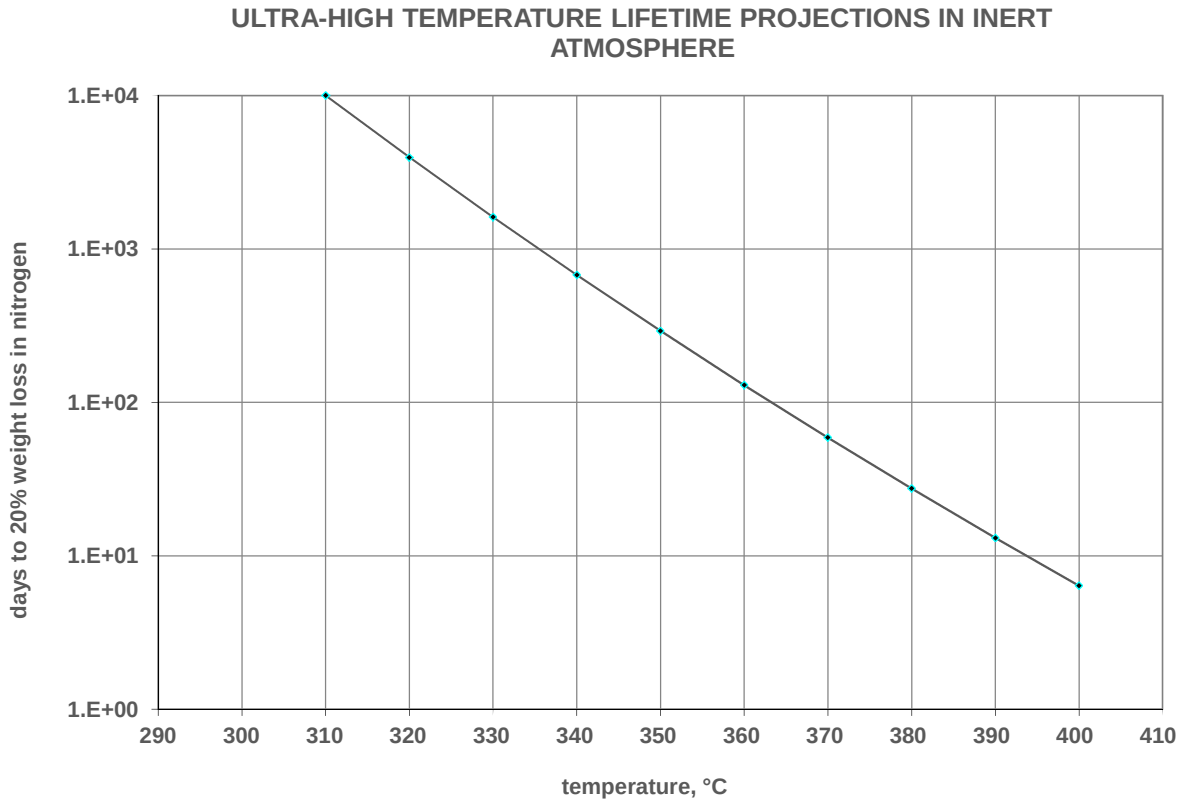

Figure 45: Lifetime projections for the Microquartz PI coated fiber in an inert environment at high temperature.

Under these conditions a much longer lifetime is expected. Even at the target 374°C the fiber can be expected to survive about 60 days or longer.

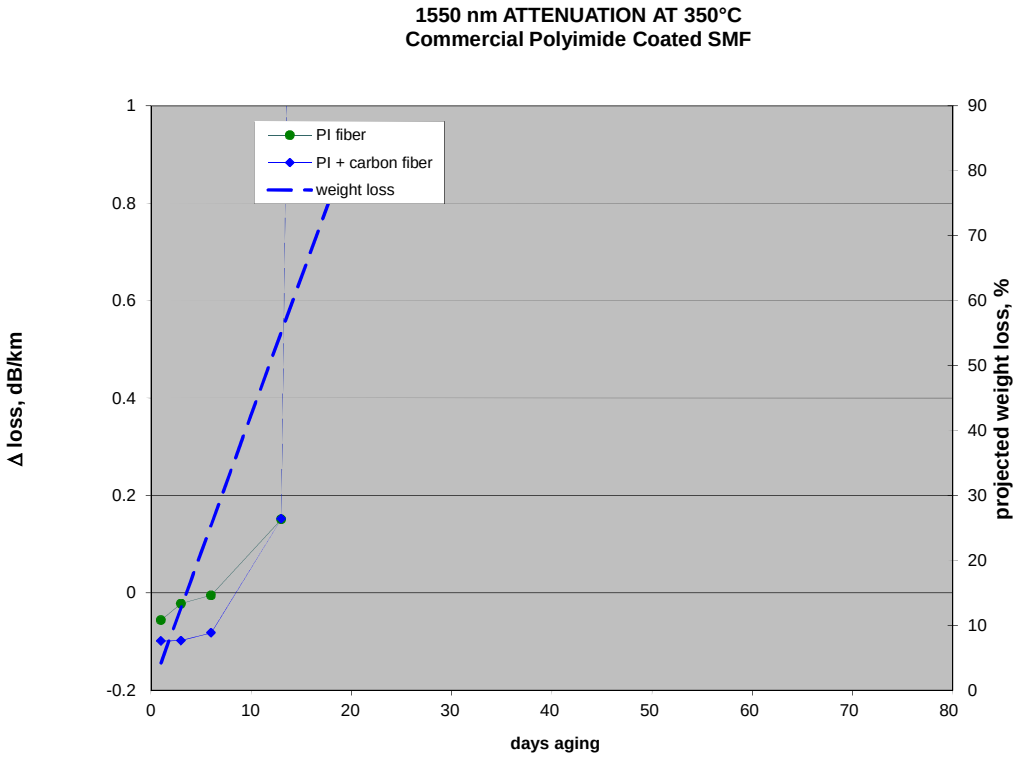

Figure 46: 350°C aging results for the commercial PI fiber and the PI/carbon coated fiber.

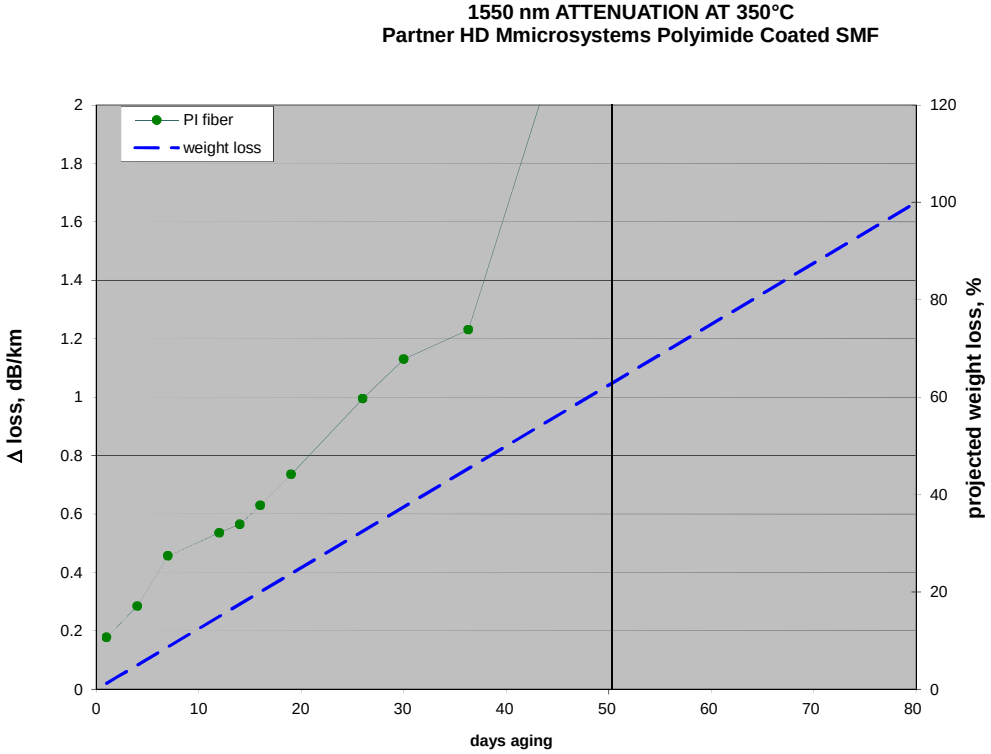

Figure 47: 350°C aging results for the Partner HD Microsystems PI coated fiber.

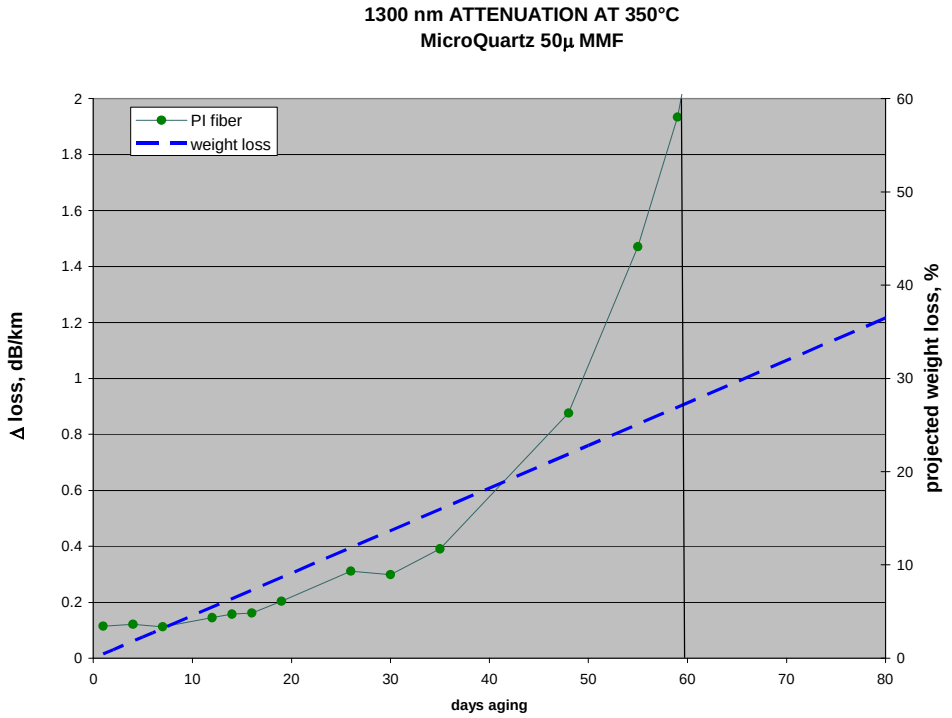

Figure 48: 350°C aging results for MicroQuartz PI coated fiber.

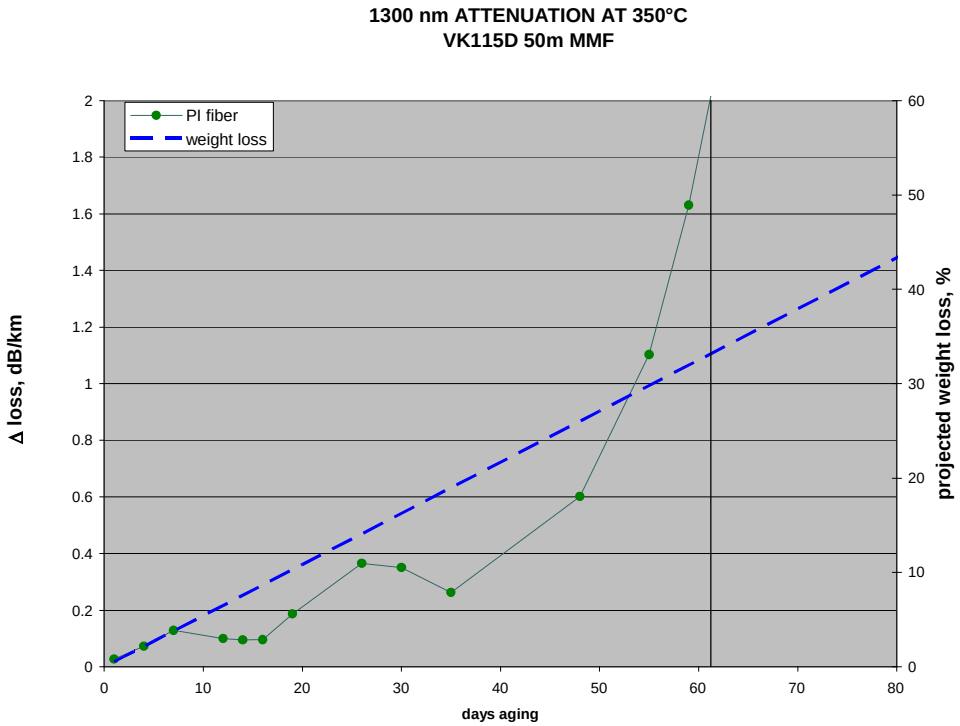

Figure 49: 350°C aging results for the VK115D PI coated fiber.

The commercial fibers showed some relaxation in attenuation initially, but then failed at 13 days aging. The other samples did not show initial relaxation, and the time to failure and the weight loss projected by the TGA data are shown in Table 14 below.

Fiber Aging at 350°C Air Atmosphere				
Fiber Type	Source	Polyimide	Days to Fiber Failure	Projected Weight Loss, %
Singlemode	Commercial PI Fiber	Unkown	13	60
Singlemode	Partner HD Microsystems Fiber	PI2574/PI5878G	50	60
Multimode	Microquartz - Eindhoven	MQ-pri/MQ-sec	60	25
Multimode	Tetramer - Eindhoven	VK115D	60	30

Table 14. Summary of 350°C fiber aging experiment.

The commercial fibers and the partner fiber sample continued to transmit light up to a higher projected weight loss than anticipated. This is because of the lower microbending sensitivity of the singlemode fiber design versus the multimode fiber. Nevertheless, the order of failure is as predicted by the TGA data, and the relative time to failure remains roughly as projected by TGA as well.

Finally, the modification of the VK115D to allow a 60% higher solids content in the application solution proved to have a significantly diminished thermo-oxidative stability, Figure 44, so work with the Tetramer formulations reached a termination with the original VK115D. The VK115D requires more passes down the draw tower to achieve the necessary thickness, but this is a feasible process.

Resistance to High Temperature/High Pressure Steam

Some end-users of high temperature fiber require carbon hermetic coating on the glass. The principal concern is as a hydrogen barrier, but a secondary concern is the environment, where it has been believed that the carbon coating provides protection against a harsh (moist and hot) atmosphere as well. Since it is already known that the carbon coating loses hermeticity against molecular hydrogen as temperatures approach about 200°C, it was desired to determine if the carbon coating continues to provide a barrier against moisture in a high temperature, aggressive environment. A simple experiment was designed, using commercially available fiber having a polyimide coating system on the glass. One specimen was coated with polyimide only, and the other had the same polyimide system over glass that first had the hermetic carbon layer deposited.

First tests were carried out in the Prysmian coatings lab at relatively low temperature and pressure created by superheated steam. The equipment used is an autoclave operating at 130°C with 100% moisture saturation (1 atmosphere gauge pressure). The commercially available fiber

specimens were coated with a polyimide system, some with carbon hermetic coating under the PI.

- Method:
  - Fibers placed under stress in 2-point bending inside precision diameter quartz tubes (static fatigue setup)
  - Tubes held in autoclave at above conditions
  - Time to failure for stressed specimens recorded
- Failures over time in the autoclave are shown in Figure 50.
  - Polyimide-only fiber failures are indicated at different stress levels
  - No carbon coated fibers broke under any conditions

This first experiment showed clearly that the carbon hermetic coating gives superior protection against the moisture attack that catalyzes flaw growth in silica under stress.

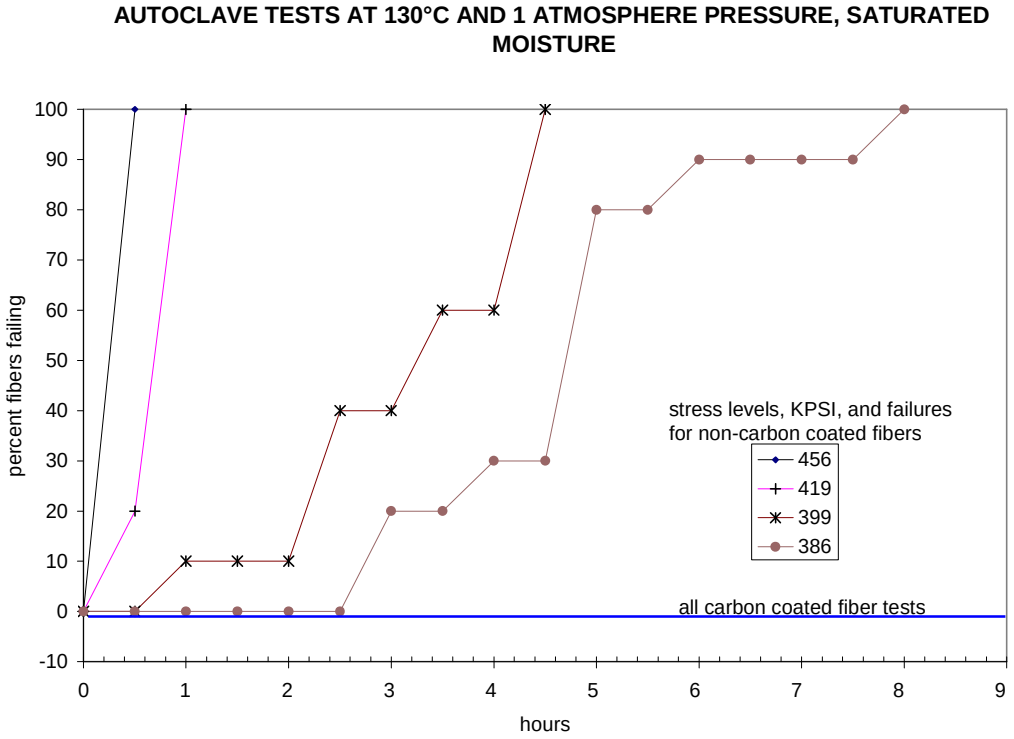

Figure 50: Time to failure for the individual specimens in 2-point bending at the indicated maximum stress levels and placed in the autoclave at 1 atmosphere of steam at 130°C

Facilities were needed to expose fibers under stress to temperatures of 250°C and higher with superheated steam. The kind of vessels and conditions for such testing are prohibitive for the Prysmian laboratory. A search for resource led to Southwest Research Institute (SwRI), which has extensive facilities for testing materials at high temperature and pressure. Safety features include internally-designed pressure vessels with metal-to-metal sealing, constant pressure monitoring, blast-proof rooms for vessels, controlled environment in rooms to

ensure constant temperature. They also have a deep experience level in studying corrosion of metal under extreme conditions in the Oil and Gas industry.

Four lengths of new fiber were obtained:

- 2030m, SMF-40-P-125-1
- 1025m, MMF-50-6-P-125-6
- 2030m, SMF-40-CP-125-1
- 1025m, MMF-50-6-CP-125-6

P denotes polyimide coating only and CP denotes carbon hermetic coating plus polyimide coating. Samples of the four fibers were sent by carrier to SwRI in preparation, and sets of precision quartz tubes were also sent ahead:

- 7.50mm radius = 87 KPSI nominal stress
- 3.10mm radius = 214 KPSI nominal stress
- 2.73mm radius = 244 KPSI nominal stress

The much larger tube was provided in the event that the smaller tubes resulted in 100% breaks.

Protocol

- Samples loaded into vessels, in 2 point bend tubes
- 50 ml water placed into the vessels
- Vessels pressurized at room temperature for 8 hours to ensure the seal
- Vessels taken to temperature (~ 4 hours to equilibrate)
- Desired time at temperature
- Vessels cooled (~ 4 hours to cool)
- Vessels opened and specimens examined for breaking

The first test was an effort to establish a benchmark, with the three tube sizes containing 10 specimens each tube, two fiber types, 250°C, 20 atmospheres pressure with superheated steam, and held for four hours. No specimens broke in either fiber type at any of the stress levels.

Most or all of the water was observed re-condensed in the vessel, so the vessels did have superheated steam. This result was surprising in light of the fast breaking of the older polyimide-only fibers in the autoclave test, even though the stress levels were much lower.

A second test was set up on site, basing conditions on the results of the first.

Second test conditions:

- 300°C, 20 atmospheres pressure, 50 ml water, 8 hours exposure after equilibrated to temperature
- Determined after inspection of first test results
- Tube loading technique was reviewed and found to be OK

Results:

- Carbon coated fibers broke at 214 KPSI and 244 KPSI stress levels (see photo in Figure 51.)
- There were no breaks in polyimide-only fibers

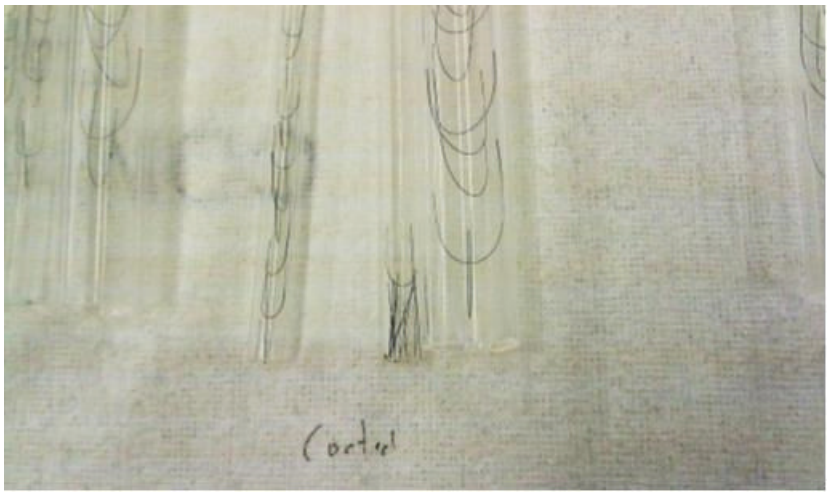

Figure 51: Photograph of broken carbon-coated specimens in the bottom of the precision diameter quartz tubes.

Additional quartz tubes were shipped overnight, adding the new stress levels in blue below to the ones already in use:

- 456 KPSI
- 419 KPSI
- 399 KPSI
- 386 KPSI
- 352 KPSI
- 244 KPSI
- 214 KPSI
- 87 KPSI

Test #2 had shown that 8 hours at 300°C differentiated between the two fiber types. Test #3 would be also 300°C for 8 hours equilibrated, with 50 ml water in the vessel, with higher stress levels made possible by the smaller diameter quartz tubes. The differentiation at much higher stress levels would complete the picture for 300°C with superheated steam. The results of Test #3 are shown in Figure 52 as percentage of fibers failing at each stress level during the high temperature treatment.

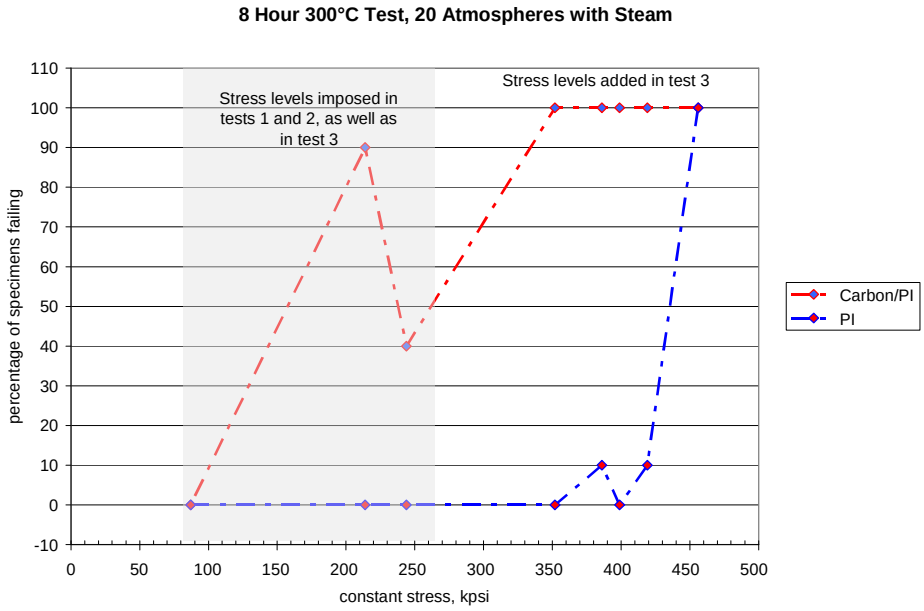

Figure 52: PI coated high temperature fibers, with and without carbon hermetic coating, percent specimens failing under stress at 300°C/20 atmospheres superheated steam.

The response of the two fiber types was definitively demonstrated:

- Carbon coated fiber fails at much lower stress than the non-carbon coated fiber
- High temperature and superheated steam rapidly corroded the strength of the carbon coated fiber

The carbon hermetic coating process results in a lower median strength, a narrow distribution of strength but 20% to 25% lower than non-carbon coated fiber. Clearly, the carbon structure opens up at 300°C, allowing moisture to attack the surface, not hermetic at this temperature. It's hard to explain the large difference in response across the range of stress levels by the difference in intrinsic strength alone, but carbon hermetic coating is detrimental to the integrity of the optical fibers at these high temperatures, and since the glass design for the GFOC project is inherently hydrogen-insensitive no further activity on developing a carbon-coated version was pursued.

2.3.5 Selection of Best High Temperature Coating

Based on the following criteria:

1. Thermo-oxidative stability at highest temperatures
2. Toughness
3. Ease of application
4. Availability

the Microquartz primary and secondary polyimide coating system was selected for the GFOC fiber.

The systems developed at Tetramer Technologies show promise in the event that more development can be done, but at this point it is necessary to finalize the choice. The GFOC fiber will have a polyimide coating system of a primary and secondary coating applied as solutions in DMSO, exhibiting an industry-leading resistance to degradation in the aggressive environment of geothermal energy wells.

2.3.6 Scale-Up Selected Final Coating

The coating with the best balance of processing and performance characteristics was selected for production scale-up. The mechanical properties of the scaled-up polyimide coated fiber were tested and reported in the following sections.

Tensile Strength and Dynamic Fatigue

Tensile strength testing was performed using 5 percent per minute as the strain rate and a 0.5 meter gauge length for the fiber. The mechanical laboratory is controlled to an environment of 22°C +/- 1°C and 50% RH +/- 5% RH.

Dynamic fatigue data were obtained at four stress rates covering 3 orders of magnitude. All testing was performed in the controlled environment laboratory.

All aging environments are achieved using Espec chambers for temperature plus humidity and by Blue M chambers for high temperature alone (uncontrolled humidity). All chambers are checked for calibration twice annually.

Two fiber samples from different draws were used for all tests.

Tensile Strength of Unaged Fiber

Tensile strength Weibull distributions are shown in Figure 53.

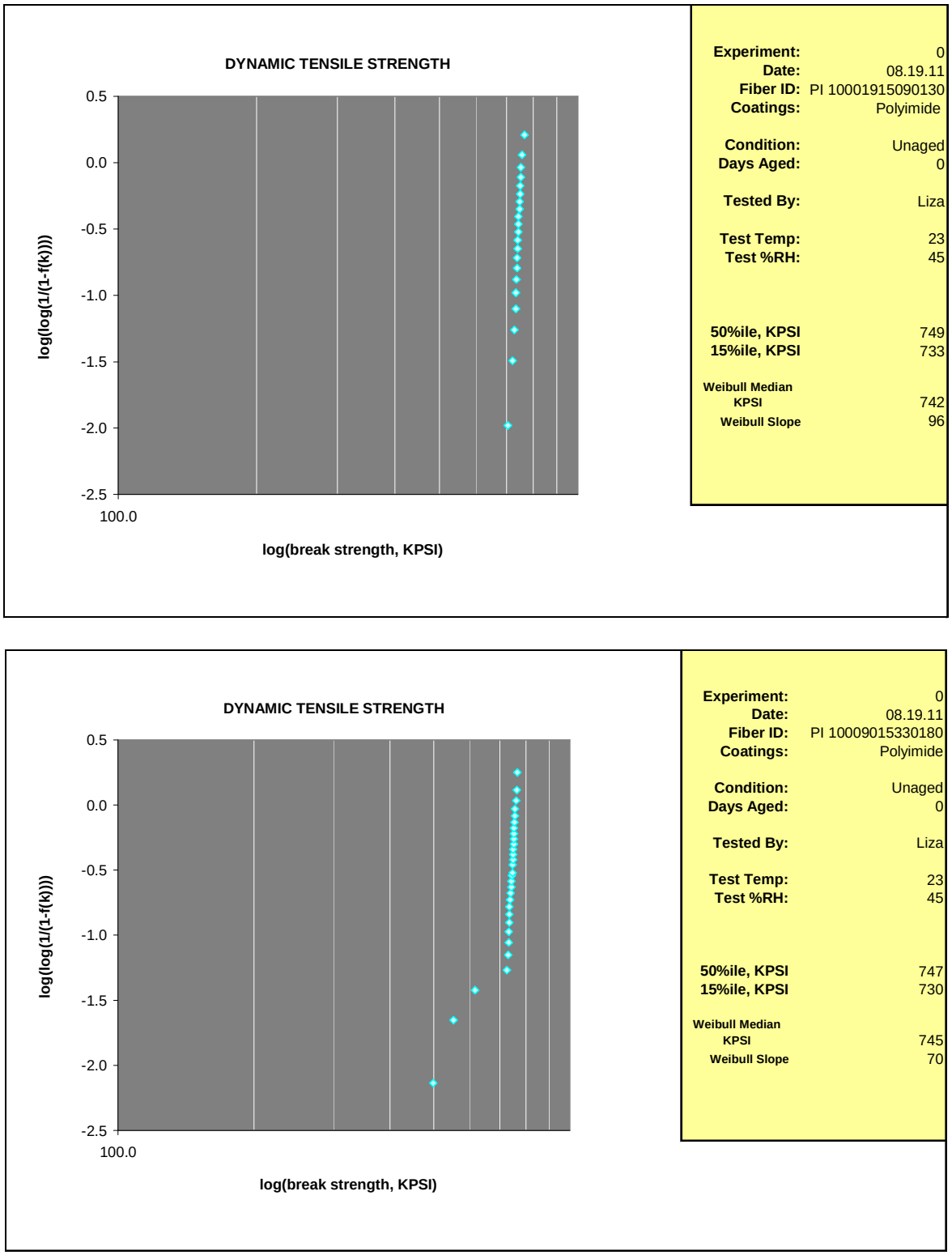

Figure 53: Tensile strength distributions of the unaged Prysmian PI fiber.

Damp Heat Aged

Tensile strength of fiber aged 30 days at 85°C/85% RH are shown in Figure 54.

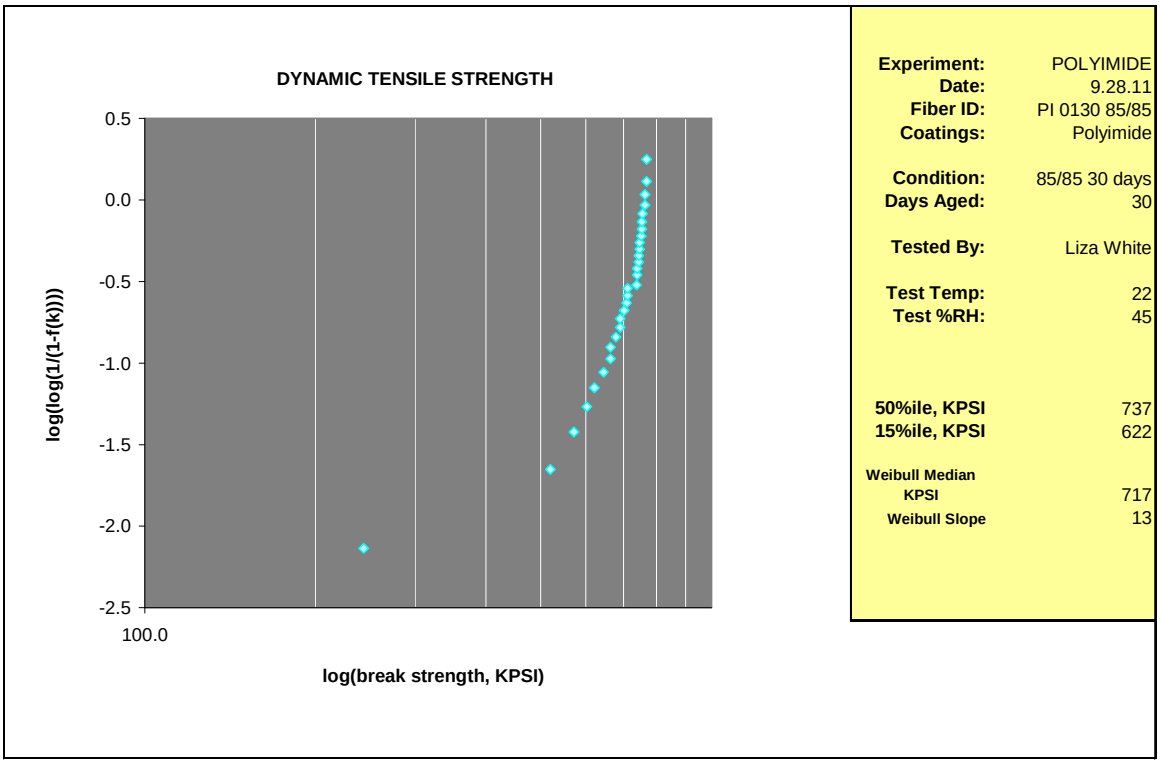

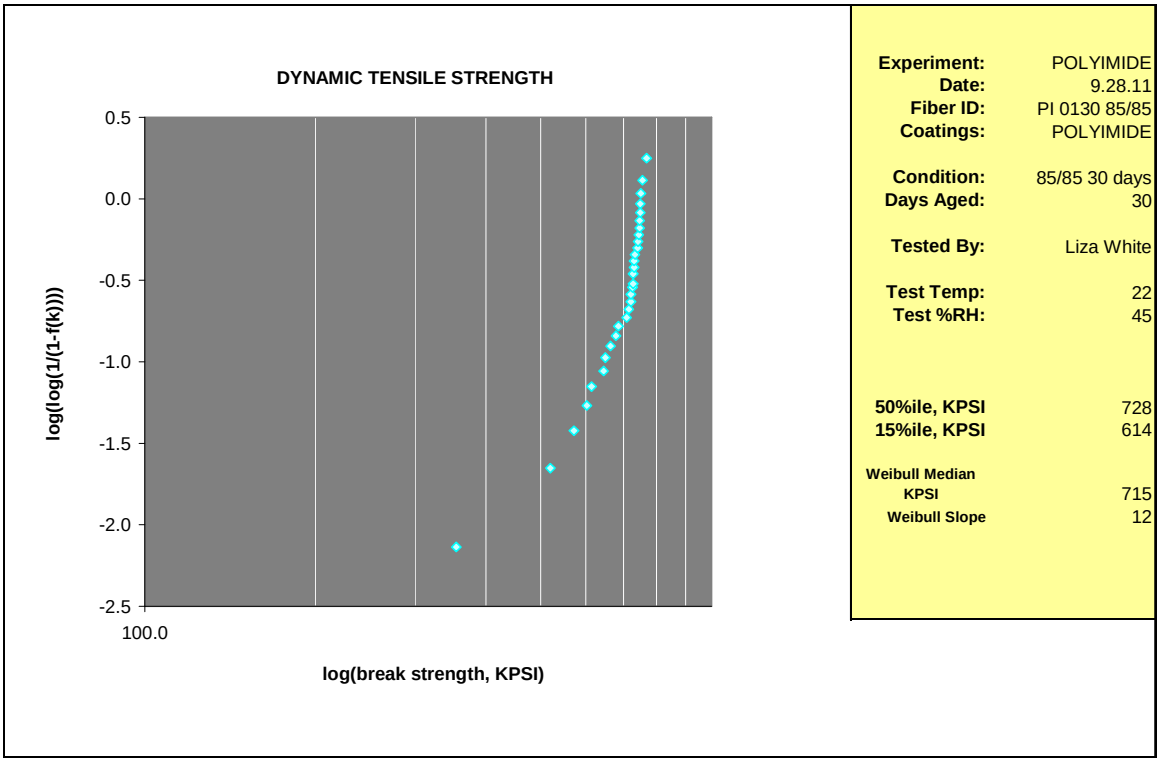

Figure 54: Damp heat aged Prysmian PI fiber tensile strength.

85°C Water Aged

Tensile strength of fiber aged 30 days in 85°C water is shown in Figure 55.

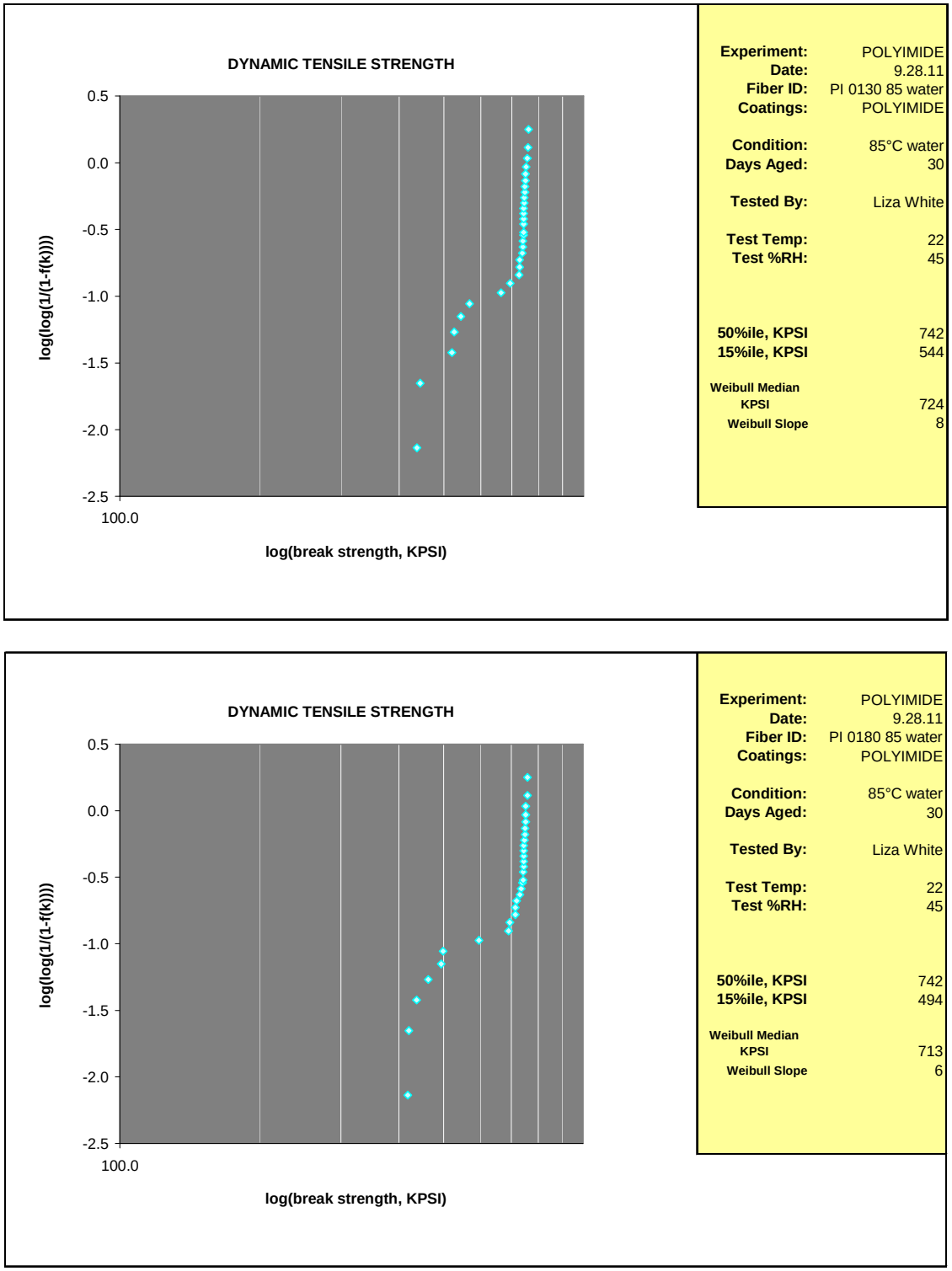

Figure 55: Tensile strength after 30 days in 85°C water.

Aged 1000 hours 300°C

Tensile strength after aging 1000 hours at 300°C is shown in Figure 56.

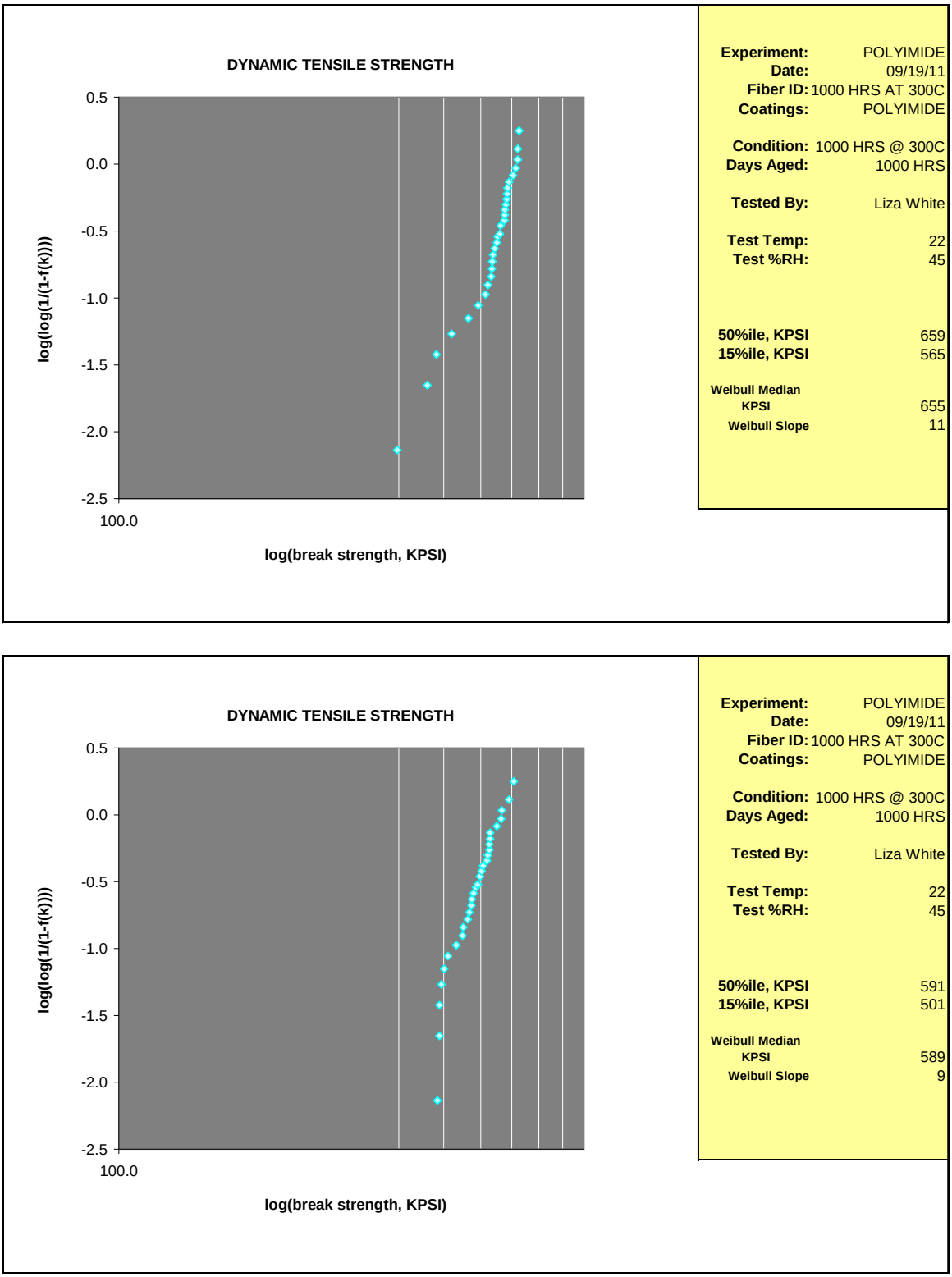

Figure 56: Tensile strength after 1000 hours at 300°C

Stress Corrosion Factor

The stress corrosion factors for the two fibers were measured before aging and after the same treatments covered in tensile strength.

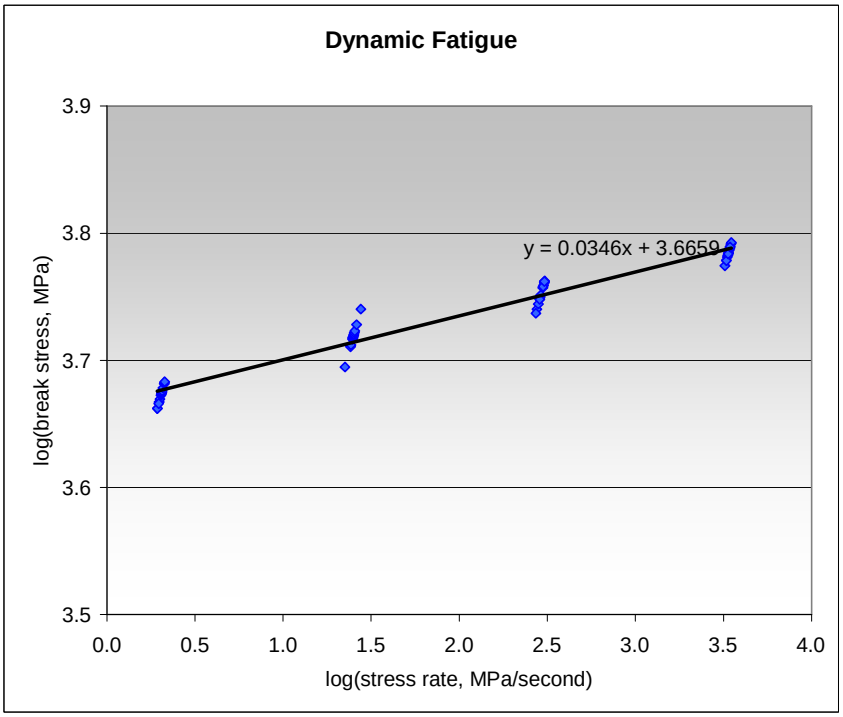

Fiber ID	Draka HT Polyimide Coarted Fiber
Color	
Primary	
Secondary	
Test Date	05/11/11
Tested by	Liza White
Temperature, °C	23
Humidity, %RH	50
n-value	28.0
Upper 95% limit	29.8
Lower 95% limit	26.4

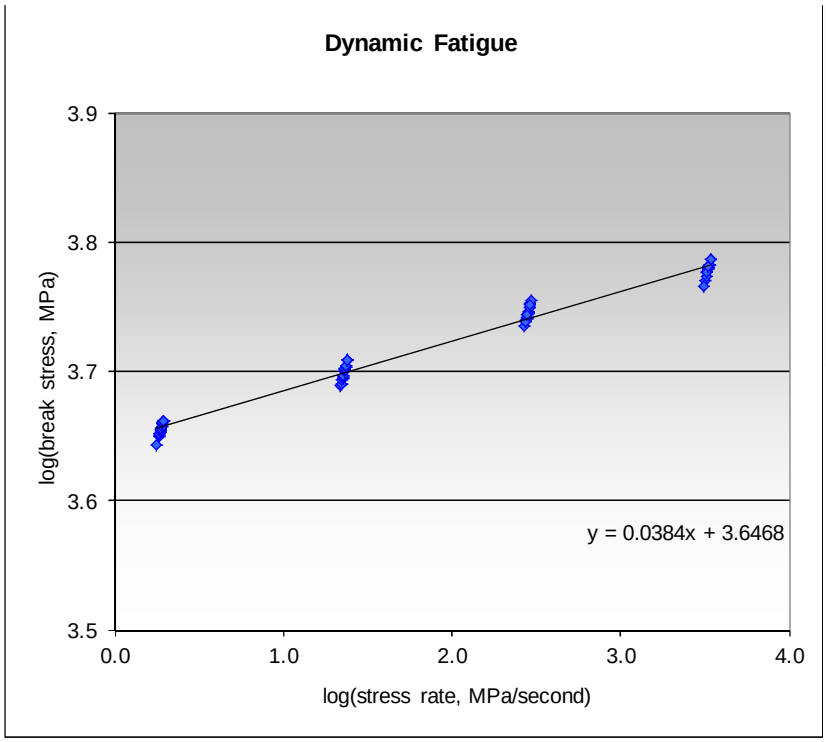

Fiber ID	Commercial PI Fiber
Color	
Primary	
Secondary	
Test Date	05.13.11
Tested by	BJO
Temperature, °C	23
Humidity, %RH	50
n-value	25.0
Upper 95% limit	25.9
Lower 95% limit	24.2

Figure 57: Stress corrosion factors obtained from the dynamic fatigue tests.

Dynamic Fatigue 85°C/85% RH Aged

The dynamic fatigue curves for polyimide fibers after 30 days damp heat aging are shown in Figure 58.

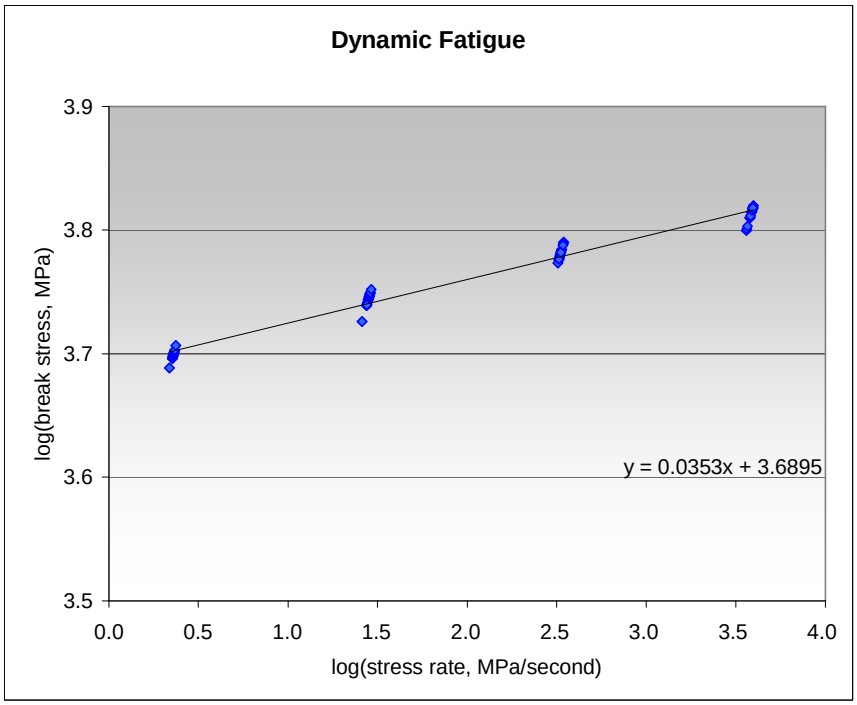

Fiber ID	PI 0130 85/85
Color	
Primary	
Secondary	
Test Date	09.30.11
Tested by	Liza White
Temperature, °C	23
Humidity, %RH	50
n-value	27.3
Upper 95% limit	28.4
Lower 95% limit	26.3

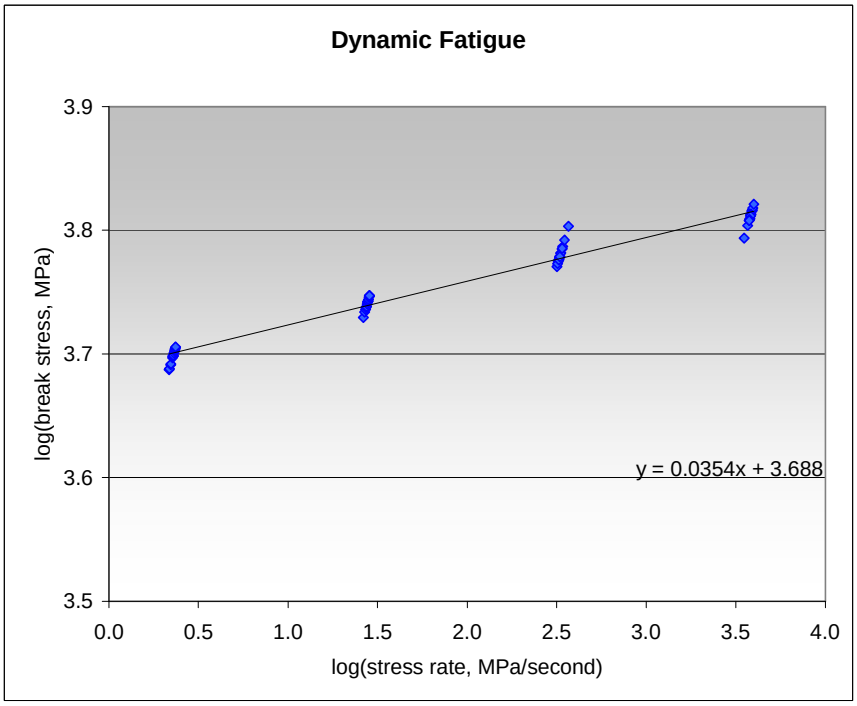

Fiber ID	PI 0180 85/85
Color	
Primary	
Secondary	
Test Date	09.30.11
Tested by	Liza White
Temperature, °C	23
Humidity, %RH	50
n-value	27.3
Upper 95% limit	28.5
Lower 95% limit	26.1

Figure 58: Dynamic fatigue for damp heat aged PI fibers.

Dynamic Fatigue 85°C Water Aged

The dynamic fatigue curves for polyimide fibers aged 30 days in 85°C water are shown in Figure 59.

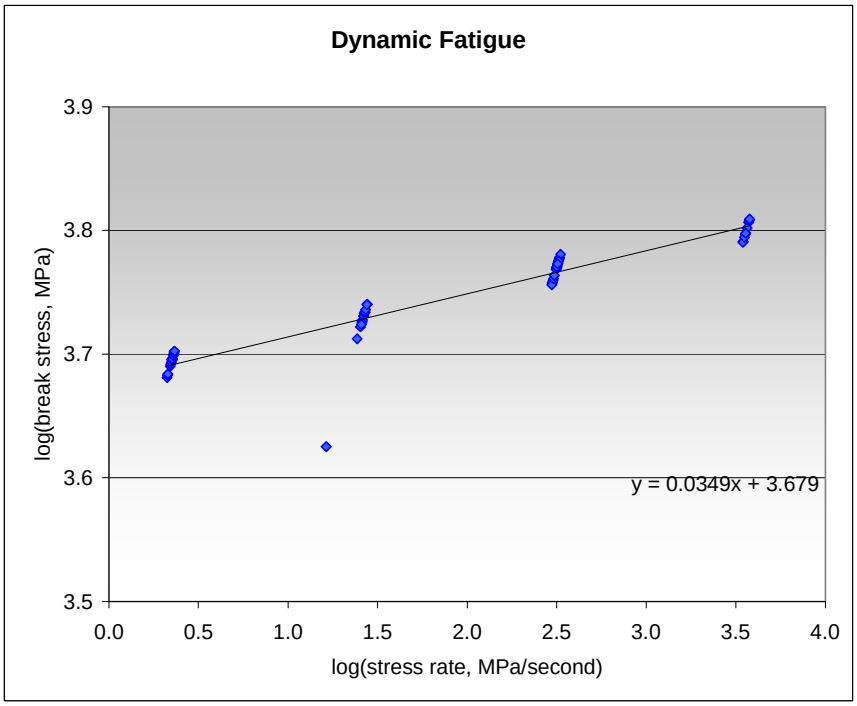

Fiber ID	PI 0130 85 Water
Color	
Primary	
Secondary	
Test Date	09.30.11
Tested by	Liza White
Temperature, °C	23
Humidity, %RH	50
n-value	27.7
Upper 95% limit	30.8
Lower 95% limit	25.2

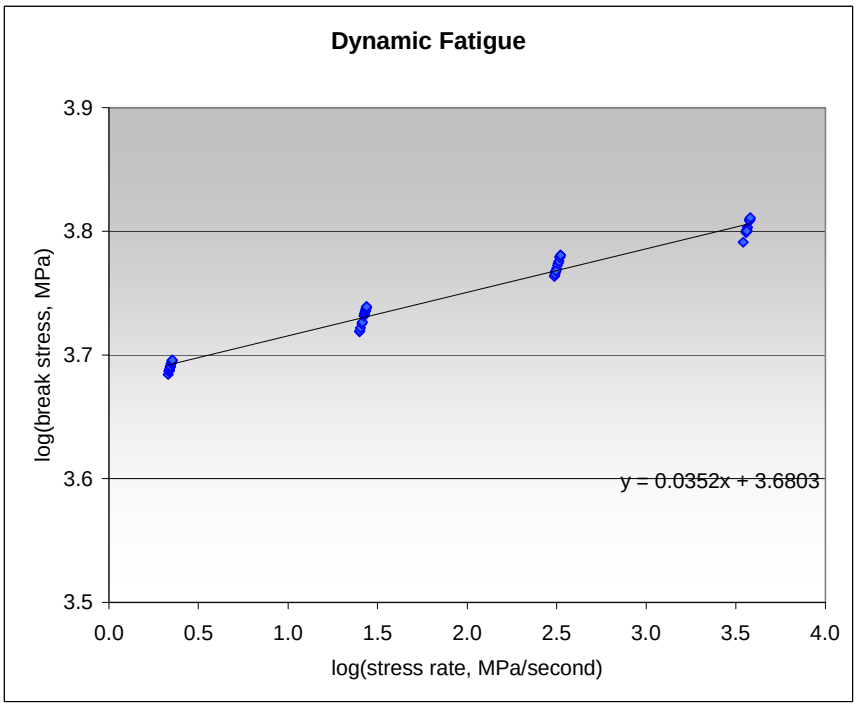

Fiber ID	PI 0180 85 Water
Color	
Primary	
Secondary	
Test Date	09.30.11
Tested by	Liza White
Temperature, °C	23
Humidity, %RH	50
n-value	27.4
Upper 95% limit	28.5
Lower 95% limit	26.5

Figure 59: Dynamic fatigue for 85°C water aged PI fibers.

Dynamic Fatigue 300°C Aged

Dynamic fatigue curves for fibers aged 1000 hours at 300°C are shown in Figure 60.

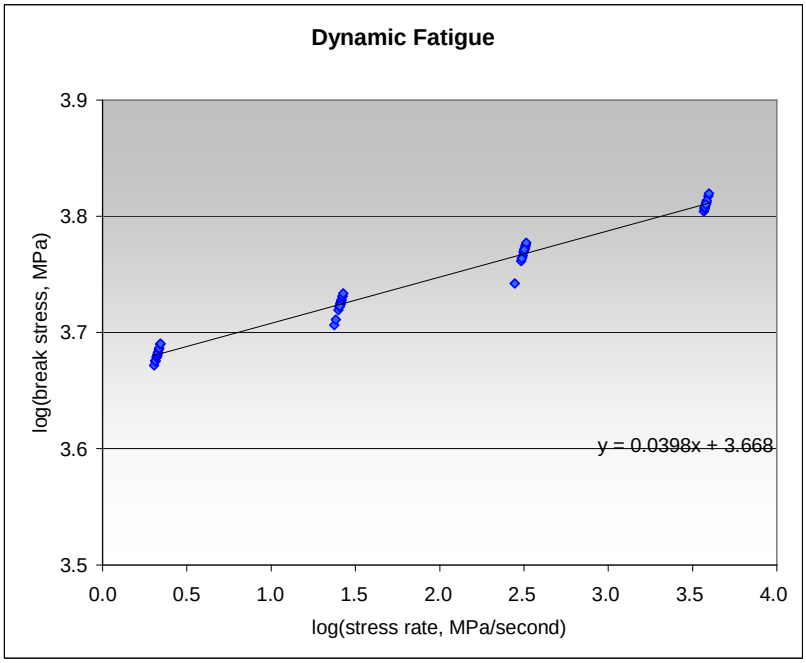

Fiber ID	PI 0180 1000 hrs @ 300°C
Color	
Primary	
Secondary	
Test Date	09.30.11
Tested by	Liza White
Temperature, °C	23
Humidity, %RH	50
n-value	24.1
Upper 95% limit	24.9
Lower 95% limit	23.3

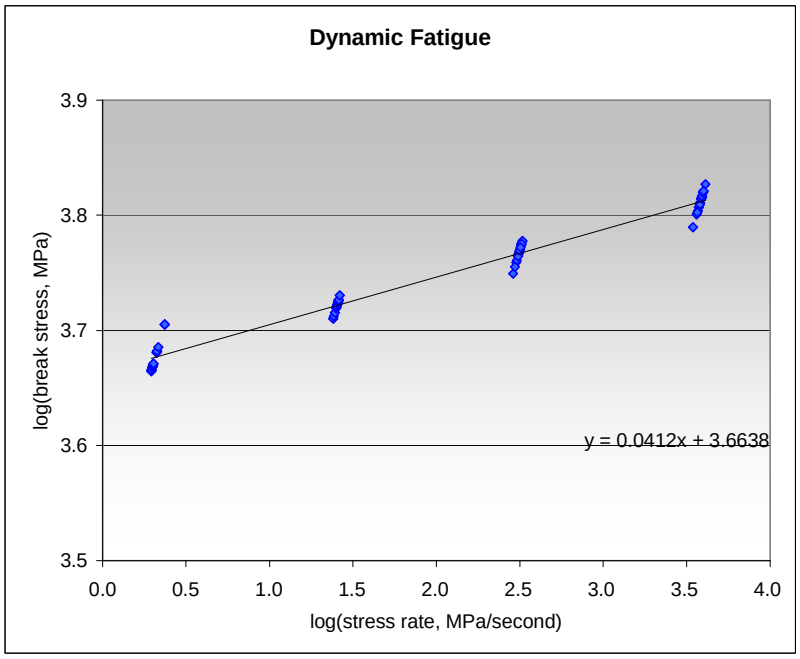

Fiber ID	PI 0130 1000 hrs @ 300°C
Color	
Primary	
Secondary	
Test Date	09.30.11
Tested by	Liza White
Temperature, °C	23
Humidity, %RH	50
n-value	23.2
Upper 95% limit	24.4
Lower 95% limit	22.2

Figure 60: Dynamic fatigue for 300°C aged PI fibers

Summary

A summary of the strength and fatigue parameters before and after aging is given below.

Tensile Strength		50%, kpsi	15%, kpsi	50%, Gpa	15%, Gpa
	GR-20 unaged	550	455	3.80	3.14
	GR-20 aged	440	400	3.03	2.76
Fiber 1	Unaged	749	733	5.17	5.06
	85°C/85% RH	728	614	5.02	4.23
	85°C Water	742	544	5.12	3.75
	300°C (1000 hrs)	659	565	4.54	3.90
Fiber 2	Unaged	747	730	5.15	5.03
	85°C/85% RH	737	622	5.08	4.29
	85°C Water	742	494	5.12	3.41
	300°C (1000 hrs)	591	501	4.08	3.46

Dynamic Fatigue		n_d		
	GR-20 unaged	18 minimum		
	GR-20 aged	18 minimum		
		n_d	UCL95%	LCL95%
	Unaged Avensys Control	24.9	25.8	24.0
Fiber 1	Unaged	28.0	29.8	26.4
	85°C/85% RH	27.3	28.4	26.3
	85°C Water	27.7	30.8	25.2
	300°C (1000 hrs)	23.2	24.4	22.2
Fiber 2	Unaged	-	-	-
	85°C/85% RH	27.3	28.5	26.1
	85°C Water	27.4	28.5	26.5
	300°C (1000 hrs)	24.1	24.9	23.3

Table 15: Tensile Strength and Dynamic Fatigue after aging.

2.3.7 Conclusion

A new, advanced high temperature polyimide coating system has been developed for the geothermal fiber optic cable featuring the highest resistance to thermo-oxidative degradation of any polymer coating system. Fibers with this coating are projected to have a five year lifetime in air at 300°C, demonstrated to survive 60 days or more (for multimode fiber, significantly longer for singlemode fiber) in air at 350°C. If the cable protection limits environmental oxygen to very low concentrations, the fiber can be expected to survive 374°C for 60 days or longer.

2.4 TASK 3: FIBER TESTING AND VALIDATION

Generally, hydrogen tests are made to study irreversible HIL due to hydrogen by using accelerated ageing conditions in terms of temperature and hydrogen partial pressure, in order to

limit exposure time. For GFOC applications, the situation is strongly different as real external conditions are almost impossible to reach by using experimental hydrogen tests.

The goal of hydrogen tests in GFOC is then firstly to help in screening specific glass compositions and coatings able to resist to severe temperature (up to 300°C) and strong hydrogen partial pressure (up to several tens of atmospheres) in conditions as close as possible to the ones that will be experienced by the fibers in cable, secondly to give data input helpful in building specific ageing models for high temperature/high pressure conditions.

For this, different hydrogen tests have been considered, taking into account GFOC Consortium experiences and capabilities in this field.

Low hydrogen pressure (0.01 atmosphere of hydrogen) / high temperature (150°C and 300°C) hydrogen tests have been involved both in off-line and in-line versions. They give practical information while being much easier to realize then their high pressure counterparts. It notably allows:

- To study hydrogen sensitivity of optical fibres at high temperatures (>150˚C) and give an approximation of the hydrogen effects under high pressures. Indeed, temperature is the main parameter that defines reactions of hydrogen with glass, as high pressure only increases the HIL level.
- To screen the different glass fiber compositions and define the best candidates for high hydrogen pressure tests.
- To give information on thermal resistance of coating before launching high pressure tests.

High pressure (up to 15 hydrogen atmospheres) / high temperature (150°C and 300°C) hydrogen tests have been involved both in off-line and in-line versions. It allows:

- To evaluate hydrogen sensitivity of optical fibers (singlemode and multimode) in environment representative of the requirements for EGS systems.
- To give comprehensive interpretation and technical elements to be diffused and exploited (intermediary performances, final conclusions).
- To orient final choice of fiber composition and coatings versus application.
- To support Prysmian's proposal on complete fiber/copper cable solution for long-term temperature and pressure measurement in supercritical reservoir and EGS Wells.
- To develop new ageing models taking into account reversible HIL due to hydrogen presence in fiber core.

2.4.1 Development of Test Procedures

To be efficient, the different hydrogen tests have been organized in different locations as shown in Figure 61 below:

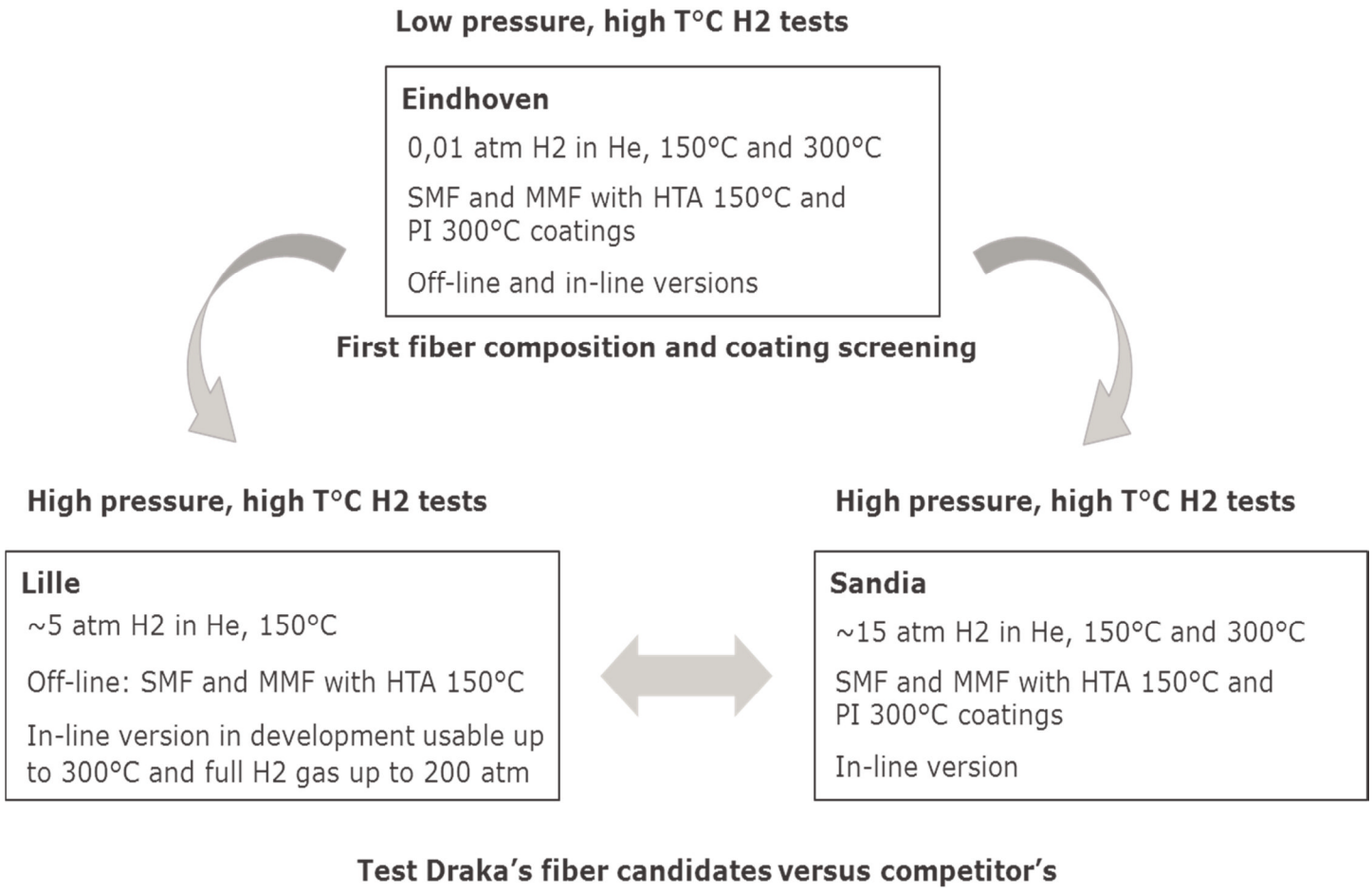

Figure 61: Location and characteristics of hydrogen tests organized for GFOC Project

To prevent bottle-neck in this part during the project, experiments have been run in parallel in Eindhoven, Lille University and Sandia Labs.

Eindhoven place has the experience and equipment adapted to the realization of low pressure hydrogen tests for singlemode and multimode fibers:

- Specific equipment has been dedicated to the realization of hydrogen tests for the GFOC project needs.

Complementary high pressure, high temperature hydrogen tests have been conducted in Lille University, which has the capability of doing off-line pressurized tests at 150°C:

- High pressure hydrogen tests within Prysmian are not possible to perform; therefore a key requirement for success has been the establishment of an external partnership with Lille University that are used to perform these tests.
- To fulfill the requirements, hydrogen test apparatus has been adapted.
- Lille University has also begun to develop during the Project capabilities to realize high pressure hydrogen tests up to 200 atmospheres of pure H2 at 300°C to increase possibilities to study hydrogen behavior in optical fibers under severe conditions.

The Geothermal Research Department at Sandia National Laboratories (Sandia) is considered to have the best facilities for evaluating fiber for EGS. Sandia has tested hydrogen insensitive candidate singlemode and multimode fibers at temperatures up to 300°C in a pressurized environment containing hydrogen at the appropriate concentrations to simulate a geothermal well.

- Prysmian has provided the fibers for the tests and worked with Sandia to develop a test procedure compatible with Sandia's testing facility that meets the goals of the proposal.

Hydrogen test procedures have been defined for the different set-ups in Eindhoven, Lille University and Sandia Labs.

Eindhoven: Low hydrogen pressure, high temperature tests

Testing capabilities, testing setup, and test procedures at the Eindhoven facility are shown below in Table 16, Figure 62, and Table 17 respectively.

Parameter	**Test capability**	**Remarks**
Gas	1% H_2 in He	Grade 2.2 supplier Hoekloss.
Pressure	1 bar	Low pressure for safety reason
Temperature ***(T_{target})***	<300°C	300°C is the maximum temperature of the furnace
Test duration ***(t)***	Approximately 150hrs	Test can run for any time but 150hrs is the standard test duration
Optical measurement	1 fiber online, 1 fiber offline	Data are collected and stored in an Excel file for analysis.

Table 16: Test Capabilities at Eindhoven

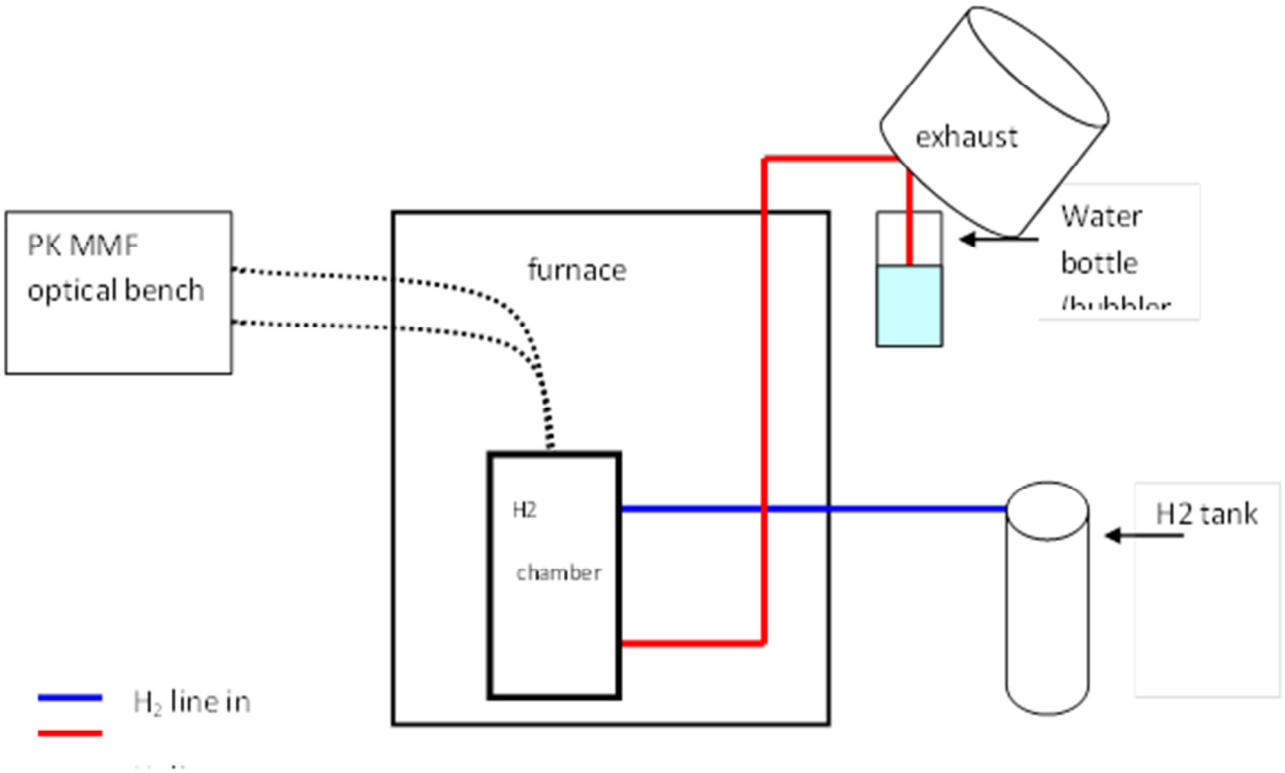

Figure 62: Schematic of Test Setup at Eindhoven

Step	Action to realize
1	Rewind 1000 m of fiber on a metal collapsing spool. Leave approximately 5 m from both ends for optical measurements.
2	Place the metallic spool inside the hydrogen chamber, collapse the spool and carefully close the chamber. Make sure to leave 5 m of fiber out of the chamber.
3	Seal the fiber pinhole with high temperature epoxy.
4	Verify that the hydrogen line-out is in the water bottle below the exhaust.
5	Measure the attenuation of the fiber using the cut-back method. (Save the files as before at 23°C)
6	Turn the furnace on.
7	Wait until T_{target} is reached (approximately 30min). Verify that all fumes are collected by the exhaust. Otherwise, place the exhaust in the correct position.
8	Wait 24 hrs for reaching T_{target} temperature inside the chamber.
9	Measure the attenuation using the cut-back method. (Save the files as: before@T_{target}°C)
10	Connect the online fiber to the PK bench and fix the offline fiber on a safe surface.

11	Use the fence to limit access to the setup.
12	Wait 4 hours for the online fiber to stabilize.
13	Run the online measurement program.
14	After the first online measurement, flush the chamber with hydrogen.
15	Set a low and constant flow of hydrogen
16	Stop online measurement program when target time (*t*) is reached.
17	Measure attenuation using the cut-back method. (Save the files as: after@T_{target}°C)
18	Turn furnace and hydrogen off and wait 24hrs for cooling down to room temperature.
19	Measure attenuation using the cut-back method. (Save the files as: after@23°C)
20	Remove the fibers from the chamber and tidy up the set-up.
21	If possible rewind the fibers on spool and store
22	Analyze test data and make plots.

Table 17: Test Procedure

Safety and Environmental Considerations and Precautions:

- Gas cylinder is fixed to the wall according to Eindhoven safety procedures.
- Hydrogen concentration used in this test (1% in He) is below the explosion limit of hydrogen (4%) for safety reasons. The use of this gas has been approved by the safety group in Eindhoven.
- Hot zones may present a risk. Use safety gloves and glasses when operating the equipment.
- A fence is used to limit access to the setup when furnace is on. Safety notices are visible.

Lille: High hydrogen pressure, high temperature tests

Testing capabilities, testing setup, and test procedures at Lille University are shown below in Table 18, Figure 63, and Table 19 respectively.

Parameter	**Test 1**	**Test 2**	**Remarks**
Gas	3% H_2 in Ar	100% H_2	Grade 2.2
Pressure *(P_{target})*	<300 bar	<300 bar	Chamber's maximum operational pressure
Temperature *(T_{target})*	<400°C	<110˚C	
Test duration *(t)*	Approx 150hrs	Approx 150hrs	Test can run for any time but 150hrs is the standard test duration
Optical measurement	2 fibers offline	2 fibers offline	Data is collected and stored in an Excel file. Data is available for analysis.

Table 18: Testing Capability

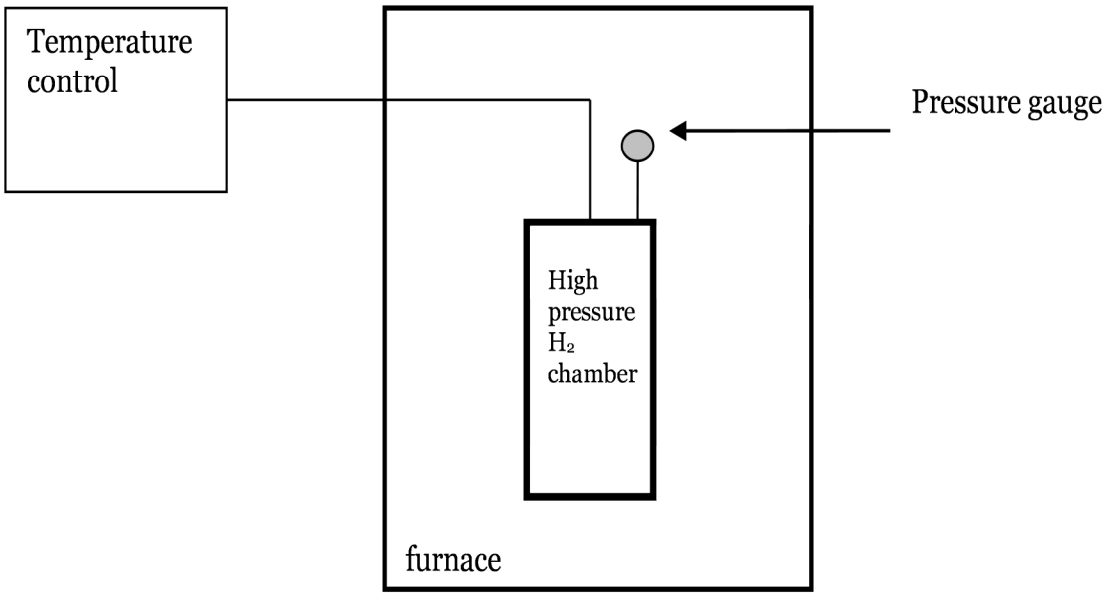

Figure 63: Schematic of hydrogen test setup at Lille University

Step	Action to realize
1	Deliver fibers will to Lille University on plastic shipping spools.
2	Rewind approximately 1000 m of fiber on a 5cm metal spool.
3	Measure attenuation from 850-1700nm using the cut-back method, white light source and OSA.
4	Place the metallic spool inside the high pressure hydrogen chamber, seal the chamber following standard procedure.
5	Fill the chamber with hydrogen gas at room temperature and pressure *P*. (*P* will be experimentally determined to obtain P_{target} at T_{target}.)
6	Place the chamber inside the furnace.
7	Ramp the temperature 5˚C/minute until reaching T_{target}.
8	Leave the fiber in the chamber for *t* hours.
9	Turn off the furnace and wait 24 hrs to cool down.
10	Remove the spools from the hydrogen chamber. At this moment hydrogen out diffusion starts.
11	Measure attenuation from 850-1700nm using the cut-back method, white light source and OSA. Please perform this measurement within 1 hour after removing spool from the chamber to limit hydrogen out diffusion.
12	If possible rewind the fibers on shipping spools and send them back to Eindhoven.
13	Save attenuation measurements on Excel file.

Table 19: Test Procedure

Sandia Labs: High hydrogen pressure, high temperature tests

Sandia Labs in New Mexico is the acknowledged experts for testing of optical fiber at high temperature /high hydrogen pressure. Sandia has performed validation tests using an interrogation box supplied by Prysmian. Sandia have performed fiber tests and discussed results with Prysmian.

Testing capabilities, testing setup, and test procedures at Sandia Labs are shown below in Table 20, Figure 64, and Table 21 respectively.

Parameter	**Test capability**	**Remarks**
Gas	5% H_2 in Ar	
Pressure (P_{test})	< 5kpsi	Pressure rating of the autoclave
Temperature (T_{target})	<600°C	600°C is the maximum temperature of the furnace
Test duration (t)	Approx 300hrs	Test can run for any time but 300hrs is the standard test duration
Optical measurement	2 test fibers online, 1 reference fiber online	Data is collected and stored in an Excel file. Data is available for analysis.

Table 20: Test Capabilities

A special test configuration was built for conducting these tests. This test configuration has reproduced the test configuration described by Normann *et al*[3]. A schematic of the test configuration is shown in Figure 10 below. All test fibers see the exact same environment within the autoclave and the same broadband light source. To insure the light source is not changing over time, a calibration fiber is used. This calibration fiber does not enter the autoclave but instead, simply connects the lamp to the spectrum analyzer. The fiber bundle from the light source to the patch panel was never disconnected once testing was started. This greatly reduced the chance of connector induced error.

[3] Normann. R. *et al.* "Development of fibers optic cables for permanent geothermal wellbore deployment" *Proceedings of 26th workshop on Geothermal reservoir Engineering*, 2001.

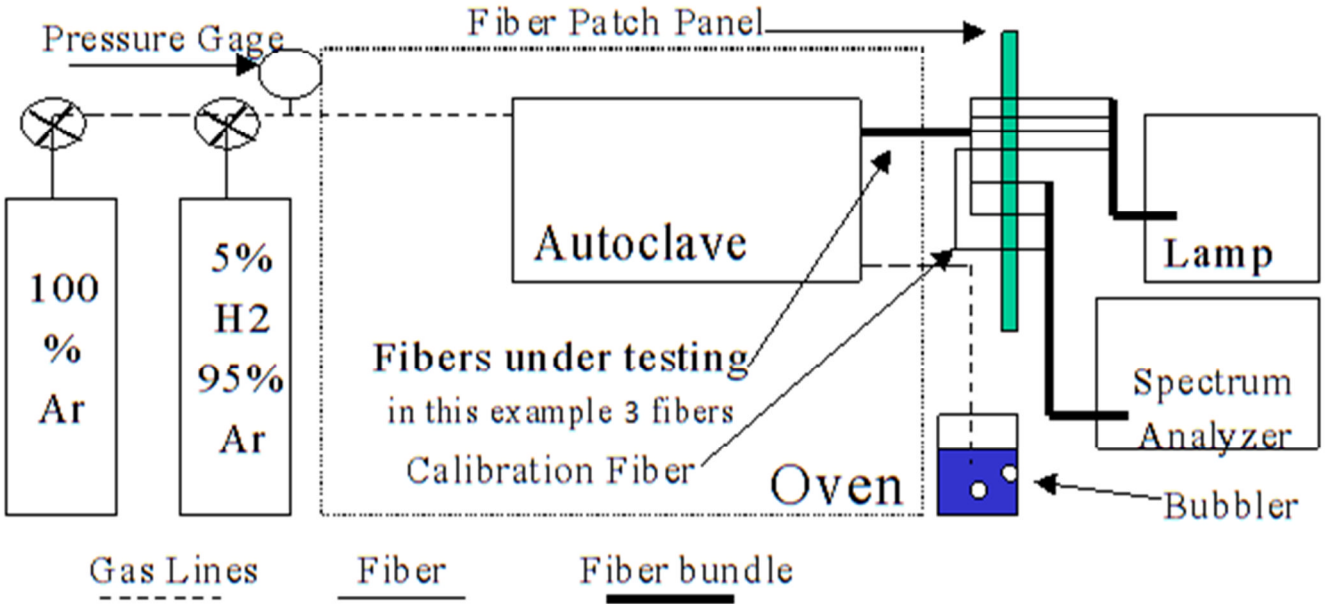

Figure 64: Shematic of Test Configuration at Sandia Labs

Test configuration for hydrogen exposure of optical fibers. Here 3 fibers (2 test fibers and 1 reference fiber) are being tested in 5% hygrogen gas. A temperature probe is located inside the autoclave.

Step	Action to realize
1	Clean the autoclave and matching hardware and then bake at 250°C for 24 hrs to remove any cleaning materials.
2	Rewind 500 ft of test fibers on metallic spools. Rewind 200 ft of reference fiber on metallic spool. The reference fiber is a hydrogen sensitive fiber that will be used to demonstrate that the test fibers have been exposed to hydrogen. The same reference fiber will be used in all the tests at Sandia.
3	Place the metallic spools inside the H_2 autoclave and carefully seal it.
4	Connect the 2 test (reference and calibration) fibers to the broadband source and OSAs.
5	Measure the attenuation of the fibers in the wavelength window 600-1700nm. Save the files as: attenuation before_hydrogen_room_temperature.
6	Purge the autoclave with 10 volumes of argon gas prior to heating.
7	Bring the autoclave to test temperature (T_{target}), increase the temperature at rate of 20°C/hr.
8	Once at temperature wait 24 hrs and take attenuation measurement. Save the file as: attenuation_before_hydrogen_ T_{target}.
9	Start online measurements; periodically taking spectrum readings (every 30 min.)
10	Expose the fibers at P_{test} partial pressure of hydrogen with 5% hydrogen in Ar gas.
11	Stop online measurement program when target time (t_{test}) is reached.
12	Measure attenuation; Save the files as: after_hydrogen_T_{target}
13	Turn furnace and bring autoclave to atmospheric pressure, flush the autoclave with Ar. Wait 24hrs for cooling down to room temperature.
14	Measure spectral attenuation; save the files as: after_hydrogen_at 23°C.
15	Remove the fibers from the chamber.
16	Save all data in an Excel file, send file to Prysmian.
17	Send fibers to Eindhoven for other tests.

Table 21: Test Procedure

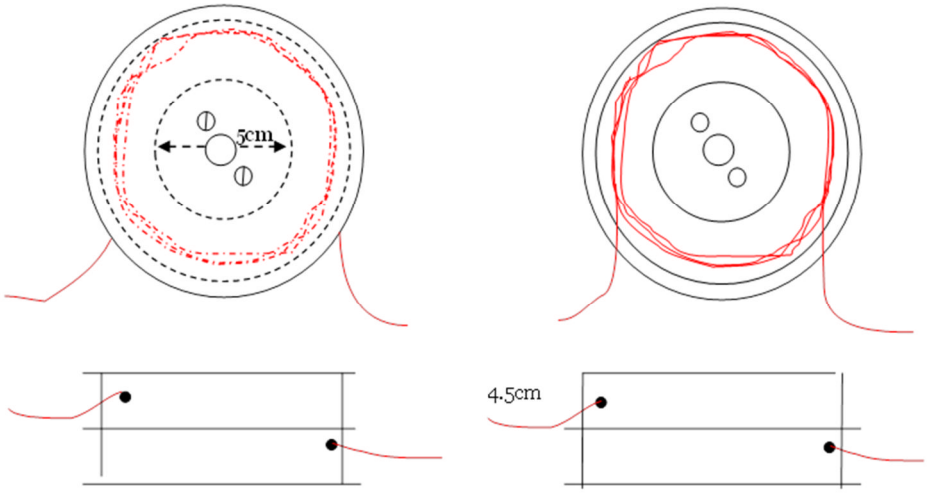

Fiber box for high temperature (>300°C) hydrogen tests

To do the fiber testing at temperature near 300°C, polyimide (PI) high temperature resistant coating coating was chosen to protect fiber. PI being a rather hard coating, the steel wool spools developed for the HTA-150°C coating can't be used as it would cause too much micro bending to be able to measure the PI coated fibers after hydrogen test. To solve this problem, a new fiber box has been designed where the fiber is lying loose, to prevent micro bending.

Resistance against temperature and material lightness is ensured by using aluminum. Moreover, as the same boxes will be used on all sites, the dimensions of the test chamber of Sandia (diameter 10.5cm max and a height of 28.9cm, so that 6 boxes can fit in) was taken as a reference. The box is however designed as wide as possible so that fiber will lose in the box with minimal micro bending. The box has a center hole, so it can be put on a rod for lowering one or more boxes at once, into the test chamber. Lastly, the outside of the box has two grooves where the fiber can be winded for transport. Figures 65 and 66 show a schematic and photographs of the box respectively.

Figure 65: Schematic of fiber box.

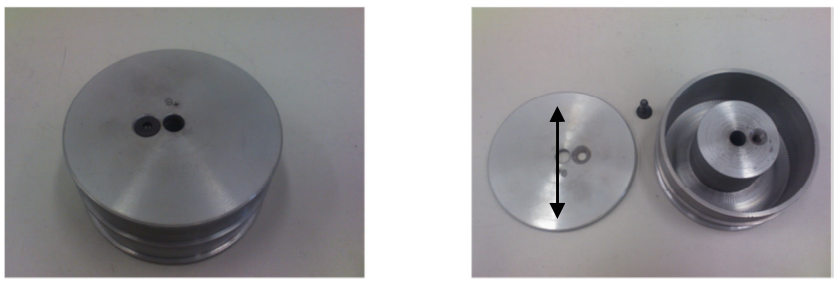

Figure 66: Photograph of the fiber box

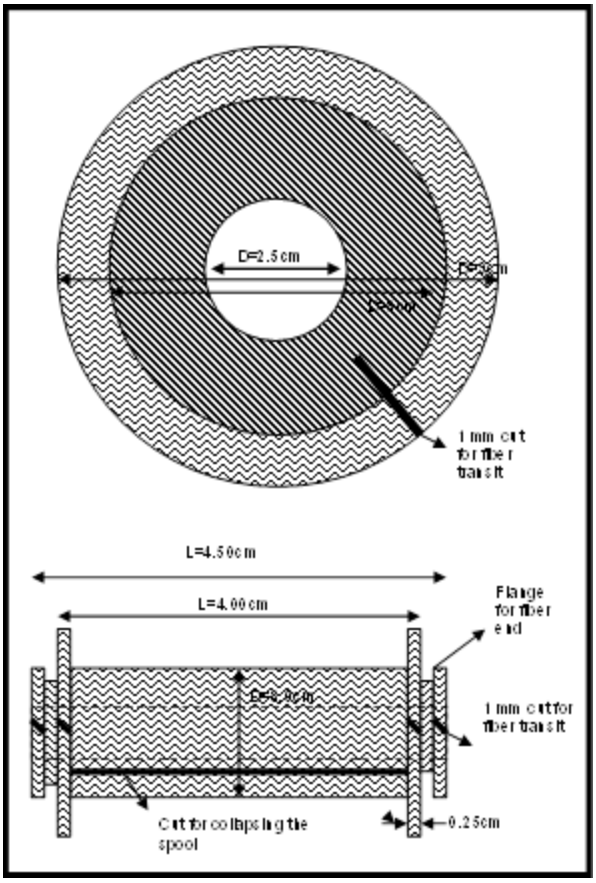

The Collapsible spool

A collapsible spool for filling the boxes was also designed. This spool has the same design as the INOX spools, used for testing HTA coating. But this one is synthetic and the inner ring is collapsible. Figures 67 and 68 illustrate the collapsible spool in photograph and schematic respectively.

Figure 67: The collapsible spool

Figure 68: Schematic of the Collapsible Spool

Table 22 gives the procedure to fill the fiber box.

Step	Action to realize
1	Wind the desired fiber length for the test on the collapsible spool. Make sure you have 5 – 10 m on the outer ring, so you can reach the measurement equipment outside the oven and if necessary do some extra measurements.
2	Open the box.
3	Unwind 5 – 10m from the top of the collapsible spool and secure the fiber so it can't unwind further.
4	Pull the fiber from the inside out through the lower fiber gap from the box.
5	Remove the bolt from the collapsible spool and remove the flange with no fiber.
6	Place the rest of the collapsible spool on top of the fiber box, so that the fiber and collapsible ring go inside the box.
7	Unwind the fiber from the flange.
8	Hold the fiber, so it can't unwind out of the box, and remove the flange and collapsible ring.
9	Pull the fiber end coming from the flange from the inside out through the upper fiber gap.
10	Close the box.
11	Fixate both out coming fiber with high temperature PI-tape to the box. This to prevent pulling fiber out of the box. This tape can be left there during testing.
12	For transport wind both fiber ends on the outside of the box and fixate again with PI-tape.

Table 22: Procedure to fill the fiber box

2.4.2 Validation Tests

Variable fiber parameters for hydrogen tests

The Table 23 below summarizes the main parameters that have been varied on fiber in order to develop reliable hydrogen tests and to define the right glass composition for singlemode and multimode fibers to be used in GFOC application.

Variable parameter	Qualitative or quantitative argument	Comments
Fiber type	Singlemode; multimode	Two different application resulting in different glass optimization
Coating	High Temperature Acrylate (HTA-150°C); polymimide (PI)	Ability to resist to hydrogen test temperature without microbending losses issue due to coating
% Germanium in core	0-16 weight % in glass	Evaluate influence of glass composition on irreversible HIL
Test Temperature	150°C; 250°C; 300°C	Evaluate reversible and irreversible HIL prints with temperature
Hydrogen partial pressure	0.01 atm; ~5 atm; ~15 atm	Extrapolate HIL prints level towards GFOC values
Test condition	Off-line; in-line	Evaluate HIL shape and level evolution at different wavelengths versus time
Test duration	120h to 800h	

Table 23: Variable parameters for hydrogen tests

Low hydrogen pressure tests

More than 30 tests have been realized under low hydrogen pressure, most of them being under in-line conditions.

The first purpose of these tests was to be sure of coating resistance under high temperatures and to define fiber conditioning during test that ensure no fiber breakage and/or microbending issues after test. These points are crucial to check before launching time and cost consuming high pressure in-line hydrogen tests:

- A new high temperature acrylate coating (HTA) has been adapted for tests to be realized at 150°C. This coating has been involved for fibers tested in high pressure off-line hydrogen tests made in Lille University.
- For tests to be realized at 300°C polyimide coating (PI) could be validated, however, tests results showed that with hard coating specific tensionless fiber conditioning must be involved to avoid microbending issues. Consequently, a specific fiber box has been designed to allow this kind of handling and testing.

The second purpose was to select fibers and temperatures to be tested under high hydrogen, particularly at Sandia Labs (in-line).

The following Tables 24 and 25 present the selected multimode and singlemode fibers, according to results of hydrogen tests in Eindhoven.

MMF	Origin	Coating	Wt% Ge in core	Test temperature
1	Competitor	PI/Carbon	-	150°C ; 300°C
2	Draka	HTA-150°C	7.5	150°C
3	Draka	HTA-150°C	12	150°C
4	Draka	PI	0	300°C
5	Draka	PI	7.5	150°C ; 300°C
6	Draka	PI	9.5	300°C
7	Draka	PI	12	300°C

Table 24: Selected MMF and temperatures for high hydrogen pressure in-line tests

SMF	Origin	Coating	Wt% Ge in core	Test temperature
1	Draka	HTA-150°C	0	150°C
2	Draka	HTA-150°C	8	150°C
3	Draka	HTA-150°C	16	150°C
4	Draka	PI	0	300°C
5	Draka	PI	8	300°C
6	Draka	PI	16	300°C

Table 25: Selected SMF and temperatures for high hydrogen pressure in-line tests

2.4.3 Prototype Screening Fiber Tests

High hydrogen pressure tests

Five 150-170h tests have been realized in pressurized atmosphere (representing ~5 atm of hydrogen partial pressure) both on singlemode and multimode fiber. A maximum of 3 fibers could be tested off-line at the same time. These off-line hydrogen tests were conducted at 150°C in Lille University.

All tests are summarized in Table 26 below:

Fiber	Test 1	Test 2	Test 3	Test 4	Test 5
Multimode (MMF)					
Draka MMF 0 wt% Ge HTA	x	x	x	x	x
Draka MMF 1.5 wt% Ge HTA		x			
Draka MMF 1.8 wt% Ge HTA	x				
Draka MMF 3.3 wt% Ge HTA	x				
Draka MMF 5 wt% Ge HTA		x			
Draka MMF 7.5 wt% Ge HTA					x
Draka MMF 12 wt% Ge HTA			x		
Singlemode (SMF)					
Draka MMF 5 wt% Ge HTA				x	
Draka MMF 8 wt% Ge HTA					x
Draka MMF 12 wt% Ge HTA			x		

Table 26: high hydrogen pressure tests realized in Lille at 150°C on selected singlemode and multimode fibers

2.4.4 Optimization Fiber Tests

Five 400-500h tests have been realized in pressurized atmosphere (representing ~15 atm of hydrogen partial pressure) both on singlemode and multimode fiber. A maximum of 5 fibers could be tested off-line at the same time. These were in-line hydrogen tests at 150°C and 300°C in Sandia Labs.

All tests are summarized in Table 27 below:

Fiber	Test 1 (300°C)	Test 2 (150°C)	Test 3 (150°C)	Test 4 (300°C)	Test 5 (300°C)
Multimode (MMF)					
Competitor PI + Carbon	x	x	x		x
Draka MMF 0 wt% Ge PI				x	x
Draka MMF 7.5 wt% Ge PI	x	x		x	x
Draka MMF 9.5 wt% Ge PI	x				
Draka MMF 12 wt% Ge PI	x				
Draka MMF 7.5 wt% Ge HTA		x	x		
Draka MMF 12 wt% Ge HTA		x			
Singlemode (SMF)					
Draka SMF 0 wt% Ge HTA			x		
Draka MMF 8 wt% Ge HTA			x		
Draka MMF 16 wt% Ge HTA			x		
Draka SMF 0 wt% Ge PI				x	x
Draka MMF 8 wt% Ge PI				x	x
Draka MMF 16 wt% Ge PI				x	

Table 27: High Hydrogen Pressure Tests realized in Sandia at 150°C and 300°C on selected singlemode and multimode fibers

Irreversible hydrogen sensitivity versus fiber characteristics and external conditions

Results of high pressure and high temperature tests have been used to evaluate optical fiber sensitivity to hydrogen under specific severe conditions.

Irreversible HIL characteristics in the 800-1700nm window have been correlated to the core glass composition (weight % of Germanium) and test temperature (150°C and 300°C). Results are made on fibers after test and full hydrogen out-gassing, which fully eliminates effect of reversible HIL due to hydrogen presence in fiber core.

At this stage, we have considered that results are not significantly influenced by the design (singlemode or multimode) of the fiber but mainly by core glass composition and temperature at a given hydrogen pressure.

Figure 69 below shows that at this temperature the irreversible HIL is mainly driven by hydrogen reactions with silicon defects to form SiOH species which absorb in the 1380-1400nm band. After more than 400h at 15 atm of hydrogen the worst behavior is obtained with pure silica core fiber, while the fiber appears much more hydrogen insensitive if the core is doped by germanium.

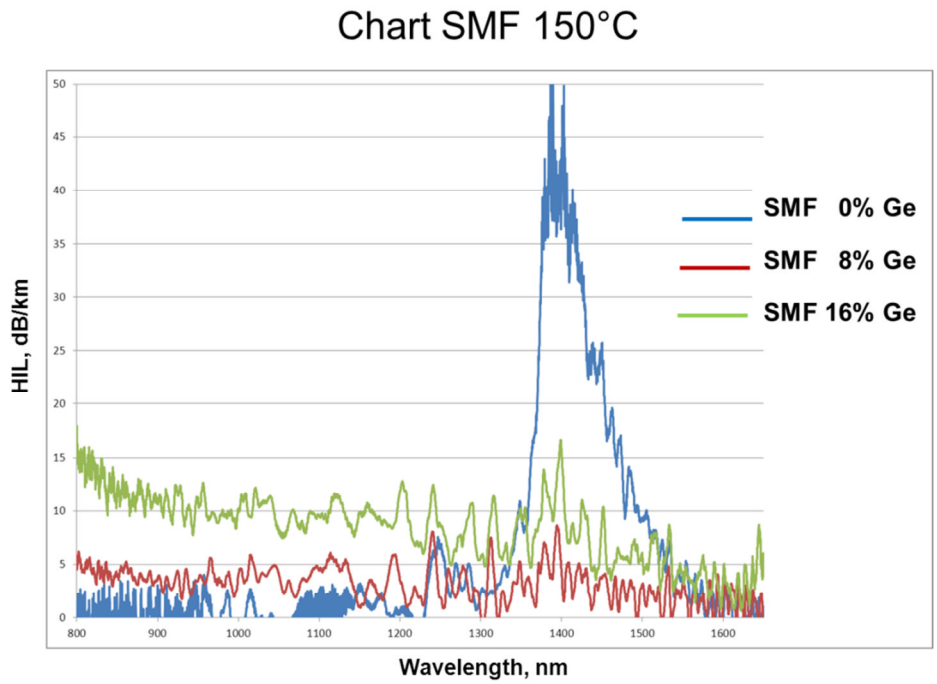

Figure 69: Influence of fiber core composition on hydrogen sensitivity at 150°C

Figure 70 below shows the influence of the fiber core composition at 300°C. We can see that at this temperature, the situation is completely changed compared to what was observed at 150°C.

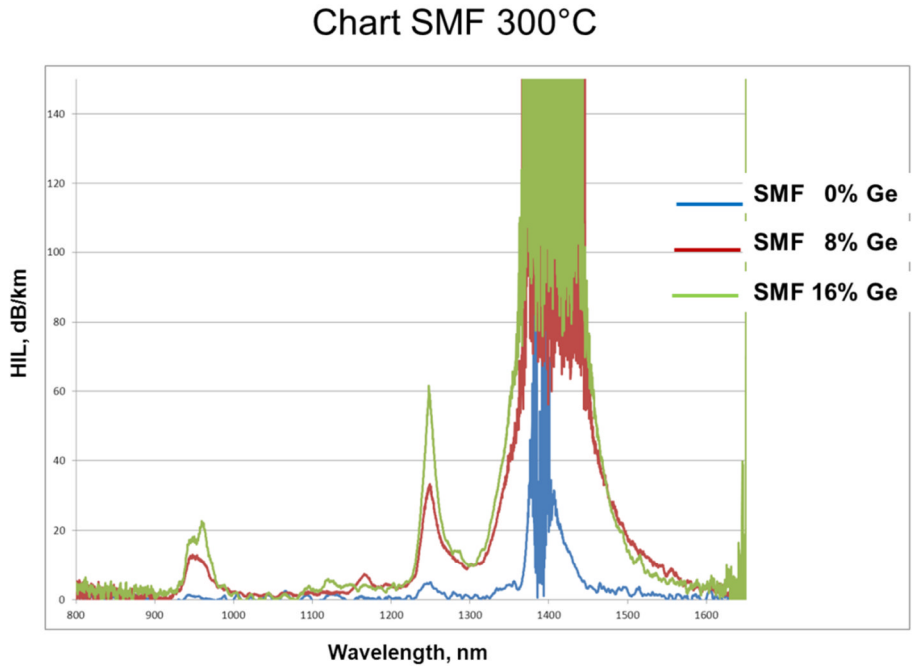

Figure 70: Influence of fiber core composition on hydrogen sensitivity at 300°C

The fibers having germanium in core behave very badly compared to the pure silica one. Moreover, the more the germanium content, the more the fiber is sensitive to hydrogen. In Figure 71 below, we can verify that the effect is similar on multimode fibers.

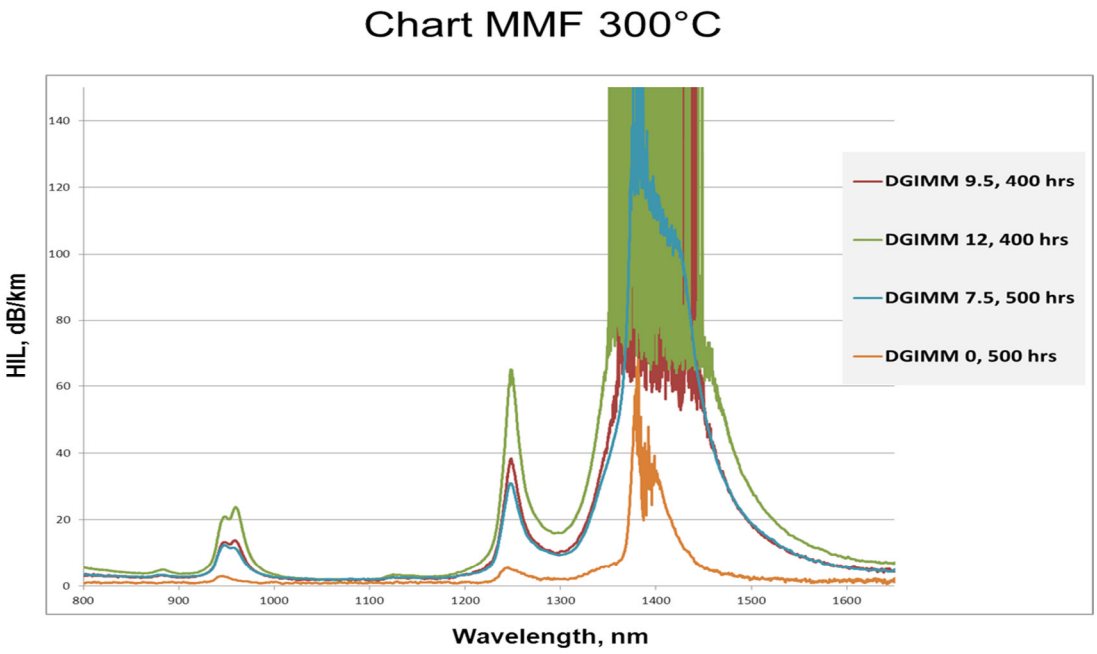

Figure 71: Irreversible HIL due to germanium in multimode fiber at 300°C

The problem is linked to a specific reactivity of hydrogen with germanium network at very high temperature (probably higher than 250°C) giving rise to huge formation of Ge-OH absorbing species. The presence of Ge–Si and Ge–Ge oxygen vacancy in the ideal glass tetrahedral network are notably responsible for this process. The photosensitive property of oxygen-deficient germania defects have been widely exploited to inscribe Bragg grating in hydrogen loaded germanium doped fibers. From these studies, it is known that hydrogen molecules will react in the glass from thermally driven reactions at Si–O–Ge sites, forming OH species and germanium-oxygen deficiency centers[4].

This phenomenon is strong enough to induce some new HIL bands around 950nm and 1240nm corresponding to vibrations related to the main GeOH absorption band around 1410nm.

As far as we could observe, it seems that the effect is not saturable within the conditions of the tests and lead to a complete darkening of the fibers in the 1375-1450nm band. If we consider the tail of this huge HIL band, the impact on fiber attenuation is significant between 1200-1600nm. HIL due to reaction of hydrogen with silica defects seems to be saturable, which limits the impact of hydrogen sensitivity in the 1000-1200nm window.

[4] Andreas Othonos. "Fibre Bragg Grating" *Rev. Sci. Instrum., Vol 68, N°12,* **1997**, p4309-4341.

Development of a model for reversible HIL due to hydrogen presence in core

To be able to evaluate the full HIL impact on fiber attenuation due to hydrogen under GFOC conditions, a critical point is to monitor and simulate the impact of hydrogen molecule presence in fiber core on attenuation in the full 800-1700nm window according to temperature and external partial hydrogen pressure.

A model has been developed that allows calculating the full spectrum shape of hydrogen in glass and thus its reversible HIL impact at any wavelength of interest.

To achieve this result, we had firstly to consider that the overall line shape originates from the sum of all the individual hydrogen molecule vibrations which are also controlled by its environment and temperature. There are several models that can be involved to monitor vibration band shape. The Gaussian profile works well for solid samples, as the Lorentzian profile works best for gases. We have considered that for gas trapped in a solid glass environment at high temperatures, the line shapes should have features of both Gaussian and Lorentzian character. In this case, the model had to take into account a combination of these two components.

Figure 72 below shows the model that has been defined to simulate reversible HIL due to hydrogen according to wavelength, temperature, external hydrogen partial pressure and time.

$$HIL(\lambda,T,p,\tau) = HIL_{1240}(T,p,\tau)\cdot\sum_{i=1}^{n} I_{\lambda_i,norm}(T)\left(A(T)\cdot\exp\left(-0.5\cdot\left(\frac{\lambda_i-\lambda}{a_{\lambda_i}(T)}\right)^2\right)+\frac{B(T)}{\left[1+\left(\frac{\lambda_i-\lambda}{a_{\lambda_i}(T)}\right)^2\right]}\right)$$

$$\text{where} \quad I_{\lambda_i,norm} = \frac{I_{\lambda_i}(T,p,\tau)}{I_{1243}(T,p,\tau)} = f(T)$$

Figure 72: Expression of reversible HIL model due to hydrogen molecule in glass

The model validity has been checked by using an in-line hydrogen test realized at 150°C on multimode fiber without germanium in core. Indeed, at this temperature, the bands due to hydrogen have higher intensity than at 300°C and are less impacted by irreversible HIL resulting from reaction of hydrogen with glass defects.

Figure 73 below shows the very good correlation of main hydrogen peaks (between 1050-1600nm) over time with experimental results.

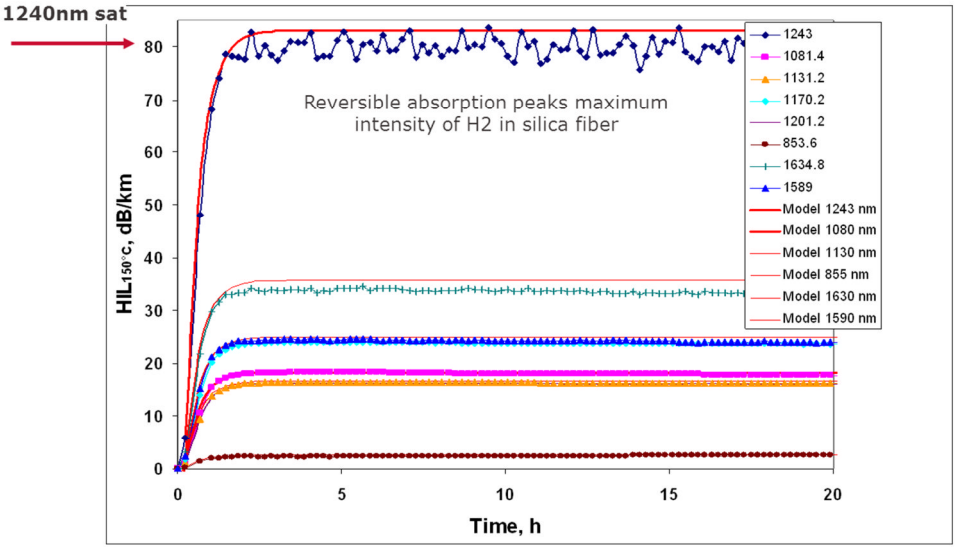

Figure 73: Confrontation of experimental results and reversible HIL model for hydrogen peaks between 1000-1600nm

We can notably point out an efficient representation of the hydrogen loading in core and equilibrium level according to external hydrogen partial pressure at 150°C.

Figure 74 below shows in the same manner for the 900-1300nm window how the model is able to simulate the overall reversible HIL spectrum.

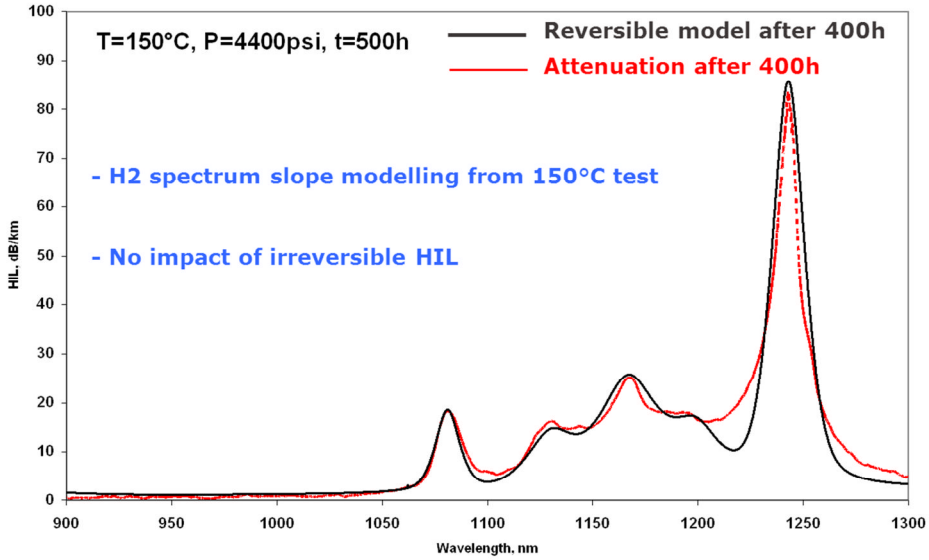

Figure 74: Confrontation of experimental results and reversible HIL model for overall reversible HIL spectrum in the 1000-1300nm window

This model will allow us to discriminate HIL due to reversible and irreversible process in fibers put in a high pressure high temperature environment. Figure 75 below shows a simulation of the reversible HIL for an in-line hydrogen test realized at 300°C on a germanium doped fiber, for which we know that irreversible HIL due to reaction of hydrogen with glass defects is the predominant process.

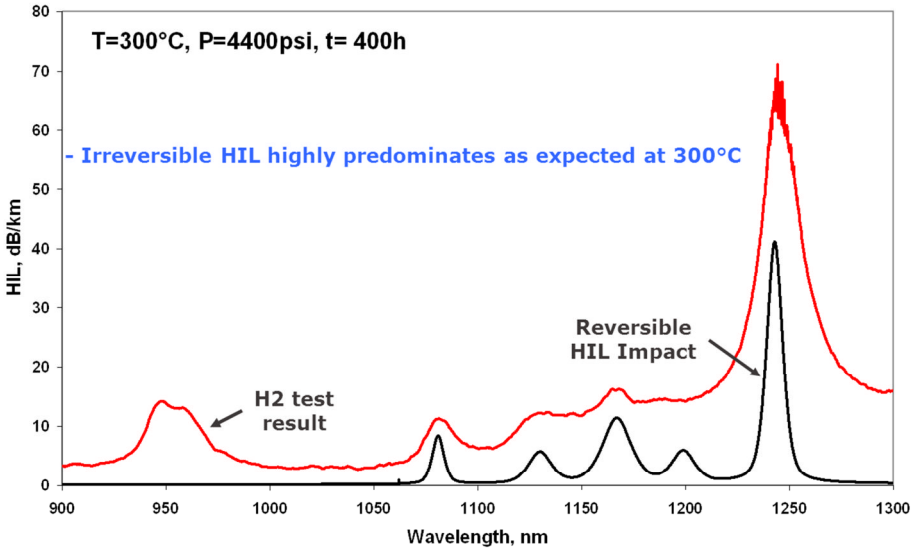

Figure 75: Simulation of the reversible HIL shape at 300°C on a germanium doped fiber

Thanks to this model, it becomes possible to calculate the irreversible HIL part by removing the reversible component. It is a first step towards development of a full high temperature / high pressure HIL model.

Influence of carbon coating on hydrogen ingression and HIL in fiber core at 300°C

We can observe in the Figures 76 below that for a given glass composition, carbon coating has no impact on the final HIL experienced by a fiber at 300°C. At every temperature, we can state that only the glass composition can have an impact in limiting irreversible HIL.

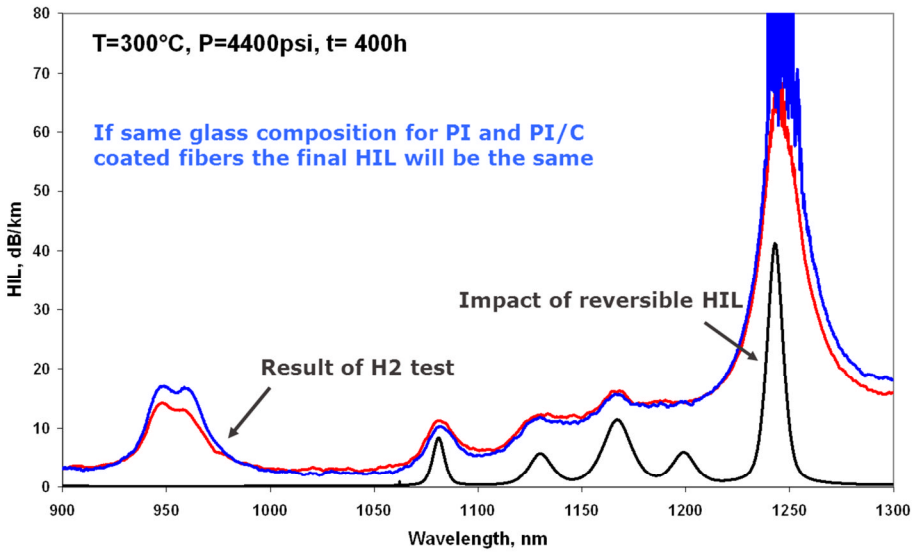

Figure 76: Simulation of the reversible HIL shape at 300°C on a germanium doped fiber

As expected, carbon coating becomes also no more efficient above at 300°C in avoiding hydrogen ingression in fiber core. As shown in Figure 77 below, compared to polyimide-coated fiber with no carbon, it only slows down the time needed for hydrogen to reach final steady state value and the time of out-gazing process.

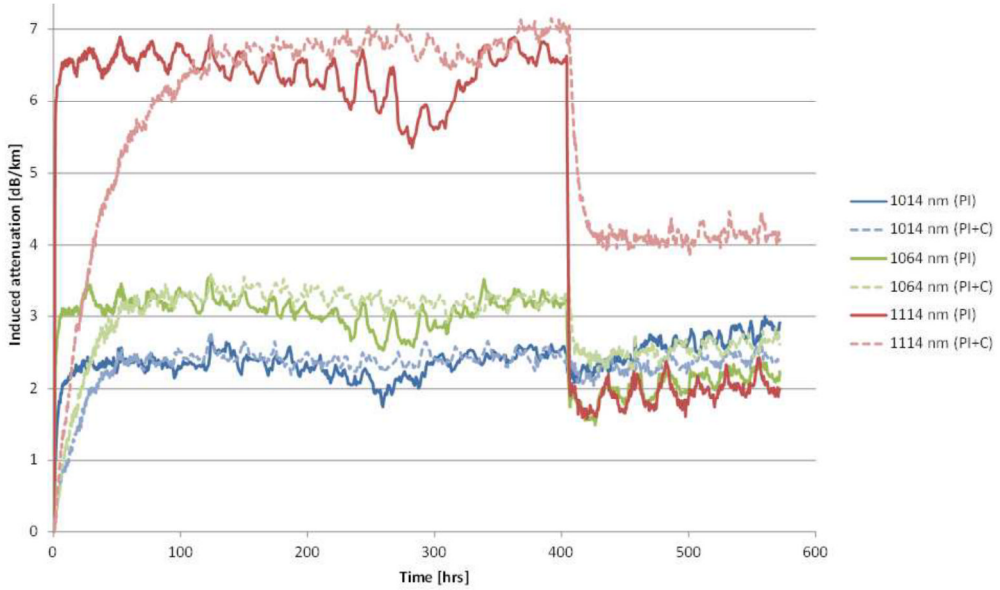

Figure 77: Influence of carbon coating at 300°C against hydrogen ingression in fiber core

2.4.5 Qualification Fiber Tests - Synthesis of Test Results and Recommendations for Fibers in GFOC Applications

The GFOC project anticipates using multimode fiber as a temperature sensor in the 1000-1100nm window and a singlemode fiber as a stress or temperature sensor at 1550nm. Figure 78 below illustrates the projected HIL impact at 300°C after 400h and 15 atm of hydrogen on a standard germanium doped fiber.

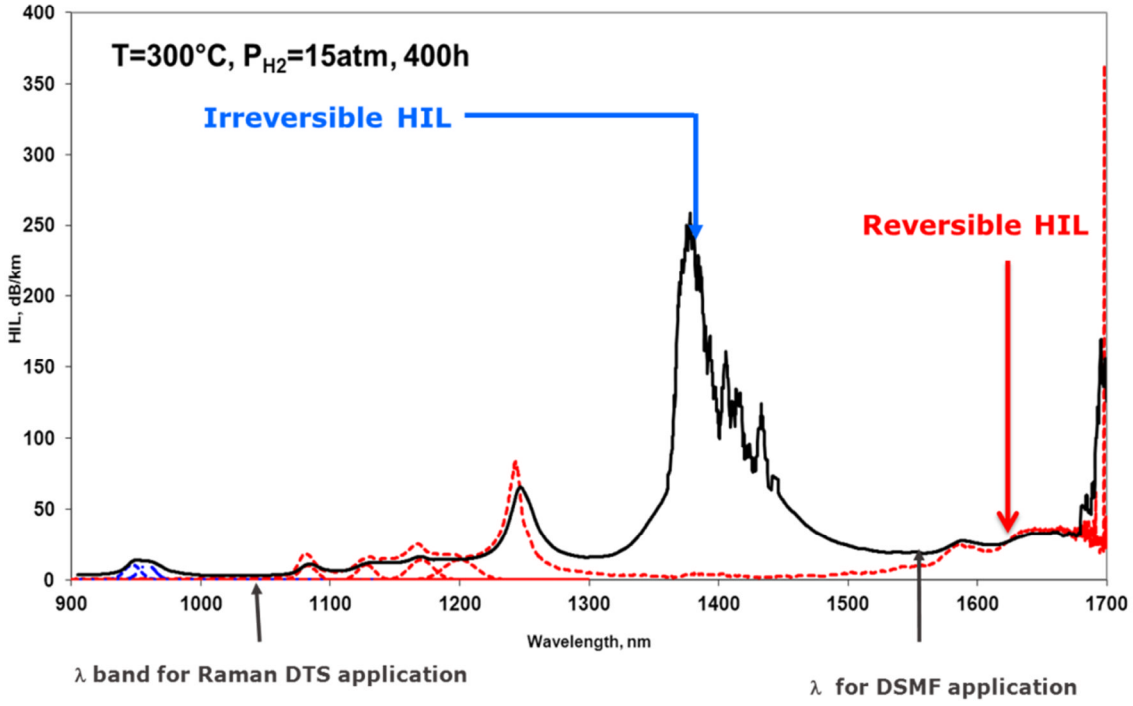

Figure 78: Overview of full HIL experienced by a germanium doped fiber in high hydrogen pressure and high temperature conditions

From this status, it is evident that singlemode and multimode fiber sensor have to be considered separately, taking into account the specific knowledge on fiber sensitivity under GFOC conditions.

Multimode temperature sensor

The Figure 79 below focuses on the 1064 nm ± 100nm band of interest:

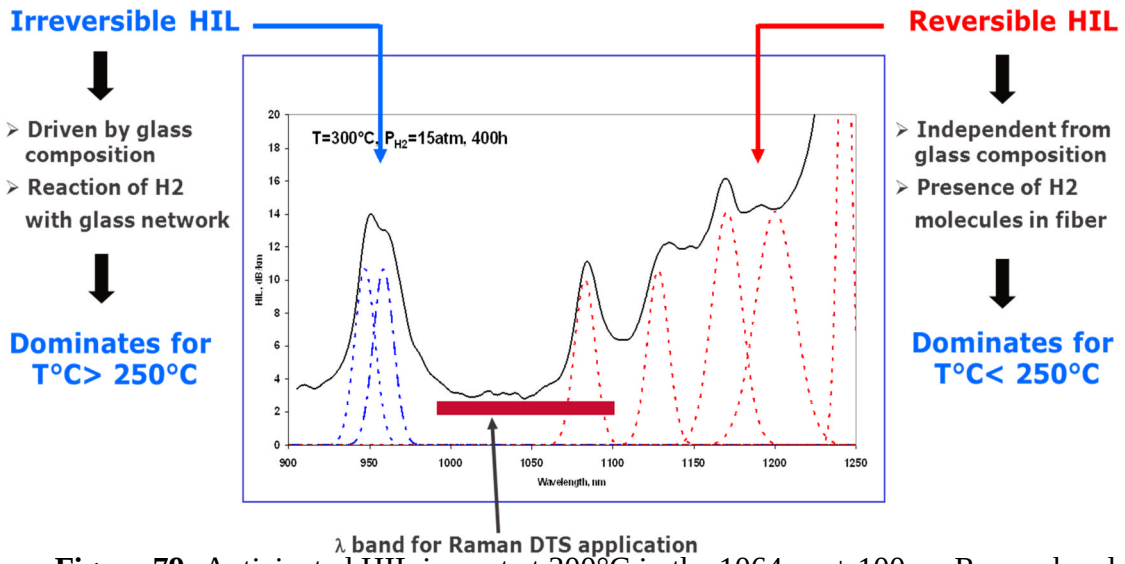

Figure 79: Anticipated HIL impact at 300°C in the 1064nm ± 100nm Raman band

At these wavelengths, we know that the most impacting HIL process will be the reversible one, coming from the tail of hydrogen absorption bands in the 1100-1300nm window. However, this effect will become all the more limited as long as temperature is high and the selected wavelength is close to 1064nm. The irreversible HIL around 950nm will remain acceptable and could even be totally avoided by using germanium free fiber.

Thus, using a wavelength around 1000nm in a germanium free multimode fiber should be the best solution for temperature sensing in GFOC application, as depicted in Figure 80. However, small amount of germanium could be acceptable at these wavelengths.

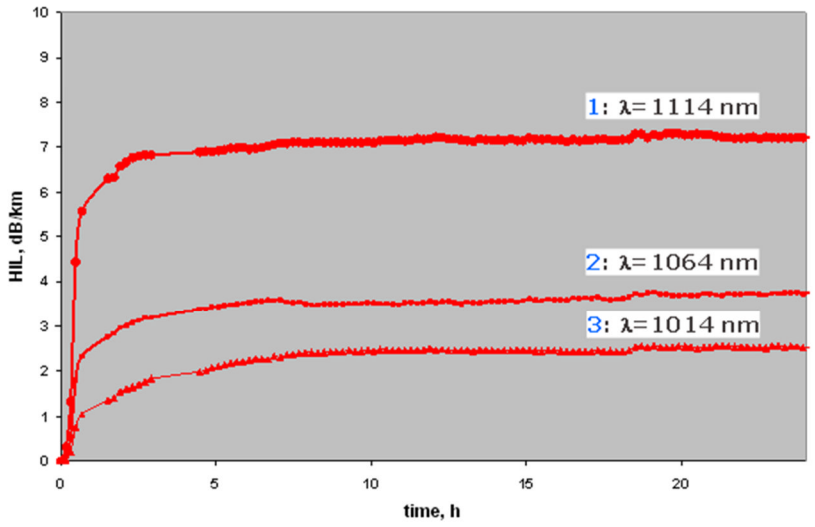

Figure 80: HIL evolution for multimode fiber in the selected 1064nm ± 100nm window

Singlemode temperature sensor

The Figure 81 below focuses on the 1550nm region of interest:

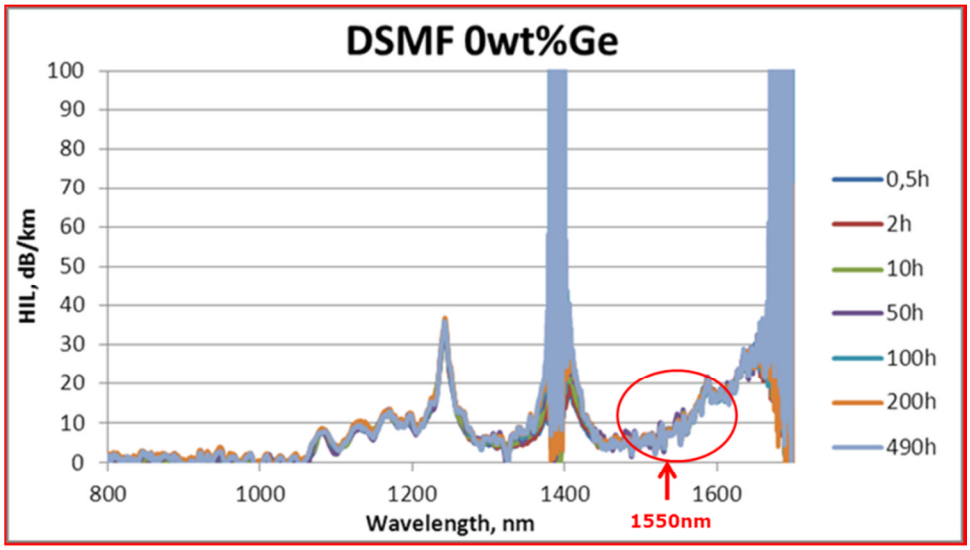

Figure 81: Anticipated HIL impact at 300°C for a singlemode fiber around 1550nm

At these wavelengths, we anticipate a non-negligible impact of either reversible or irreversible HIL processes so that it will be necessary to find out an acceptable trade-off between these two components. The reversible HIL comes from the tail of the huge hydrogen bands above 1600nm which will remain significant even at high temperatures. The irreversible impact due to the tail of the –OH absorption bands will require avoiding any germanium doping in fiber core.

Thus, using 1550nm wavelength for stress sensing in GFOC application will be a much more difficult task than for temperature sensing, even using a germanium free fiber. It could be interesting to finely select a wavelength in the 1500-1500nm window that will limit as much as possible at the same time the impact of reversible and irreversible HIL. As can be seen in Figure 82 below, the ideal solution, if the appropriate instrumentation could be obtained, would be to select a wavelength in another window for example, in the 1000-1100nm band or around 1310nm.

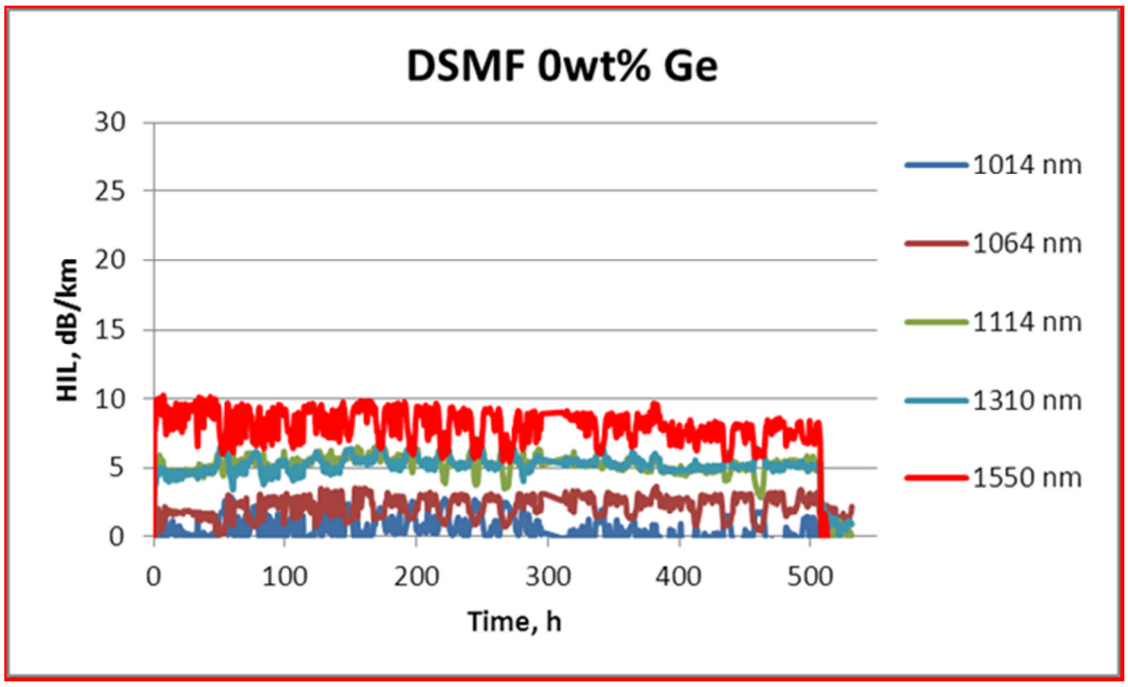

Figure 82: HIL evolution in the selected 1000-1550nm window versus time

2.4.6 Conclusion & Perspectives on Hydrogen Sensitivity

Hydrogen sensitivity has been widely studied in the frame of GFOC application in order to be able to select the best suitable glass composition for high hydrogen pressure and high temperature conditions.

Hydrogen tests together with utilization procedures taking into account security issues have been adapted and/or involved through external collaborations:

- Low hydrogen pressure and high temperature tests were available in the Eindhoven facility
- High hydrogen pressure and high temperature were available in off-line version in Lille University up to 150°C and in in-line version in Sandia Labs up to 300°C.
- Specific coatings were involved to fit fiber thermal stability requirements under test temperature and specific handling means were designed to avoid fiber damages and microbending loss issues.

A hydrogen tests plan was defined and realized in order to screen and select the best fiber candidates both in multimode and singlemode designs:

- Main physic-chemical processes responsible for HIL in fibers under high temperature and high hydrogen pressure conditions have been deeply studied.

- Irreversible HIL process has been pointed out according to temperature and core glass fiber composition. Effect of germanium-linked reaction at high temperature has been notably put in evidence.
- An efficient model has been developed to monitor reversible HIL prints due to hydrogen molecules in fiber core versus temperature, hydrogen partial pressure, wavelength and time. It can indirectly give access to irreversible HIL.

Technical recommendations concerning the most suitable glass composition both for singlemode fiber to be used as stress sensor at 1550nm and multimode fiber to be used as temperature sensor in the 1000-1100nm band could be given:

- Firstly, we come to the conclusion that carbon coating is not efficient for applications at 300°C, as it only slows down hydrogen ingression in fiber core.
- Secondly, we recommend using germanium free fiber for singlemode stress sensor. While the impact of reversible HIL could be limited if the operating wavelength of 1550nm were replaced with a wavelength in the 1000nm-1100nm band or around 1310nm, this solution is unlikely due to the instrumentation available in these bands.
- Thirdly, we recommend using germanium free fiber for multimode temperature sensor at operating wavelength the closest as possible to 1000nm. We however admit that a small amount of germanium in fiber could be acceptable for this application.

Concerning the hydrogen sensitivity knowledge under high temperature and hydrogen pressure, the perspective is now to develop a full model able to predict fiber ageing in severe conditions encountered in GFOC application.

For this, it will be needed to develop specific hydrogen test with high capability in terms of achievable hydrogen pressure and temperature together with in-line data acquisition.

The development of this kind of specific hydrogen set-up has been initiated in Lille University during the Project. Equipment have been acquired and almost fully installed. Once validated from security and technical point of view, it will offer a wide range of experimental conditions up to 300°C and 200 atm of pure hydrogen.

It will be a precious tool to design specific tests and build fiber aging models that could be exploited to address specific hydrogen sensitivity requirements and specifications for various applications and products.

2.5 CONCLUSIONS

Phase 1 of this project successfully concluded with the development and manufacture of a novel class of optical fibers which has a hydrogen-insensitive glass chemistry, a refractive index profile optimized to produce values above 500 MHz.km in the 900-1100 nm range, and an advanced high temperature polyimide coating system featuring the highest resistance to thermo-oxidative degradation of any polymer coating system for the GFOC application. High pressure/high

temperature hydrogen atmosphere test procedures and tests have validated the optical fiber design such that these fibers are projected to have a five year lifetime in air at 300°C and could survive much higher temperatures (of up to 374°C) for extended periods depending on environmental oxygen present.

To increase the hydrogen resistance of the fiber for GFOC application, the content of germanium in the fiber core must be limited or managed as much as possible. The capabilities of the PCVD fiber manufacturing process will facilitate the incorporation of Fluorine and help finely control refractive index profiles.

Bandwidth for the GFOC fiber can be optimized to values above 500 MHz.km in the 900 – 1100 nm range with the help of the newly developed correction curve program for Fluorine doped depressed multimode fibers. Fluorine doped depressed multimode fiber bandwidths are wavelength independent when compared with Germanium doped 'Datacom' multimode fibers. Measuring bandwidth at 850 and 1300 nm (standard wavelengths for 'Datacom') is enough to check bandwidths in the 900 – 1100 nm range.

It is clear from the experiments that there is a positive effect of a trench on the micro and macro bending for single mode fibers. No clear or a slight improvement is visible for multimode fibers.

With this information, a novel class of fibers that includes unique hydrogen-insensitive glass chemistry and a defined refractive index profile for proper bandwidth has been developed for the GFOC application.

A new, advanced high temperature polyimide coating system has been developed for the geothermal fiber optic cable featuring the highest resistance to thermo-oxidative degradation of any polymer coating system. Fibers with this coating are projected to have a five year lifetime in air at 300°C, demonstrated to survive 60 days or more (for multimode fiber, significantly longer for singlemode fiber) in air at 350°C. If the cable protection limits environmental oxygen to very low concentrations, the fiber can be expected to survive 374°C for 60 days or longer.

Fibers manufactured based on these investigations have been tested and been incorporated in the cable designed in Phase 2 and tested in Phase 3 of the project.

3.0 Phase 2: Cable Development

3.1 INTRODUCTION

Phase 2 of the project successfully developed a complete EGS cable package including optical fibers, fiber protection, high temperature insulated conductors and protective cladding for cable components. Much of Phase 2 work was performed in parallel with the fiber development activities of Phase I.

Phase 2 focused on four key tasks:

- High Temperature Buffer Tube Development: Development of a protective metal coating for the fibers to protect the fiber from shock, vibration and varying rates of thermal expansion.

- Cable Insulation Development: Development of an extrudable, high-temperature electrical insulation to isolate wire conductors from each other and internal cable components.

- Metal Clad Encapsulation Development: Development of a robust cable package capable of incorporating and protecting cable components during well installation and deployment.

- Pre-Field Environmental Testing and Validation: Test of the final cable construction using simulated EGS well conditions in Prysmian's accredited testing laboratory prior to field trials.

3.2 HIGH TEMPERATURE BUFFER TUBE DEVELOPMENT

The Geothermal Fiber Optic Cable (GFOC) is designed to be used in very hot geothermal water wells more than 5km deep. In the project proposal hot water is specified as higher than 300°C up to 374°C (Super Critical Water). This part of the project, Phase 2, Task 1 describes the Fiber In Metal Tube (FIMT) development to be used in the downhole cable construction, employing the specially designed optical fibers. An example of the intended cable design is depicted below in Figure 83.

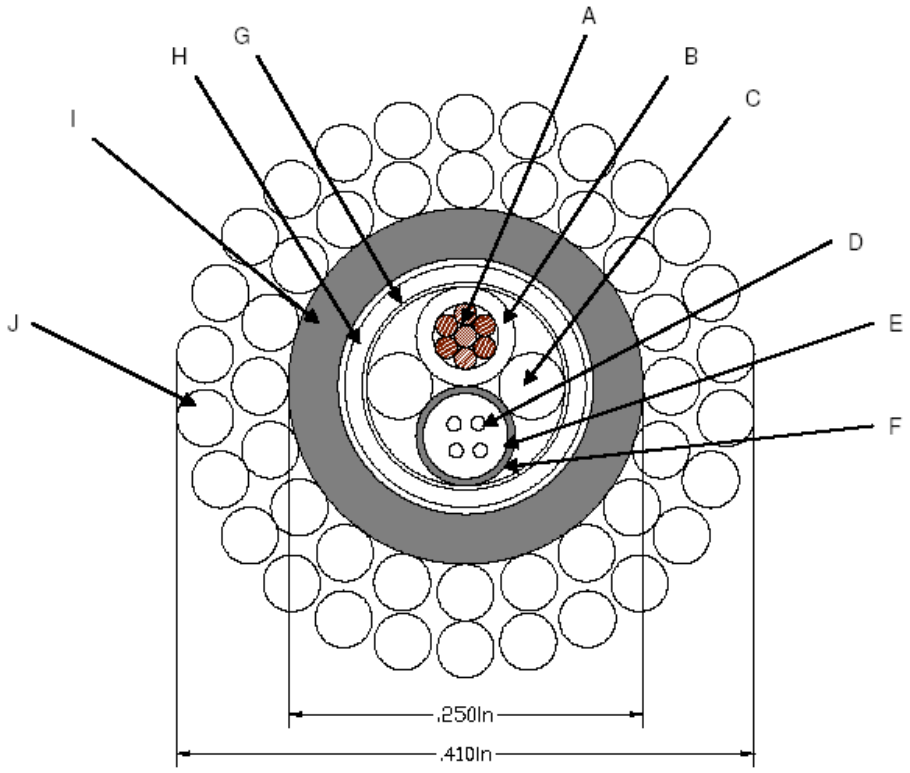

Components:

A. #18 AWG 7/26 ETP NP 2% Copper; O.D.:1.16mm (0.046") nominal
B. ECCtreme ™ ECA 3000 Fluoroplastic; O.D.: 1.78mm (0.070") nominal
C. Fillers: Fiberglass rod covered with ECCtreme ™ ECA 3000 Fluoroplastic; O.D.: 1.22mm (0.048") nominal
D. Optical fibers: 2 x 50/125 Draka polyimide coated H2 tolerant & 2x single mode Draka polyimide coated H2 tolerant
E. Gel: silicone bases gel
F. A625 Incoloy FIMT: 1.5/1.8mm (I.D. x O.D.)
G. Tape: PTFE tape wrap; thickness: 0.076mm (0.003")
H. ECCtreme ™ ECA 3000 Fluoroplastic rated to 300°C; O.D.: 4.32mm (0.170") nominal
I. A825 Incoloy alloy tube; Wall thickness: 0.89mm (0.035"); O.D.: 6.35mm (0.250") nominal
J. A825 Incoloy armor, First layer 20/1mm (0.040") preformed RHL at 20°; Second layer 26/1mm (0.040") preformed LHL at 20°

Note: Components (A B), C, and E are cabled with 5.5 inch Left Hand Lay

Figure 83: Example of the intended cable design.

In this first section the FIMT and cable construction is analyzed; looking at this particular FIMT application in terms of materials in the context of the total cable construction. The extreme high application temperature is analyzed and the vertical deployment of the cable is discussed. Finally, the importance of excess fiber length (EFL) in the design is discussed, and the theoretical requirements for the FIMT are summarized. Excess fiber length is additional fiber added during the manufacturing process that allows the optical fiber to operate over a wide temperature range without strain induced by thermal expansion of cable elements with a greater coefficient of thermal expansion and when the cable is elongated by tensile stress.

Temperature requirement

Looking to a standard FIMT there are two materials that cannot withstand temperatures above 300°C: the optical fibers and the filling gel. The optical fiber solution is discussed in Phase 1 of this project.

The oil-based, standard gels normally employed in FIMT's have three problems at elevated temperatures. The first problem is that the standard gels have a flash point of about >200°C, which is not high enough for our application. The second problem is that the viscosity decreases at higher temperatures. Projected for use on the vertical deployment, standard gels become more or less liquid and will drop out the bottom end of the cable, or if there is an end plug, the gel will gather in the lower part of the FIMT and the upper part will be "dry". The third problem is that the air inside the FIMT will expand at elevated temperatures and pushes the gel out of the tube.

Thus, the criteria for a suitable filling material are a material that:
1. doesn't burn or separate in different components at higher temperatures;
2. has a stable texture from normal ambient temperature, (±20°C) up to temperatures above 300°C;
3. cannot be pushed out by the increase of the internal pressure; and
4. is soft enough to respect the vulnerable optical fibers and won't cause high attenuations, steps or fiber breaks.

Standard stainless steel, for example 304 or 316, can easily withstand temperatures above 300°C, however, there is an important point of attention. The Coefficient of Thermal Expansion (CTE) of 304 and 316 stainless steel is higher than the coefficient of glass. For normal temperature ranges up to 150°C or 200°C most cable designs can adapt these differences. But for higher temperatures the difference in CTE of standard stainless steels to that of the glass fibers is too much to be practical considering the space considerations in this application. Further complicating this, due to the vertical deployment, the cable will elongate by the weight of its own construction. This elongation works in the same direction as the differences in thermal expansion. Stainless steel 304 and 316 have a CTE of about18 µm/m/K. Glass has a CTE of about 8 µm/m/K, a difference of 10 µm/m/K. Thus, for every 100°C temperature increase there is a decrease of 0.1% Excess Fiber Length (EFL) available. Going up in temperature from 20°C to 320°C means that the cable construction has a loss of 0.3% available EFL. This value combined with the cable elongation caused by its own weight and the compact design of the cable forces us to look for a stainless steel alloy with a thermal expansion coefficient closer to that of the CTE of glass.

Vertical deployment

In a vertical deployment there is a constant downward force in the longitudinal direction of the cable. This force increases with the length of the cable. Therefore the design of the cable is very robust with two layers of high tensile steel wires over the outside. All the elements in the cable, except the optical fibers, are supported by these high tensile steel wires by frictional forces between the construction elements.

Normally a FIMT rated for 300°C is a dry loose tube FIMT with minimal friction between steel tube and fibers. Due to the stranded construction of the core, initially the fibers are held by the friction in the FIMT. Due to gravity, there is always a small force pulling the fibers down. This small force combined with temperature variations and the difference in thermal expansion coefficient between the FIMT and the glass of the fibers, will result in a creep downwards of the fibers. Finally the upper part of the downhole cable will have no EFL and the lower part will have too much EFL. Both cases result in an attenuation increase in the optical fibers and the possibility of a fiber breakage. Therefore, it is a goal of this development to link the fibers in some way to the steel tube in order to prevent these problems.

Cable construction

A cross section drawing of the proposed cable design is depicted in Figure 83. In Figure 83 the lay length of the stranded core elements is specified; this is an important design parameter because it contributes to excess fiber in the cable. The maximum EFL in a 1.5/1.8mm (1.5 mm ID/1.8 mm OD) FIMT is 0.20 to 0.25%. As a result of the thermal expansion combined with the elongation of the cable caused by the tension of its own weight, the cable construction needs to adapt much more free cable elongation than the 0.2% EFL in the FIMT. The rest should come from the helical construction of the cable core.

Requirements for the FIMT

The development of the FIMT designed for a geothermal well can be split in four sub tasks:

1. Calculations on the EFL of the fibers in the steel tube and calculations on the free Elongation of the cable design,
2. Search and evaluate the processability of a stainless steel alloy with a CTE close to the expansion coefficient of glass,
3. Search and evaluate the processability of a "filling material" that can be applied in extreme high temperatures (>300°C), that is soft enough to avoid damage of the optical fibers and can be added to the FIMT during the production process,
4. Tests of the materials and the newly developed FIMT.

3.2.1 Define Optimal Excess Fiber Length (Calculations on free cable elongation)

According the proposed cable design in Figure 83, the FIMT in the cable core is stranded together with a copper wire with the same outer dimension. In the FIMT are 4 Polyimide (PI)-coated fibers, each with an outer diameter of 0.155mm. The bundle diameter of these 4 fibers is theoretical $(1+\sqrt{2})$ times the fiber diameter, is 0.38mm. Based on these parameters, listed in Table 28, it is possible to calculate the radius of curvature and the free cable elongation for a number of different lay-lengths.

Diameter central element	0
Outer diameter tube	1.8 mm
Inner diameter tube	1.5 mm
Number of tubes in the first layer	2
Diameter fiber bundle	0.38 mm

Table 28: Parameters to calculate the free cable elongation

Lay-length	Radius of curvature	FIMT-length	Add. Length	Free cable elongation
40mm	45.93mm	40.40mm	0.99%	0.85%
50mm	71.26mm	50.32mm	0.64%	0.54%
60mm	102.22mm	60.27mm	0.44%	0.38%
70mm	138.81mm	70.23mm	0.33%	0.28%
80mm	181.03mm	80.20mm	0.25%	0.21%
90mm	228.87mm	90.18mm	0.20%	0.17%

Table 29: Calculation of the Radius of Curvature and Free Cable Elongation

The minimum lay-length is determined by the minimum radius of curvature of the fibers. Normally the radius of curvature should be larger than ±75mm, but preferred is ±100mm. This means that the minimum lay-length is 60mm which results in a free cable elongation of 0.38%. Together with the 0.20-0.25% EFL of the FIMT gives a total free elongation of >0.58%.

In the next section concerning thermal expansion, A825 is calculated to have a thermal expansion of 0.168% (~0.17%) when the temperature rises from 20°C up to 300°C. Based on the calculations above, this means that 0.41% elongation (0.58%-0.17%) is available for tension due to the vertical deployment when employing A825.

Thermal expansion

Previously it was discussed why a stainless steel alloy with a lower Coefficient of Thermal Expansion (CTE or α) than the standard A304 or A316 is needed for the current FIMT application. However, CTE is not the only selection criterion for a stainless steel alloy. The other important criteria are:

- Weldability of both the longitudinal weld and the cross welds.
- Elongation at break, because immediately after the FIMT is welded the diameter is reduced by a set of dies. Normally the minimum reduction coefficient is 0.85 (18% reduction) and the maximum reduction coefficient is 0.70 (43% reduction), so the elongation at break has to be more than 45%
- Availability in the usable dimensions. Steel alloys are normally blended, cast and rolled in large quantities. Therefore it is not possible to select an alloy only on its theoretical properties but on its availability on the market, and the ease of cutting it to the correct width.

Thermal expansion of Chrome-Nickel alloys compared to glass

Stainless steel 304 and 316 have a CTE of 17.8 µm/m/K (304) and 16.2 µm/m/K (316) respectively. Glass has a CTE of about 8µm/m/K. Because of the difference of CTE between these stainless steels and the glass fibers is about 10µm/m/K, EFL decreases 0.1% every 100°C increase of temperature. The proposed small cable construction (O.D. ±10.5mm) is not able to adapt the elongation caused by gravity, the vertical deployment, and a difference in thermal expansion of 0.3% (△T: +300°C). A steel alloy with a CTE closer to the value of glass is needed.

From theoretical knowledge it is known that the CTE of a steel nickel alloy strongly depends on the amount of nickel. The Swiss physicist Charles Édouard Guillaume invented Invar (circa 1896), a steel nickel alloy with a CTE close to zero. The graph in Figure 84 shows the CTE (α) as function of the amount of nickel in the alloy. The sharp minimum occurs at the Invar ratio of 36%

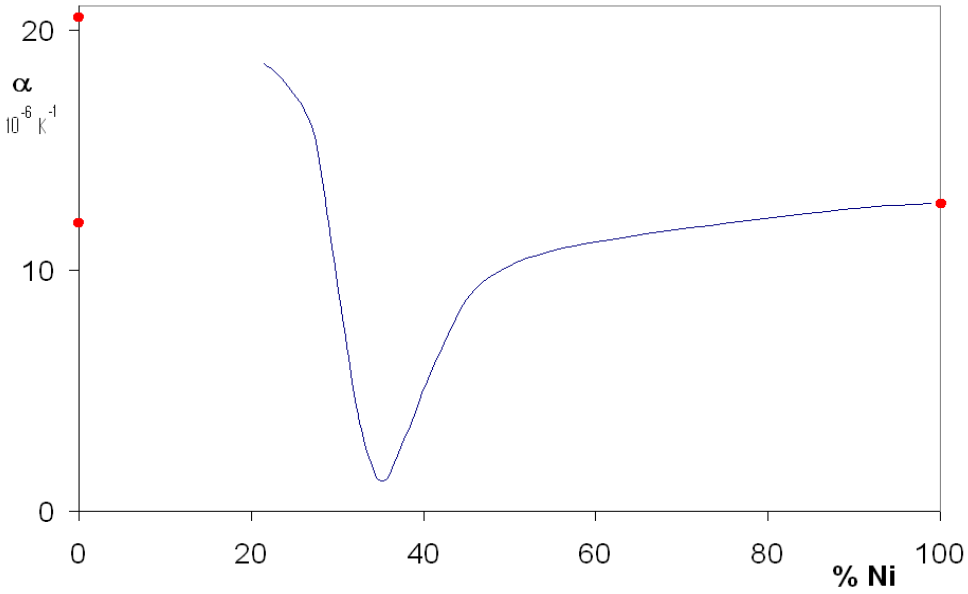

Figure 84: A sharp minimum in CTE occurs at the Invar ratio of 36% Nickel.

Table 30 shows the most important properties of nine steel alloys evaluated for this application.

	A304; DIN 1.4301	A316; DIN 1.4401	A825; DIN 2.4858	A625; DIN 2.4856	A925	A718; DIN 2.4668	A X-750; DIN 2.4669	A 909	Ivar
Physical Properties	Metric	Metric	Metric	Metric	Metric	Metric	Metric	Metric	Metric
Density	8 g/cc	8 g/cc	8.14 g/cc	8.44 g/cc	8.05 g/cc	8.19 g/cc	8.28 g/cc	8.19 g/cc	8.125 g/cc
Mechanical Properties									
Tensile Strength, Ultimate	505 MPa	580 MPa	690 MPa	880 MPa	1210 MPa	1375 MPa	1250 MPa		470 MPa
Tensile Strength, Yield	215 MPa	290 MPa	310 MPa	460 MPa	810 MPa	1100MPa	850MPa		
Elongation at Break	**70 %**	**50 %**	**45.0 %**	**50.0 %**	**24.0 %**	**25.0 %**	**30.0 %**	**15.0 %**	**30.0 %**
Electrical Properties									
Electrical Resistivity	72 µohm-cm	74 µohm-cm	113 µohm-cm	129 µohm-cm	117 µohm-cm	125 µohm-cm	122 µohm-cm		80 oµhm-cm
Magnetic Permeability	1008	1008	1005	10006	1001	10011	10035		
Curie Temperature			<= -196 °C	<= -196 °C		-112°C	-125°C		240°C
Thermal Properties									
CTE, linear	**17.8 µm/m/K**	**16.2 µm/m/K**	**14.0 µm/m/K**	**12.8 µm/m/K**	**13.2 µm/m/K**	**13.0 µm/m/K**	**12.6 µm/m/K**	**7.7 µm/m/K**	**2.0 µm/m/K**
Specific Heat Capacity	0.5 J/g-°C	0.5 J/g-°C	0.440 J/g-°C	0.410 J/g-°C	0.435 J/g-°C	0.435 J/g-°C	0.431 J/g-°C		0.385 J/g-°C
Thermal Conductivity	16.2 W/m-K	16.3 W/m-K	11.1 W/m-K	9.80 W/m-K		11.4 W/m-K	12.0 W/m-K		14.7 W/m-K
Melting Point	1400 - 1455 °C	1370 - 1400 °C	1370 - 1400 °C	1290 - 1350 °C	1311 - 1366 °C	1260 - 1336 °C	1390 - 1430 °C		
Solidus	1400 °C	1370 °C	1370 °C	1290 °C	1311 °C	1260 °C	1390 °C		
Liquidus	1455 °C	1400 °C	1400 °C	1350 °C	1366 °C	1336 °C	1430 °C		
Component Elements Properties									
Aluminum, Al			<= 0.20 %	<= 0.40 %	<= 0.30 %	0.20 - 0.80 %	0.40 - 1.0 %	<= 0.15 %	
Boron, B						<= 0.0060 %			
Carbon, C	<= 0.08 %	<= 0.08 %	<= 0.050 %	<= 0.10 %	<= 0.01 %	<= 0.080 %	<= 0.080 %	<= 0.06 %	<= 0.04 %
Chromium, Cr	18.0 - 20.0 %	<=18.0 %	19.5 - 23.5 %	20.0 - 23.0 %	21.0 %	17.0 - 21.0 %	14.0 - 17.0 %		
Copper, Cu			1.50 - 3.0 %		1.8 %	<= 0.30 %	<= 0.5 %		
Cobalt, Co				<= 1.0 %		<= 1.0 %	<= 1.0 %	12.0 - 16.0 %	
Iron, Fe	66.345 - 74 %	0,62	>= 22.0 %	<= 5.0 %	28.0 %	17.0 %	5.0 - 9.0 %	balance	balance
Manganese, Mn	<= 2.0 %	<= 2.0 %	<= 1.0 %	<= 0.50 %		<= 0.35 %	<= 1.0 %		0.2 - 0.4 %
Molybdenum, Mo		<= 3.0 %	2.50 - 3.50 %	8.0 - 10.0 %		2.80 - 3.30 %			
Nickel, Ni	8 - 10.5 %	<=14 %	38.0 - 46.0 %	>= 58.0 %	44.0 %	50.0 - 55.0 %	>= 70.0 %	35.0 - 40.0 %	35.0 - 36.6 %
Phosphorous, P		<= 0.045 %		<= 0.015 %		<= 0.015 %			<= 0.008 %
Silicon, Si	<= 1.00 %	<= 1.00 %	<= 0.50 %			<= 0.35 %	<= 0.50 %	0.25 - 0.50 %	<= 0.25 %
Niobium, Nb (Columbium, Cb)				3.15 - 4.15 %		4.75 - 5.50 %	0.70 - 1.20 %	4.3 - 5.2 %	
Sulfur, S	<= 0.030 %	<= 0.030 %	<= 0.030 %	<= 0.015 %		<= 0.015 %	<= 0.010 %		<= 0.0015
Titanium, Ti			0.60 - 1.20 %	<= 0.40 %	2.1 %	0.65 - 1.15 %	2.25 - 2.75 %	1.3 - 1.8 %	

Table 30: Nine Steel Alloys and Their Most Important Properties

Table 30 shows that:

- A304 and A316 are included in the table as a reference to the others.
- A909 has a CTE of 7.7µm/m/K, which is very close to the CTE of glass. However an elongation at break of only 15% makes A909 unsuitable for the FIMT.
- Invar has a very small CTE, but the CTE difference with respect to glass is about 6µm/m/K. The elongation at break is much better than it was for A909, but still not enough for the FIMT of this project.
- A925, A718 and A X-750 have CTE's of about 13µm/m/K, a difference of 5µm/m/K from that of glass. However the elongation at break is also not sufficient.
- A625 and A825 have a CTE that is 5 and 6 µm/m/K larger than glass respectively and have a elongation at break that is larger than required for our production process (A625: 50% and A825: 45%). By using A625 or A825 the reduction of free cable elongation by a temperature increase of 300°C is 0.15% for A625 and 0.18% for A825. These two alloys look to be the best candidates for the FIMT.

One of our main stainless steel suppliers, Zapp, has a stock of small amounts (25 up to max 1000kg) of different stainless steel alloys and in different thicknesses. We were able to buy a about 200 kg of A625 in the right dimensions: 7.9x0.15mm. From a technical point of view, A625 may have the right properties, but it is a very expensive material, almost $79/kg for about 200 kg. In greater quantities (>2500kg) A625 is more reasonable, but still expensive, about $70/kg. Compared to A304, at about $11/kg and A825 at about $44/kg, A625 is very expensive. However, because of the availability of small amounts and the delivery time of less than 1 month, buying stock from Zapp was an important advantage.

Trials with low thermal expansion FIMTs

In order to make the small steel strips into longer lengths to fabricate the FIMT, the short coils of A625 steel strip must be cross welded into longer lengths. The goal is to achieve cross weld samples that have the same strength as samples without a cross weld. After 6 trials we found the right parameters on our cross weld machine to achieve this goal, see Table 31.

Cross weld line 3710 (window side)

Trial nr	Power	Speed	Focus	Gas	Single sided / double sided	Visually	Break	Elongation
1	Steel strip without cross weld							34.7%
2	Steel strip without cross weld							35.3%
3	202	750	12.5	He	Single	OK	Weld	14.7%
4	202	750	12.5	He	Single	OK	Weld	18.7%
5	174	750	12.5	He	Double	OK	Weld	30.7%
6	150	750	12.5	He	Double	OK	Weld	33.0%
7	125	750	12.5	He	Double	OK	Not on weld	35%
8	125	750	12.5	He	Double	OK	Not on weld	35%

Table 31: Parameters to make a good cross weld

Note from Table 31 that the unwelded steel strip had an elongation at break of only 35%, while usually A625 has an elongation at break of 50%. This could be possibly explained by the fact the A625 came from a small amount from the stock of Zapp. Possibly this batch was not annealed as much as it should have been.

During the longitudinal welding trials we were not able to make the desired 1.5/1.8mm (44% reduction) tube because of the limited elongation at break of the steel strip. Instead, it was decided to make a 1.7/2.0mm FIMT, which needs only a 30% reduction. Welding of the longitudinal seam was not a problem. After a few trials good welding parameters were found as seen in Table 32.

Speed	Laser power	Focus	Tube
7m/min	610W	12.0mm	1.7/2.0mm

Table 32: Parameters for the longitudinal weld

Thermal expansion of the construction

The thermal expansion of the construction is determined by the thick-walled A825 Incoloy tube and the A825 armor of the larger cable construction (see I and J in Figure 83). The cross-section of the A825 Incoloy tube is 15.3mm² and the armor wires have a total cross-sectional area of 36.1mm². The FIMT has a cross-section of 0.778mm², which is negligible when compared to the A825 components. When considering the entire cable construction and the thermal expansion, the A825 components will dominate the thermal expansion. Thus it is not important if the FIMT is made of a stainless steel with a low CTE such as A625 or a stainless steel comparable to A316.

The CTE of A825 is only slightly higher than A625 (14.0µm/m/K compared to 12.8µm/m/K), and A825 is a commonly used alloy for welding the 6.35mm tube and also for high tension steel wires. The CTE of the construction will be ~14µm/m/K which is 6µm/m/K more than the CTE of the optical fiber. In other words if the temperature rises from 20°C to 300°C the EFL will reduce by 0.168% compared with 0.134% for A625.

The difference in length between the A825 (CTE=14.0µm/m/K) construction and the A304 (CTE = 17.8 µm/m/K) FIMT if the temperature rises from 20°C to 300°C is 3.8 (difference in CTE between A825 and A304)*280K = 0.106%. Along a cable length of 3km, this is 3.18m. Using A316 for the FIMT this length difference would be 1.85m.

Conclusion: A316 is the best compromise to use for the FIMT because it is a well-known and often used alloy for FIMTs, and it has acceptable thermal expansion behavior in the context of the entire construction. If the FIMT is not part of a cable construction that mainly consists of A825 components, then A625 is the preferred alloy for the FIMT.

3.2.2 Determine Optimal Gels or Buffer Tubing Construction

As discussed previously, optical fibers in a dry FIMT in vertical deployment can cause the fibers to move downwards and have too much EFL at the bottom of the tube and a lack of EFL at the top of the tube. A material is needed to give friction between the FIMT and the fibers in it. The requirements on such a material are:

- soft enough to avoid damage and high attenuation of the optical fibers;
- can withstand extreme high temperatures, higher than 300°C;
- doesn't drip out in case of vertical deployment;
- is not pushed out by the pressure increase inside the FIMT at high temperatures; and

- can be added to the FIMT during welding.

Search of high temperature resistant materials

We approached some known suppliers and did additional research to select candidates for the high temperature resistant material. Table 33 lists the materials which had the best potential for this application with some of their properties.

Name	Supplier	Max application temperature	Materials group	Hardness	Tested
JS 533 (5398)	Loctite	350°C	Silicone based, curing by contact with humidity	Shore A35	Yes
5612	Loctite	220°C (300°C Peak)	Silicone based, curing by mixing 2 components	Shore A45	Yes
5928	Loctite	350°C	Silicone based, curing by contact with humidity	Shore A23 - 38	No
5399	Loctite	350°C	Silicone based, curing by contact with humidity	Shore A33	Yes
Duraseal 1531	Cotronics	650°F (= 340°C)	Silicone based, curing by contact with humidity	Shore A31	Yes
Siliconen AB	Silicones & More	320 - 380°C	Silicone based, curing by mixing 2 components	Shore A40	No
XTS 320	Intek adhesives	320°C	Silicone based, curing by contact with humidity	Shore A35	No
FortaFix	Mincouk	800°C	Silicone based, curing by contact with humidity	VPN 6	No
HT 192	Master Adhesive	not known	based on Krytox®[5] 407	not known	Yes
Tetramer Technologies		Development project		not known	No

Table 33: List of high temperature resistant materials.

The list of candidate materials was subsequently reduced as two suppliers (Silicones & More and Intek) showed interest in the project. Despite best efforts Tetramer's development efforts did not leave their own laboratory. It was quickly determined that the FortaFiz material was too hard. However, tests were conducted on the Loctite materials, Cotronics (Duraseal), and Master Adhesive materials.

In the laboratory three tests were performed,

- a sample of the material was placed on a saucer in the oven up to 350°C for ±24 hours;
- samples were injected into an empty steel tube (2.8/3.2mm x 50cm) and placed vertically in an oven up to 300°C;
- an Oxygen Index Test (OIT) up to 400°C for 90minutes.

The test with a sample on a saucer in an oven was performed on 5 materials: JS 533, 5612, 5399, Duraseal 1531 and HT192.

[5] *Kyrtox is a registered trademark of E.I, du Pont Nemours and Company*

Laboratory test on high temperature filling materials

Loctite 5612

Loctite 5612, a 2 component material, was tested up to 300°C in the oven on a saucer. Up to 250°C the material was still soft and without cracks. At 300°C the sample on the saucer became partially loose from the saucer and cracks formed on the surface. The surface became inflexible but was still soft on the inside as shown in see Figures 85 and 86.

Figure 85: Loctite 5612 at 250°C

Figure 86: Loctite 5612 at 300°C

The OIT test of Loctite 5612 in Figure 87 shows that there is an event at 265° C and at 334°C. This is corresponding with the results of the sample on the saucer in the oven. Between 250°C and 300°C the material starts to change.

When the Loctite 5612 was injected in a steel tube, testing showed that, even the cured material is pushed out of the tube, as seen in Figures 88 and 89. At 150°C some material is pushed out of both tube ends but at 200°C much more material is pushed out. At 250°C no additional material is pushed out. At 300°C the silicones that were pushed out became hard.

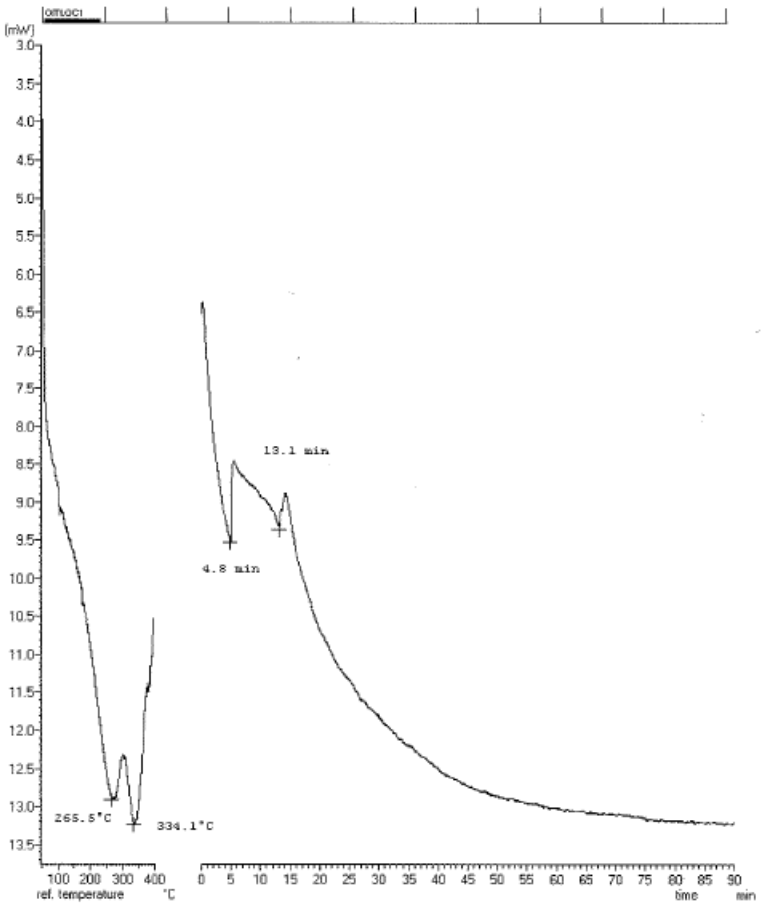

Figure 87: OIT curve Loctite 5612

Figure 88: Tube and saucer sample in the oven at 150°

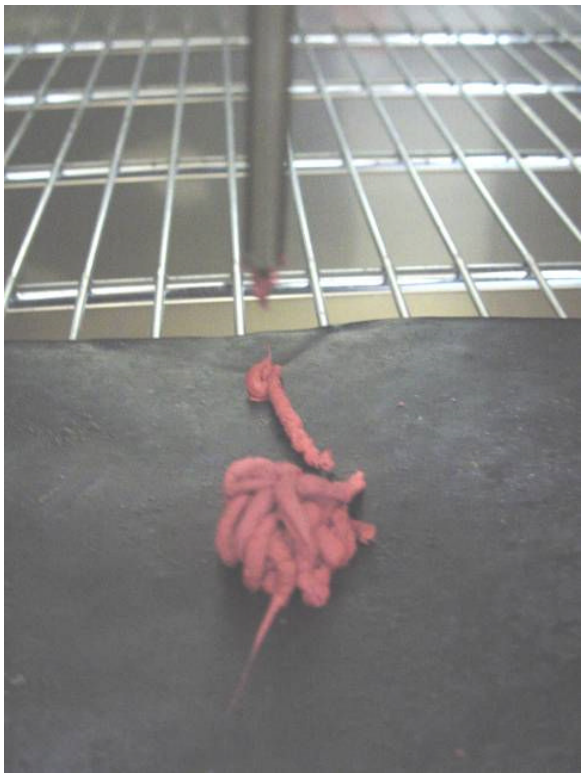

Figure 89: Silicone pushed out the tube at 200°C

The Loctite 5399

Loctite 5399 is a one component material and was tested in the same way as described above for the 5612 material, as can be seen in Figures 90 and 91.

Figure 90: Tube and saucer sample in the oven at 150°.

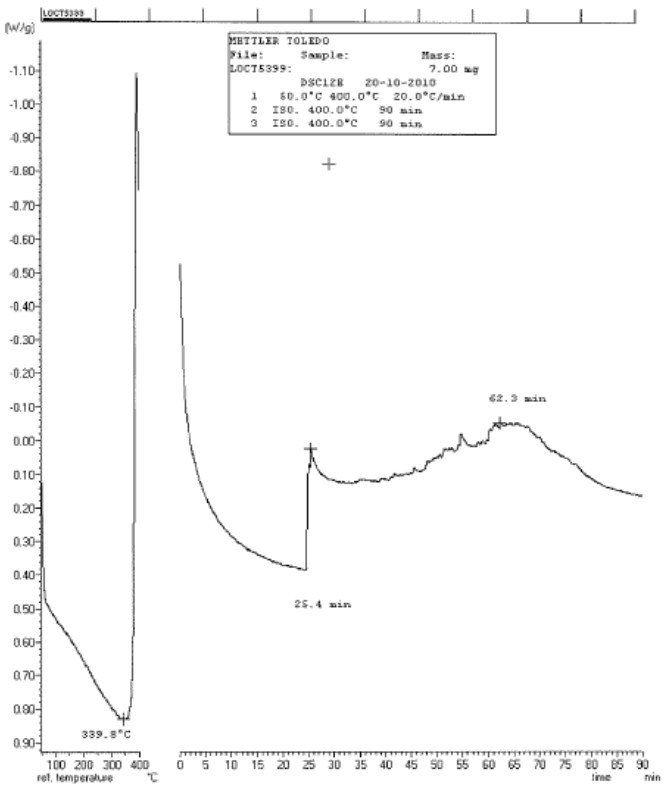

Figure 91: OIT curve Loctite 5399.

Figure 92: Silicone pushed out the tube at 250°C

Figure 93: More silicone pushed out the tube at 300°C

Up to 250°C almost no material was pushed out of the tube samples. The 5399 material began coming out of the tube at 250°C and increases flow at 300°C as can be seen in Figures 92 and 93. The OIT curve shows an event at 340° C. The sample on the saucer is still soft at 300°C.

The Loctite JS533

Loctite JS 533 is a one component material. JS533 was packed in a metal tube of 100ml, at the same time the Loctite 5399 is the same material but packed in a 310ml plastic cylinder.

Figure 94: Tubes and a saucer filled with Loctite JS533 in an oven at 300°C.

Figure 95: Tube filled with JS533; nothing is pushed out at 300°C.

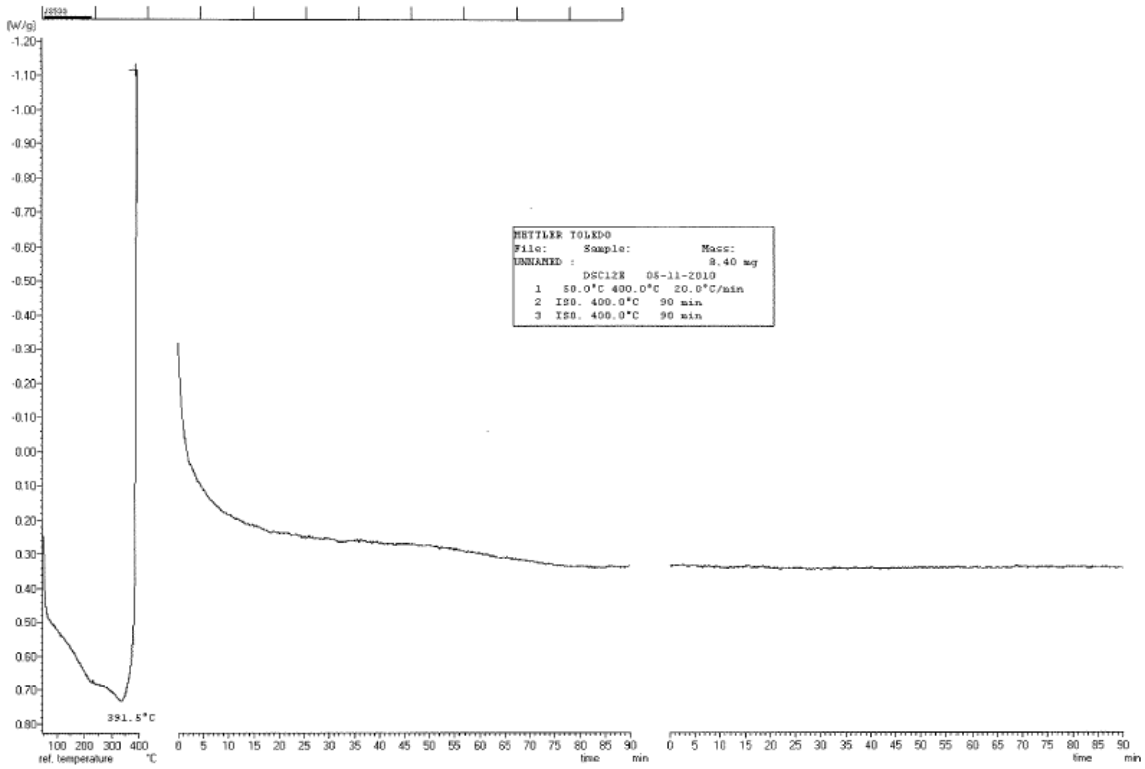

Figure 96: OIT curve Loctite JS 533

Before curing, JS533 has a much lower viscosity than 5399.

Up to 300°C (max temperature oven) no material was pushed out of the tubes as can be seen in Figures 94 and 95. The OIT curve in Figure 96 shows an event at 391°C.

After these tests Loctite 5399 and JS533 were placed in a small oven for higher temperatures (see Figure 97). At 350°C both materials remained soft and flexible, but both exhibited a thin, slightly harder skin. There were also some air bubbles between the saucers and the samples. After cooling down there were cracks in both materials.

Figure 97: Loctite 5399 and JS533 in a small over at 350°C

Duraseal 1531

Duraseal 1531 is a one component material. Filling the stainless steel tube with samples was not possible because of the very high viscosity/stiffness of the material.

On the saucer at 300°C the material was still soft inside but had a harder skin, see Figure 98.

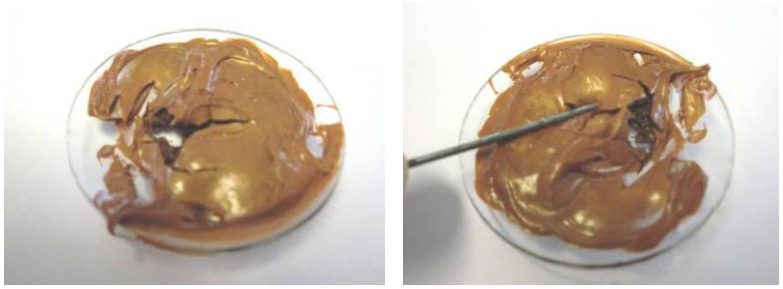

Figure 98: Samples Duraseal with hard skin

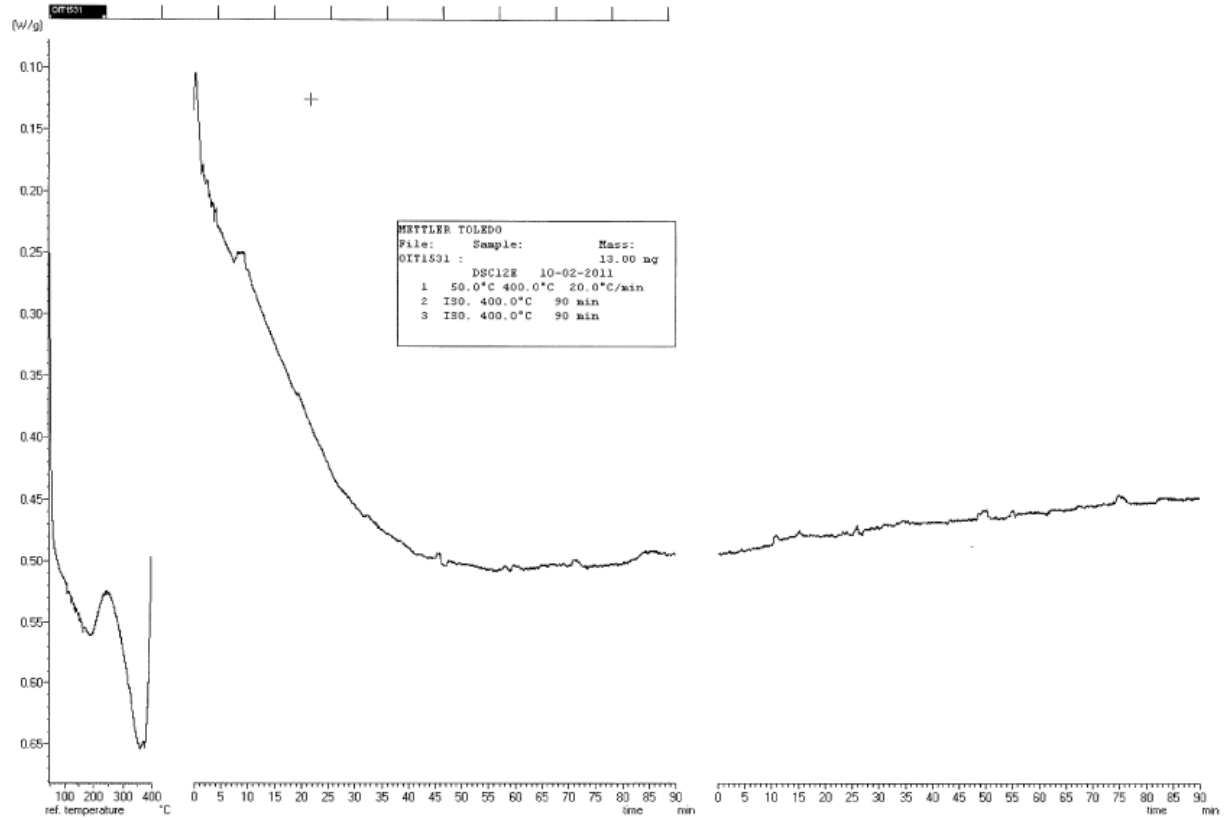

Figure 99: The OIT test of Duraseal shows an event at ±370°C

Master Adhesives HT192

A sample of the Master Adhesives gel was tested in an oven at 200°C, 250°C and at 300°C. At 200°C and 250° no visible change in the structure was noticed. At 300°C, the oil separated from the other components of the material, as can be seen in Figures 100 and 101. The non-oil components were white and a bit crumbly after the oil separation. The oil and the separated components can be re-mixed, but the mixture is not as smooth as the original material.

Figure 100: Oil and other components separate

Figure 101: Magnified view of Figure 100

Figure 102: Tube filled with HT192 in the oven

Figure 103: HT192 is pushed out of the metal tube, top and bottom

Figures 102 and 103 give an impression of what was dripped out. Most of the material dripped already out of the stainless steel tube after 21 hours at 200°C. After 6 hours at 250°C nothing dipped out. After 18 hours at 300°C the oil had dripped out and had separated from the other components again. Some crumbly material was still in the stainless steel tube. After this test at 300°C, 4.2.gr (60%) had dripped out, 2.9 gram (40%) was still in the tube (specific gravity HT 192 = 1.95kg/liter)

Thermal Gravimetric Analysis (TGA) on JS533 and Master Adhesives HT192

In Figure 104, the 300 °C weight loss is tracked for the following materials:

- Silicone adhesive used for the "non-conventional" gel (JS533)
- Master Adhesives (MA) material based on Krytox® 407 (HT192)

The silicone (JS533) undergoes an immediate mass loss associated with the cure followed by mass loss at 300°C at a much lower rate. The MA material (HT192) undergoes a rather steady mass loss at 300°C. Mass loss for both materials is at about 35% at 250 hours. The MA material also shows very obvious oil separation at 300°C. No official oil separation tests were performed, but the material would clearly fail normal tests done for telecomm cables. A low viscosity fluid separates from the MA gel at 300°C. If the FIMT is not sealed at the connector, the fluid could drip out at 300°C.

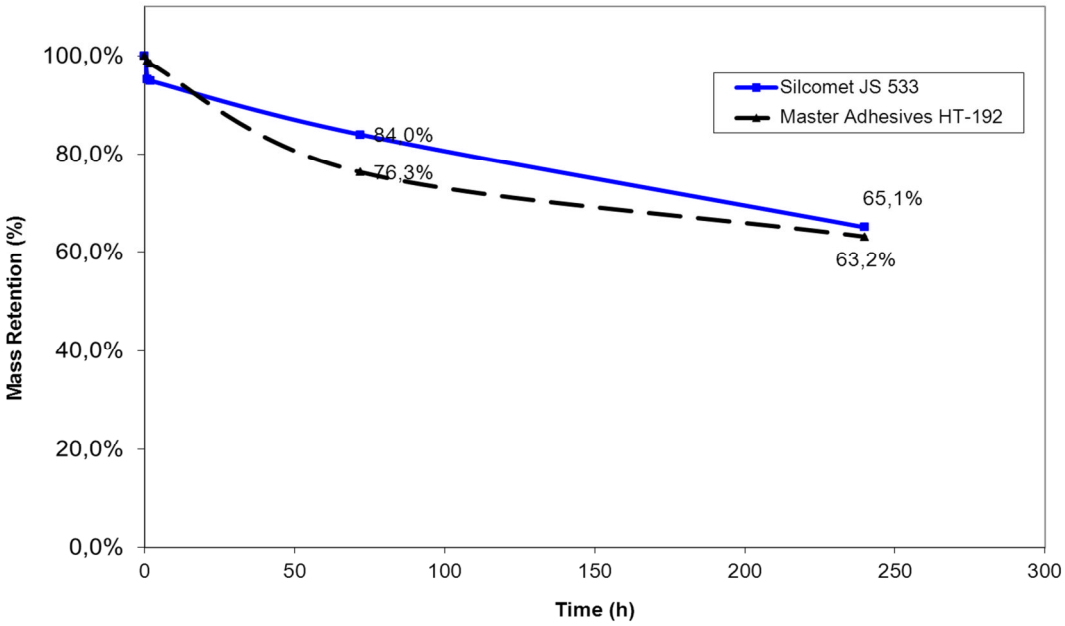

Figure 104: Mass retention versus time

Conclusion of the laboratory tests

Three of the five tested materials survived the tests at 300°C: Loctite 5399 and JS533 and Duraseal 1531. It was decided to continue with production trials using JS533 and Duraseal 1531. Loctite JS533 was preferred above 5399 because of its lower viscosity before curing.

FIMT trials with high temperature materials, intermittent plug

In the context of the GFOC project several trial FIMTs were made between autumn 2010 and autumn 2013. Table 34 lists the trial lengths made. The lengths were produced and rewound in the Netherlands and then shipped to Draka USA for further analysis. After production and after rewinding, the fibers in the FIMTs were tested by OTDR.

The first trial lengths,1A and 1B (see Table 34) were made with currently available technology using Verrillon polyimide (PI) coated fibers in a dry FIMT and in a FIMT filled with 2 component gel respectively. The drawback of the dry FIMT is that the distribution of the EFL along the tube can easily change at vertical deployment. The drawback of the 2-component gel is that is can only be used up to ±230°C

The second batch of trial lengths, 2A, 2B and 2C (see Table 34) were made with the first Draka PI-coated fibers and 1 Verrillon PI-coated fiber. The fibers are used in FIMTs filled with Sepigel (standard telecom gel for FIMTs), 2 component gel (max 230°C), and the first high temperature gel material, Duraseal 1531 (max 340°C) respectively.

Nr	Date	Type	Fibers	Gel	Length	Result after welding	Result after rewinding
1A	Nov 2010	1.5/1.8	Verrillon PI coated	No gel, dry	500m	Good attenuation	Good attenuation
1B	Nov 2010	1.5/1.8	Verrillon PI coated	2 component	500m	Good attenuation	Good attenuation
2A	Mar 2011	2.8/3.2	3x Draka PI coated + 1 Verrillon PI coated coated	Sepigel	350m	1 Draka fiber broken on pay-off, attenuation OK	Good attenuation
2B	Mar 2011	2.8/3.2	3x Draka PI coated + 1 Verrillon PI coated	2 component	500m	Good attenuation	Good attenuation
2C	Mar 2011	2.8/3.2	3x Draka PI coated + 1 Verrillon PI coated	Duraseal 20m/5cm manually	500m	Good attenuation	Increase attenuation, not straight
3A	May 2011	1.7/2.0	SM telecom	JS533 85% filled, strip lubricated with water	250m	Unknown	High attenuation, JS533 cured
3B	May 2011	1.7/2.0	SM telecom	JS533 85% filled, strip NOT lubricated with water	250m	Good attenuation	High attenuation, JS533 NOT cured
3C	May 2011	1.5/1.8	SM telecom	JS533 Intermittent 20m/ 2cm; NOT water	250m	Good attenuation	Good attenuation
4A	June 2011	2.8/3.2	3x Draka PI coated + 1 Verrillon PI coated	JS 533 Intermittent 20m/2cm	500m	Good attenuation	1 fiber not straight
4B	June 2011	2.8/3.2	3x Draka PI coated + 1 Verrillon PI coated	Duraseal Intermittent 20m/2cm	500m	Good attenuation	1 fiber not straight
5A	Feb 2012	2.8/3.2	4x SM telecom	JS533 Intermittent 20m; injected	500m	Good attenuation	Not straight @1550nm
5B	Feb 2012	2.8/3.2	JS533 Intermittent 25m; injected	JS533 Intermittent 20m; injected	500m	3 fibers OK, 1 fiber not straight	3 fibers OK, 1 fiber not straight
6	June 2012	1.7/2.0 A625	4x Draka PI coated	JS533 Intermittent 25m; injected	900m	3 fibers OK, 1 fiber broken	3 fibers OK, 1 fiber broken
7	July 2012	1.5/1.8	4x Draka PI coated	JS533 Intermittent 25m; injected	4000m	1 fiber OK, 3 fibers were broken	1 fiber OK, 3 fibers were broken
8	Sept 2012	1.4/1.7	4x SM telecom	JS533 Intermittent 25m; injected	1000m	3 fibers OK, 1 fiber broken	Unknown
9	Sept 2012	1.5/1.8	3x SM telecom	JS533 Intermittent 25m; injected	1000m	Good attenuation	Good attenuation
10	Oct 2012	1.5/1.8	4x Draka PI coated	No gel, dry	3500m	Good attenuation	Good attenuation
11A	Nov 2012	1.5/18	3x SM telecom	JS533 Intermittent 25m; injected	1000m	Good	Unknown
11B	Nov 2012	1.5/18	4x Draka PI coated	JS533 Intermittent 25m; injected	1400m	2 fibers OK, 2 fibers broken	Cut on fault location, Re-winded on small AL-drum
12A	Feb 2013	1.5/1.8	3x SM telecom	JS533 Intermittent 25m; injected	640m	Good attenuation	
12B	Feb 2013	1.5/1.8	4x Draka PI coated	JS533 Intermittent 25m; injected	1000m	Good attenuation	Good attenuation
12C	Feb 2013	1.7/2.0 A625	4x Draka PI coated	JS533 Intermittent 25m; injected	450m	Weld failure, broken fibers	
13A	Feb 2013	1.5/1.8 A625	3x Draka PI coated + 3	No gel, dry	420m	Steel strip folded double	Cut on fault location, Re-winded on small AL-drum
13B	Mar 2013	1.7/2.0 A625	3x Draka PI coated + 3	No gel, dry	400m	Good attenuation	Re-winded on small AL-drum
13C	Sept 2013	1.7/2.0 A625	1x Draka PI coated	No gel, dry	400m	Good attenuation	Re-winded on small AL-drum
14A	Mar 2013	1.5/1.8 A304	4x Draka PI coated	JS533 Intermittent 25m; injected	1100m	1 broken fiber	1 fiber not straight
14B	June 2013	1.5/1.8 A304	4x Draka PI coated	JS533 Intermittent 25m; injected	635 & 500	Good attenuation	
14C	Sept 2013	1.5/1.8 A316	4x Draka PI coated	JS533 Intermittent 25m; injected	3000m	Good attenuation	Good attenuation

Table 34: List of trial FIMTs

The 2C FIMT with Duraseal was the first FIMT with intermittent plugs. The viscosity of the Duraseal is very high and it was difficult to apply the material in the tube during welding. Applying of the Duraseal 1531 was done manually.

The third batch of trial FIMTs, 3A, 3B and 3C (see Table 34) was made to investigate two things: first, can the high temperature materials be used as a normal filling compound, longitudinal filling of about 85%, or is an intermittent plug necessary; and second, will a one component material cure inside the FIMT. Trial FIMT 3A was made with a 85% filling degree of JS533. Before the JS533 silicone material was put in to the tube, the inside of the steel strip was lubricated with water because this one component silicone needs humidity for the curing, see Figures 105 and 106.

Figure 105: Lubrication of the steel strip

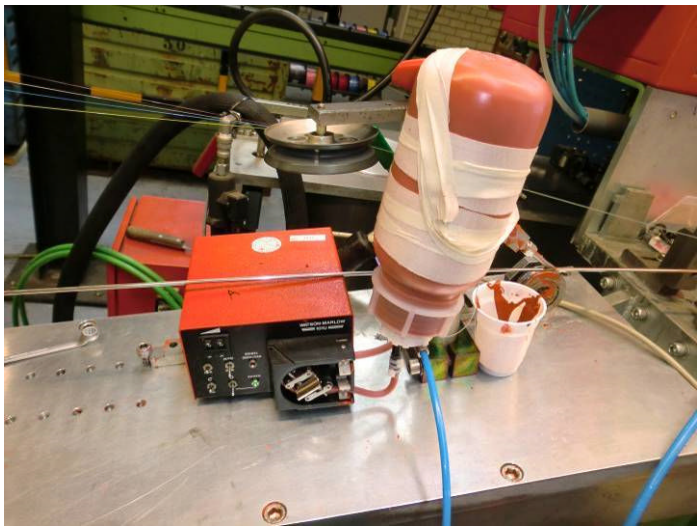

Figure 106: The roller pump feeds the JS533 in to the tube

Immediately after 3A was produced, the water lubrication was removed, and the second trial with JS533 was made, trial 3B. Before making the third trial length the roller pump was also removed. During the production of trial 3C intermittent plugs were injected manually every 20m. From these (3A-3C) trials, we learned:

- high temperature materials like JS533 causes high attenuation after rewinding / curing;
- entire filling of a FIMT needs water lubrication to cure the one component silicone;
- intermittent plugs don't need lubrication to cure the silicone inside the FIMT; and
- intermittent plugs don't cause high attenuation values, even after rewinding.

In the fourth batch of trial lengths, 4A and 4B (see Table 34) we tested the two most promising high temperature materials with PI-coated fibers in an oversized 2.8/3.2mm FIMT with manual injection of the intermittent plugs, as shown in Figures 107 through 109. The goal of this trial was to test the fibers and intermittent plug materials at high temperatures. An oversized FIMT is used in order to be able to put enough fiber excess length (EFL) in the tube, more than 0.3%, because of the coefficient of expansion of the A304.

Figure 107: Manual injection of the plug

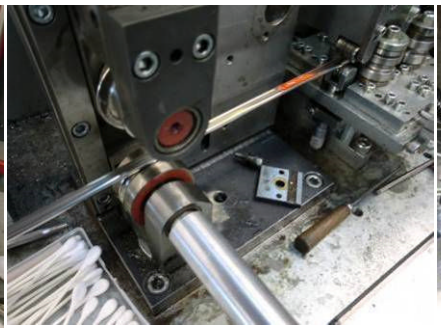

Figure 108: A JS522 plug

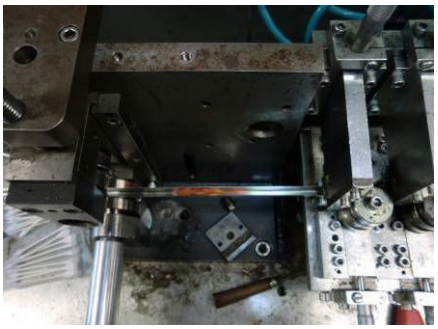

Figure 109: A Duraseal 1531plug

Both FIMTs were tested at Draka USA in an oven at the following temperatures:

1.0 at room temperature,
2.0 increased in temperature at 50°C, 100°C, 150°C 200°C, 250°C and 300°,
3.0 ageing for 3 and 11 days at 300°C, and
4.0 cycled between 50°C and 300°C .

The results of the ODTR and Brillouin Optical Time Domain Analyzer (BOTDA) measurements are depicted below in Figures 110, 111, and 112.

The MM-fiber in the Duraseal FIMT has very high attenuation at 300°C while the MM-fiber in the JS533 FIMT has a more stable attenuation.

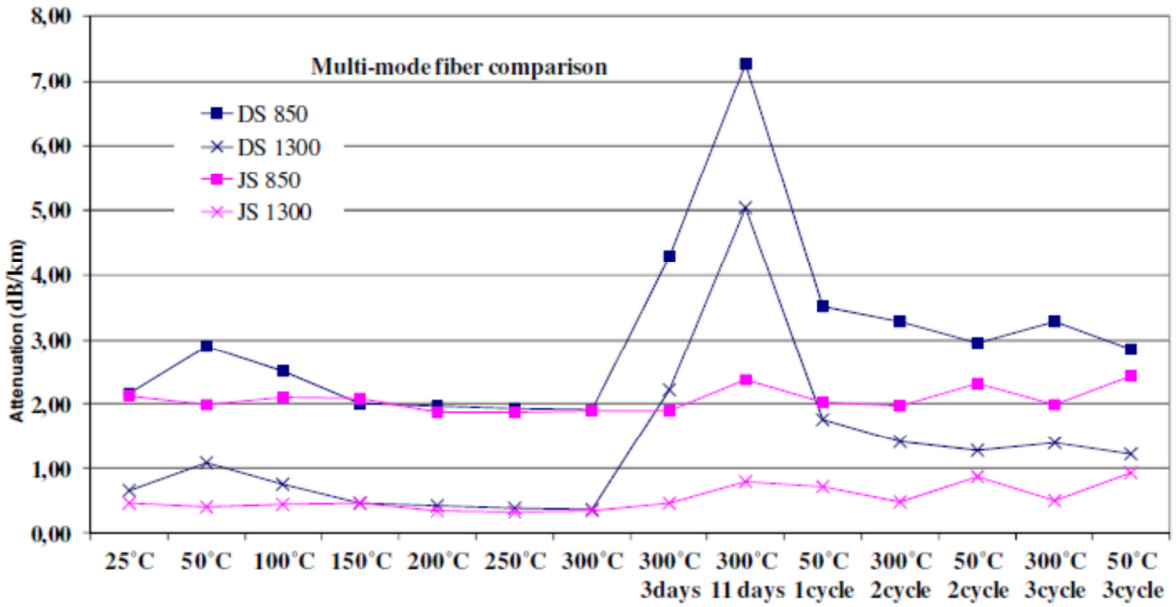

Figure 110: OTDR results (850nm & 1300nm) of the MM-fibers in the JS533 FIMT (red) and the Duraseal FIMT (blue)

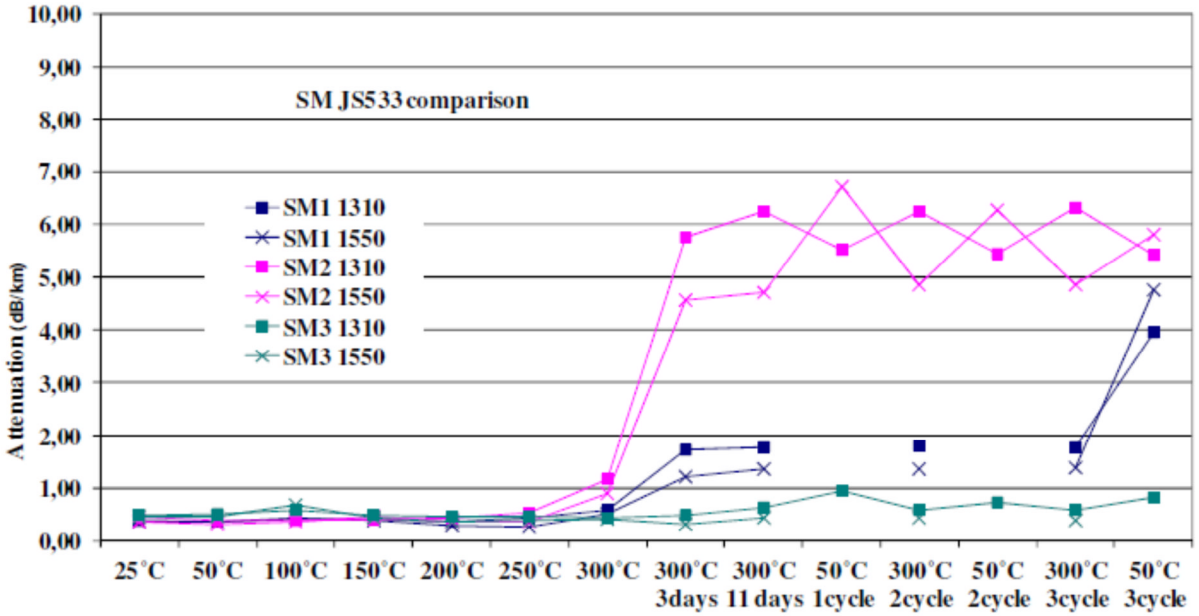

Figure 111: OTDR results (1310nm & 1550nm) of the SM-fibers in the JS533 FIMT

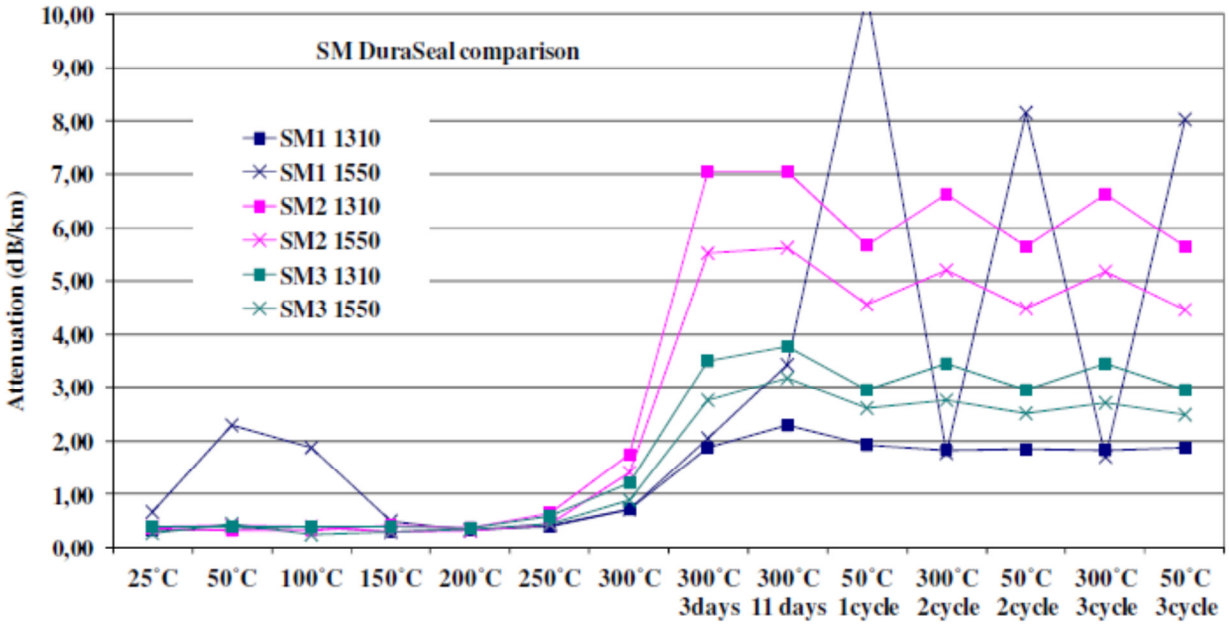

Figure 112: OTDR results (1310nm & 1550nm) of the SM-fibers in the Duraseal FIMT

The SM fibers in both FIMTs have high attenuation at 300°C, and the attenuation stays high even when the temperature comes down to 50°. One fiber however, the SM3 in the JS533 FIMT, maintained an acceptable attenuation at 1310nm (<1.0dB/km). This was the only Hydrogen tolerant fiber of both FIMTs. Spectral attenuation measurement after the test proves that Hydrogen is the cause of the high attenuation. But there is also another effect that causes the high attenuation. At the fourth part of the test, the cycling between 50°C and 300°C, the attenuation at 1550nm at 50°C is always very high. The wavelength 1550nm is always much more sensitive for micro bending than 1310nm. So the fibers are under stress at 50°C, which is probably caused by the shrinkage of the

tube at lower temperatures; the EFL becomes too much at some places. Both phenomena's are happening in both FIMTs

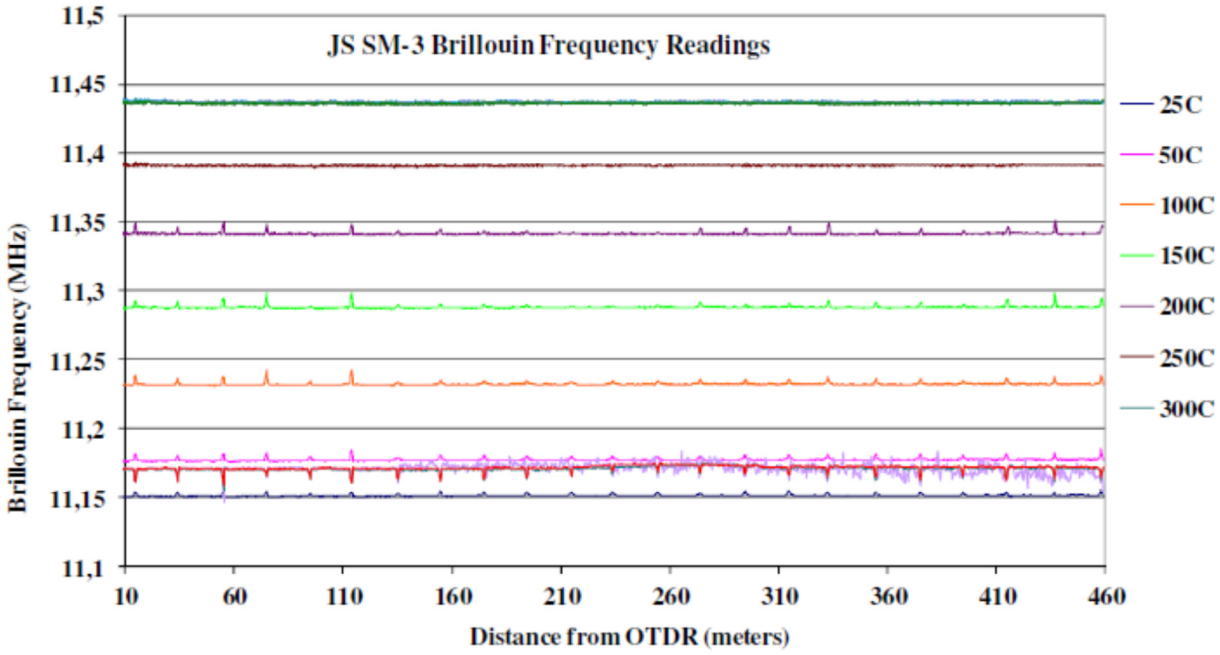

Figure 113: Brillouin readings at different temperatures

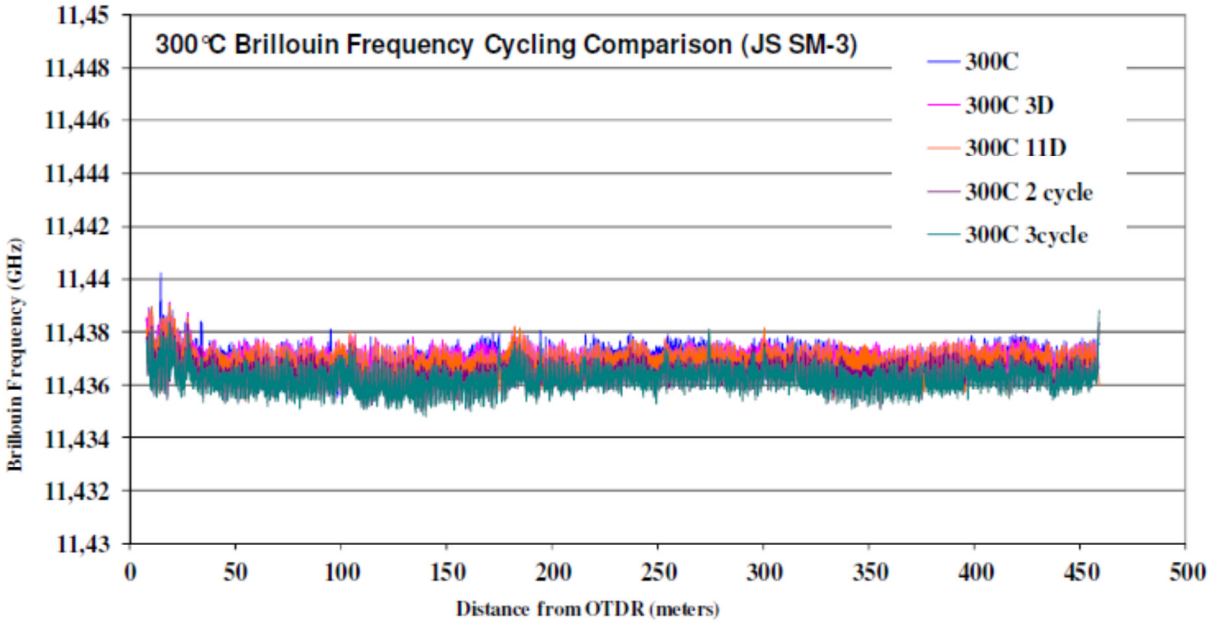

Figure 114: Zoomed in on the 300°C readings

Brillouin measurements were done on the Hydrogen tolerant fiber in the JS533 FIMT also, as shown in Figures 113 and 114. At lower temperatures the Brillouin spectrum scans shows the

intermittent plug points along the FIMT as very small pikes. The frequency shift between the successive higher temperatures is very stable, always about 0.05MHz. The repeatability of the readings through the temperature cycling is very good. All the measurements at 300°C are within a band of 0.003MHz

After the test, the plugs inside the FIMTs were investigated. The Duraseal material changed from a rubbery, soft texture to a hard material that crumbled when handled. This shows serious degradation. The Loctite material (JS533) remained soft and rubbery with no visible signs of degradation. As a result this material was chosen as the superior material. For the next trials the JS533 was always used because of its better performance at 300°C and because of its lower viscosity before curing. The lower viscosity makes the injection easier. The injection pump described in the next section is designed based on the JS533.

The rest of the trial FIMTs, trials 5 through 13, are described in the next sections because they are all done to improve the injection.

Injection pump

At the first trials with an intermittent plug the silicone material was added manually between the first set of rolls, making a U-form of the steel strip and the second set of rolls, closing the U-form to a circle. This method was chosen for its ease to implement, but has the following disadvantages:

A. the amount of injection is not exactly determined and not always the same;
B. injection in a large tube, for example the 2.8/3.2mm FIMT, is not as critical as the injection in a small tube as the 1.5/1.8mm FIMT where excess silicone material can easily cause a weld failure;
C. as a result of the reduction of the tube size after welding by two dies, the fibers are moving faster than the steel strip until the last die. This difference in speed is the main reason the intermittent plugs were much longer than desired. These long plugs are the likely reason for the discontinuities in the OTDR traces;
D. manual injection can be done for a short trial length but is not acceptable for a long production length that runs for several hours.

For reasons A, B and D, low pressure equipment that gives the right dose would be satisfying. But for reason C the injection of the silicone material should be as close as possible to the reduction dies. The closer the injection occurs to the dies, the less the effect of the speed difference between fibers and steel tube. So the goal is to use an injection pump that is able to inject a well-defined dose of silicone material along a long thin needle just before the dies. The dimensions of the needle are determined by the machine setup and the size of the welded tube, ±70cm long with an outer diameter of ±2mm, including a small separate tube for the fibers.

Injection Pump Design

We didn't find a pump on the market that could be used, even with some modifications, for our application. So we decided to design and make our own injection pump. The basic design is illustrated in Figure 115.

The JS533 tube is inside a plastic tube that can be pressurized. The pneumatic cylinder activates the piston, and the one-way-valve prevents the silicone material from being pushed back in the JS533 tube.

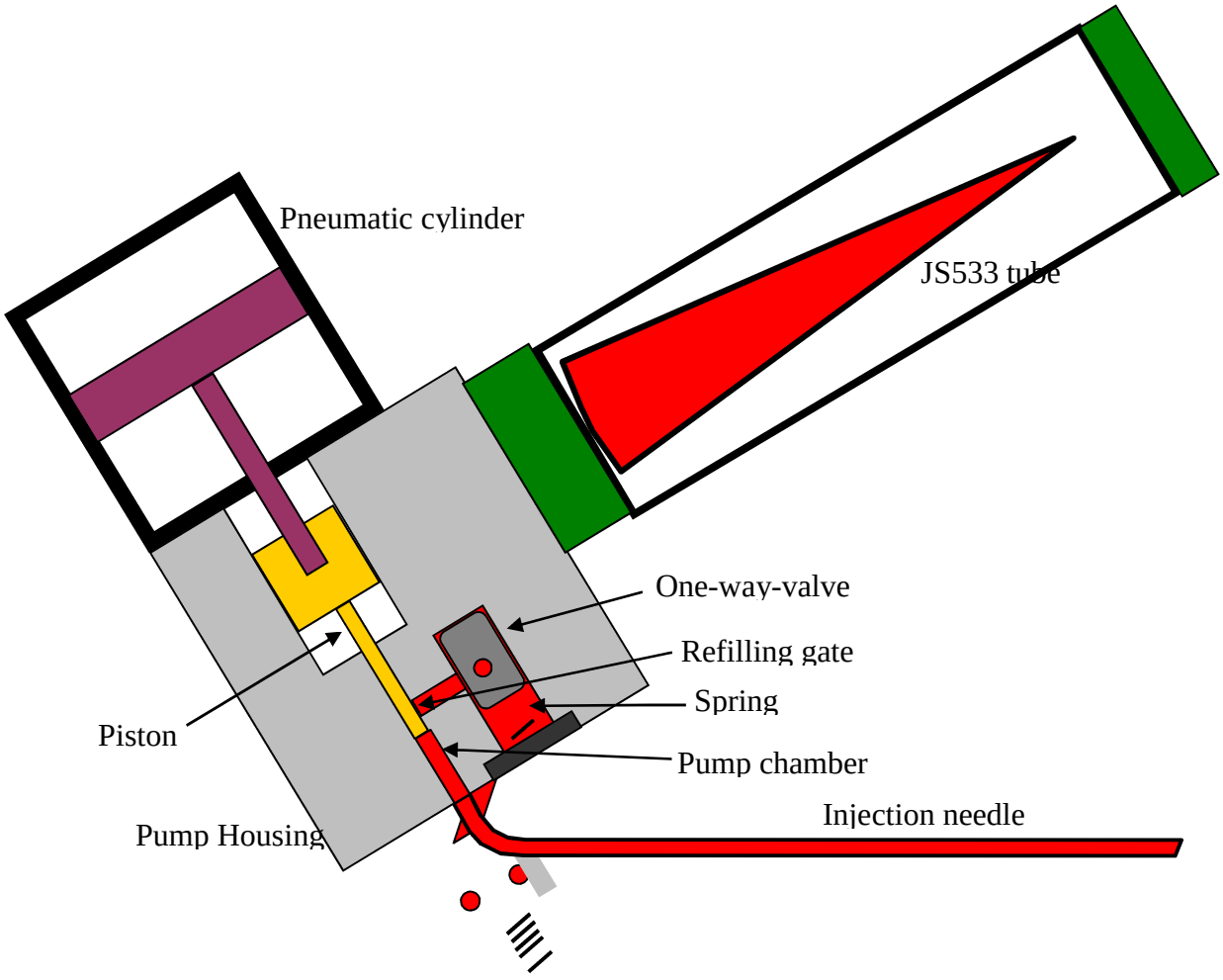

Figure 115: Schematic drawing of the injection pump

One injection cycle consists of the following steps:

1. the tube around the JS533 tube is pressurized so the JS533 is also under pressure;
2. the pneumatic cylinder, and the piston are moving upwards so the refilling gate becomes open;
3. then the JS533 material can flow from the pressurized JS533 tube along the one-way-valve and the refilling gate into the pump chamber;
4. then the pneumatic cylinder and the piston are moving downwards. The JS533 in the pump chamber cannot flow backwards due to the one-way-valve. So the piston is pushing the JS533 into the injection needle

This design was worked out in technical drawings. Some standard parts were available on the market such as:

- The pneumatic cylinder: Festo ADVU Ø40x45, double acting and spring return.
- One-way-valve: Bosch Rexroth M-SR10KE,
- and the JS533 the from Loctite

The other parts are specially made for this application.

After using the pump, it has to be cleaned immediately because of the curing of the JS533. All loose parts of the pump have to be removed and first cleaned by compressed air as well as the pump housing itself. All these loose parts are put in Kroon oil in order to prevent curing until there is time to complete cleaning. The needle is a throwaway component and needs to be replaced each production run.

Trial FIMTs with intermittent plug

The first trials with the new injection pump were 5A and 5B, both 2.8/3.2mm FIMTs of ±500m. For trial 5A standard telecom fibers were used, and for 5B, PI-coated fibers. The standard telecom fibers had good attenuation after welding but the OTDR traces were not straight after rewinding. The trial with the 4 PI-coated fibers had 1 broken fiber after welding. For both trials the pneumatic cylinder was controlled manually so the timing was not very accurate. The dies were placed directly after the weld fixture in order to make the length where the fibers have a higher speed that the steel tube as small as possible. See also Figure 116: the injection pump mounted on the machine, Figure 117: the needle beyond the welding point, and Figure 118: the dies immediately after the weld fixture.

Trial number 6 was made with A625 steel. As mentioned previously, the A625 has less elongation at break (35%, normal >40%, ±44%) so it was not possible to make a 1.5/.8mm FIMT. Instead a 1.7/2.0mm FIMT was made with 4 PI-coated fibers. This time the injection pump was activated by compressed air and 2 electrical valves controlled by the PLC of the machine. The dies were cooled by an emulsion as is standard practice. At the OTDR measurements it was noticed that 1 of the 4 fibers was broken. The OTDR measurements of the other 3 fibers were acceptable.

Trial number 7 was meant to be used in the experimental downhole cable, and therefore much longer than the other trial lengths, 4km. The set-up of the injection process was the same as used for

trial 6. The steel strip however was standard A304. The FIMT was 1.5/1.8mm, as will be needed for a real downhole cable. 3 of the 4 fibers were broken after welding. Investigation of the fiber breaks showed that there are 2 reasons for the fiber breakages:

1. The quality of the fibers is not always 100% along the length. The microscopic in Figure 119 shows that 1 of the broken fibers exhibits a kind of "spike" in the cross section of the fiber, and that the PI- coating is not concentric; and
2. Due to the long needle (±70cm) and the viscosity of the JS533, the needle is "bleeding" a long time after an injected plug. Figure 120 shows that traces of JS533 were found over 170cm of the fibers. This means that the fibers are adhered to the tube over a long distance which induces stress on the fibers.

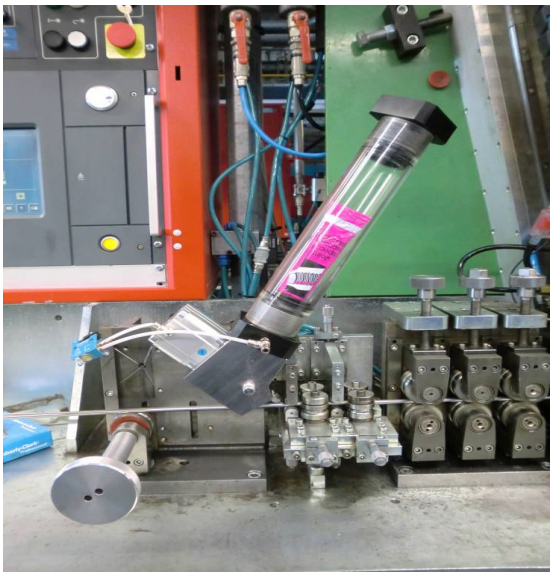

Figure 116: Injection pump on the machine

Figure 117: End of the needle beyond the welding point

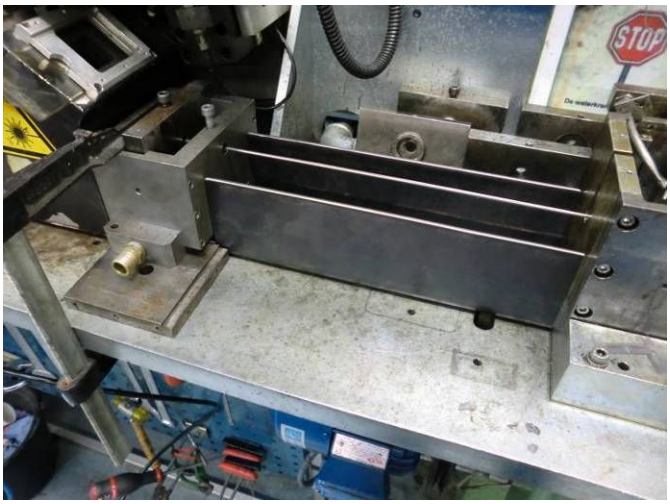

Figure 118: Dies immediately after weld protection

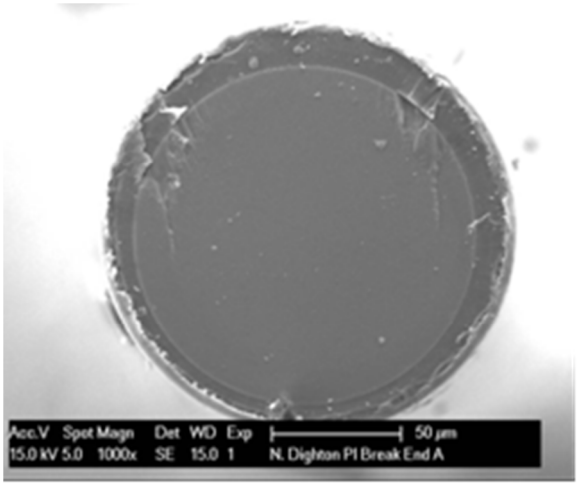

Figure 119: Cross-section of a non-concentric PI-coated fiber.

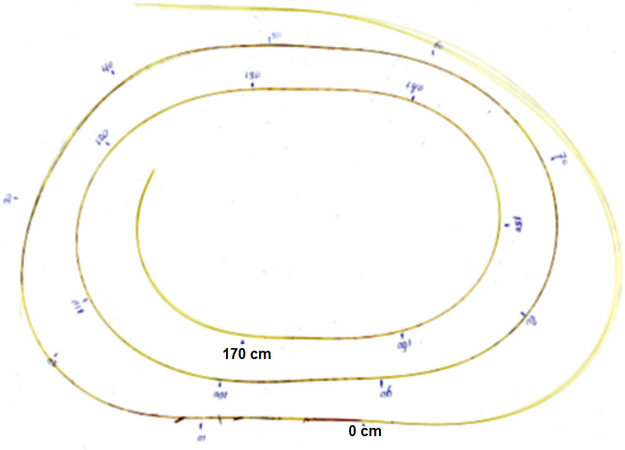

Figure 120: Traces of JS533 were found over 170cm length of fiber

After the poor results of trial FIMT 7 it became clear that it was necessary to solve the problem of the bleeding needle. We devised 2 basic solutions:

1. don't reduce the diameter of the welded FIMT so the speed of the fibers is the same as the speed of the steel strip. If the speed of both is the same, the intermittent plug can be applied in the half open tube between the first set of rolls making a U-shape of the steel strip and the second set of rolls, closing the u-shape to a circular shape; and
2. retract the piston immediately after the injection so the pressure inside the needle is released.

In trial 8 a 1.4/1.7mm FIMT was made of 4.8x0.15mm steel strip without using reducing dies. With a short needle it is easier to inject a plug without after bleeding, but is was much more difficult to inject the correct amount of material to prevent cause weld failures. A little bit too much silicone material causes immediate weld failure. After some trial and error, useful injection parameters were found. Standard telecom fibers were used for this trial length, but after welding one of the four fibers was broken.

Retracting the piston was first tried on trial FIMT 9. After the injection pulse the piston is moved backwards by a stack of Belleville springs. A stack of 6 Belleville springs retract the piston about 0.7mm, see Figure 121. A long injection needle injected the JS533 material directly before the dies. After some adjustments in timing and air pressure useful parameters were found. Three standard telecom fibers were used, and the OTDR measurements after both welding and rewinding showed no broken fibers.

FIMT 10 was a long length of 3.5km, intended to be used in an experimental downhole cable. Because the intermittent plug was still not reliable enough to be used on a long length with PI-coated fibers, a dry FIMT was made. The dry 1.5/1.8mm FIMT with 4 PI-coated fibers ran without problems.

Trial runs 11A and 11B were made to repeat the results of trial 9 (11A) and to test the more vulnerable PI-coated fibers with the same injection parameters (11B). Repeating the trial 9 was no problem, and the 3 standard telecom fibers had good attenuation values. After the good result of 11A, the standard telecom fibers were replaces by 4 PI-coated fibers. Again, 2 of the 4 PI-coated fibers were broken. The conclusion was that PI-coated fibers are much more vulnerable than standard telecom fibers, and that more sophisticated changes on the injection pump are necessary to improve the injection plug, i.e. smaller amount of injection and more retracting of the piston.

Redesign injection pump

For further improvement of the injection, the pump needed a few items of redesign. The main changes are:

- retracting of the piston by a spring in the pneumatic cylinder; and
- making the piston diameter smaller so the amount of injection and also the retraction can be better defined.

The retraction of the piston by a stack of Belleville springs was not enough. The movement backwards was less than 1mm. A spring in a pneumatic cylinder is a well-known method to move a cylinder backwards. However we don't want the cylinder moving backwards until the end of the cylinder. It should only be moving backwards halfway because the piston has to block the refilling gate until the next injection. The backward movement by the spring is limited by two bolts inside the pneumatic cylinder, as shown in Figure 122. The refilling gate becomes free if the cylinder is activated by compressed air again.

For the 2.8/3.2mm FIMTs the Ø5mm piston worked fine. However for the 1.5/1.8mm the movement of the piston has to be limited so much that it is not practical anymore. Therefor a new Ø3mm piston was made. If the piston is smaller the pump chamber also has to be smaller. To achieve this, a 12mm bolt with a Ø3mm hole was screwed in the pump house.

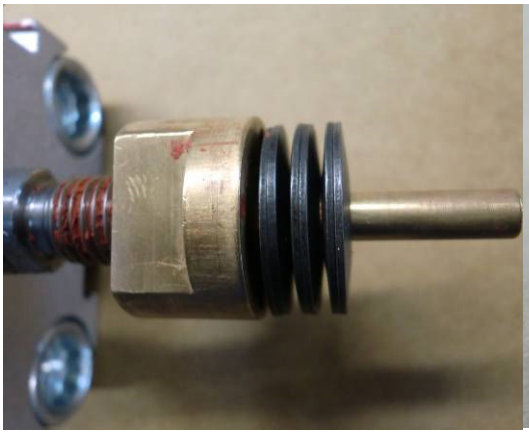

Figure 121: Stack of Belleville springs

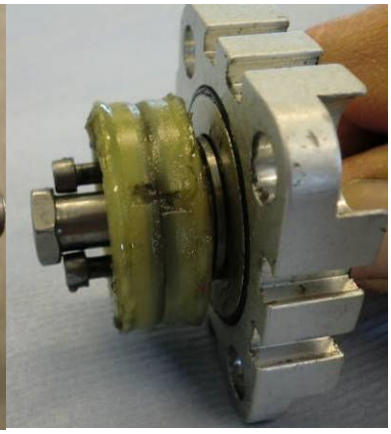

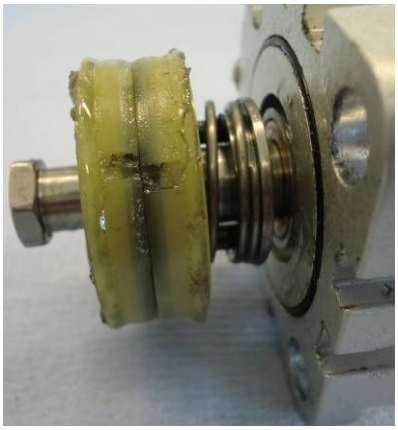

Figure 122: The spring inside the pneumatic cylinder is pressed at injection and it sprung back subsequently

Trials with improved injection pump

The first trial with the redesigned injection pump was 12A with 3 standard telecom fibers. Inspection of the intermittent pug showed that there was a big improvement. The material of the plug was within an area of 12cm to 15 cm without traces of JS533 before or after the plug. The 3 telecom fibers had all good attenuation after production. The second trial, 12B, was made on the same day with 4 PI-coated fibers. This trial had good attenuation and no fiber breaks.

With this good result in mind a new trial with A625 was made, trial 12C. This trial was not a success because after 450m there was a weld failure and one of the fibers was broken again. Also the investigation of the intermittent plug showed that there were traces of JS533 before and after the plug itself. We had the impression that the retraction of the piston was not working because of too much friction of the piston. To improve the visibility of the injection process, sensors were mounted on the pneumatic cylinder to detect the movement /position of the cylinder. These sensors were read by the PLC that generates a red light if the cycle of the cylinder is not right, as shown in Figures 123 and 124.

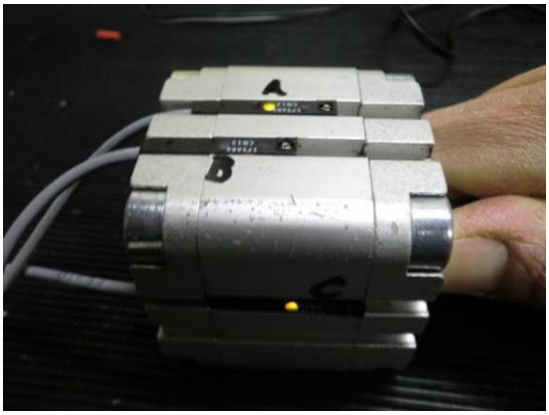

Figure 123: sensors mounted on the pneumatic cylinder

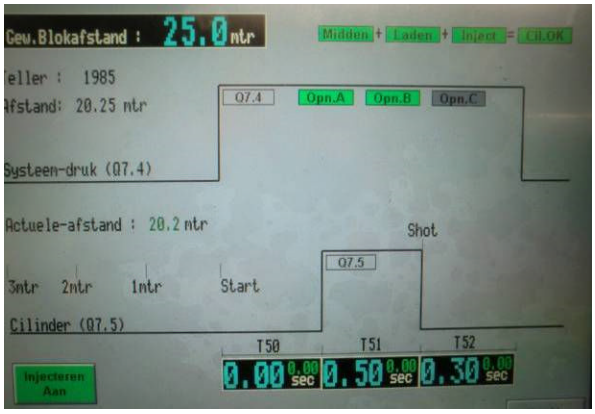

Figure 124: PLC generates a red or green light

3.2.3 Test and Validate Buffer Tube and Fiber Construction Prototype with Draka Fiber

Most of the FIMT trials produced were sent to Draka USA for tests and investigations. A few temperature tests were done in Delfzijl.

Test 1.5/1.8mm A304 FIMT

During rewinding of FIMT 11B on the small aluminum spool, the best part was cut out. On the small aluminum spool were no broken fibers. This spool was put in an oven and the attenuation was measured by OTDR at different wave lengths for SM and MM fibers. First the temperature was raised in steps of 50°C until 300°C (max temperature of the oven), stabilized at 300°C for a few days, cooled until 50°C and then again raised up to 300°C. The results of the OTDR measurements are depicted in the graphs of Figure 125.

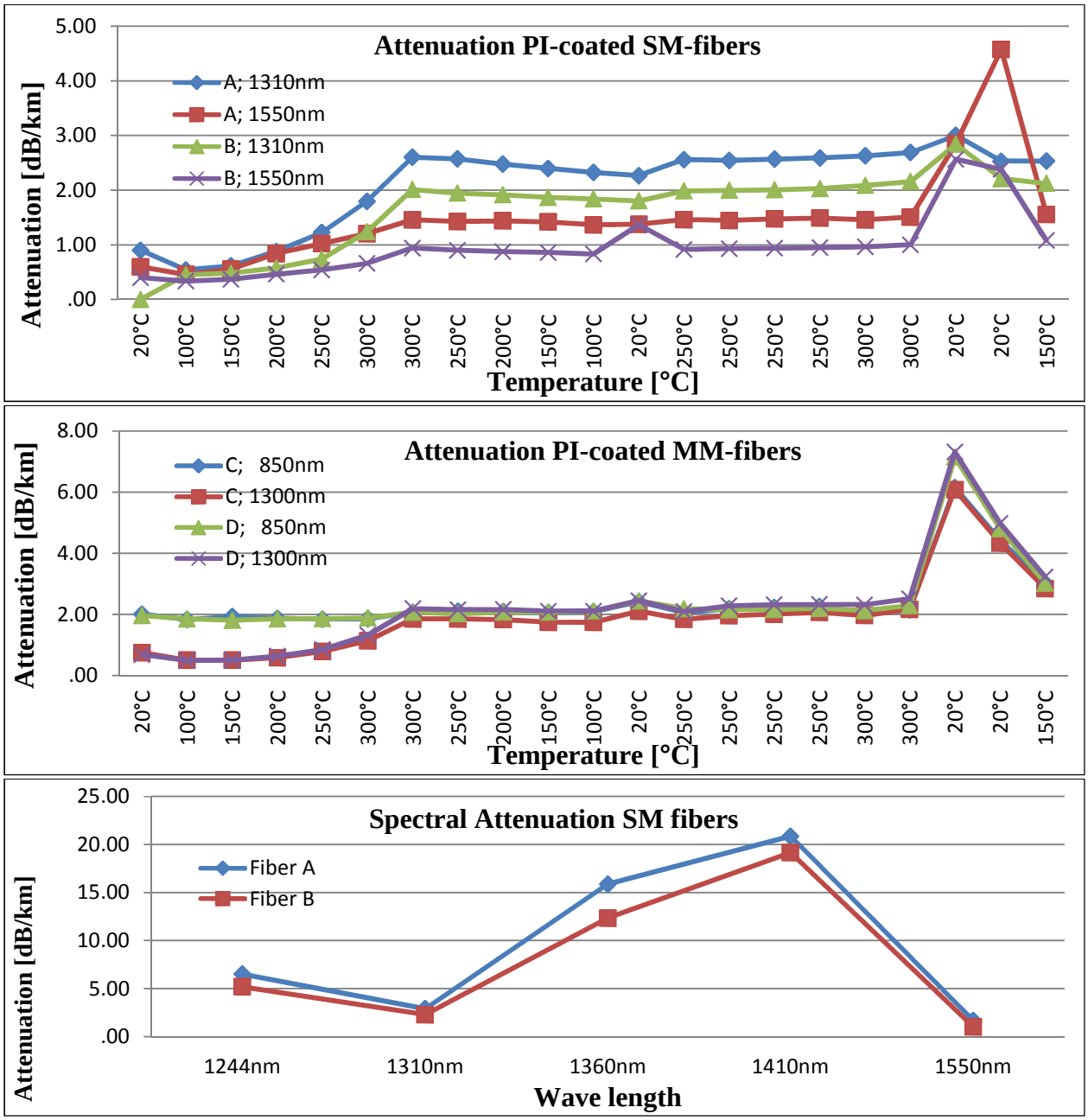

Figure 125: OTDR measurements at high temperatures.

The graphs in Figure 125 show an attenuation increase above 150°C until 300°C for both type of fibers SM and MM, however the attenuation increase at 850nm is negligible. OTDR measurements on more wavelengths, especially at wavelengths where hydrogen can be detected, 1244nm and around the OH-peak at 1383nm, 1360 and 1410nm, show that there is hydrogen in the fibers. Hydrocarbons inside the FIMT are cracked at these high temperatures. One of the sources of hydrocarbons inside the FIMT is most likely the lubrication we used during welding. The lubrication of the steel strip before it enters the forming rolls makes the welding process more stable and reliable. In a next trial the FIMT will be made without using the lubrication oil.

Another phenomenon that can be identified from the attenuation measurements is that at the end, at lower temperatures, the attenuation rises to very high values, especially at 1550nm for the SM-fibers and on both wave lengths for the MM-fibers. This is probably caused by the EFL of the fibers in the tube. The alloy of the FIMT was A304 which has a higher CTE than the glass of the fibers.

Test 1.7/2.0mm A625 FIMT, with and without lubrication of the steel strip

In order to search for the source of the Hydrogen in the FIMT, two additional short trial lengths were made, both without the intermittent plug, FIMT 13A and 13B. For both FIMTs A625 steel was used because it has a CTE of only 12.8µm/m/K. Because there was less elongation in this steel strip the FIMT size increased to 1.7/2.0mm. The first length was made without lubrication oil on the welding machine and the second was made with lubrication oil. The one without lubrication oil failed after 420m because the steel strip folded double between roll 6 and 7. Both FIMTs contained 3 PI-coated fibers, 1 MM hydrogen sensitive fiber, 1 MM hydrogen tolerant fiber, and 1 SM hydrogen sensitive fiber.

One of the reasons that the attenuation increased after cooling down in the previous test could be aluminum reel that was used in the oven. Aluminum has a CTE of 22.2µm/m/K so it is possible that the FIMT is elongated at high temperature in the oven. In order to protect the FIMT from this effect a modified aluminum reel was used. This time the reel had a 3mm wide kerf at one side, see Figure 126.

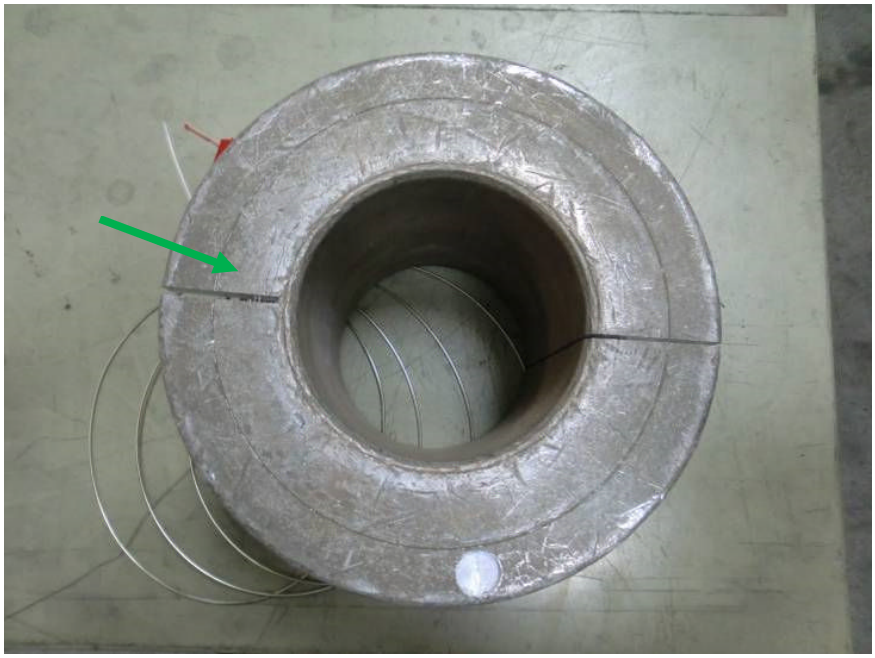

Figure 126: Aluminum reel that is able to adapt the difference in CTE

The results of the OTDR measurements of these 2 trial lengths are depicted in the graphs of Figures 127 and 128.

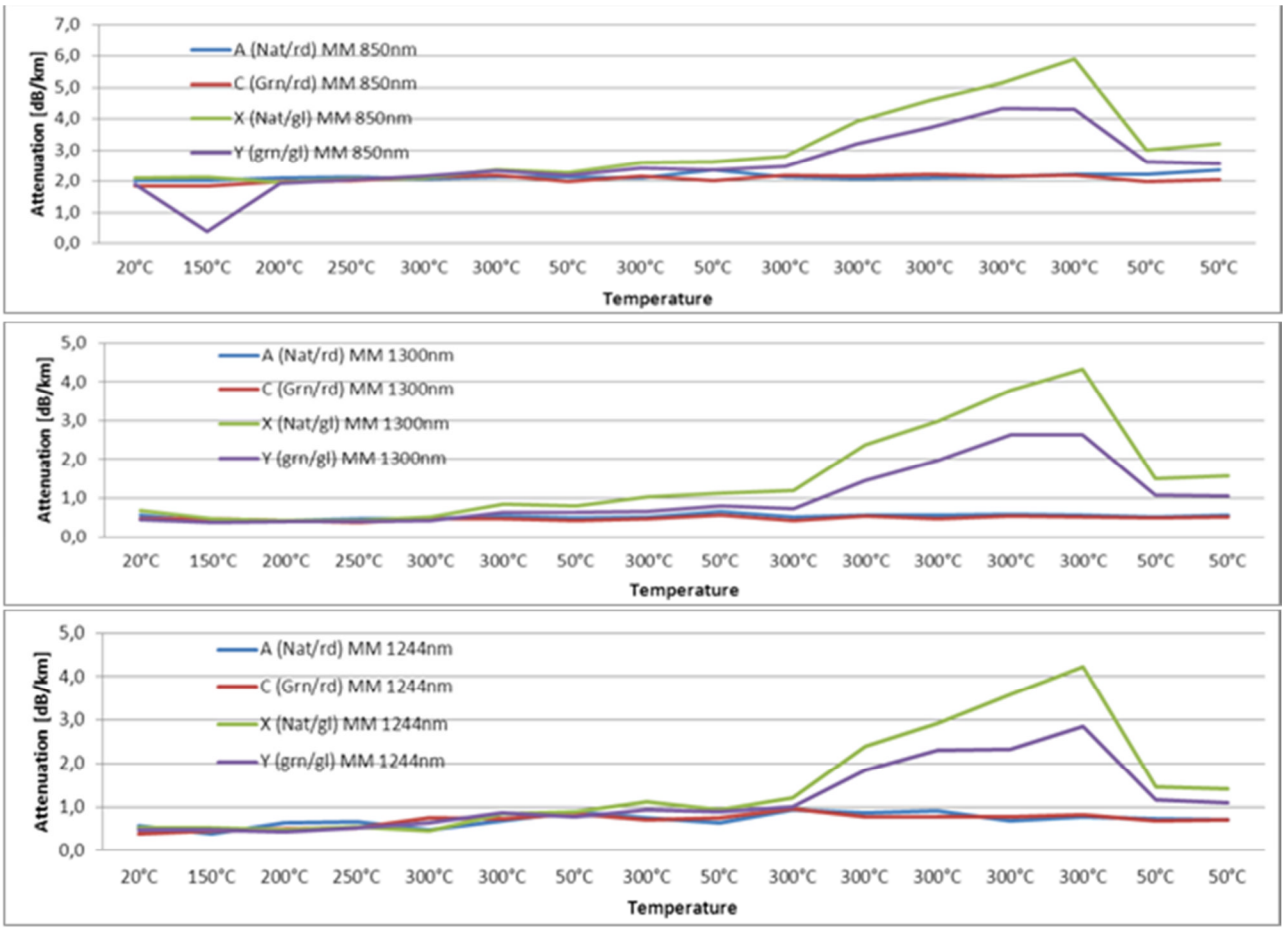

Figure 127: OTDR measurements of the MM fibers at high temperatures

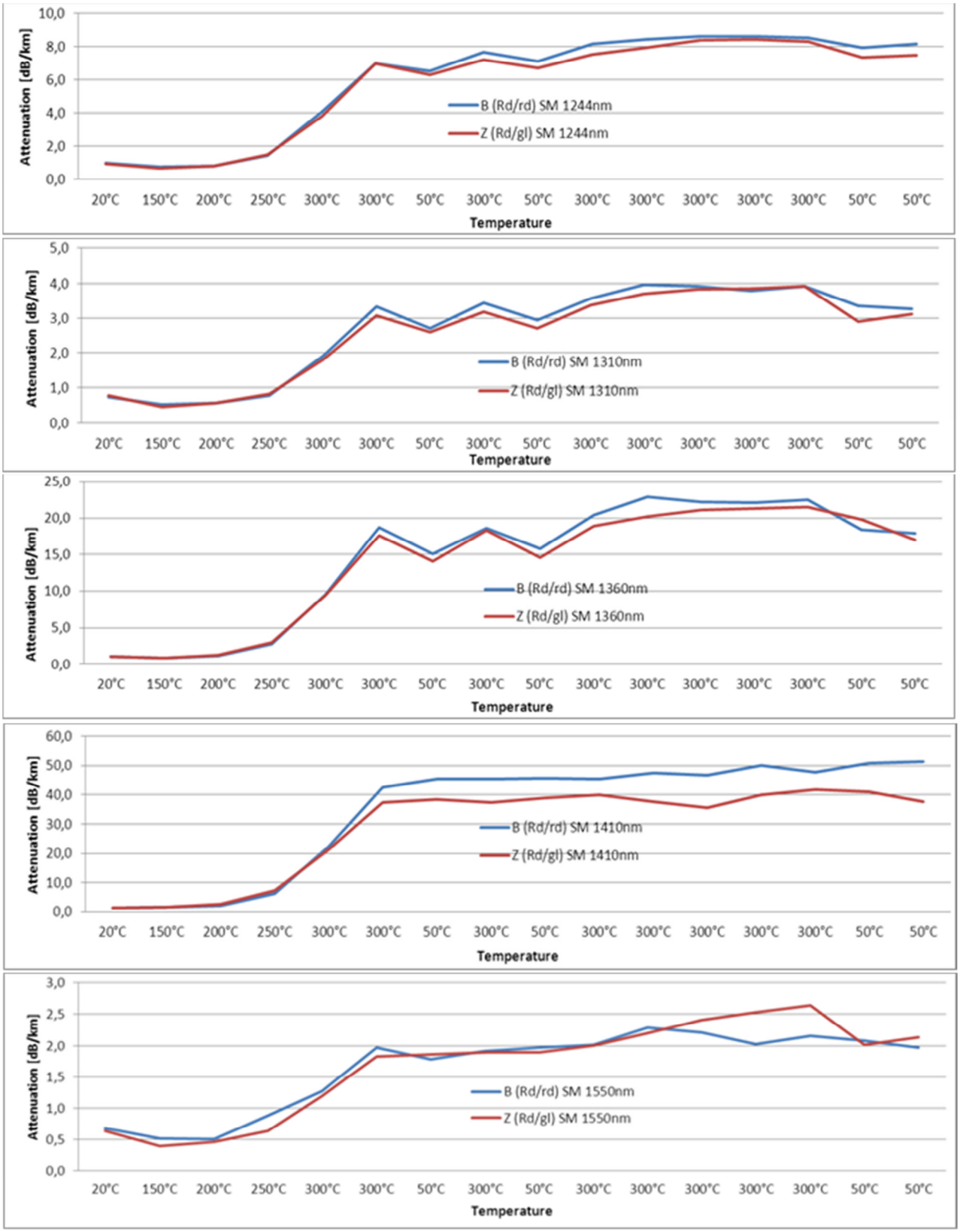

Figure 128: OTDR measurements of the SM fibers at high temperatures

The graphs in Figures 127 and 128 show that there is still hydrogen in the FIMTs, and there is no difference between the FIMT produced with or without the lubrication oil. This tells us also that the intermittent plug was not the source of the hydrogen in previous trials (for example FIMT 11B). The second lesson is that hydrogen tolerant fibers, the MM fibers A and C, have very good attenuation values during the whole test. The third lesson is that cooling down and rising the temperature again during test has no major influence on the attenuation values. Because four parameters were changed in the trial setup: steel strip alloy, FIMT size, no intermittent plug, and adapting aluminum reel; it is not evident which of the differences was responsible for this improvement. The fourth lesson is that the MM fibers show attenuation increase after a few days at 300°C, and the attenuation increase of the SM fibers starts immediately at 300°. The reason behind this phenomenon is not clear, but is probably because of the wavelengths 850nm and 1300nm are less sensitive for hydrogen.

Test 1.7/2.0mm A625 FIMT, with pre-treated Polyimide fiber

After removing the lubrication oil and the intermittent plug, the FIMT was still generating hydrogen at 300°C. Searching for a possible explanation it was noticed that the Polyimide fiber changed in color from light brown (gold color) to more dark brown. Could it be possible that the Polyimide is generating the hydrogen? In order to investigate this, a hydrogen sensitive SM-fiber was rewound on an aluminum reel that was able to adapt differences in CTE (kerf at one site of the reel). The tension on the fiber was released by compressing the kerf in the aluminum reel and the fiber was placed in the over at 300°C for 3 days. After this pre-treatment the fiber was rewound on a normal fiber reel and used in a 1.7/2.0mm A625 FIMT, FIMT 13C. The A625 steel was also pre-treated at 300°C and no intermittent plug was used. For lubrication of the steel strip a non-hydrocarbon perfluoropolyether Krytox® oil was used. The 400m long trial FIMT was rewound on the aluminum reel that was able to adapt differences in CTE and put in the oven at 300°C. The results are depicted in the graph of Figure 129.

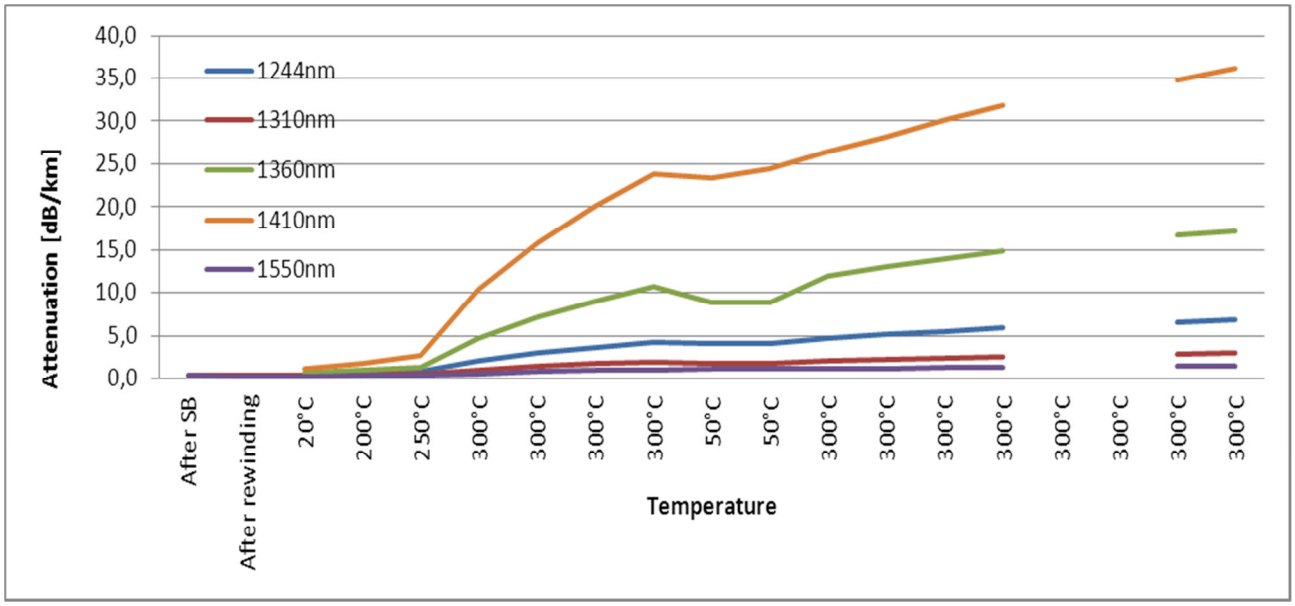

Figure 129: OTDR measurements of the pre-treated SM polyimide fiber

Although there is still some hydrogen generated in the FIMT, this process is much slower compared to the FIMTs without pre-treated Polyimide fibers. So pre-treatment of the fibers can slow down the hydrogen generation, but it can't eliminate it.

Until now it is not clear what is causing the hydrogen generation inside the FIMT at 300°C. Probably the lubrication of the steel strip and the Polyimide coating of the fiber are important items, but there is more. However, we were not able to eliminate the hydrogen generation inside the FIMT. The use of hydrogen tolerant fibers doesn't increase the attenuation of the fibers due to hydrogen presence. In a geothermal well, eventually over time and increasing temperature, hydrogen will penetrate inside the FIMT and fibers, so it is preferred to always use hydrogen tolerant fibers.

FIMT in hydrogen environment

Even though a welded FIMT seems to be a good protection against the hydrogen in the well, operators of oil, gas and thermal wells are still concerned about the risk of hydrogen darkening of the fibers used in wells. In order to investigate this phenomenon we produced a dry 1.5/1.8mm FIMT with a 150°C acrylate coated SM-fiber and put it in a 4.6/5.1mm stainless steel tube. The space between the small FIMT and the outer tube is filled with 100% pure hydrogen at ±4bar. This 650m long tube in tube construction is placed in an oven at 150°C. The design of this experiment is depicted in Figure 130. The attenuation was measured by OTDR at five wave lengths, 1244nm, 1310nm, 1360nm, 1410nm and 1550nm. The results are depicted in Figure 131. After a month the hydrogen bottle was empty.

This experiment shows that under high temperature and high pressure, a stainless steel FIMT is not a hermetic shield around the fiber inside. After time, depending on temperature, pressure, and hydrogen concentration, the attenuation of the fibers in the FIMT will increase.

It is unlikely that the hydrogen inside the FIMT is generated by the hydrocarbons inside the FIMT. As demonstrated in the previous tests (13 A, 13B, 13C, and the last experiment reported above) this process starts above 200°C (±250°C). This experiment illustrates that in oil, gas and thermal wells, hydrogen tolerant fibers should always be used.

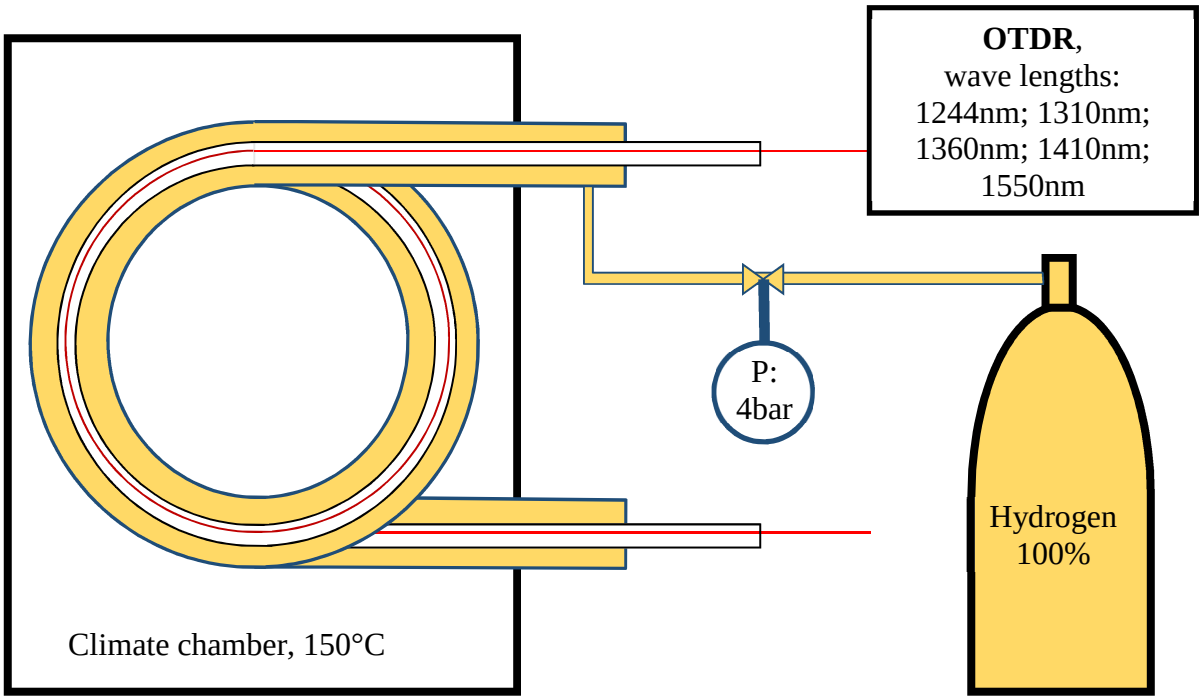

Figure 130: Setup FIMT in hydrogen environment

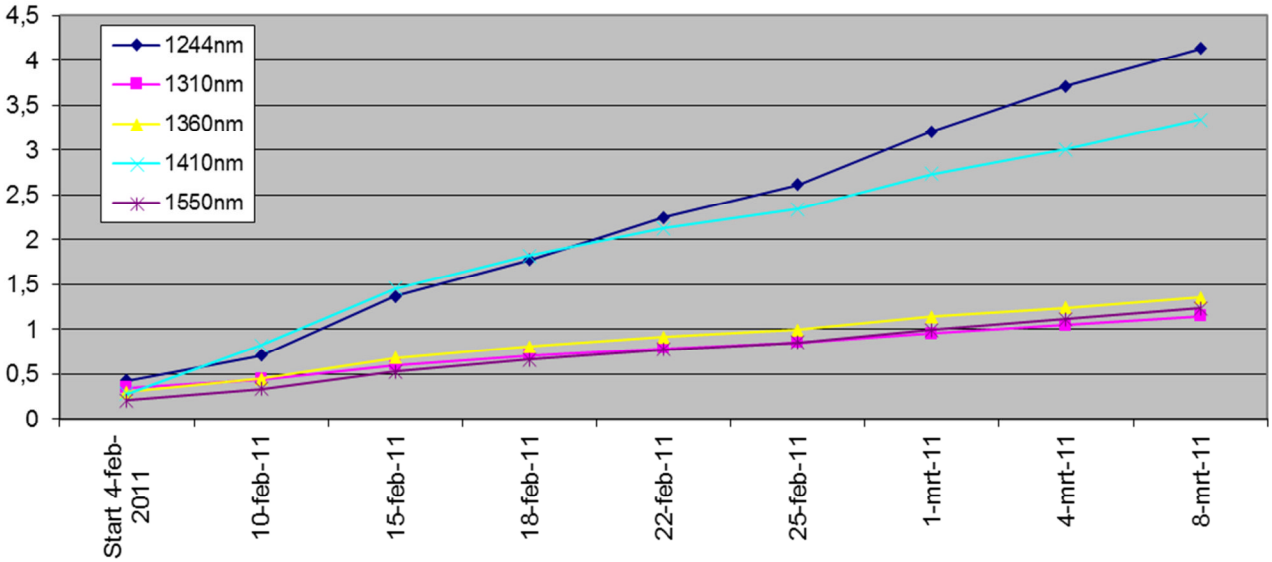

Figure 131: Attenuation increase during hydrogen test in dB/km

Production lengths

The goal of this project is not only to make short trial lengths, but also a 3km+ production length that can be used in a real geothermal well. A dry version of this 1.5/1.8mm FIMT with Polyimide coated fibers was made in October 2012 (FIMT 10 in Table 34.) In this section the production of the FIMTs with intermittent plugs is described, FIMTs 14A, 14B and 14C.

March 2013 trial for a long production length with intermittent plug

The first trial to make a more than 3km long production length was in March 2013 using the modified injection pump controlled by the PLC. The JS533 intermittent plug was injected every 25m (amount of injection: ±0.04gr). After 1100m we had a broken fiber on the fiber pay-off. Because of this broken fiber the production was stopped. Measuring the 1100m showed that there was another broken fiber in the FIMT at 434m from the outer end. Both broken fibers were MM-fibers. After rewinding, one of the SM-fibers didn't have a straight OTDR curve. A summary of the OTDR measurements is given in Table 35.

Attenuation after welding	850nm	1300nm	1310nm	1550nm		Length [m]
Fiber A	-	-	0.414	0.340	dB/km	1120
Fiber B	-	-	0.453	0.406	dB/km	1120
Fiber C	-	-	0.829	0.632	dB/km	1120
Fiber D	-	-	2.425	2.879	dB/km	434
Attenuation after rewinding						
Fiber I	-	-	0.891	0.610	dB/km	1070
Fiber II'	-	-	0.895	1.043*	dB/km	1070
Fiber III'	2.476	1.312	1.495	0.968	dB/km	1070
Fiber IV	2.360	1.266	1.549	1.018	dB/km	700
* trace not straight						

Table 35: OTDR measurement results first production trial 14A

Figure 132: Broken PI-fiber

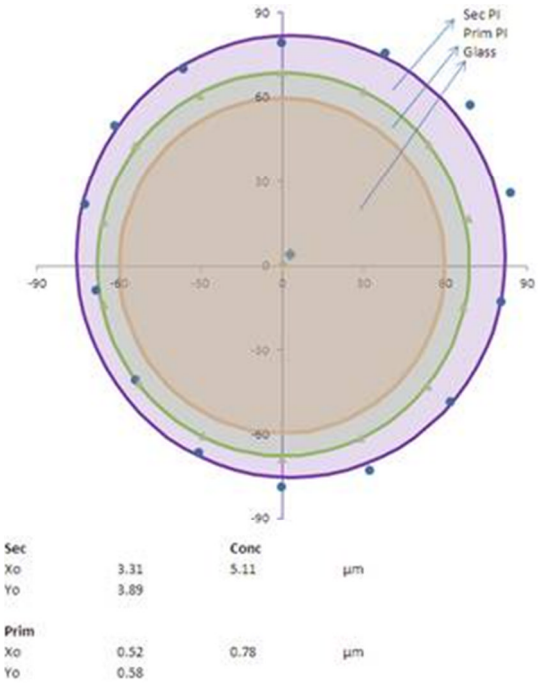

Figure 133: Cross section broken fiber

Analyzing the broken fiber showed that the second layer of PI-coating was not centric. This most likely caused the weak spot in the fibers, see Figure 133.

June 2013 trial for a long production length with intermittent plug

The second trial (14B) was made in June 2013 using the same setup as in March. Again one of the MM-fibers broke on the pay-off after ±650m (pay-off tension ±160cN). The original length of the fibers was a little more than 3.6km so the machine was restarted immediately for another trial. This time after 500m, a weld failure occurred due to damage on the long injection needle. The long injection needle was welded together with the tube in production. A summary of the OTDR measurements is given in Table 36.

First trial	850nm	1300nm	1310nm	1550nm	Length
Fiber I	2.024	0.875	0.989	0.656	659m
Fiber II	1.960	0.848	1.037	0.696	659m
Fiber III	-	-	1.096	0.892	659m
Fiber IV	-	-	0.663	Forgot to print	659m
Second trial	850nm	1300nm	1310nm	1550nm	Length
Fiber A	-	-	0.678	0.507	526m
Fiber B	1.985	0.963	1.057	0.722	526m
Fiber C	2.054	0.937	1.139	0.759	526m
Fiber D	-	-	1.061	0.783	526m

Table 36: OTDR measurement results second and third production trial, FIMT 14B

Analyzing the broken fiber showed once again a non-centricity (3%) of the secondary PI-coating. The minimum wall thickness (of PI coating) was 16 µm.

September 2013 trial for a long production length with intermittent plug

In September 2013 a new set of fibers was available to make a production length (trial 14C). Again 1 fiber broke on the fiber pay-off after 360m. We decided to continue production but didn't use the rolls on the fiber pay-offs in the normal S-shape. This time the fiber touched only the top of one roll as shown in Figure 134. In order to prevent the long injection needle from welding together with the tube in production, the injection needle was a little bit shorter compared to the previous trials and stopped just before the welding point. In Table 37 the most important process parameters are listed.

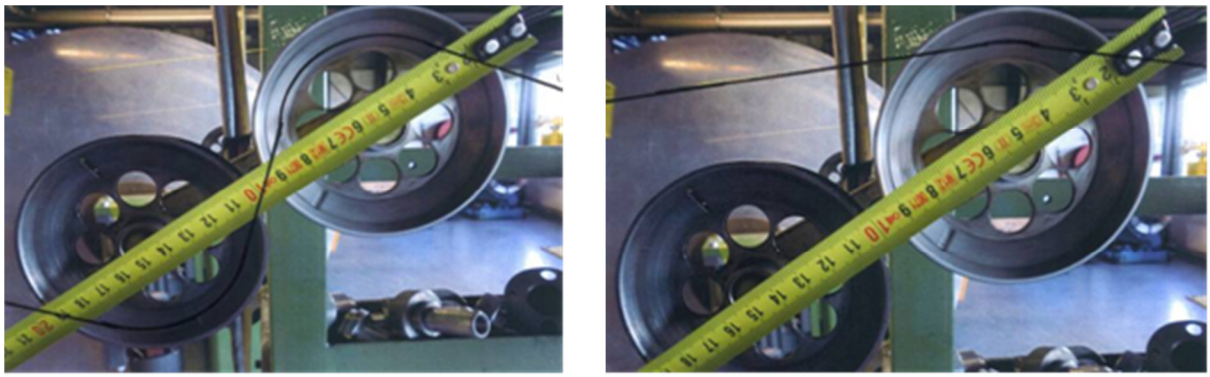

Figure 134: Fiber along the pay-off rolls before (S-shape) and after the broken fiber.

Steel strip	7.9x0.15mm, DIN 1.44004		
Tension on fibers	125cN	Take-up tension	80N
Tube size	1.5/1.8mm	EFL reduction rolls	3x Ø80mm
Line speed	8m/min	Measured EFL	0.24%
Focus	12.0mm	Intermittent plug	25m
Laser power	600W	Plug material	JS533: 0.035gr/plug

Table 37: Process parameters steel tube welding

After the broken fiber no other problems occurred and the production continued until the first fiber reel was empty. After steel tube welding, the FIMT was rewound on a transport reel. The results of the OTDR measurements are in Table 38.

Attenuation after welding	850nm	1300nm	1310nm	1550nm		Length [m]
Fiber A	1.955	0.437	-	-	dB/km	3610
Fiber B	-	-	0.476	0.365	dB/km	3610
Fiber C, broken on fiber pay-off	not measured	0.470			dB/km	3220
Fiber D			0.379	0.258	dB/km	3610
Attenuation after rewinding						
Fiber I	1.984	0.895	-	-	dB/km	3180
Fiber II	-	-	0.644	0.380	dB/km	3180
Fiber II	-	-	0.969	0.623	dB/km	3180
Fiber IV	2.011	0.927	-	-	dB/km	3180

Table 38: OTDR measurement results production trial, FIMT 14C

3.2.4 Conclusions on High Temperature Buffer Tube Development

Using a FIMT in a hot geothermal well requires high demands on the design and production of this FIMT. Because of the high temperature in the well, normal cable gels can't be used, and a special alloy of stainless steel is needed. Normal gels will become liquid, pushed out and burn. Normal stainless steel alloys have a too high CTE, and the cable construction is not able to adapt to the difference in length for a temperature change of 300°C.

Steel

Alloy 625 has a CTE much closer to the CTE of glass and has good processability on a FIMT welding line. Alloy 825 has also a CTE close to glass but is less processable on the FIMT welding line. However, alloy 825 is a metal that is often used for encapsulation tubes and armoring wires in the downhole cable construction. In the cross section of the downhole cable, the A825 dominates the CTE of the construction, so the small amount of stainless steel of the FIMT is not so important. If the FIMT is part of this kind of cable design, A316 is a good alloy to use. If the FIMT is part of a less massive construction A625 is preferable.

Filling material

Instead of a normal cable gel, it may be better not to use any gel at all. A dry FIMT with PI-coated fibers inside can be used up to 300°C. A downhole cable for geothermal wells containing a dry FIMT with PI-coated fibers has been made and is undergoing tests in Phase 3 of this project. The vertical deployment and variations in temperature however may cause problems to the fibers. Over time it is possible that the fibers sink downwards, and the fibers are under tension in the upper part of the cable and buckle stress in the lower part of the cable. In order to prevent the creep downwards, some kind of adhesive between fibers and FIMT is needed. Several commercially available materials have been tested. Loctite JS533, a silicone based material, was selected as the best available material. Applying the JS533 all along the FIMT caused high attenuation on the fibers. Therefore an intermittent plug was employed. Patent US8929701B2 entitled: Loose-tube optical-fiber cable was granted January 6, 2015. Every 25m a small amount of JS533 was injected in the tube. This is enough to prevent the fibers from creeping downwards. If this small amount (±0.04gr) is injected on a small spot in the FIMT, it doesn't have a negative influence on the attenuation of the fibers. In order to be able to inject such a small amount of JS533 on a very local spot in the FIMT, a special injection pump was designed and made. After a lot of trials and improvements a 3km long FIMT with an intermittent plug was made. Because of the problems described and the time factor, this FIMT with intermittent plug hasn't been used in a downhole cable trial.

High temperature tests

Short trial lengths of ±400m have been tested in an oven at 300°C. In all these tests hydrogen is causing attenuation increase. One of the possible causes is the lubrication of the steel strip. Another possible cause could be the PI-coating of the fibers. We were not able to make a FIMT that doesn't have attenuation increase at 300°C over time. Another test of a FIMT in a hydrogen environment at elevated temperatures (150°C) and pressure (4bar) showed that the stainless steel tube is not a hermetic barrier for hydrogen. Over time, the hydrogen will increase the attenuation of the fibers in the FIMT. So over time hydrogen will affect the fibers anyhow. Therefore it is important to use hydrogen tolerant fibers in a downhole cable. These hydrogen tolerant fibers were developed and

reported on in Phase 1 of this project.

3.3 HIGH TEMPERATURE CABLE DEVELOPMENT

The scope of this task was to develop an extrudable insulation or other alternative insulation for the electrical conductors with performance characteristics suitable for EGS use.
Manufacture lengths of cable using insulation candidates and evaluate the material performance. The candidate material with the best combination of resistance to temperature and fluids and manufacturability will be selected for the final cable design. A key success factor is manufacturability, the material developed needs to be manufactured using existing equipment.

3.3.1 High Temperature Cable Jacketing and Insulation

Prior to the award of this development program, the highest temperature rated extruded insulation was 260°C. Inorganic insulation materials had been used at higher temperatures, however the electrical properties of these materials are significantly poorer than extruded materials and the properties were not stable with changes in temperature. As we are not experts in high temperature polymer development, we sought assistance from several experts in this development. From work previously performed, we were confident that the Fluoroplastic family had promise of being able to meet temperatures higher than 260°C. The Chemours Corporation expressed interest in pursuing the development of a melt extrudeable insulation material rated at 300°C. They developed a proprietary process to manufacture a new class of Fluoroplastic that exhibited the following enhanced properties:

- High thermal stability
- High melting point (320 °C)
- Excellent dielectric properties
- Excellent chemical and permeation resistance
- Broad wire processing window of operation

This material was subjected to testing by Draka, Chemours as well as Underwriters Laboratories to establish that the new material was suitable for operation at 300°C. In addition, this material demonstrates enhanced properties (e.g., higher melting point, increased melt viscosity, improved stress crack resistance) when subjected to post processing heat treatment. This effect, known as epitaxial co-crystallization (ECC), occurs when the resin is heated between 280-300 °C for a prolonged period. This material has been designated as Chemours™[6] ECCtreme™[7] ECA 3000 fluoroplastic resin

[6] *Chemours is a registered trademark of the Chemours Company FC, LLC*
[7] *Ecctreme is a registered trademark of the Chemours Company FC, LLC*

Key material certifications and evaluations are:

- Underwriters Laboratory certification for continuous-use at 300°C in accordance with UL Standard 746B.
- Chemical Resistance Evaluation by Chemours where the material physical properties did not degrade when exposed to the following chemicals for 90 days.
    - Ammonium Hydroxide 35%
    - Hydrochloric Acid 37%
    - Hydrofluoric acid 20%
    - Nitric Acid 63%
    - Sulfuric Acid 98%
    - Sulfuric Acid 98% @ 150˚C
- Resistance to Fluids at High Temperature and Pressure Evaluation by Chemours where the modulus did not decrease when exposed to the following fluids and conditions:
    - Diesel Fuel at 300°C and 5000psi for 2 weeks
    - Brine at 300°C and 5000psi for 4 weeks
    - Krytox® at 300°C and 5000psi for 4 weeks
    - Stream at 300°C and 1200psi for 3 months

An alternate insulation using mica tape and fiberglass was considered for operating temperatures greater than 300°C, up to 400°C. A prototype was manufactured and the insulation resistance was not stable. The insulation improved over time at high temperature indicating the need to add processing steps to pretreat the cable core prior to installing in the metalclad tube. Another disadvantage of the mica tape and fiberglass braid insulation system is the manufacturing expense. Taping and braiding are much slower manufacturing process than extrusion and associated labor costs are approximately six times greater than extruded insulation. Ultimately the extruded ECCtreme™ ECA 3000 extruded insulation material was selected for the final cable design because other cable elements were limited to 300°C operation.

3.3.2 Trial Cable

Following the development of the insulation material, prototypes of the downhole cable were manufactured and tested at 300°C in our laboratory to qualify the cable for operations at 300°C both for performance of the fiber and the electrical conductor. Performance of the fiber and buffer tubes were addressed in detail in previous sections of this report and the overall cable design is addressed in the next section of this report; the focus of this section is the ECCtreme™ ECA 3000.

The ECCtreme™ ECA 3000 material processed well on existing equipment and there were no significant challenges. Though, there was initially a high in-process dielectric failure rate. This was resolved when the material was run without color concentrate and based on supplier recommendation an alternate more compatible color concentrate can be used if color coded products are required. Several prototype cables were manufactured and subjected to routine factory inspection tests where the material performed well. Cable samples were subjected lab tests where the insulation electrical performance was evaluated at 300°C and insulation passed 1000VDC

dielectric withstand test and there was no capacitance change compared to measurement at room temperature.

3.4 METAL CLAD CABLE DEVELOPMENT

The technical challenge of this task was to extend the performance of Draka's existing tube encapsulated cable (TEC) with the product name Metalclad cable with enhanced materials and manufacturing methods for required core fillers, water and gas blocking, securing of internal components, exterior encapsulation, and strength members needed for unsupported vertical installations. This required identification and validation of materials and cable designs intended to operate at 300°C. Manufacture of cable prototypes to determine optimum geometry of internal components, manufacturing processes, and whether internal polymeric or metallic anchors will hold the components securely.

3.4.1 Develop High Temperature Core Filler

The core filler are the cable elements that occupy unused space in the core to achieve a round core that will fit firmly in the overall metal tube. Key properties of the materials used are similar to the high temperature insulation discussed in section 3.3. Therefore the ECCtreme™ ECA 3000 was selected as the filler material.

3.4.2 Evaluate Securing Buffer Tube and Twisted Pair Within Cable

Conductors and buffer tubes along with fillers needed to create a round assembly are secured to each other by twisting; an overall tape wrap and an extruded jacket are also be used to hold the twisted assembly together. The twisted assembly jacket is extruded with an overall diameter necessary to frictionally secure the assembly in the metal tube. The diameter of the jacketed assembly outside diameter is typically 2 to 5 mils less than the inside diameter of the metal tube and this secures the core well enough to yield a pull out resistance of 2 to 50 pounds over a one foot length. This pull out force has been proven to be sufficient to secure the twisted core in the tube during service and also allows field personnel to strip the cable ends for termination.

In addition to securing cable elements together the twisted assembly increases the excess fiber length in the buffer tube and increases the optical fibers frictional resistance to movement in the dry buffer tubes. Typically buffer tubes are filled with gel to prevent moisture intrusion and mechanically protect optical fibers cables. For application where cables are operating at very high temperatures there are no suitable gels available and dry buffer tubes must be used. Without twisting the dry buffer tube with other cable elements to increase frictional resistance to movement of the optical fibers within the tube, the optical fibers would fail in long vertical deployments. Twisting also increase the total exceeds fiber available in the cable. Excess fiber is needed to prevent fiber strain due to thermal expansion and elongation of the cable. Excess fiber length and buffer tube filling gels design considerations are discussed in detail in section 3.2 of this report.

3.4.3 Metalclad Cable Prototypes

Metal clad cable prototypes were manufactured using best industry practices to produce mechanically robust cables while preventing damage to all cable components and preventing introduction of hydrogen producing water or machine oils into the cable. The term Metalclad refers to the metal tube installed over the cable core elements for protection. The Metalclad tube is typically 0.25 inches in diameter with a wall thickness between 0.028 inches and 0.049 inches and made of 316 SS or incoloy 825, though tubes are also manufactures in other sizes and using other alloys. The metal clad tube is manufactured using clean dry metal strip that is formed and weld without adding machining oil. The welded tubes are inspected using eddy current to detect small imperfections after welding. Tubing is then drawn through dies to achieve the final dimensions and inspected one more time using eddy current to ensure no defects. These manufacturing practices have been developed and refined over decades of manufacturing metal clad cables for the oil and gas industry. Where the metal clad cable prototypes differ from cables used in the oil and gas industry is the need to be self-supporting to depths greater than 10,000 feet.

Quarter inch metal clad cables have a maximum vertical self –supporting operating length between 4360 feet and 5980 feet. This length is based on the cable weight, yield strength and other factors. The need to minimize optical fiber strain is an important consideration for determining the self-supporting length where cable elongation will decrease the excess fiber available in the cable. The self-supporting cable length is calculated as follows:

$$SSL = \frac{L_{YS}(1 - S_T) - (M_T + F_R)}{UW \times SF}$$

Where:
L_{YS} = Load at Yield Strength (lbs)
M_T = Weight of tool or bob at bottom of cable (lbs)
UW = Unit weight of cable (lbs/ft)
S_T = Strength loss percentage at operating temperature (%)
SF = Safety factor
F_R = Maximum force induced during tool removal (lbf)
SSL = Self-Supporting Length (ft)

For the case of a 316L tube with a 0.035inch wall for use at 300˚C and the following assumptions:

L_{YS} = 2128 lbs
M_T = 100 lbs
UW = 0.1 lbs/ft
SF = 2
F_R = 500 lbs
S_T = 25 % (300˚C for SS)

SSL = 4980 ft

With similar assumptions the maximum self-supporting lengths for 0.25 inch diameter cold work hardened 316SS and incoly 825 metalclad with 0.028inch to 0.049inch walls and 90kpsi yield strength is between 4360 and 5980 feet.

For long self-supporting vertical installations Metalclad cable with fiber optic elements sensitive to strain require additional strength members. To increase the self-supporting cable strength three approaches were considered. One approach is to add strength members inside the metal clad tube, but due to the limited space available inside the tube this method would not substantially increase the cable strength. Another approached is to attached the metalclad to a parallel strength members, this approach result is flat cable assemble and will be difficult to remove from a well and redeploy. The approach selected was a multi wire overall strength member as shown in Figures 83and 135. The strength member consists of 46 hardened wires with 200kpsi yield strength, each wire is 0.040inches in diameter, the first layers is applied with a right hand lay and contains 20 wires, the second layer has 26 wire applied with a left hand lay. Adding this strength member to the example above increases self-supporting length from 4980ft to 13,830feet. The overall multi wire strength member also allows the cable to retain its flexibility and can be easily sealed at the well head.

3.5 CONCLUSIONS

The greatest challenge encountered during the high temperature cable development was the FIMT manufacture and identification of a suitable filling material. Much progress was made refining the intermittent plug filler manufacturing process and a long length was successfully manufactured though not in time to be incorporated into the field trial of phase three of the project. The intermittent plug design was validated in lab tests and offers a promising alternating to dry buffer tubes in the absence of filling gel suitable for use at 300°C. Chemours's development of ECCtreme™ ECA 3000 was as key contribution, where the rated operating temperature of extrudable electrical material was increased from 260°C to 300°C. The final cable design uses the coated fiber developed in phase one to the project inside the FIMT developed in phase two, the FIMT is twisted together with an electrical conductor with Chemours's ECA3000 insulation and installed in a metalclad tube. The metal clad tubes have been refined over decades of use in the oil and gas industry and an additional strength member was added over the quarter inch metalclad to provide the strength needed to achieve self –supporting vertical lengths greater than 10,000 feet. The cable developed in Phase 2 of the project and used in Phase 3 Cable Testing and Validation is shown in Figure 135 below.

Components

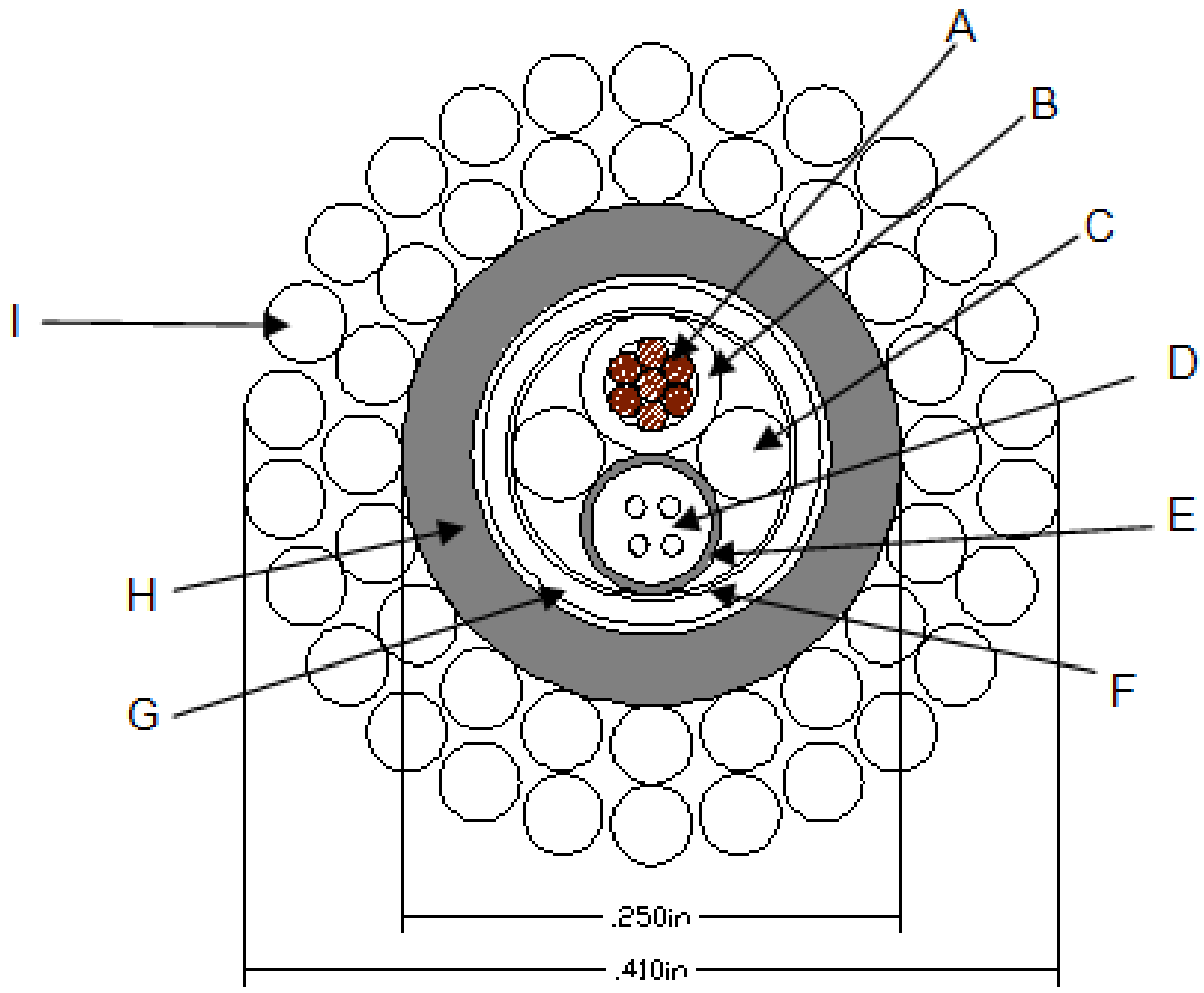

A:	#18 AWG 7/26 ETP NP 2% Copper; O.D.: 1.16 mm (0.046") Nominal
B:	Natural ECCtreme ™ ECA 3000 Fluoroplastic ; O.D.: 1.78 mm (0.070") Nominal
C:	Fillers: Fiberglass Rod covered with ECCtreme ™ ECA 3000 Fluoroplastic; O.D.: 1.22 mm (0.048") Nominal
D:	Fibers: 2 x 50/125 Draka Polyimide Coated H2 resistant & 2 x Single Mode Draka Polyimide Coated H2 resistant
E:	625 Incoloy FIMT: 1.5 mm x 1.8 mm (ID x OD)
F:	Tape: PTFE Tape Wrap Thickness: 0.076 mm (0.003")
G:	ECCtreme ™ ECA 3000 Fluoroplastic rated to 300˚C; O.D.: 4.32 mm (0.170") Nominal
H:	825 Incoloy Alloy Tube; Wall Thickness: 0.89 mm (0.035"); O.D.: 6.35 mm (0.250") Nominal
I:	Stainless Steel Armor; First layer 20/.040" preformed RHL at 20˚; Second layer 26/0.40" preformed LHL at 20˚

Figure 135: Final Cable Design

4.0 Phase 3: Cable Testing and Validation

4.1 INTRODUCTION

Field testing and validation of the cable developed was performed at Nevada Geothermal Power Blue Mountain power plant. The well made available for testing was 6300 feet deep and highest temperature recorded during previous surveys was 196°C, a well bore schematic is provided in Figure 136 and previous survey data is provided in Figure 137. Field testing was performed in three parts; short-term, medium-term and long-term. Short-term testing consisted of installing and removing a trial cable to make sure the cable worked well existing handling equipment and then installing a long-term test cable for the remainder of the field tests. The medium-term test consisted of measurements to evaluate the cable performance in the well after on month. The long-term tests consisted of evaluation of the cable performance from four to ten months and a final evaluation after removing cable from the well.

The cable design installed for evaluation is shown in Figure 135. The total cable was 6800 feet and when installed there was 6200 feet of cable inside the well. The cable was subjects to factory electrical and optical inspections prior to being shipped to well site, where the cable passed all electrical inspection and exhibited high optical attenuation. Optical fiber attenuation measured at each step of manufacturing are shown below in Table 39. Typical maximum acceptable attenuation for downhole cables is 0.5dB/km for singlemode fibers at both 1310nm and 1550nm, and 1.5dB/km at 1300nm and 3.5dB/km at 850nm for multimode fibers. During manufacturing the FIMT is subjected to several operations were the FIMT tube is bent and heated, this can induce stress and strain on the optical fibers. Based on attenuation measurements shown below and Brillouin fiber strain measurements the most likely cause is microbend induced attenuation from increased excess fiber related to the FIMT and metalclad tubing length being reduced during manufacturing. The most significant attenuation increase occurred during armoring where it is believed excessive use of tubing straightening devices reduced the overall tubing length.

Fiber	Wave length	Attenuation (dB/km)				
		As Received	After Cabling	After Jacketing	After Metal Clad Tube	After Armor
Singlemode	1310nm	0.53	0.59	0.69	0.67	1.50
	1550nm	0.34	0.46	0.71	0.71	1.55
Multimode	850nm	1.88	2.19	2.92	3.02	5.45
	1300nm	0.47	0.77	1.42	1.50	3.91

Table 39: Optical fiber attenuation during manufacturing

Cable testing and validation proceeded with the cable described above for two key reasons. Exceess fiber in the cable will decrease when the cable is deployed in the well and should improve, and as shown Table 40 this proved to occur. The second reason was window of time to have a cable installed and sufficient time to complete the long-term test was closing and not using this cable for testing and validation would jeopardize completion of phase three of the project.

4.2 SHORT-TERM TEST

The short-term test consisted of two parts, the first part a non-critical trial cable was installed to ensure the installation process would not damage the critical cable intended for long-term installation. The non-critical cable was installed using 150lbs of sinker bars and was installed to a depth of 1000 feet with no problems. The cable was removed from the well and no damage was found to cable or installation equipment. Results of the first part of the short-term test demonstrated the cable was more flexible than expected and the weight of sinker bars used to install the critical long-term cable could be reduced.

The second part of the short-term test was to install the cable developed for long-term evaluation, shown in Figure 135. This design permitted multiple measurement tecniques to be used during the field trial.

1) The electrical conductor provided power and communication link with downhole tool equipped with pressure and temperature transducers. The high temperature/high pressure (HT/HP) tool and surface receiver were provided by Perma Works and capable of continuous logging of well conditions at the bottom end of cable installation.
2) Singlemode optical fibers in the FIMT were used for distributed temperature sensing (DTS) using a Brillouin frequency shift measurement technique. The instrument used to perform these DTS measurements was provided by Omnisens. This measurement technique required a round-trip optical signal though both single mode fibers and the fiber ends were fusion spliced in a cavity of the (HT/HP) tool to form a continuous loop back to the surface.
3) Multimode optical fibers in the FIMT were used for distributed temperature sensing (DTS) using a Raman backscatter measurement technique. The instrument used to perform these DTS measurements was provided by Sensortran.
4) Optical fiber attenuation was also measured with an OTDR to evaluate how well the cable system is protecting the fibers during operation.

Cable design installed for the long-term test is shown in Figure 135; cable was installed in the well using a100lbs of sinker bars and the measurements describe above were performed.

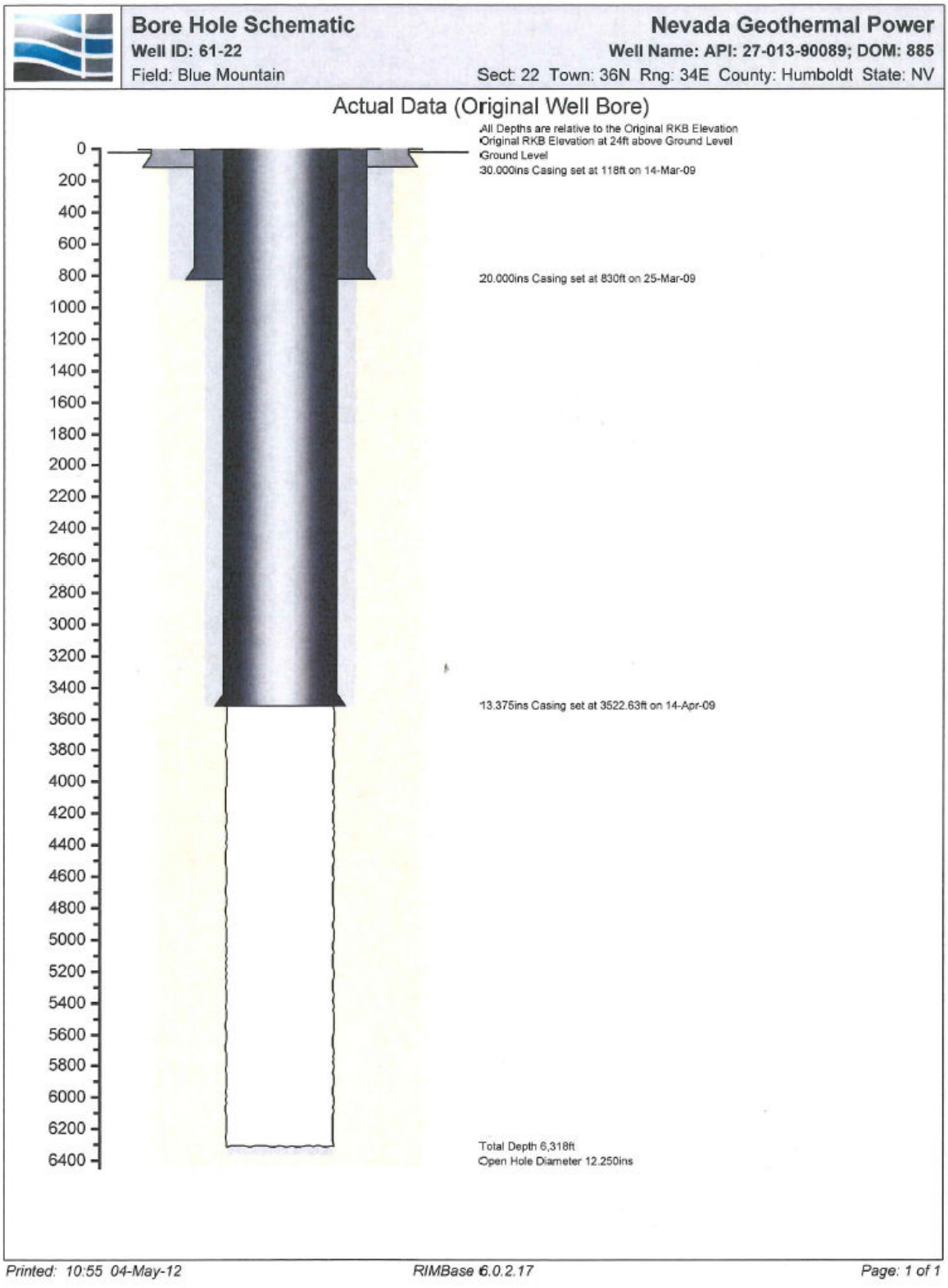

Figure 136: Well Bore Schematic

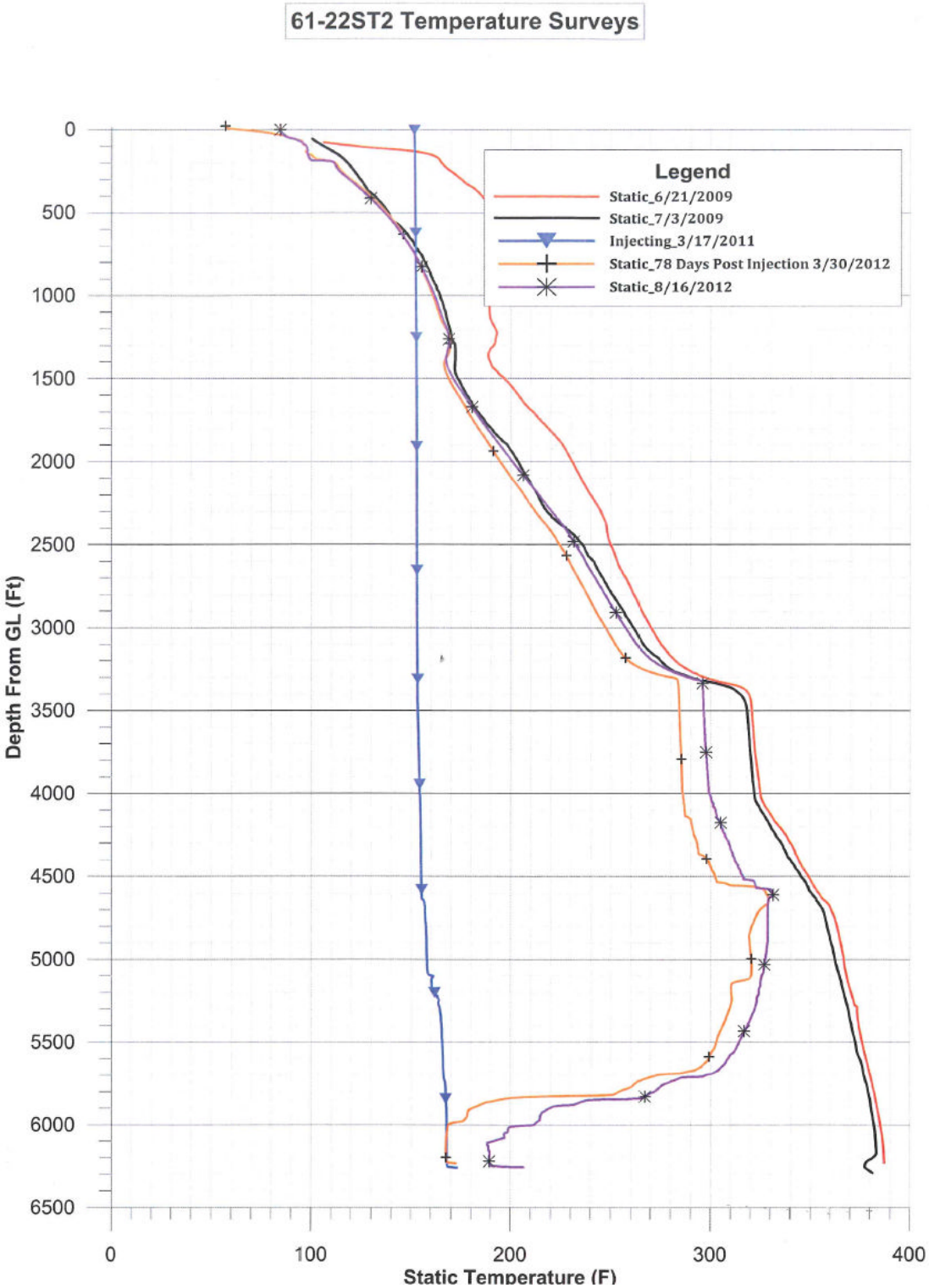

Figure 137: Previous Well Surveys

Measurements performed three to four hours after installation in well demonstrated all cable elements were functioning properly. Distributed temperature measurements using Brillouin and Raman measurement techniques are shown below in Figures 138 and 139 respectively, both figures show one data point for the Perma Works HT/HP tool where well temperature and pressure were measured at the bottom end of cable.

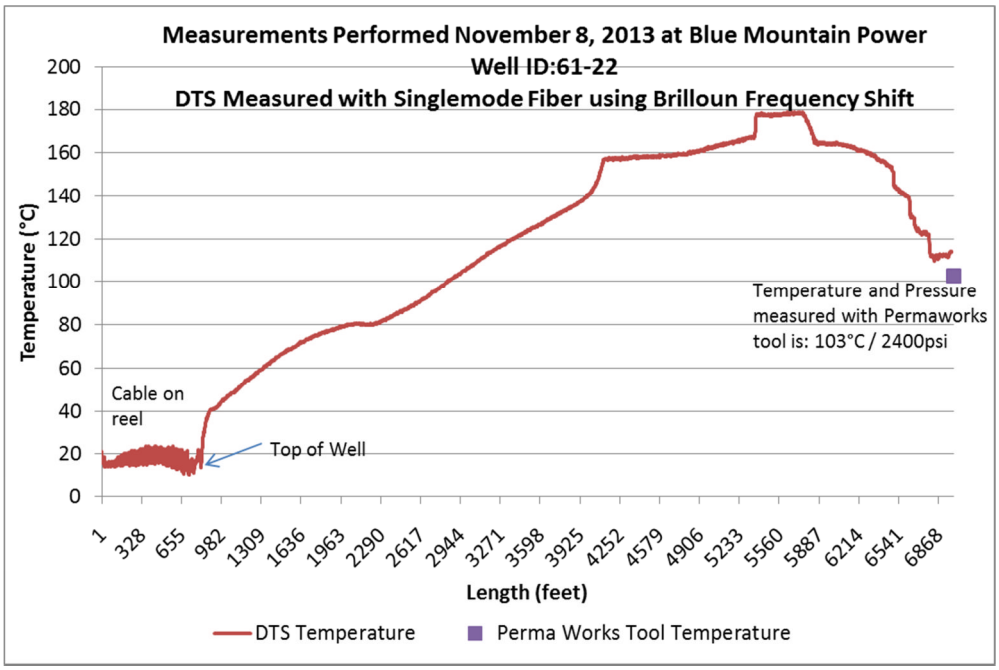

Figure 138: DTS measurements using Brillouin measurement technique, day one.

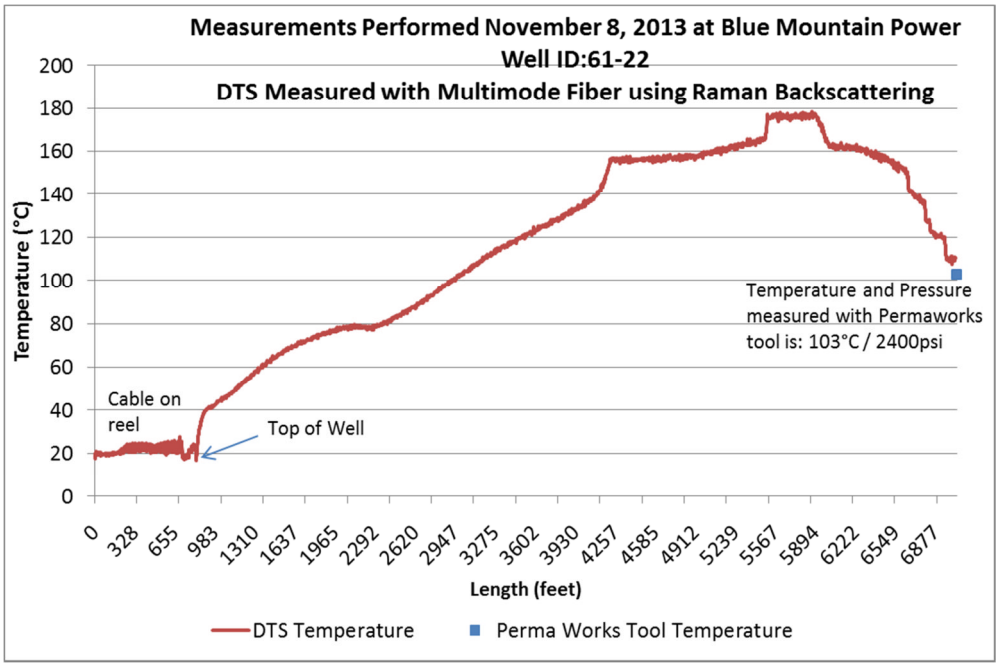

Figure 139: DTS measurements using Raman measurement technique, day one.

Optical fiber attenuation measurements were performed and results indicate the cable was installed without damage or additional stress applied to fibers. OTDR measurements are shown below in Table 39.

Fiber Type	Wave length	Attenuation (dB/km)
Singlemode fiber	1310nm	0.47
	1550nm	0.38
Multimode fiber	850nm	2.08
	1300nm	0.64

Table 40: Optical fiber attenuation immediately after installation in well

4.3 MEDIUM-TERM TEST

Additional measurements were preformed 27 days after the cable installed in the well. Optical fiber attenuation measurements are shown below in Table 40. Attenuation of all fibers increased, most notably the singlemode fiber attenuation doubled at 1550nm from 0.38dB/km to 0.77dB/km. DTS measurements were performed using Raman measurements over multimode fiber and data is shown in Figure 140.

Fiber Type	Wave length	Attenuation (dB/km)
Singlemode fiber	1310nm	0.67
	1550nm	0.77
Multimode fiber	850nm	2.22
	1300nm	1.08

Table 41: Optical fiber attenuation after 27 days in well

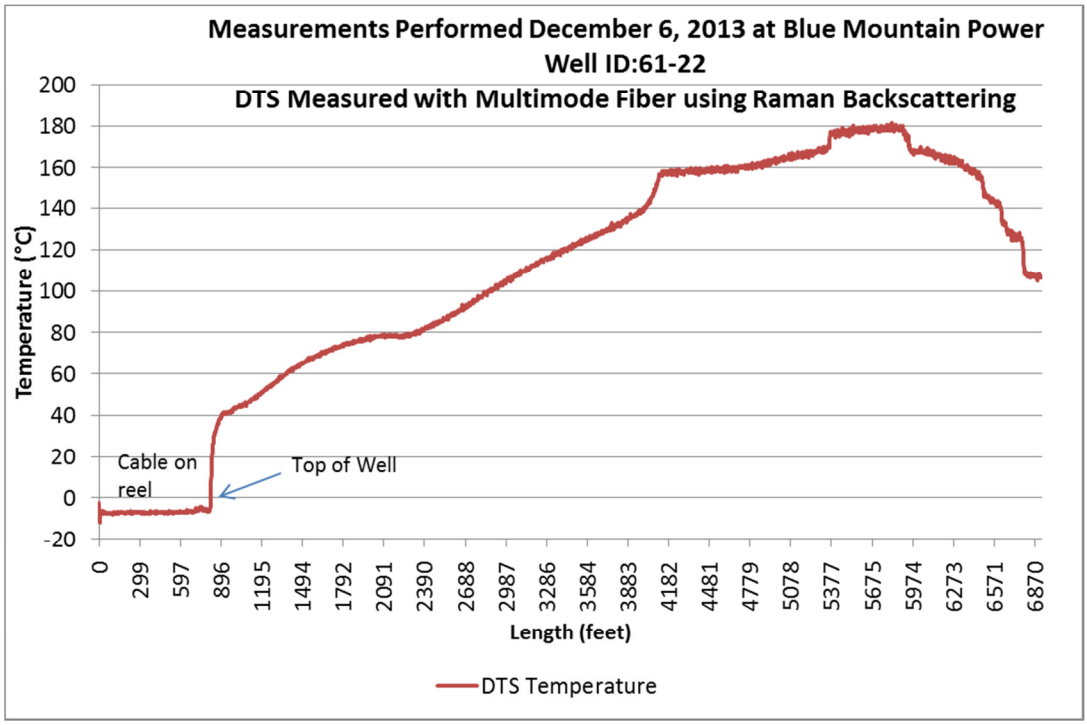

Figure 140: DTS measurements using Raman measurement technique, after 27 days

Do to extreme temperatures at the well site the fusion slicer was not operating properly and singlemode fibers could not be spliced to perform DTS measurements with the Brillouin measurement system. The Perma Works surface receiver was also inoperable and needed to be repaired by the factory.

4.4 LONG-TERM TEST

The long-term tests was a continuation of previous tests with the cable performance monitored for up to 10 months and inspected after removal from well. The long-term test included two site visits were optical attenuation measurements were performed and operating condition of other measurement systems were checked.

The first site visit for the long-term test was 131 days after the cable installation. During this visit problems encountered during the medium-term test were addressed, the Sensortran Raman based DTS systems was setup to perform periodic measurements, and Blue Mountain power plant were trained to perform periodic Brillouin DTS measurements. Optical fiber attenuation measurements were performed and values more than double for both singlemode and multimode fiber types, measurements are shown below in Table 41. DTS measurements were performed using Brillouin and Raman measurement techniques are shown below in Figures 141 and 142 respectively. The well temperature profile was significantly different than prior measurements because of difference flow conditions in the well. During previous measurements the well was closed and static, in early 2014 water was begun being pumped in the well from the surface. The reason for this was to keep water in the surface pipes from freezing. The water flow into the well was low and the well was not intended to serve as an injector well in the field. Nonetheless, the water flowing into the well significantly changed the temperature profile of the well. DTS temperature profiles were similar for both measurement techniques indicating attenuation increase did not significantly affect the optical fibers capability to serve as DTS sensing elements.

The HT/HP tool and receiver was set up during the 131 day site visit and programmed to log continuously. Initial measurements were 96°C and 2405PSI. The system stopped logging and a new log could not be initiated during the 10 month site visit. When the system was returned to the manufacturer for evaluation the HT/HP tool was found to be in good working condition, but the surface receiver has a failed output transistor. There was also evidence of a mouse nest inside the receiver unit that may have contributed to the failure.

Fiber Type	Wave length	Attenuation (dB/km)
Singlemode fiber	1310nm	1.63
	1550nm	2.28
Multimode fiber	850nm	4.95
	1300nm	4.12

Table 42: Optical fiber attenuation after 131 days in well

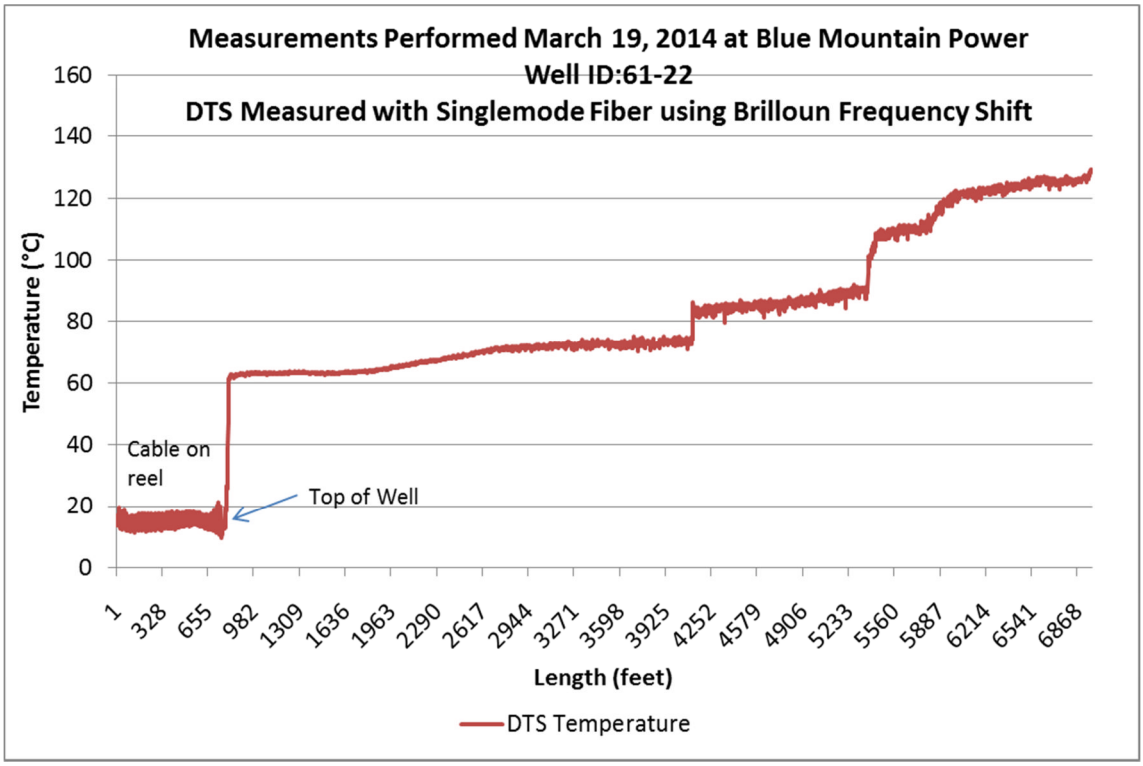

Figure 141: DTS measurements using Brillouin measurement technique, after 131 days

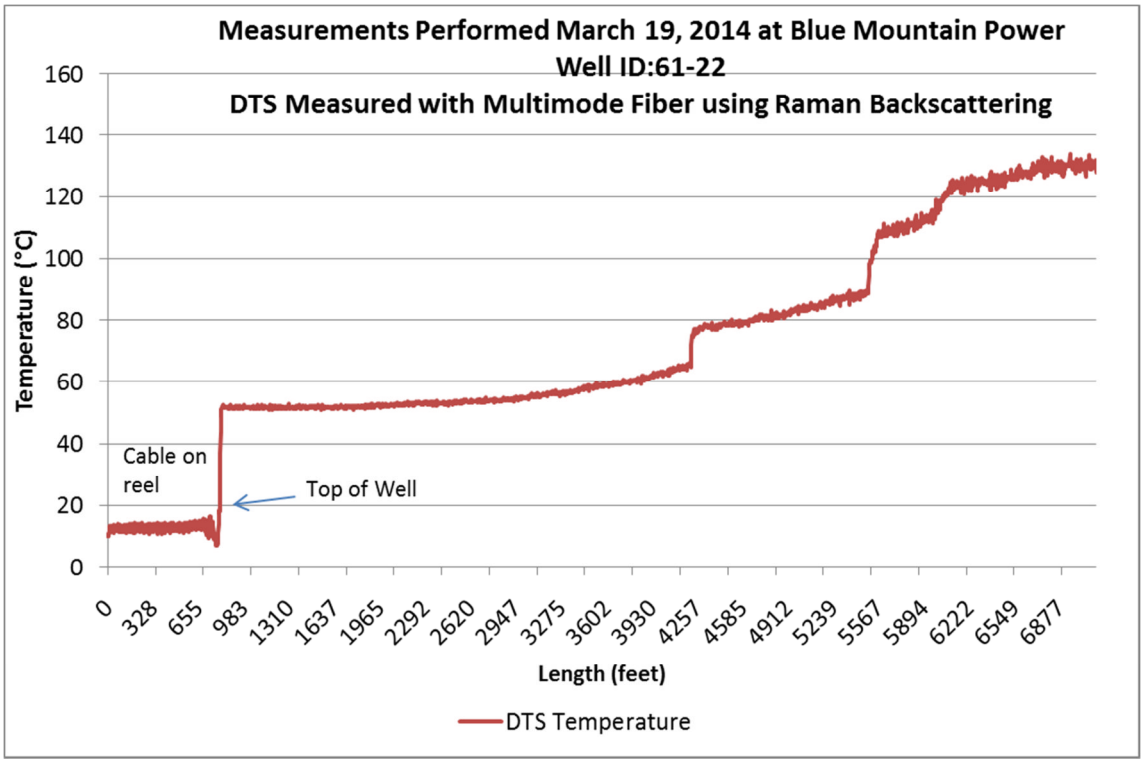

Figure 142: DTS measurements using Raman measurement technique, after 131 days

During the 10 month site visit the Sensotran Raman DTS was found malfunctioning. The unit was programmed to perform measurements periodically at one hour intervals during the 131 day site visit. The unit did perform measurements during the period between site visits, but a hardware failure occurred in August approximately nine months into the test that prevented further measurements.

Due to hardware failure of HT/HP tool receiver and Raman DTS system the only measurements that could be perform at the 10 month site visit were Brillouin DTS measurements and OTDR attenuation measurements. DTS measurements performed throughout the 10 month the test using Brillouin technique is shown below in Figure 143. There are two sets of temperature profiles corresponding to a closed or open well. As previously mentioned the well was closed during the initial measurements on November 2013, this same condition applies to the final measurements on September 2014. During the period between January 2014 and August 2014 there water being pumped into the well from the surface.

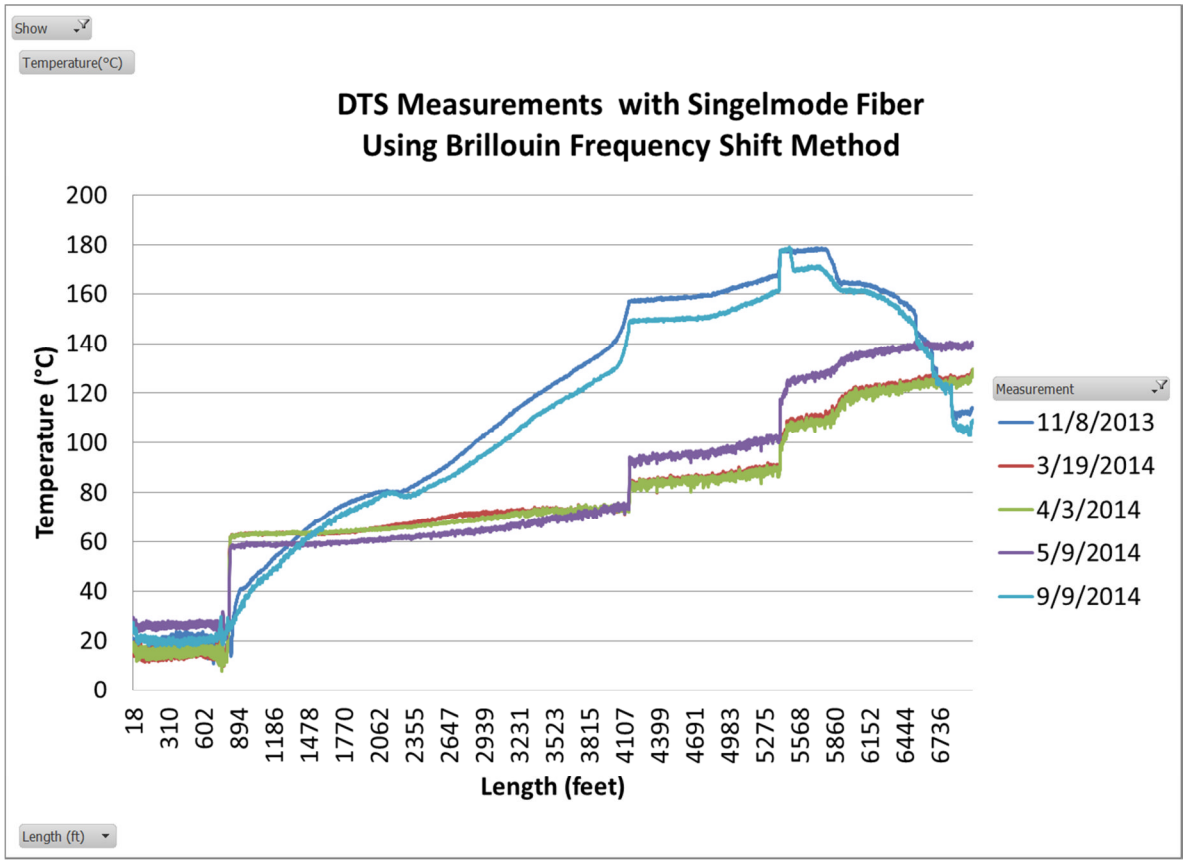

Figure 143: DTS measurements using Brillouin measurement technique during 10 month test.

Attenuation measurements were performed during the final site visit and again after the cable was removed from the well and allowed to cool, these measurements along with previously reported attenuation values are shown in Table 42.

Fiber	Wave length	Attenuation (dB/km)				
		Day1	Day 27	Day 131	Day 305	After removed
Singlemode	1310nm	0.47	0.67	1.63	1.49	1.36
	1550nm	0.38	0.77	2.28	2.04	2.31
Multimode	850nm	2.08	2.22	4.95	2.25	3.23
	1300nm	0.64	1.08	4.12	1.87	2.53

Table 43: Optical fiber attenuation measurements

After removal from the well the cable was shipped back to the Draka factory and subjected to factory electrical inspection. The cable passed all electrical inspections and had no visible corrosion or other damage.

4.5 CONCLUSIONS

Field testing was successfully demonstrating both cable design strengths and identified performance weakness. Field testing demonstrated the cable design was easily handled by standard downhole cable equipment where the cable proved to be more flexible than field personnel expect. All metal and dielectric materials withstood the well environment with no discernible degradation. The design weakness was evidenced by the attenuation increase both during manufacturing and when installed in the well. The manufacturing process can be adjusted to manage the total available excess fiber in the completed cable, but a high temperature gel or alternative to a dry tube is needed to mitigate other factors contributing to increase optical fiber attenuation. Although the attenuation did not prevent DTS measurements, it must be remembered that the well temperature and depth was less than those of the cable design goals.

5.0 Conclusions

Work done during the project has contributed to advances in high temperature optical fiber coatings, hydrogen resistant optical fibers, and high temperature electrical insulation materials. These are advances are each critical enabling technologies for well sensing cables and together make possible a complete fiber/copper cable solution for long-term temperature and pressure measurements up to 300°C, with optical fiber cables capable of operating in supercritical wells up to 374°C for up to 60days. Although these advances represent the current state of the art, the objective of a complete long-term solution of a cable capable of operating for five years in a well environment with temperatures up to 374°C was not fully attained.

Barriers to attaining the objective of a cable that can operate at 374°C were related to the polymeric materials, i.e., optical fiber coating, electrical insulation, and buffer tube gel. Much effort was expended developing an alternative to using buffer tube gel that performed well in lab tests scheduling constraints prevented use of the technology in the field test cable. Nonetheless, a gel suitable for use in buffer tubes at 300°C and greater would yield a more robust cable than a dry buffered design such as the cable used in the field test of phase three. Higher temperature fiber coatings and electrical insulation materials are available using non-polymeric materials. Where metal coated fibers and mica electrical insulation may be used at 374°C and higher temperatures.

Use of metal coatings was outside the scope of this project. In phase 2 of the project a prototype using mica/fiberglass insulation system was manufacture, this may be a viable solution to achieve 374°C, but for a 300°C cable design the ECCtreme™ ECA 3000 is a more robust and economical solution.

APPENDIX

LIST OF PUBLICATIONS

Title: An Optical Fiber with Advanced Polyimide Coating

Authors: Bob Overton
Frans Gooijer
Gertjan Krabshuis

Published: 2012 IWCS Conference Proceedings

INVENTION/PATENT APPLICATIONS

Title: Multimode optical fibre (Depressed Graded-Index MMF with Trench)

Inventors: Denis Molin
Pierre Sillard
Marianne Bigot-Astruc

Date Reported: July 8, 2011

DOE"S" No: S-127,412

Patent Number: EP2541292 B1

Title: Loose-tube optical-fiber cable (Loose Tube Construction with Intermittent Fiber Support)

Inventors: Jan Jonker
Mark Lowell
Tyler Angers

Date Reported: Aug. 16, 2012

DOE"S" No: S-131,138

Patent Number: US8929701 B2

PRODUCTS RESULTING FROM WORK

1. **Product Name**: DrakaElite™ High Temperature Optical Fiber - Hydrogen Tolerant High Pressure and High Temperature Single Mode Fibers

   Organization: Prysmian Group (Draka Communications)

   Product Information:
   http://www.prysmiangroup.com/en/business_markets/markets/fibre/downloads/datasheets/DrakaElite---High-Temp-Family_2012.04.pdf

2. **Product Name**: DrakaElite™ High Temperature Optical Fiber - Hydrogen Tolerant High Pressure and High Temperature Graded Index Multi Mode Fibers

   Organization: Prysmian Group (Draka Communications)

   Product Information:
   http://www.prysmiangroup.com/en/business_markets/markets/fibre/downloads/datasheets/DrakaElite---High-Temp-Family_2012.04.pdf

3. **Product Name**: ECCtreme ™ ECA 3000 Fluoroplastic Resin

   Organization: Chemours

   Product Information:
   https://www.chemours.com/Ecctreme/en_US/assets/downloads/Chemours_Ecc_treme-ECA_3000_Tech_Data_K24282.pdf

   Note: Product was developed by Chemours with assistance from Prysmian Group (Draka Cableteq USA)